

ABSTRACT

Title of Document:

TRAPPING LABILE ADDUCTS FORMED
BETWEEN AN ORTHO-QUINONE
METHIDE AND DNA

Michael Patrick McCrane, Doctor of Philosophy,
2012

Directed By:

Professor Steven E. Rokita, Department of
Chemistry and Biochemistry

Exogenously generated electrophiles are capable of alkylating DNA. If not repaired, the resulting DNA adducts can lead to mutations and either cancer or cell death. Electrophilic *ortho*-quinone methides (*o*-QM) are reactive intermediates that alkylate DNA and are generated during xenobiotic metabolism of a variety of compounds including environmental toxins and therapeutic agents. Identifying the full alkylation profile of *o*-QM towards DNA would allow for the genotoxicity of *o*-QM precursors to be better understood.

From model studies based on nucleosides, *o*-QMs react most readily, but reversibly with the strong nucleophiles 2'-deoxycytidine (dC) N3, 2'-deoxyguanosine (dG) N7, and 2'-deoxyadenosine (dA) N1 and less efficiently, but irreversibly with the weak nucleophiles dG N1, dG N², and dA N⁶. The reverse reactions complicate analysis of their products in DNA, which requires enzymatic digestion and chromatographic separation. Selective oxidation by

bis[(trifluoroacetoxy)iodo]benzene (BTI) can transform the reversible *o*-QM-DNA adducts into irreversible derivatives capable of surviving such analysis. To facilitate this analysis, a series of oxidized *o*-QM-dN adducts were synthesized as analytical standards.

Initial oxidative trapping studies with an unsubstituted *o*-QM and dC demonstrated the necessity of an alkyl substituent *para* to the phenolic oxygen to block over-oxidation. A novel *o*-QM included a methyl group *para* to the phenolic oxygen that successfully blocked the over-oxidation allowing for generation of a stable MeQM-dC N3 oxidized product. Further oxidative trapping studies with MeQM and dG resulted in the formation of three stable MeQM-dG oxidized products (guanine N7, dG N1, and dG N²).

Initial studies with duplex DNA optimized the enzymatic digestion and confirmed that the assay conditions were compatible with oxidative trapping. The low yielding MeQM alkylation of duplex DNA needs to be scaled up prior to the oxidative trapping studies.

Alternative studies quantified the release of MeQM from DNA with the use of β-mercaptoethanol as a nucleophilic trap. These studies revealed single stranded DNA as a superior carrier of MeQM than duplex DNA and, therefore, a better target DNA for the oxidative trapping studies due to increased yield of MeQM adducts. With the increased MeQM-DNA yield, the intrinsic selectivity and reactivity of MeQM towards DNA can be determined.

TRAPPING LABILE ADDUCTS FORMED BETWEEN AN ORTHO-QUINONE
METHIDE AND DNA

By

Michael Patrick McCrane

Dissertation submitted to the Faculty of the Graduate School of the
University of Maryland, College Park, in partial fulfillment
of the requirements for the degree of
Doctor of Philosophy
2012

Advisory Committee:

Professor Steven E. Rokita, Chair
Professor Philip DeShong
Professor Lyle Isaacs
Professor Herman O. Sintim
Professor Daniel Stein

© Copyright by
Michael Patrick McCrane
2012

Lay Abstract

A number of drugs and environmental toxins are metabolized in our cells resulting in compounds that can react with and cause damage to many different cellular components, including DNA. The type, amount, and location of the DNA damage, known as lesions, determines the biological response which may consist of repair or cell death. If the biological response is insufficient to correct the DNA lesions, mutations may occur possibly leading to cancer or cell death. Many anti-cancer drugs also work by damaging DNA. Understanding the biological response to a specific DNA damaging compound would allow for the assessment of that compound's toxicity. To accomplish this goal, the DNA lesions formed by a specific compound must first be identified. This would allow for the relationship between a lesion and a specific biological response to be established.

One type of DNA damaging compound is quinone methide (QM). The QM functional group is found upon metabolism of a number of anti-cancer compounds, the most well known is mitomycin C. QMs are also found in cells upon metabolism of certain environmental chemicals, such as the food preservative BHT. QMs have the unusual ability to form both irreversible and reversible products with DNA. The reversible products exist long enough to elicit a biological response, but not long enough for standard analysis. To effectively assess the toxicity of QMs, the reactivity and selectivity of a simple QM towards DNA is a necessity and requires a method of trapping the reversible products. In this way, the product profile can be “frozen” at any given time and will not change during the long process of breaking down DNA. The compound bis[(trifluoroacetoxy)iodo]benzene (BTI) can transform the reversible

products into irreversible products through an oxidation mechanism. Most importantly, BTI performs this transformation quickly, completely, and in the near physiological conditions used for the QM reaction of DNA. These points are important as they will allow for the analysis of the QM reaction of DNA at short (< 24 hr), but biologically relevant times leading to a much better understanding of its reactivity and selectivity than previous studies have allowed.

To help with the eventual analysis of the reaction between QM and DNA, a number of analytical standards were synthesized from nucleosides. This was accomplished by first reacting individual nucleosides with QM to form the QM-nucleoside product and second the product was oxidized with BTI to form the analytical standard. Initially, the first nucleoside to be studied was 2'-deoxycytidine (dC) because it forms only one, slowly reversible, product with QM. During these studies, the simplest QM was observed to form a complex, and unexpected, product after reaction with BTI. A new QM, which featured the addition of a methyl group to limit the reactivity of QM with BTI, was developed to avoid the formation of the unexpected complex product. The new QM (MeQM) successfully reacted with dC and formed the expected product upon reaction with BTI.

After the MeQM-dC product was synthesized and its structure determined, the three products between MeQM and the nucleoside 2'-deoxyguanosine (dG) were synthesized. Additionally, MeQM forms two products with the nucleoside 2'-deoxyadenosine, and these products were studied by my undergraduate mentee Omer Ad. Previous studies have shown that 2'-deoxythymidine (dT) does not react with

QM and it was not studied. In total, six analytical standards were made for use with the analysis of the reaction between MeQM and DNA.

With the help of the six analytical standards, the reaction between MeQM and DNA was investigated. However, not enough MeQM reacted with the DNA and therefore future work will increase the amount of MeQM that reacts with DNA. Once the reaction between MeQM and DNA can be studied, information on the associated lesions (such as their type, amount, and location) can be used to determine why QMs elicit specific biological responses and how to assess the toxicity of QM based DNA damaging compounds.

Dedication

For Randi and Luke

Acknowledgements

I would like to thank my advisor Professor Steve Rokita for welcoming me into his lab and for his endless support and encouragement. With your influence and your trust I have become a much better and more independent scientist. You were always there for a discussion and I somehow always left our meetings feeling more enthusiastic about my research.

I would like to thank my committee of Professors DeShong, Isaacs, Sintim, and Stein for taking the time out of their busy schedules to accommodate me. Professor DeShong, also thank you for improving my knowledge of chemistry and for being available for friendly discussion. Professor Isaacs, you taught me more about structure determination than I thought possible and were also a great help with my presentation skills during my 2nd year seminar. Professor Sintim, you taught me a great deal about organic synthesis and methodology and did it with an enthusiasm that made it easy to come to class.

Thank you to the other professors who I've had for classes during my time in College Park. Professors Falvey, Davis, Eichorn, and Cropp were instrumental in improving my knowledge of chemistry and improving my work ethic.

I would like to thank Dr. Yiu-Fai Lam and Dr. Gene Mazzola for all of the time that they spent teaching me the ins and outs of NMR. Thank you also for always being available to help me interpret data or just for a friendly chat. Also, thank you to Dr. Yue Li for his help with running many samples on the mass spectrometer and the LC/MS. Additionally, thank you to Bill Griffin and Levi Gayatao for always being

helpful in the stock room and loading dock. I'm going to miss talking about the Yankees with you Bill.

Thank you to all of the Rokita lab members, past and present. Everyone has been incredibly friendly and inviting since the first day I stepped into the lab. Especially Drs. Patrick McTamney, Neil Campbell, and Jen Buss for showing me that grad school can be a lot of fun when I was just starting. A big thank you to Dr. Chengyun Huang for tolerating me constantly playing music in the lab and for also being a fantastic labmate. Good luck back home in China! Thank you to Omer Ad for being a great student to mentor and a great person to share the lab with. Good luck in Grad School, I know you'll do great! Thank you to Fazel Fakhrai (I'm still going to call you AB) for being a good friend for the last 4 years and a great source of chemistry knowledge. And a final thank you to Petrina Boucher for always being there to complain about science or life when I needed to and also for many useful discussions about class and research.

I would like to thank my Mom and Dad because without them, I'm obviously not here. Thank you for teaching me that I can accomplish anything that I put my mind to and for always believing in me. Thank you to my sister Jess for being a great sister and friend.

And last, but certainly not least, thank you to my loving wife Randi and son Luke. Randi, you have been my biggest supporter and I don't know if I could have accomplished this without you. Words cannot express how much you mean to me. And Luke, I can't wait until you're older so I can buy you your first chemistry set!

Table of Contents

Lay Abstract.....	ii
Dedication.....	v
Acknowledgements.....	vi
Table of Contents.....	viii
List of Tables	x
List of Figures.....	xi
List of Schemes.....	xv
Abbreviations.....	xvii
Chapter 1: Introduction.....	1
1.1. DNA Alkylation.....	1
1.2. The Importance of Detecting Labile DNA Adducts.....	3
1.3. Extensively Studied Labile DNA Alkylating Agents.....	4
1.4. DNA Alkylation by Quinone Methides.....	9
1.5. Requirements for a QM-DNA Trapping System.....	15
1.6. Oxidation of the QM Phenol as an Effective Trap.....	17
Chapter 2: Formation and Oxidation of QM-dC and MeQM-dC Adducts	21
2.1. Introduction.....	21
2.2. Results and Discussion	23
2.2.1. Oxidation of QM-dC N3.....	23
2.2.2. Synthesis of a Novel <i>o</i> -Quinone Methide Precursor to Block Over-Oxidation	27
2.2.3. Alkylation of dC with MeQM	29
2.2.4. Initial Attempts at MeQM-dC N3 Oxidation.....	30
2.2.5. Oxidation of MeQM-dC N3	38
2.3. Summary.....	44
2.4. Materials and Methods	44
Chapter 3: Formation and Oxidation of MeQM-dG Adducts	50
3.1. Introduction.....	50
3.2. Results and Discussion	53
3.2.1. Alkylation of dG with MeQM	53
3.2.2. Oxidation and Isolation of the MeQM-dG adducts	66
3.3. Summary.....	81
3.4. Materials and Methods	82
Chapter 4: Alkylation of DNA by MeQM and Subsequent Enzymatic Digestion.....	86
4.1. Introduction.....	86
4.2. Results and Discussion	90
4.2.1. Optimization of the Enzymatic Digestion of DNA	90
4.2.2. Alkylation of DNA by MeQM	98
4.3. Summary.....	107
4.4. Materials and Methods	107
Chapter 5: Quantifying Quinone Methide Release from DNA with β -Mercaptoethanol	110

5.1. Introduction.....	110
5.2. Results and Discussion.....	112
5.2.1. Synthesis of the Water and β -Mercaptoethanol Adducts of MeQM.....	112
5.2.2. Determination of Extinction Coefficients for MeQM-H ₂ O, MeQM- β ME, and Internal Standards.....	121
5.2.3. Quantifying MeQM Released from Nucleoside Adducts by Trapping with β -Mercaptoethanol.....	123
5.3. Summary.....	153
5.4. Materials and Methods.....	155
Chapter 6: Conclusions.....	160
Appendices	166
Appendix A. Supporting Information for Chapter 2	166
Appendix B. Supporting Information for Chapter 3.....	178
Appendix C. Supporting Information for Chapter 4.....	191
Appendix D. Supporting Information for Chapter 5	195
References.....	201

List of Tables

Table 2.1. The effect of pH on the stability of the major product of MeQM-dC N3 oxidation during purification.	32
Table 2.2. Parameters for the Sep-Pak assisted solvent exchange of the major product of MeQM-dC N3 oxidation.	33
Table 3.1. Comparison of UV-Vis and t_r data between MeQM-dG and QM-dG.	60
Table 3.2. ^1H NMR comparison between MeQM-dG and QM-dG (ppm).	61
Table 3.3. HPLC gradient optimization for the fractionation of the MeQM-dG alkylation.	63
Table 4.1. Enzymatic digestion conditions for the initial ctDNA experiments, compared to the literature precedent.	93
Table 5.1. Calculated molar extinction coefficients (ϵ) at $\lambda_{280\text{ nm}}$ of the compounds of interest in the βME trapping of MeQM.	123
Table 5.2. Reaction conditions without a DNA nucleophile expected to produce a maximum amount of MeQM- H_2O and a minimum amount of MeQM- βME .	126
Table 5.3. Reaction conditions used to compare the effect of reaction vessel on the persistence of MeQM and subsequent formation of MeQM- βME .	132
Table 5.4. Reaction conditions used to compare the effect of shaking the reaction vessel on the persistence of MeQM and subsequent formation of MeQM- βME	132
Table 5.5. Reaction conditions for the control experiment which measures the persistence of MeQM or 4-MeBrQMP in solution in the absence of DNA.	133
Table 5.6. Reaction conditions for the comparison between the ability of various nucleoside based nucleophiles to extend the lifetime of MeQM in solution using potassium phosphate as a buffer.	140
Table 5.7. Comparison between the ability of various nucleoside based nucleophiles to extend the lifetime of MeQM in solution using <i>m</i> -cresol as the internal standard instead of the previously used phenol.	150

List of Figures

Figure 2.1. ^1H - ^{13}C HMBC of 2.2 in $\text{DMSO}-d_6$ at 600 MHz.	25
Figure 2.2. ^1H NMR of 2.15 in $\text{DMSO}-d_6$ at 400 MHz.	41
Figure 2.3. ^1H - ^{13}C HMBC of 2.15 in $\text{DMSO}-d_6$ at 400 MHz.	43
Figure 3.1. Watson-Crick base pairing in DNA with the major and minor grooves labeled.	52
Figure 3.2. HPLC analysis of a “one-pot” MeQM-dG oxidation.	54
Figure 3.3. HPLC analysis of the alkylation of dG with MeQM.	55
Figure 3.4. HPLC analysis of MeQM-dG alkylation with 50 mM 4-MeBrQMP and 22.5 mM dG in a 1.8:1:1.2 mixture of DMF:CH ₃ CN:H ₂ O.	57
Figure 3.5. HPLC analysis of a 2x scale MeQM-dG alkylation of Figure 3.4.	57
Figure 3.6. HPLC analysis of the MeQM-dG alkylation that consisted of a 1:1 mixture of DMF:H ₂ O with 4-MeBrQMP (25.0 mM), dG (12.5 mM), and KF (250 mM).	59
Figure 3.7. HPLC analysis of the MeQM-dG N7 NMR sample that was stored in $\text{DMSO}-d_6$ for 24 hours at -20 °C.	62
Figure 3.8. HPLC analysis of MeQM-dG alkylation using a 42.5% DMF percentage.	64
Figure 3.9. HPLC analysis of MeQM-dG alkylation. Injection volume was 200 μL .	64
Figure 3.10. HPLC analysis of MeQM-dG alkylation. Injection volume was 1 mL.	65
Figure 3.11. Crude oxidation of MeQM-dG N1 with BTI.	66
Figure 3.12. ^1H NMR of the product formed by oxidation of MeQM-dG N1 in $\text{DMSO}-d_6$ at 400 MHz.	67
Figure 3.13. HPLC analysis of the crude oxidation of the mixture of MeQM-dG N1 (3.2) and MeQM-dG N ² (3.3) with BTI.	69
Figure 3.14. ^1H NMR of the material collected between 21 and 36 minutes of HPLC analysis of the crude oxidation of the mixture of MeQM-dG N1 (3.2) and MeQM-dG N ² (3.3) with BTI (Figure 3.13).	70
Figure 3.15. HPLC analysis of the ^1H NMR sample from Figure 3.14 .	70

Figure 3.16. $^1\text{H} - ^{13}\text{C}$ HMBC of 3.7 in DMSO- d_6 at 600 MHz.	72
Figure 3.17. $^1\text{H} - ^{13}\text{C}$ HMBC of 3.8 in DMSO- d_6 at 600 MHz.	74
Figure 3.18. HPLC analysis of the crude oxidation of the mixture of MeQM-dG N7 (3.4) and MeQM-guanine N7 (3.5) with BTI.	76
Figure 3.19. ^1H NMR of the material collected between 9 and 13 minutes of HPLC analysis of the crude oxidation of the mixture of MeQM-dG N7 (3.4) and MeQM-guanine N7 (3.5) with BTI (Figure 3.18).	77
Figure 3.20. HPLC analysis of the ^1H NMR sample from Figure 3.19 .	78
Figure 3.21. $^1\text{H} - ^{13}\text{C}$ HMBC of 3.10 in DMSO- d_6 at 600 MHz.	80
Figure 3.22. Structural similarities between MeQM-dG N1 (3.2), MeQM-dG N ² (3.3), and MeQM-dC N3 (2.8).	81
Figure 4.1. Fully characterized products of the BTI oxidation of MeQM-dC N3 (2.15), MeQM-dG N1 (3.7), MeQM-dG N ² (3.8), MeQM-guanine N7 (3.10), and MeQM-dA N ⁶ (4.3).	87
Figure 4.2. Synthesized complimentary oligonucleotide sequences used as target duplex DNA.	94
Figure 4.3. HPLC analysis of the enzymatic digestion of a reaction consisting of salDNA, sodium phosphate, and NaF in an 80:20 solution of H ₂ O:CH ₃ CN.	95
Figure 4.4. HPLC analysis of the enzymatic digestion of a reaction consisting of salDNA, sodium phosphate, and NaF in an 80:20 solution of H ₂ O:CH ₃ CN. BTI was added to the reaction and held for 5 minutes prior to work-up and digestion.	96
Figure 4.5. HPLC analysis of the enzymatic digestion of a reaction consisting of OD1/OD3, sodium phosphate, and KF in an 70:30 solution of H ₂ O:CH ₃ CN.	98
Figure 4.6. HPLC analysis of an alkylation reaction consisting of each dN, sodium phosphate, NaF, and 67 mM 4-MeBrQMP in an 80:20 solution of H ₂ O:CH ₃ CN.	99
Figure 4.7. HPLC analysis of an alkylation reaction consisting of each dN, sodium phosphate, KF, and 240 mM 4-MeBrQMP in a 70:30 solution of H ₂ O:CH ₃ CN.	100

Figure 4.8. HPLC analysis of an alkylation reaction consisting of salDNA, sodium phosphate, KF, and 240 mM 4-MeBrQMP in a 70:30 solution of H ₂ O:CH ₃ CN.	101
Figure 4.9. HPLC analysis of an alkylation reaction consisting of salDNA, sodium phosphate, KF, and 100 mM 4-MeBrQMP in a 70:30 solution of H ₂ O:CH ₃ CN.	102
Figure 4.10. HPLC analysis of an alkylation reaction consisting of OD1/OD3, sodium phosphate, KF, and 100 mM 4-MeBrQMP in a 70:30 solution of H ₂ O:CH ₃ CN.	104
Figure 4.11. Expansion of Figure 4.10 to better show the products of MeQM alkylation of OD1/OD3.	105
Figure 4.12. HPLC analysis of an alkylation reaction consisting of OD1/OD3, sodium phosphate, KF, and 100 mM 4-MeBrQMP in a 70:30 solution of H ₂ O:CH ₃ CN. The reaction was stirred in a 0.3 mL glass Reacti-vial for 1 hour at 37 °C prior to an addition of BTI in CH ₃ CN.	106
Figure 5.1. ¹ H NMR of 5.9 in CDCl ₃ at 400 MHz.	116
Figure 5.2. HPLC analysis of the ¹ H NMR (CD ₃ CN) sample of the MeQM-βME reaction at 23 hours.	119
Figure 5.3. HPLC purification of MeQM-βME following a first purification by chromatotron.	120
Figure 5.4. HPLC chromatogram from the reaction detailed in Table 5.2.	126
Figure 5.5. HPLC chromatogram of the MeQM-H ₂ O stability test.	128
Figure 5.6. HPLC chromatogram of the MeQM-βME stability test.	129
Figure 5.7. HPLC chromatogram of the stability test without a potential MeQM source.	130
Figure 5.8. Example HPLC chromatogram of the βME trapping reaction detailed in Table 5.4 , including ctDNA at 4 mM nts.	135
Figure 5.9. ¹ H NMR of the proposed MeQM-MOPS adduct (5.10) in CD ₃ CN at 500 MHz.	137
Figure 5.10. ESI ⁺ -MS of MeQM-MOPS (5.10).	138

Figure 5.11. Comparing the formation of MeQM- β ME in the presence of various nucleoside based nucleophiles.	141
Figure 5.12. Synthesized oligonucleotide sequences used as model of dsDNA and ssDNA.	144
Figure 5.13. Measuring the release of MeQM from OD1/OD3 by quantifying the amount of MeQM- β ME formed.	147
Figure 5.14. HPLC chromatogram of the reaction detailed in Table 5.6 with OD1/OD3 as the DNA nucleophile.	148
Figure 5.15. HPLC chromatogram of the reaction detailed in Table 5.7 with OD1/OD3 as the DNA nucleophile.	149
Figure 5.16. Measuring the formation of MeQM- β ME in the presence of various DNA based nucleophiles.	151

List of Schemes

Scheme 1.1. Proposed mechanism for the depurination of N7-alkyl dG residues.	2
Scheme 1.2. Ring opening in 7-methylguanine (1.9) to yield the FAPy-7MeG (1.11) adduct.	3
Scheme 1.3. Malondialdehyde (1.12) can tautomerize to β -hydroxyacrolein (1.13).	5
Scheme 1.4. M ₁ dG (1.14) and <i>N</i> ² OPdG (1.15) can interconvert under aqueous conditions.	6
Scheme 1.5. Initial alkylation of dG by acrolein (1.16) followed by the reversible interchain cross-link with an opposing dG (1.19 – 1.21).	7
Scheme 1.6. Structure of Et 743 (1.22).	8
Scheme 1.7. Proposed mechanism of the reversible alkylation of dG by Et 743 (1.22).	9
Scheme 1.8. Structures of <i>p</i> -QM (1.27) and <i>o</i> -QM (1.28).	10
Scheme 1.9. Proposed mechanism for the alkylation and cross-link formation of DNA by mitomycin C (1.30).	10
Scheme 1.10. Formation of BHT-QM (1.37) and BHTOH-QM (1.39) by enzymatic oxidation.	11
Scheme 1.11. Proposed mechanism for the fluoride activation of BrQMP (1.40) to <i>o</i> -QM (1.28).	13
Scheme 1.12. Structures of the <i>o</i> -QM-dN adducts.	14
Scheme 1.13. Proposed mechanism for the reverse reaction of an <i>o</i> -QM-dN adduct (1.42).	17
Scheme 1.14. Generic oxidative de-aromatization of 2-hydroxymethylphenol (1.49) to 2-hydroxymethylbenzoquinone (1.50).	18
Scheme 1.15. Proposed mechanism for the BTI (1.52) oxidation of phenol (1.51) to 1,4-benzoquinone (1.57).	19
Scheme 2.1. Formation of <i>o</i> -QM (1.28) and subsequent alkylation of dC (1.48) resulting in QM-dC N3 (1.42).	22
Scheme 2.2. Oxidation of QM-dC N3 (1.42) and the expected product 2.1 .	23
Scheme 2.3. Synthesis of 4-MeBrQMP (2.6).	28

Scheme 2.4. Formation of MeQM (2.7) and subsequent alkylation of dC (1.48) resulting in MeQM-dC N3 (2.8). Scheme 2.5. Oxidation of MeQM-dC N3 (2.8) with BTI and the expected product 2.9 . Scheme 2.6. Synthesis of 1-methylcytosine (2.12a) and 1-propylcytosine (2.12b). Scheme 2.7. Formation of MeQM (2.7) and subsequent alkylation of 1-MeC (2.12a) resulting in MeQM-MeC N3 (2.13). Scheme 2.8. Oxidation of MeQM-MeC N3 (2.13) with BTI and the expected product 2.14 . Scheme 2.9. Oxidative trapping of MeQM-dC N3 (2.8) with BTI. Scheme 2.10. Two possible products from the BTI oxidation of MeQM-dC N3 (2.9 and 2.15). Scheme 3.1. Structures of products formed from the alkylation of dG (3.1) by MeQM (2.7). Scheme 3.2. Proposed structure of the product (3.7) formed by oxidation of MeQM-dG N1 (3.2). Scheme 3.3. Proposed structure of the product (3.8) formed by oxidation of MeQM-dG N ² (3.3). Scheme 3.4. Proposed structure of the product (3.11) formed by oxidation of MeQM-dG N7 (3.4) and the subsequent deglycosylated product (3.10). Scheme 4.1. Oxidative de-aromatization can trap labile MeQM-DNA adducts. Scheme 5.1. Reaction scheme for nucleophilic trapping of MeQM (2.7) with βME to form MeQM-βME (5.3). Scheme 5.2. Synthesis of MeQM-H ₂ O (5.2) in one step by reduction of 5-methylsalicylaldehyde (2.3). Scheme 5.3. Synthesis of MeQM-βME (5.3) from 5-methylsalicylaldehyde (2.3). Scheme 5.4. Proposed mechanism for the reduction of dithioacetal 5.9 by 1,4-CHD. Scheme 5.5. Scheme for the trapping of MeQM with βME.	30 31 34 35 36 40 42 51 71 73 75 89 111 113 115 117 124
--	---

Abbreviations

SAM - *S*-adenosylmethionine

BER - base excision repair

bisQMP – bi-functional quinone methide precursor

BTI - bis[(trifluoroacetoxy)iodo]benzene = PIFA - phenyliodosyl bis(trifluoroacetate)

BrQMP – brominated quinone methide precursor

BHT – butylated hydroxytoluene

ctDNA – calf thymus DNA

COSY – correlation spectroscopy

1,4-CHD – 1,4-cyclohexadiene

dA - 2'-deoxyadenosine

dC - 2'-deoxycytidine

M₁dG - 3-(2'-deoxy-β-D-erythro-pentofuranosyl)pyrimido[1,2-α]purin-10(3*H*)-one

dG - 2'-deoxyguanosine

dN – 2'-deoxynucleosides

DNA – 2'-deoxyribonucleic acid

drib – 2'-deoxyribose

dT - 2'-de oxythymidine

FAPy-7MeG - 2,6-diamino-4-hydroxy-5*N*-methylformamidopyrimidine

1,2-DCE – 1,2-dichloroethane

Et₂O – diethyl ether

DMF – N, N-dimethylformamide

DMSO – dimethylsulfoxide

DEPT - Distortionless Enhancement by Polarization Transfer

dsDNA – double stranded DNA

Et 743 - ecteinascidin 743

ESI – electrospray ionization

EtOH – ethanol

EtOAc – ethyl acetate

FDA – Food and Drug Administration

g – gram

HMBC – heteronuclear multiple bond correlation

HSQC – heteronuclear single quantum correlation

HPLC – high performance liquid chromatography

8-HO-PdG - 8-hydroxy-1,N²-propano-2'-deoxyguanosine

LC/MS - liquid chromatography - mass spectrometry

L - liter

pH – -log([H⁺])

MDA - malondialdehyde

MS – mass spectrometry

βME – β-mercaptoproethanol

1-MeC- 1-methylcytosine

5MeC - 5-methylcytosine

7MeG - N7-methylguanine

O⁶MeG - O⁶-methylguanine

MGMT - O⁶-methylguanine-DNA methyltransferase

MMS - methylmethanesulfonate

MeQM – 4-methyl *o*-quinone methide

μ L – microliter

mg – milligram

mL - milliliter

mmol – millimoles

M – molar

MOPS - 3-(N-morpholino)propanesulfonic acid

nmol - nanomoles

NMR – nuclear magnetic resonance

NER – nucleotide excision repair

nts – nucleotides

1D – one dimensional

o – *ortho*

N^2 OPdG - N^2 -oxopropenyl-deoxyguanosine

p – *para*

MMR - post-replication mismatch repair system

1-PrC – 1-propylcytosine

QM – quinone methide

QMP – quinone methide precursor

t_r – retention time

salDNA – salmon sperm DNA

ssDNA – single stranded DNA

NaHCO_3 – sodium bicarbonate

MS/MS – tandem mass spectrometry

TBDMS – *tert*-butyldimethylsilyl

TBDMS-Cl – *tert*-butyldimethylsilylchloride

THF – tetrahydofuran

TLC – thin layer chromatography

TEA – triethylamine

TEAA – triethylammonium acetate

TFA – trifluoroacetic acid

PPh_3 – triphenyl phosphine

Tris-HCl - tris(hydroxymethyl)aminomethane hydrochloride

2D – two dimensional

UHPLC – ultra high performance liquid chromatography

UV-Vis – ultraviolet-visible spectroscopy

H_2O – water

Chapter 1: Introduction

1.1. DNA Alkylation.

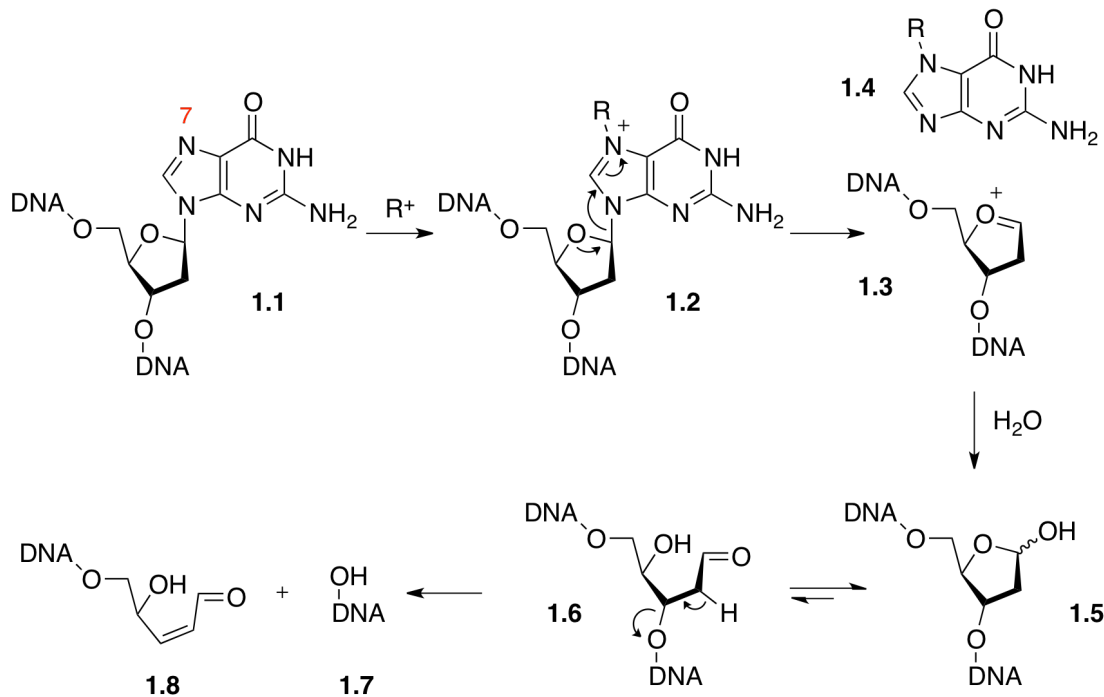
Nucleophilic sites on DNA have the potential to react with a variety of endogenously and exogenously generated electrophiles to form DNA adducts.¹⁻³ Endogenously generated DNA adducts, such as 5-methylcytosine (5MeC), are crucial to normal development in mammals by regulating a number of cellular processes.⁴⁻⁶ However, there appears to be a low level of mutagenic DNA adducts formed nonenzymatically by *S*-adenosylmethionine (SAM), showing that not all endogenous DNA alkylation is beneficial.¹ Exogenously generated DNA adducts, formed from environmental chemicals, mainly result in DNA damage. Exogenous DNA alkylating agents that target rapidly replicating cells have found success as cancer chemotherapeutic drugs by damaging the DNA of cancer cells.⁷⁻⁹ Unfortunately, exogenous DNA alkylating agents that damage genomic DNA may result in mutations if not repaired.

Regardless of how the DNA adduct is formed, each unique adduct invokes a specific cellular response. *O*⁶-Methylguanine (*O*⁶MeG), for example, is a major DNA adduct formed by alkylating agents from both endogenous and exogenous sources.^{3,10,11} The repair protein *O*⁶-methylguanine-DNA methyltransferase (MGMT) directly reverses the methylation by transferring the *O*⁶-methyl group to a cysteine residue on itself. If this repair mechanism is not successful, the adduct may cause a 2'-deoxyguanosine (dG) to a 2'-deoxyadenosine (dA) transition, permanently altering

the DNA sequence.^{12,13} The O^6 MeG:T mismatch can be lethal also due to futile cycling by the post-replication mismatch repair (MMR) system.¹²

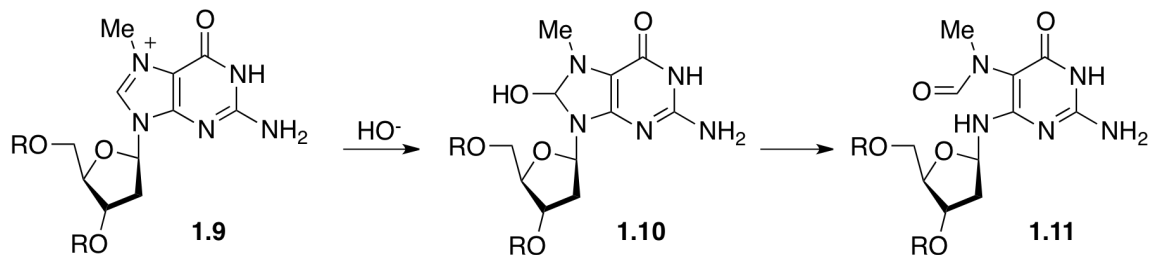
Another common DNA adduct is N7-methylguanine (7MeG). The N7 position of 2'-deoxyguanosine (dG N7) is the most nucleophilic site within the DNA bases, making it highly reactive with electrophiles.¹⁴ For example, 82% of the methylation of duplex DNA by methyl methanesulfonate (MMS) occurs at dG N7.¹⁵ While alkylation of dG N7 may be frequent, the 7MeG adduct appears to be neither mutagenic nor cytotoxic.³ A number of 7MeG degradation products exhibit mutagenicity and cytotoxicity. Alkylation at dG N7 places a positive charge on the N7 nitrogen (**1.2**), destabilizing the *N*-glycosidic bond and leading to spontaneous depurination. The resulting abasic site (**1.3**) may lead to a DNA strand break and is toxic (**Scheme 1.1**).¹⁶

Scheme 1.1. Proposed mechanism for the depurination of N7-alkyl dG residues. R⁺ is an electrophilic alkylating agent. Adapted from Gates et al.¹⁶



Another toxic 7MeG degradation product is 2,6-diamino-4-hydroxy-5*N*-methylformamidopyrimidine (FAPy-7MeG, **1.11**). FAPy-7MeG is formed from 7MeG upon opening of the imidazolium ring by hydrolysis (**Scheme 1.2**). Although only weakly mutagenic, FAPy-7MeG does block DNA chain elongation, therefore affecting DNA synthesis.^{17,18} Furthermore, the glycosidic bond in FAPy-7MeG is chemically stable under physiological conditions, unlike 7MeG.¹⁶ The removal of these adducts requires active repair, such as base excision repair (BER) which can lead to the formation of toxic abasic sites (**1.3**).³

Scheme 1.2. Ring opening in 7-methylguanine (**1.9**) to yield the FAPy-7MeG (**1.11**) adduct. Adapted from Gates et al.¹⁶



1.2. The Importance of Detecting Labile DNA Adducts.

Much of the study on DNA alkylation is focused on the irreversible process rather than the reversible process. Irreversible adducts lend themselves to simple manipulation as the adducts can survive lengthy (>22 hr) assays such as enzymatic digestion and work-up prior to tandem liquid chromatography-mass spectrometry (LC/MS).^{19,20} A much less studied area of DNA alkylation is the formation of reversible, or labile, DNA adducts. As these reversible DNA adducts may have lifetimes shorter than the time required for the assay, their presence may be

diminished or go unnoticed altogether. However, the lifetime of the reversible adduct may be sufficient to elicit a cellular response, provoking DNA damage repair pathways. The reversible DNA adducts can then release from the excised DNA and reassociate with the original DNA. This repeated regeneration of the active alkylating agent effectively extends the lifetime of these DNA alkylating agents *in vivo*. For this scenario, a lower amount of reversible alkylating agent would, therefore, be needed to achieve the same result as a higher amount of irreversible alkylating agent, which would be beneficial for therapeutic uses, but harmful with environmental toxins.

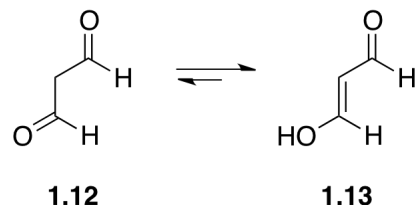
Unfortunately, the reversible nature of these alkylating agents makes their detection and analysis difficult. The ability to detect reversible DNA adducts would allow for an assessment of the genotoxicity of such an alkylating agent. Access to the full profile of adducts formed by an alkylating agent would also be instrumental in a proposed mechanism of its toxicity.^{20,21} This additional information could influence the toxicology rating of chemicals or help to design more selective DNA targeting therapeutics. It is, therefore, imperative that a method, or methods, to detect labile DNA adducts be developed.

1.3. Extensively Studied Labile DNA Alkylating Agents.

A number of known DNA alkylating agents are confirmed to form labile DNA adducts. One of these DNA alkylating agents, malondialdehyde (MDA, **1.12**), is an endogenously formed product of lipid peroxidation that is present also in a variety of

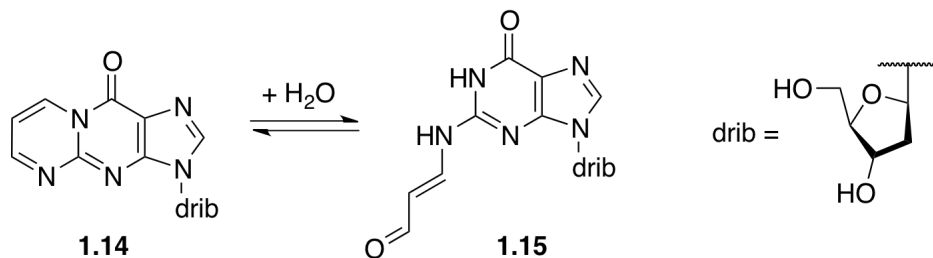
foodstuffs.^{22,23} MDA can act as both a strong electrophile and as a strong nucleophile when it forms its enol tautomer, β -hydroxyacrolein (**1.13**) (**Scheme 1.3**).²²

Scheme 1.3. Malondialdehyde (**1.12**) can tautomerize to β -hydroxyacrolein (**1.13**).



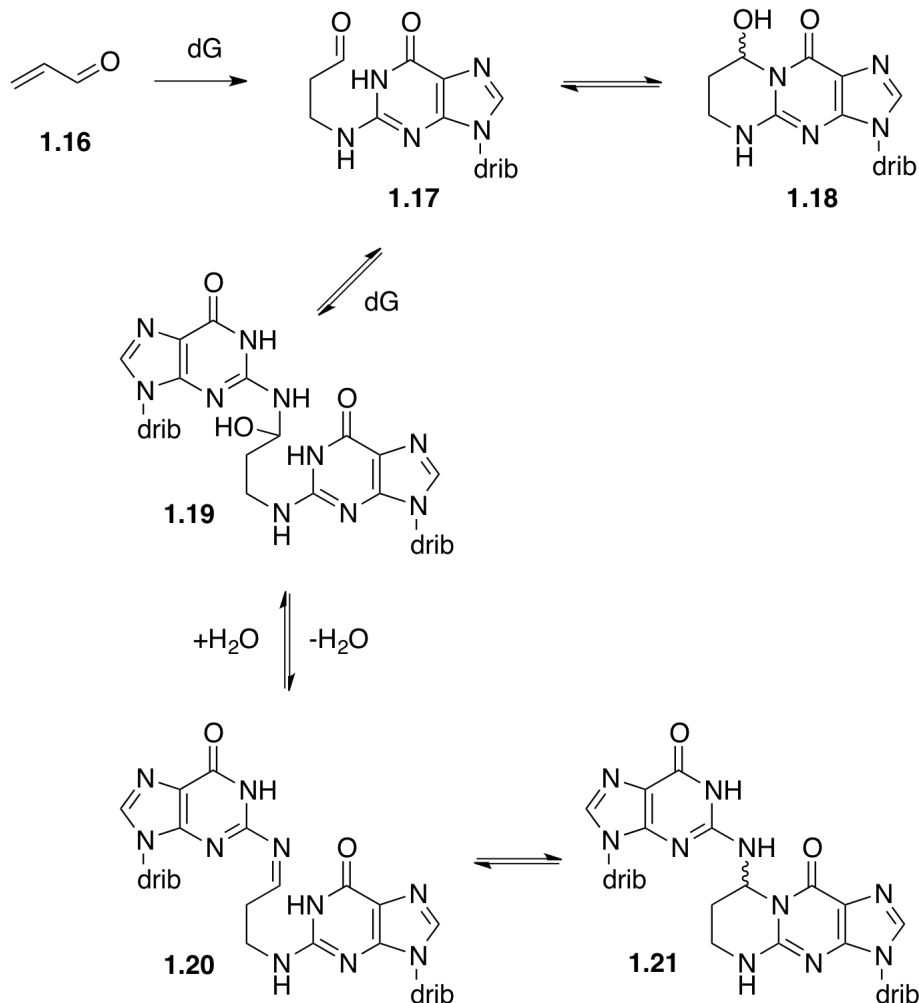
MDA forms mutagenic DNA adducts with dA and 2'-deoxycytidine (dC), but mostly with dG.²² The major adduct formed with dG is 3-(2'-deoxy- β -D-erythro-pentofuranosyl)pyrimido[1,2- α]purin-10(3H)-one (M₁dG, **1.14**) (**Scheme 1.4**).²⁴ At neutral pH, M₁dG has been shown to be reactive towards nucleophiles,²⁵ and basic conditions can cause hydrolytic ring-opening to form N^2 -oxopropenyl-deoxyguanosine (N^2 OPdG, **1.15**), which is reactive also with nucleophiles (**Scheme 1.4**).²⁶ Further studies determined that M₁dG is converted to N^2 OPdG in duplex DNA when positioned complementary to cytosine which suggests a cytosine catalyzed ring-opening.²⁷ Furthermore, the N^2 OPdG does not covalently react with the catalytic cytosine, as confirmed by NMR data. This allows N^2 OPdG to react with another nucleophile, including reforming the original ring (**Scheme 1.4**).²⁷ This result highlights the reversible linkage that allows MDA to exist effectively in two unique electrophilic forms that display different toxicity.

Scheme 1.4. M₁dG (**1.14**) and *N*²OPdG (**1.15**) can interconvert under aqueous conditions.



Acrolein (**1.16**) is another thoroughly studied DNA alkylating agent. Acrolein is also a bis-electrophile that is formed endogenously from oxidation of polyunsaturated fatty acids and is present exogenously in cigarette smoke and automobile exhaust.²⁸ *In vitro* studies reveal a number of adducts form between acrolein and each nucleoside.^{19,28-30} However, many of these adducts are monofunctional and irreversible. Unlike the monofunctional adducts, the major crosslinking adduct, 8-hydroxy-1,*N*²-propano-2'-deoxyguanosine (8-HO-PdG, **1.18**), exhibits lability to form the *N*²-(3-oxopropyl) adduct (**1.17**) (**Scheme 1.5**).^{28,31} This allows 8-HO-PdG to reversibly form interchain crosslinks if the complementary strand contains the sequence 5'-CpG opposite of the adduct (**Scheme 1.5**).³¹ This cross-link occurs at 1 – 2% of the levels of the monofunctional adduct (**1.17**), which approaches the limit of detection using current analytical methods such as LC-MS/MS (~1 adduct per 10^8 DNA bases, when 50 μg of DNA is assayed).²⁸ Even at this low level of formation, these crosslinks may be lethal to bacterial, yeast, and repair-deficient mammalian cells.^{32,33} The reversible nature of the acrolein dG *N*² crosslinks complicates their identification and analysis *in vivo*. Therefore, most studies were carried out *in vitro* with a model DNA such as calf thymus DNA (ctDNA).²⁸

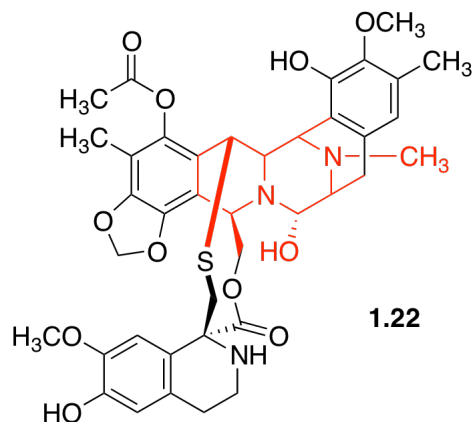
Scheme 1.5. Initial alkylation of dG by acrolein (**1.16**) followed by the reversible interchain cross-link with an opposing dG (**1.19 – 1.21**). Adapted from Kozekov et al.³¹



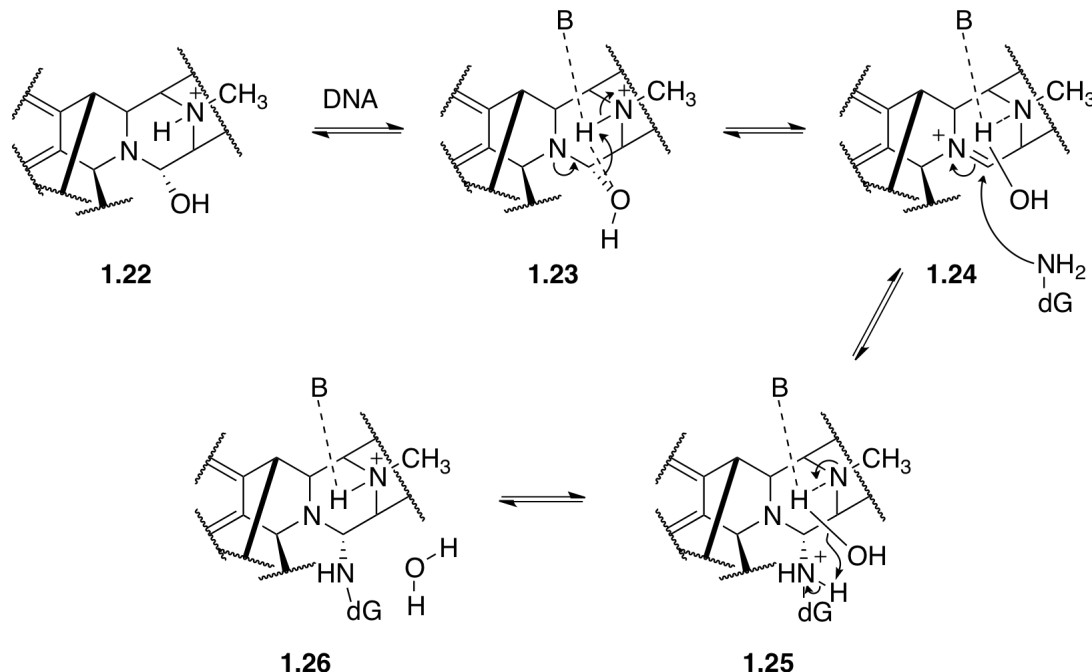
While malondialdehyde and acrolein are endogenous alkylating agents, the natural product ecteinascidin 743 (Et 743, **1.22**) represents an exogenous alkylating agent (**Scheme 1.6**). Et 743 is registered under the trade name Yondelis and is currently undergoing clinical trials for treatment of a variety of tumors.^{34,35} Et 743 selectively binds to the minor groove of duplex DNA and reversibly alkylates the same position on dG as acrolein (**Scheme 1.7**).^{36,37} Et 743 alkylates DNA with varying sequence selectivity due to recognition of three base pair sequences through

hydrogen-bonding patterns.^{36,37} Further studies have determined that the rate of reversal is dependant on the nucleotide on the 3' side of the covalent attachment due to the formation of this hydrogen-bonding network between Et 743 and the 3' nucleotide while the rate of alkylation is independent of the target sequence.³⁷ Once free from the DNA, Et 743 is free to alkylate any target sequence. The result is a gradual accumulation of the thermodynamically favorable adduct leading to the observed preference for a specific target sequence.

Scheme 1.6. Structure of Et 743 (**1.22**) with the DNA alkylating section highlighted in red.



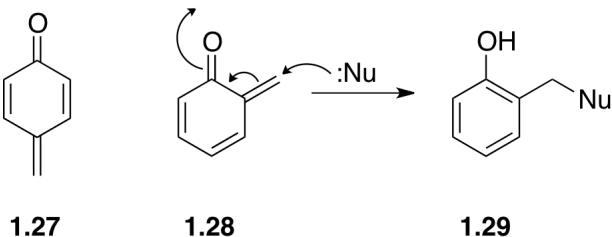
Scheme 1.7. Proposed mechanism of the reversible alkylation of dG by Et 743 (**1.22**). The scheme shows only the portion of Et 743 highlighted in red from **Scheme 1.6**. Adapted from Zewail-Foote et al.³⁷



1.4. DNA Alkylation by Quinone Methides.

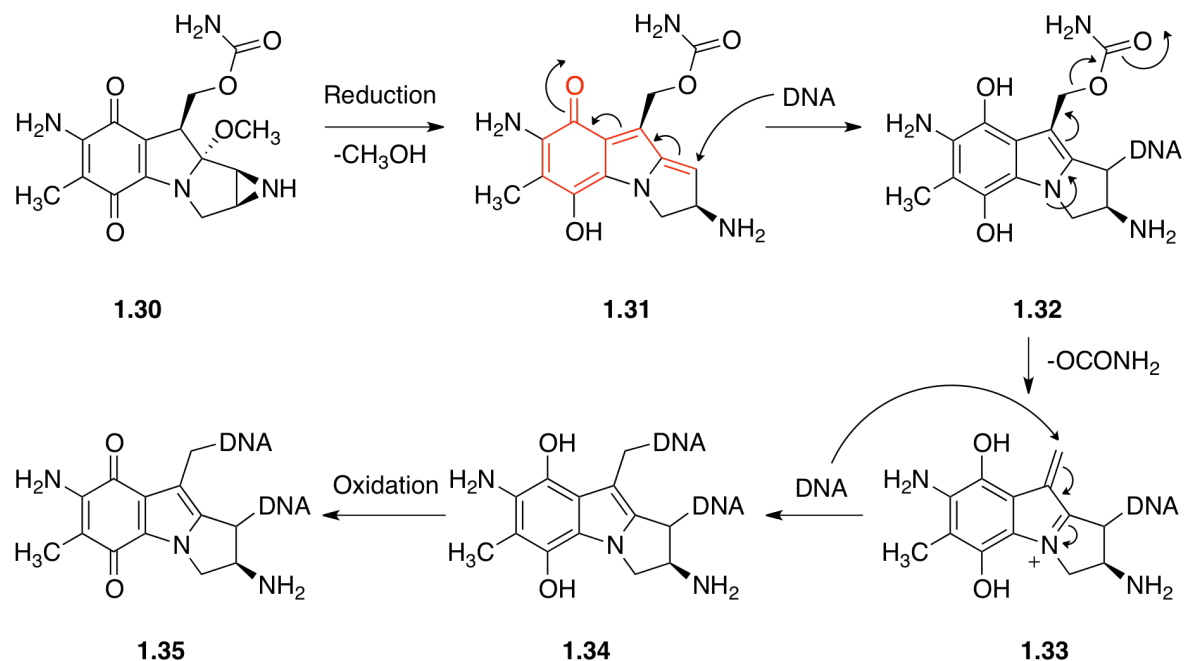
Another family of reversible DNA alkylating agents is the quinone methides (QM). QMs can exist as *para* (*p*-QM, **1.27**) or *ortho* (*o*-QM, **1.28**) isomers. QMs are highly reactive, electrophilic species that serve as Michael acceptors with nucleophilic reaction at the exocyclic methylene group (**Scheme 1.8**). Restoration of aromaticity occurs upon reaction and is the major driving force behind the reactivity of QMs. The reactivity of QMs have been compared to highly stabilized carbocations, due to the similar reactivity of each towards nucleophiles (**Scheme 1.8**).^{38,39}

Scheme 1.8. Structures of *p*-QM (**1.27**) and *o*-QM (**1.28**). The mechanism of nucleophilic addition to *o*-QM and the restoration of aromaticity is shown.



One exogenous source of QMs is the antitumor drug mitomycin C (**Scheme 1.9**).⁴⁰ Mitomycin C is enzymatically reduced *in vivo* to form the vinylogous QM **1.31**. Initial alkylation results in a monoadduct at the dG N² position in DNA (**1.32**). Upon loss of the carbamate, alkylation occurs at a second dG N² position to form the cytotoxic crosslink **1.35** (**Scheme 1.9**).^{40,41}

Scheme 1.9. Proposed mechanism for the alkylation and cross-link formation of DNA by mitomycin C (**1.30**). Adapted from Tomasz⁴⁰ and Noll et al.⁴¹



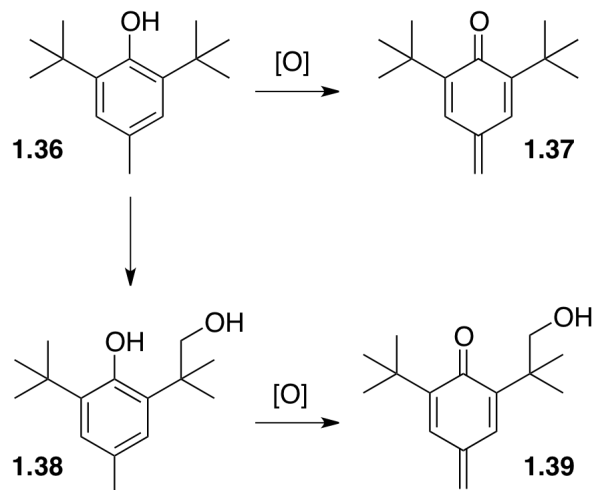
The reductive activation of mitomycin C is key to its antitumor properties.

While normal tissues are oxygen rich and therefore inhibit the activation of

mitomycin C, many solid tumors are oxygen deprived and readily activate mitomycin C. Under these reductive conditions, mitomycin C selectively alkylates dG in the minor groove. Unlike the reversible alkylating agents discussed earlier, mitomycin C is an irreversible alkylating agent. It has proven to be an effective anticancer drug and an excellent example of the alkylating power of QMs.

A second exogenous source of QMs is the food preservative 2,6-di-*tert*-butyl-4-methylphenol (BHT, **1.36**). BHT is oxidized *in vivo* by cytochrome P₄₅₀ to initially form the *p*-QM 2,6-di-*tert*-butyl-4-methylenecyclohexa-2,5-dienone (BHT-QM, **1.37**). Alternatively, hydroxylation of a *tert*-butyl group followed by oxidation affords the *p*-QM 6-*tert*-butyl-2-(2'-hydroxy-1',1'-dimethylethyl)-4-methylenecyclohexa-2,5-dienone (BHTOH-QM, **1.39**) (**Scheme 1.10**).⁴² These two *p*-QMs (**1.37** and **1.39**) can alkylate every DNA base along with a number of other intercellular nucleophiles such as glutathione and amino acids in proteins.^{43,44}

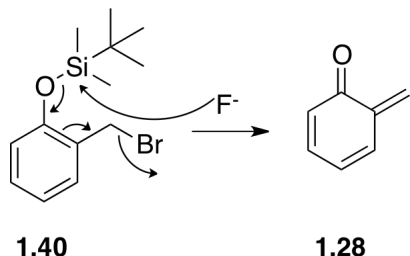
Scheme 1.10. Formation of BHT-QM (**1.37**) and BHTOH-QM (**1.39**) by enzymatic oxidation.



While most of these adducts are irreversible, the dG N7 and dC N3 adducts prove to be labile.⁴³ The dG N7 adduct decomposes through the common depurination mechanism of N7-alkylguanine residues to form the guanine N7 adduct.¹⁶ Interestingly, the dC N3 adduct reforms the active QM along with unmodified dC through a reverse reaction.⁴³ This property would allow BHT-QM to alkylate another nucleophile present in solution and contribute to the *in vivo* toxicity observed in rat and mouse models.^{42,43,45}

The reactivity of most QMs makes them too unstable to store, and QM study requires a stable precursor that can be activated when needed. Mitomycin C and BHT are enzymatically activated *in vivo* to form the transient QM intermediates. For *in vitro* studies on BHT, the QM was formed through chemical oxidation with Ag₂O.⁴³ QMs have been also formed from various precursors through oxidation with NaIO₄,⁴⁶ photochemistry⁴⁷⁻⁵⁰ and heat.^{51,52} Another chemical means of activation that was discovered by the Marino laboratory⁵³ and further developed by the Rokita laboratory⁵⁴ utilizes fluoride to cleave a silyl group protecting the phenolic oxygen, which subsequently expels a leaving group (either bromide or acetate) to form the desired *o*-QM (**Scheme 1.11**). The silyl protected *o*-QM (BrQMP, **1.40**) proved also to be stable upon storage at 0 °C either pure or dissolved in an aprotic solvent and thus can serve as an effective QM precursor (QMP).

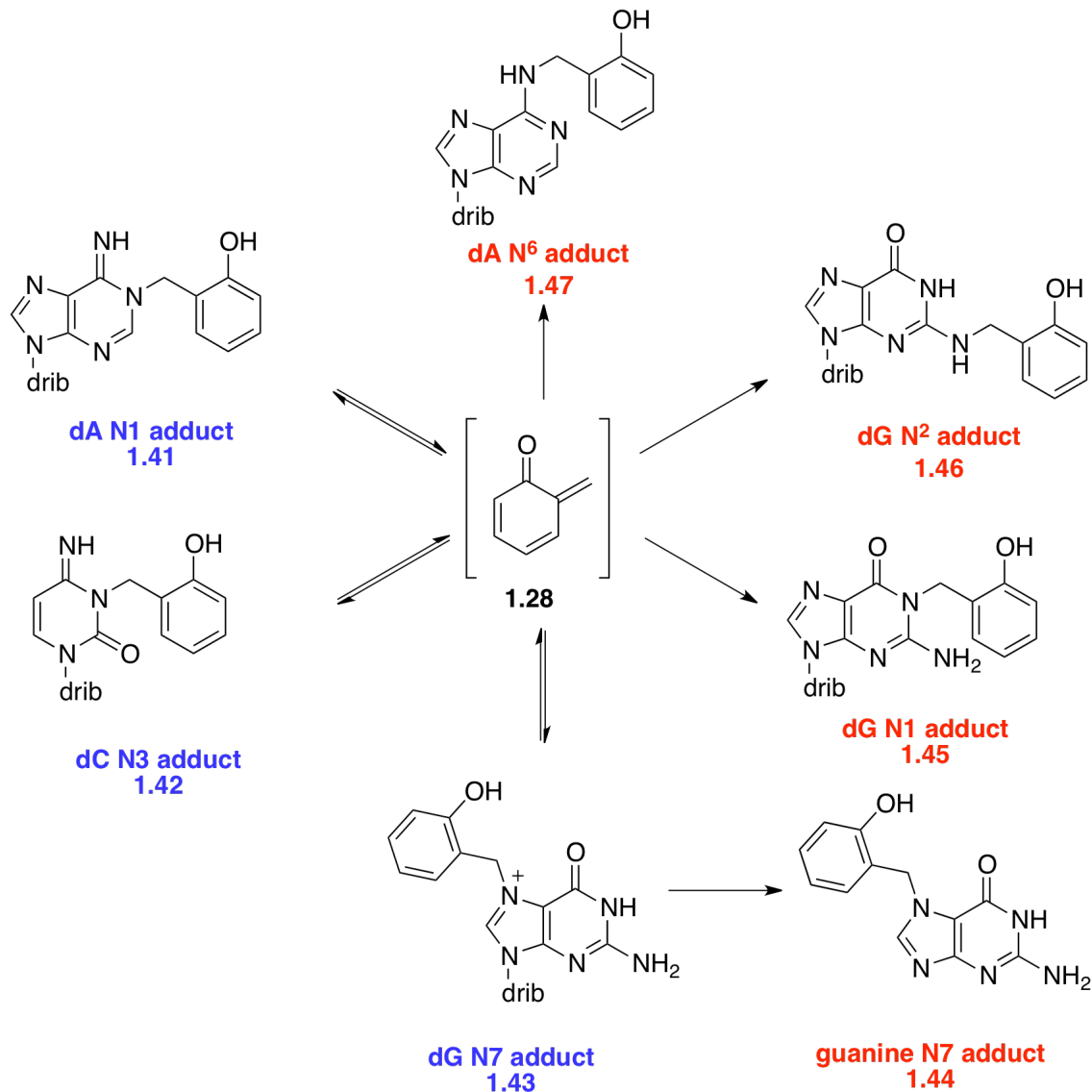
Scheme 1.11. Proposed mechanism for the fluoride activation of BrQMP (**1.40**) to *o*-QM (**1.28**).



Initial studies with the simplest *o*-QM model, **1.28**, determined that adducts were formed with dC,⁵⁵ dG,⁵⁶ and dA,⁵⁷ but not with 2'-deoxythymidine (dT).

Additional studies between **1.28** and deoxynucleosides revealed selectivity towards the stronger nitrogen nucleophiles dC N3, dG N7, and dA N1 (**Scheme 1.12**, labeled in blue).⁵⁸ These adducts form reversibly through a kinetically controlled process.⁵⁹ This reversibility was shown to also lead to a time dependant shift from these kinetically controlled products to the irreversible, thermodynamically controlled, products at dG N1, dG N², and dA N⁶ (**Scheme 1.12**, labeled in red).⁵⁸

Scheme 1.12. Structures of the *o*-QM-dN adducts. Reversible adducts are labeled in blue and irreversible adducts are labeled in red. Adapted from Weinert.⁶⁰



The result of these competing processes is an initial high yield of adducts with the stronger nucleophiles that gradually shifts to a low yield of adducts with the weaker nucleophiles that persist indefinitely. Additionally, ubiquitous water acts as an irreversible trap of *o*-QM.⁵⁸ The repeated capture and release of the *o*-QM by the stronger nucleophiles effectively extends the lifetime of this transient electrophile.⁶¹ The reversibility of these QM-dN adducts potentially allows also for the escape of *o*-

QM from cellular repair processes such as base excision repair (BER) and nucleotide excision repair (NER) leading to increased effectiveness as a therapeutic agent, as seen with the previously discussed Et 743.³⁷

1.5. Requirements for a QM-DNA Trapping System.

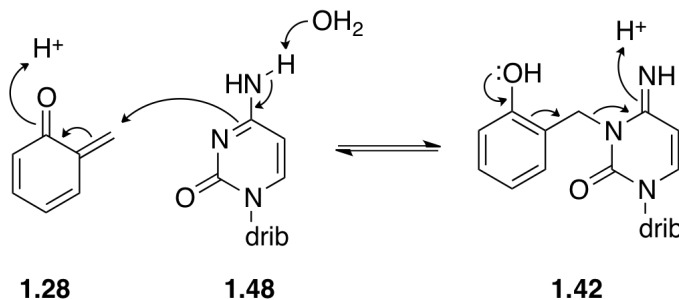
As discussed above, there are a number of positive effects stemming from the reversibility of the kinetic QM-dN adducts, most notably the extension of the effective lifetime of *o*-QM. Unfortunately, the reversibility of these QM-dN adducts is detrimental also to their detection in duplex DNA. Only the thermodynamic QM-dN adducts persist through standard enzymatic digestion and chromatographic analysis of the alkylated DNA.^{43,62,63} The time dependent shift from kinetic to thermodynamic products effectively obscures the alkylation profile of *o*-QM towards DNA at short (<4 hr) times, giving an incomplete and inaccurate alkylation profile. For example, early studies of the model *o*-QM **1.28** revealed selectivity for the weakly nucleophilic positions dA N⁶ and dG N² after a 24 hour reaction with duplex DNA.⁶² Later studies determined that the more nucleophilic position of dA at N1 was initially alkylated, but the labile adduct is no longer present after the lengthy reaction and work-up due to constant regeneration and gradual trapping to form the irreversible dA N⁶ adduct.⁵⁷ Isotope labeling with ¹⁵N further confirmed a dissociative mechanism of reversible alkylation and contradicted the possibility of an intramolecular rearrangement (Dimroth rearrangement) leading to formation of the dA N⁶ adduct.⁵⁷

Development of a method to suppress *o*-QM release from its reversible adducts is necessary for satisfactory analysis of the intrinsic selectivity and efficiency of *o*-QM alkylation of DNA. Classical approaches such as an acid or alkaline quench prior to enzymatic digestion^{57,64-66} fail with the *o*-QM adducts as they would destabilize the labile adducts.⁵⁷ Mass spectrometry (MS) can be an effective way to analyze DNA alkylation, but frequently fails to observe labile adducts, especially at the dG N7 position.⁶⁷ A further complication is that multiple *o*-QM adducts at a particular nucleoside have the same mass. For example, the QM-dA N1 and QM-dA N⁶ adducts appear as two unique compounds by HPLC, but have identical masses by MS. Therefore MS would be unable to provide important information about the position of the covalent linkage.

A chemical trap that converts the reversible *o*-QM-dN adducts to irreversible derivatives would be very useful in their analysis as it would eliminate the previously mentioned issues with labile adducts. Namely, the alkylation profile would not change from the beginning of the alkylation work-up through the ultimate HPLC analysis. There are a number of requirements for a successful trapping method. One requirement is that the trap must be effective under physiological conditions (aqueous, pH 7, 37 °C) to ensure that the target DNA is still properly annealed as B-DNA, the dominant form found in cells. The trap must not interfere with the ultimate chromatographic analysis of the digested DNA and it must also react quickly, quantitatively, and selectively with the *o*-QM phenol to accurately quench the labile QM-DNA adducts at the desired time point. By not reacting with the DNA itself, the ensuing chromatographic analysis would be simplified by decreasing the amount of

oxidation by-products formed. An effective chemical trap should focus on the *o*-QM phenol to prevent donation of the oxygen lone pair back into the nucleoside, therefore preventing regeneration of the active *o*-QM (**Scheme 1.13**).

Scheme 1.13. Proposed mechanism for the reverse reaction of an *o*-QM-dN adduct (**1.42**) (dN = dC, **1.43**, in this example).



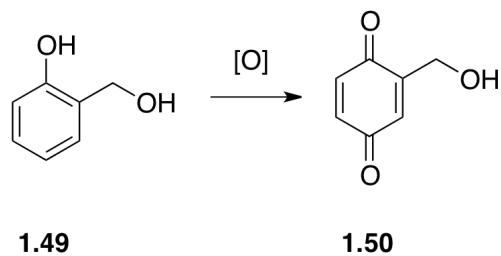
From the requirements outlined above, a number of chemical traps can be considered. Although silylation and acetylation may occur quickly with the *o*-QM phenol, reaction may also occur at the phosphate oxygens leading to multiple side-products and possibly incomplete trapping. Alkylation of the *o*-QM phenol is also possible but suffers from the same shortcomings as silylation and acetylation while also possibly forming side-products with other nitrogen nucleophiles found in DNA further confusing the origin of each adduct. Reduction of the *o*-QM phenol was also not pursued due to the reactive nature of common transition metal reducing agents towards DNA.

1.6. Oxidation of the QM Phenol as an Effective Trap.

Oxidative de-aromatization of the *o*-QM phenol has the potential to satisfy each of the requirements for a chemical trap (**Scheme 1.14**). However, not all

methods of oxidative de-aromatization would be applicable to the *o*-QM-DNA system. Singlet oxygen is frequently used for oxidative de-aromatization in synthetic procedures but would fail in this system due to its oxidation of guanine residues.^{68,69} Potassium nitrosodisulfonate (Fremy's salt) is a reagent that could selectively oxidatively de-aromatize the *o*-QM phenol.^{60,70} Initial studies with a ten-fold excess of Fremy's salt observed the oxidation of 2-hydroxymethylphenol (QM-H₂O, **1.49**) to 2-hydroxymethylbenzoquinone (**1.50**) by HPLC analysis (**Scheme 1.14**).⁶⁰ UV-Vis and high-resolution mass spectrometry confirmed the assignment of the new compound. Unfortunately, oxidation with Fremy's salt proved to be low yielding, even with a twenty-fold excess of oxidant.⁶⁰ The inability to fully convert a substituted phenol to the corresponding benzoquinone would only complicate the analysis of *o*-QM-DNA adducts and studies with Fremy's salt were abandoned.

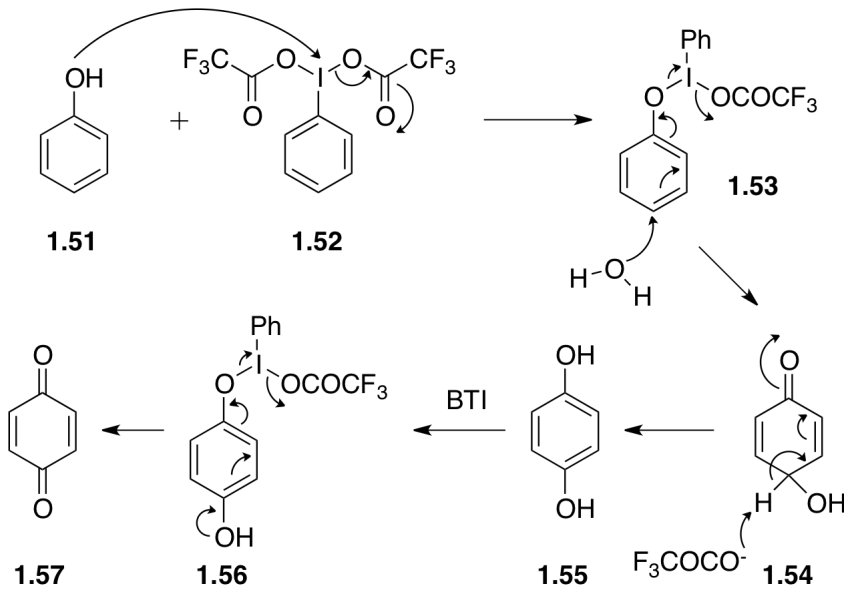
Scheme 1.14. Generic oxidative de-aromatization of 2-hydroxymethylphenol (**1.49**) to 2-hydroxymethylbenzoquinone (**1.50**).



Hypervalent iodine species, in particular bis[(trifluoroacetoxy)iodo]benzene (BTI, **1.52**, also known less commonly in the literature as PIFA which stands for phenyliodosyl bis(trifluoroacetate)⁷¹) selectively and efficiently de-aromatizes phenols under aqueous conditions (**Scheme 1.15**).⁷²⁻⁷⁵ BTI satisfies the requirements for the chemical trap due to its mild reactivity, selectivity for phenol moieties, fast reaction, and compatibility with physiological conditions. The proposed mechanism

begins with a nucleophilic addition of the phenolic oxygen to the BTI iodine, leading to the expulsion of one equivalent of trifluoroacetate (**Scheme 1.15**). Next, nucleophilic addition of water to the activated phenol occurs expelling iodobenzene and another equivalent of trifluoroacetate and forming the intermediate ketone **1.54**. A base then removes the acidic proton (*para* to the newly formed ketone) allowing rearomatization to occur. A second equivalent of BTI can then repeat the reaction leading to the formation of 1,4-benzoquinone (**1.57**).^{72,73}

Scheme 1.15. Proposed mechanism for BTI (**1.52**) oxidation of phenol (**1.51**) to 1,4-benzoquinone (**1.57**). Adapted from Tamura et al.⁷² and Barret et al.⁷³



The proof of concept experiment that involved the oxidation of 2-hydroxymethylphenol (**1.49**) to 2-hydroxymethylbenzoquinone (**1.50**) by Fremy's salt was repeated (**Scheme 1.14**). The oxidation was successful using a four-fold excess of BTI.⁶⁰ The product was formed in near quantitative yield, as determined by HPLC, after a 10 minute incubation at room temperature in aqueous CH_3CN .

Selective oxidative de-aromatization of the *o*-QM phenol by BTI appears to be a viable method for trapping the labile *o*-QM-DNA adducts. This will allow, for the first time, the intrinsic selectivity of *o*-QM alkylation of DNA to be determined. The goal of this dissertation is to synthesize and characterize the oxidation products of each individual *o*-QM-dN adduct and then use these products as analytical standards to determine the *o*-QM alkylation profile of DNA at short time points. Using the information obtained from these studies regarding the type, location, and amount of *o*-QM adducts that are formed with DNA, a relationship between the biological response to *o*-QM and toxicity of *o*-QM can be determined.

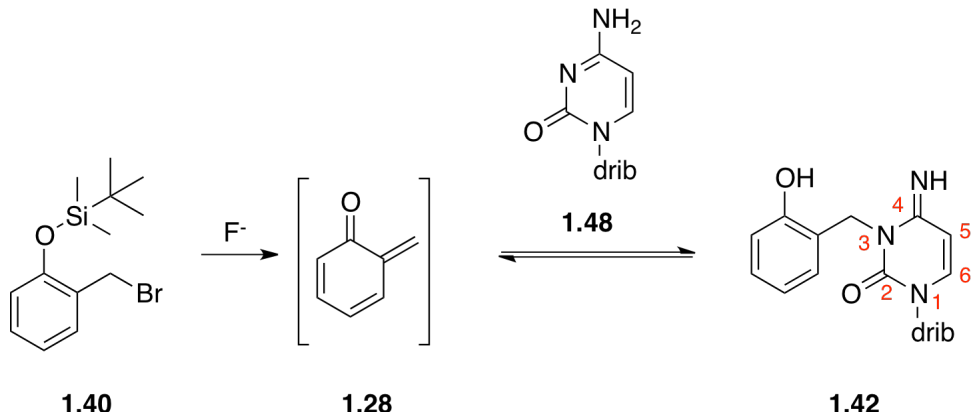
Chapter 2: Formation and Oxidation of QM-dC and MeQM-dC Adducts

2.1. Introduction.

Oxidative de-aromatization of the phenolic products formed between an *ortho*-quinone methide (*o*-QM) and DNA has the potential to quench the reversible alkylation and allow the QM-DNA adducts to survive enzymatic digestion and subsequent HPLC analysis. As discussed in Chapter 1, oxidative de-aromatization with bis[(trifluoroacetoxy)iodo]benzene (BTI) meets the criteria outlined for successful trapping of the adducts (**Scheme 1.15**). Specifically, BTI reacts quickly, quantitatively, and selectively with the QM phenol under physiological conditions.

2'-Deoxycytidine (dC) was chosen to test whether oxidation of an *o*-QM-deoxynucleoside (*o*-QM-dN) adduct forms a stable and identifiable compound with the ability to remain stable during DNA digestion conditions. Alkylation of dC by QM was previously shown to form a single adduct, QM-dC N3 (**1.42**).⁵⁵ Since dG⁵⁶ and dA⁵⁷ form multiple adducts with QM and dT does not react with QM,⁵⁸ dC would result in the least convoluted product profile and would be the simplest dN to test with oxidative trapping (**Scheme 2.1**).

Scheme 2.1. Formation of *o*-QM (**1.28**) and subsequent alkylation of dC (**1.48**) resulting in QM-dC N3 (**1.42**).

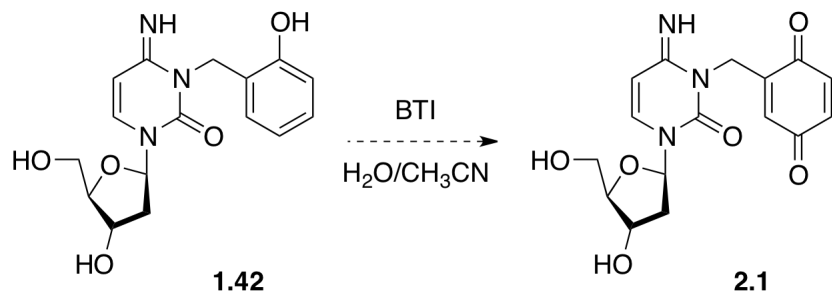


The previously studied QM (**1.28**) was chosen as the first model *o*-QM since it is the simplest *o*-QM and its dC adduct shows only modest reversibility under aqueous conditions.⁵⁸ The dC adduct is also one of the highest yielding *o*-QM-dN adducts formed by the reaction with QM **1.28**.

Initial studies were successful in isolating, but not characterizing, the product of oxidation of QM-dC N3.⁶⁰ Synthesis of QM-dC N3 in a solution of 70:30 DMF:H₂O at pH 7 was successful.⁵⁵ QM-dC N3 was then oxidized *in situ* by a four-fold excess of BTI in CH₃CN. HPLC purification resulted in the isolation of a major product. NMR spectra (¹H and ¹³C) of the product were inconsistent with the expected compound **2.1** (**Scheme 2.2**). While it was determined by ¹H and ¹³C NMR that the dC ribose and pyrimidine fragments were intact, the presumed benzoquinone protons were shifted downfield (8 - 9.5 ppm) without the anticipated ¹H-¹H coupling. The benzylic carbon and protons were also absent from the ¹H and ¹³C spectra. The most significant evidence for formation of a compound other than **2.1** was the observation of only 14 of the expected 16 carbons in the ¹³C spectra. While numerous 1D and 2D NMR experiments were run, the lack of a consistent mass

spectrum hindered the complete structural characterization of the unknown product. The goal of this chapter was to reproduce the synthesis of the unknown QM-dC N3 oxidation product and elucidate the structure. A second goal was the synthesis of a novel quinone methide precursor that would have the same alkylation selectivity as **1.40** but would be oxidized by BTI to produce an expected product. Most of the following research has been published as McCrane et al.⁷⁶

Scheme 2.2. Oxidation of QM-dC N3 (**1.42**) and the expected product **2.1**.



2.2. Results and Discussion.

2.2.1. Oxidation of QM-dC N3.

The first step in preparing enough of the oxidized QM-dC N3 adduct for structure elucidation involved repeating the previously used method.⁶⁰ The QM precursor, *o*-(*tert*-butyldimethylsilyl)-2-(bromomethyl)phenol (BrQMP, **1.40**), used with this method was synthesized according to a literature procedure, and the QM-dC N3 adduct was then generated *in situ* following literature procedure.^{55,58} After the 20 minute alkylation, the QM-dC N3 adduct was oxidized *in situ* by a four-fold excess of BTI in CH₃CN. After work-up to remove iodobenzene and other oxidation by-

products the reaction was fractionated by reverse phase HPLC. The major product matched the retention time and λ_{max} (219 nm, 271 nm, 335 nm) of the previously unidentified compound. The compound was collected and lyophilized to dryness to yield a white solid that rapidly turned brown. The isolated compound remained stable (90%) over 6 days in aqueous acetonitrile. Initial characterization by ^1H and ^{13}C NMR matched the previously unidentified compound, proving that the formation of this oxidized product of QM-dC N3 is reproducible.

Multiple HPLC runs were needed to obtain the mg quantities of oxidized QM-dC N3 adduct necessary for further analysis by NMR. Signals (^1H and ^{13}C) based on literature values⁷⁷ for both the pyrimidine and ribose groups were observed, and their assignments were confirmed by ^1H - ^{13}C HSQC and ^1H - ^{13}C HMBC analysis (Appendix A.5 – A.8). The unsaturated nature of the *o*-QM remnant was apparent from the remaining ^{13}C signals that all ranged between 116.6 ppm and 187.6 ppm (Figure 2.1). The large 2-bond coupling ($^2J_{\text{CH}} = 43$ Hz) observed for the cross peak between C11 (124.4 ppm) and H12 (9.44 ppm) in the ^1H - ^{13}C HMBC spectrum is unique to aldehydes (Figure 2.1).⁷⁸

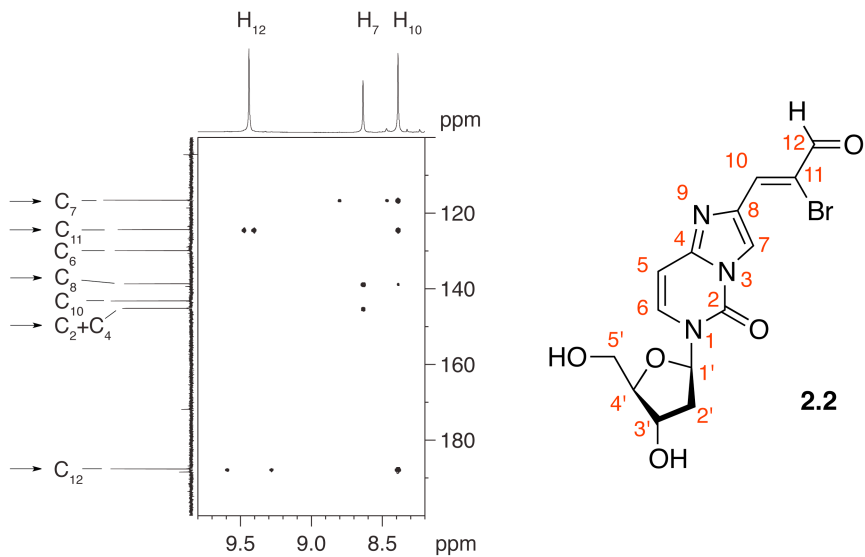


Figure 2.1. ^1H - ^{13}C HMBC of **2.2** in $\text{DMSO}-d_6$ at 600 MHz.

Connectivities between C7 through C12 were established by a combination of ^1H - ^{13}C HSQC, ^1H - ^{13}C HMBC, and ^1H - ^{15}N HMBC analysis (**Appendix A.7 – A.9**). Specifically, it was determined that C7, C10, and C12 were bonded to hydrogen from the ^1H - ^{13}C HSQC. The quaternary carbons C8 and C11 were placed in between the carbons C7, C10, and C12 based on ^1H - ^{13}C HMBC correlations and to account for the lack of ^1H - ^1H coupling. The attachment of C10 to C8 and not C7 was accomplished with data from ^1H - ^{13}C HSQC and ^1H - ^{15}N HMBC experiments, which show that N9 has a correlation to H10 and N3 does not. The remaining order of carbon atoms was determined with ^1H - ^{13}C HSQC and ^1H - ^{13}C HMBC experiments. The only unaccounted linkage was the atom attached to C11. A proton or carbon was ruled out due to each atom in the ^1H and ^{13}C spectra having been assigned. It was unlikely that the unknown functional group was -OH (from H_2O), -NH₂ (from dC), or -I (from BTI) due to the chemical shift of C11 (124.4 ppm). Computational estimates (ChemDraw Ultra 7.0) for the chemical shift of C11 attached to these functional

groups would be 163 ppm, 157 ppm, and 96 ppm respectively. A bromine (from BrQMP) attached to C11 corresponds well to the experimentally determined chemical shift of C11 (computational = 126 ppm vs. experimental = 124.4 ppm).

Initial analysis of the product by electrospray ionization mass spectrometry (ESI⁺-MS) at the University of Maryland Department of Chemistry and Biochemistry Mass Spectrometry Facility was unable to produce a consistent mass. Through collaboration with the FDA, mass spectrometry on the product was finally accomplished with the help of their much more sensitive equipment. This added sensitivity allowed for the NMR sample (in DMSO-*d*₆) to be diluted by 1000-fold in a solution of 25% CH₃CN and 75% H₂O with 0.1% acetic acid prior to infusion. The resolution of the FDA equipment was also improved as the parent mass signal had a mass accuracy of 13 ppm compared to >20 ppm at the department facility. Loss of the two carbons was confirmed by ESI⁺-MS, and the parent ion (*m/z* 384 .0141 (M+H)⁺) revealed the presence of one bromine by its distinct isotope ratio (**Appendix A.10**). MS/MS experiments generated the characteristic deglycosylation (*m/z* 267.9716 (M – drb + H)⁺) and debromination (*m/z* 304.9544 (M – Br)⁺) products to support the structural assignment based on extensive NMR data (**Appendix A.11 – A.12**).

The entire conjugated system of the QM-dC N3 oxidized adduct is illustrated in a favorable thermodynamic configuration for simplicity and has not been confirmed experimentally (**Figure 2.1**). While over-oxidation is proposed to be a driving force in the formation of the unexpected product, a mechanism by which this product forms and incorporates the bromine released from the QM precursor **1.40** is

still under consideration. Therefore, its use for quantifying QM alkylation adds an unneeded complication. Without knowing the mechanism for the oxidation of the QM phenol, it would be impossible to know which variables in the QM alkylation of DNA would affect the product formation. For example, if the bromine in the product comes from a reincorporation of the bromine from the precursor then product formation is most likely concentration dependant on the precursor and may not be successful at the lower concentrations used with DNA.

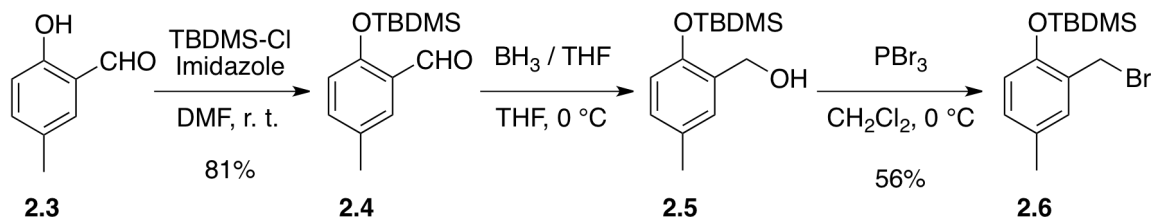
2.2.2. Synthesis of a Novel *o*-Quinone Methide Precursor to Block Over-Oxidation.

The possible over-oxidation and rearrangement that plagued the QM precursor **1.40** was addressed through the application of a novel QM precursor that generated products containing an alkyl group *para* to the phenolic oxygen.⁷²⁻⁷⁴ An alkyl group at the *para* position should block deprotonation that leads to re-aromatization of the QM phenol (**Scheme 1.15**). The oxidation would terminate at a *para*-quinol instead of allowing a second equivalent of BTI to associate with the re-aromatized QM phenol and eventually lead to the formation of a 1,4-benzoquinone.

The simplest alkyl containing precursor 2-bromomethyl-4-methyl-*O*-(*tert*-butyldimethylsilyl)phenol (**2.6**) was prepared from 5-methylsalicylaldehyde in three steps (**Scheme 2.3**). 5-Methylsalicylaldehyde (**2.3**) was protected with *tert*butyldimethylsilyl (TBDMS) to form 2-(*tert*-butyldimethylsilyl)oxy-5-methylbenzaldehyde (**2.4**). The aldehyde was subsequently reduced to a primary alcohol with borane-THF to form 2-hydroxymethyl-4-methyl-*O*-(*tert*-

butyldimethylsilyl)phenol (**2.5**). Finally, the primary alcohol was used directly and substituted with bromine using PBr_3 to form the desired QM precursor 2-bromomethyl-4-methyl-*O*-(*tert*-butyldimethylsilyl)phenol (4-MeBrQMP, **2.6**).⁷⁹ Bromination with PBr_3 was superior to the previous method of $\text{CBr}_4/\text{PPh}_3$ bromination by providing a simpler work-up and purification by forming fewer by-products such as bromoform. Furthermore, the new method resulted in a ten-fold faster reaction (1.5 hr vs. 19 hr).

Scheme 2.3. Synthesis of 4-MeBrQMP (**2.6**).

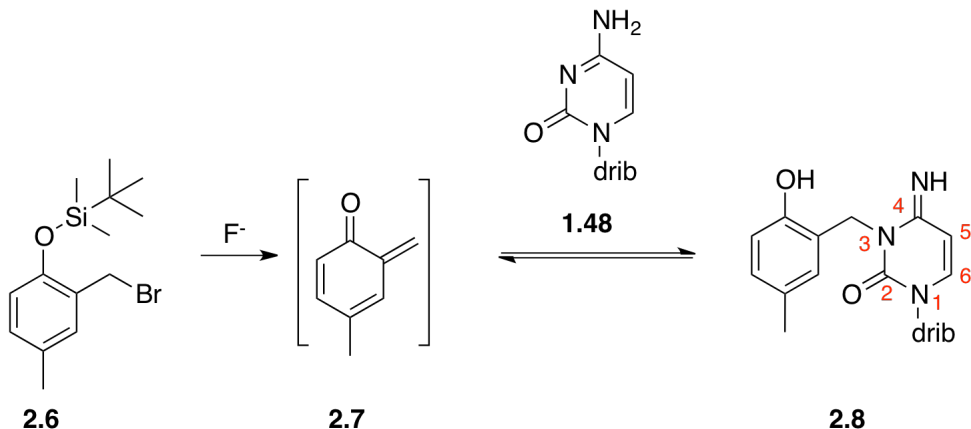


Deprotection of **2.6** with fluoride results in the formation of 4-methyl-6-methylene-cyclohexa-2,4-dienone (MeQM, **2.7**). The presence of the methyl substituent was not expected to alter the alkylation preference of the QM. A related set of substituents had not significantly altered the alkylation profile of QMs towards dNs.^{60,80} The electron-donating properties of the methyl group stabilize the electron deficient MeQM intermediate resulting in faster generation and increased lability of the resulting adducts formed by MeQM vs. those of QM.^{60,80} By blocking re-aromatization during the oxidation of phenol by BTI, the methyl-substituted model was expected to block the over-oxidation observed with the unsubstituted QM (**1.49** to **1.50**, **Scheme 1.15**).⁷²⁻⁷⁴ However, the new MeQM posed a greater challenge for the oxidative trapping due to the increased reversibility of its dC adduct.

2.2.3. Alkylation of dC with MeQM.

Prior to the start of the oxidation studies, the alkylation profile of the novel precursor (**2.6**) was determined to confirm that it is the same as the unsubstituted QM (**1.28**) and can therefore be used as a model *o*-QM. Alkylation of dC by MeQM results in the formation of a single adduct, MeQM-dC N3 (**2.8**). The MeQM-dC N3 adduct was prepared *in situ* by deprotection of 4-MeBrQMP (**2.6**) with aqueous KF in the presence of dC, under similar conditions as previously discussed for the formation of QM-dC (**1.42**) (Scheme 2.4). The major product was purified by reverse phase HPLC and its structure confirmed to be **2.8** by ¹H NMR, ¹³C NMR, and UV-Vis data (Appendix A.13 – A.14). MeQM attachment at dC N3 was also confirmed by comparison with literature values of **1.42**.⁵⁵ Evidence that MeQM alkylates dC at the N3 position comes from the similar chemical shifts of the benzylic protons, that vary by less than 0.1 ppm, (4.96 ppm for **1.42**,⁵⁵ 4.89 ppm for **2.8**). Similarly the λ_{\max} values vary by only 1 nm (278 nm for **1.42**,⁵⁵ 279 nm for **2.8**). The absorbance data is also consistent with N3-ethyl dC ($\lambda_{\max} = 280$ nm) and not N⁴-ethyl dC ($\lambda_{\max} = 270$ nm).⁸¹

Scheme 2.4. Formation of MeQM (**2.7**) and subsequent alkylation of dC (**1.48**) resulting in MeQM-dC N3 (**2.8**).

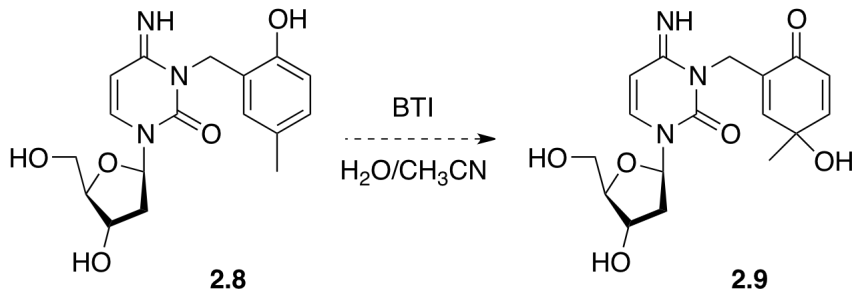


2.2.4. Initial Attempts at MeQM-dC N3 Oxidation.

Preliminary attempts to isolate and characterize the MeQM-dC N3 oxidized adduct were unsuccessful. The initial oxidation of MeQM-dC N3 used the same reaction conditions as the formation of QM-dC N3 oxidized adduct (**2.2**) (**Scheme 2.5**). However, HPLC analysis failed to reveal a major product, but mostly unresolved, low intensity peaks. The next attempt utilized a longer oxidation (1 hr vs. 20 min) to confirm that the failed HPLC analysis wasn't the result of incomplete oxidation. An alternative work-up replaced the NaHCO_3 addition with an equal volume of H_2O to limit the number of reactive species present. The HPLC method was also changed from using H_2O to 10 mM triethylammonium acetate (TEAA) buffer at pH 4 as the aqueous phase. An acidic aqueous phase has been shown to be effective in the fractionation of other substituted QM-dN adducts.⁸⁰ These conditions resulted in the detection of a new product by HPLC ($t_r = 46$ min) with a unique UV-Vis absorbance ($\lambda_{\text{max}} = 238$ nm, 289 nm, 348 nm) (**Appendix A.2**). Upon lyophilization to a white solid, analysis by $\text{ESI}^+ \text{-MS}$ failed to detect the expected

mass (m/z 364.15 ($M + H$)⁺) or any relevant fragment. These results suggest that the isolated compound decomposes or transforms to a different compound after HPLC purification.

Scheme 2.5. Oxidation of MeQM-dC N3 (**2.8**) with BTI and the expected product **2.9**.



The eluting buffer was altered in both the pH and concentration of the TEAA buffer to determine if it contributed to the decomposition of the isolated compound. The pH of the collected solution was also adjusted to values between 5.9 and 9.1 prior to lyophilization. Decomposition was observed by HPLC and ¹H NMR in the form of multiple compounds being eluted and a very congested NMR spectra (**Table 2.1**). While decomposition became less significant as the pH was adjusted from acidic towards neutral, it was never halted. Analysis by ¹H and ¹³C NMR revealed the consistent presence of TEAA, which may contribute to the decomposition of the isolated compound as both are concentrated as the solvent is removed during lyophilization.

Table 2.1. The effect of pH on the stability of the major product of MeQM-dC N3 oxidation during purification.

Step When pH is Altered	How pH is Altered	Post-Alteration pH	Method to Remove Solvent	Result ¹
During HPLC Purification	10 mM TEAA, pH 4	4.0	None (reinjected into HPLC after 1.5 hr)	No Decomposition
During HPLC Purification	10 mM TEAA, pH 4	4.0	lyophilization	Decomposition
Prior to HPLC Purification	100 mM TEAA, pH 4	4.0	lyophilization	Decomposition
After HPLC Purification	HPLC grade TEA	5.9 - 9.1	lyophilization	Decomposition ²
During HPLC Purification	5 mM TEAA, pH 5	5.6	lyophilization	Decomposition
During and After HPLC Purification	5 mM TEAA, pH 5 then HPLC Grade TEA	6.2	lyophilization	Decomposition
After HPLC Purification	HPLC grade TEA	6.0	Multiple rounds of lyophilization	Decomposition ²

¹Decomposition checked by HPLC. ²Decomposition also analyzed by ¹H and ¹³C NMR.

A small (360 mg silica) reverse phase column potentially allows for the HPLC solvent to be exchanged for a less reactive, TEAA-free solvent. The column used was a Waters Sep-Pak® Plus C18 cartridge. The Sep-Pak could be used to exchange the TEAA buffer for a less reactive, non-nucleophilic solvent by loading the isolated compound onto the column and eluting with the solvent of choice. Four different procedures were attempted (**Table 2.2**). MeQM (**2.7**) was reacted with dC and then subsequently oxidized with BTI to form the desired compound. The crude reaction was then purified by reverse phase HPLC allowing for collection of the desired compound in 20 mL of a solution of 85% 10 mM TEAA (pH 4) and 15% CH₃CN. A 65:35 mixture of 1 mM phosphate buffer (pH 7) to CH₃CN as the eluting solvent of

the Sep-Pak showed the least decomposition when analyzed by HPLC. To acquire enough compound for NMR analysis, this procedure was repeated four times and the isolated solid was combined in DMSO-*d*₆. Unfortunately, greater decomposition (in the form of a complex spectra) was observed by ¹H NMR than the preliminary results suggested (**Appendix A.4**). The Sep-Pak studies were thus abandoned for a new approach to successfully isolate the MeQM-dC N3 oxidation product.

Table 2.2. Parameters for the Sep-Pak assisted solvent exchange of the major product of MeQM-dC N3 oxidation.

Sample pre-treatment	Column pre-treatment	Column Wash	Eluting Solvent	Eluting Solvent Removal	Result ¹
Lyophilization (1 hr)	nanopure H ₂ O (5 mL)	Nanopure H ₂ O (3 × 1 mL)	CH ₃ CN (2 × 5 mL)	Streaming N ₂ (5.5 hr)	Decomp.
Dilution with 10 mL H ₂ O	nanopure H ₂ O (5 mL)	Nanopure H ₂ O (3 × 1 mL)	CH ₃ CN (2 × 5 mL)	Streaming N ₂ (5.5 hr)	Decomp.
Dilution with 5 mL H ₂ O	0.1 % TEA in H ₂ O (3 mL)	0.1 % TEA in H ₂ O (3 × 2 mL)	CH ₃ CN (3 mL)	Streaming N ₂ (overnight)	Decomp.
Dilution with 5 mL H ₂ O	nanopure H ₂ O (5 mL)	Nanopure H ₂ O (3 × 2 mL)	65:35, 1 mM phosphate buffer pH 7: CH ₃ CN (2 × 5 mL)	Lyophilization (16 hr)	Less Decomp. ²

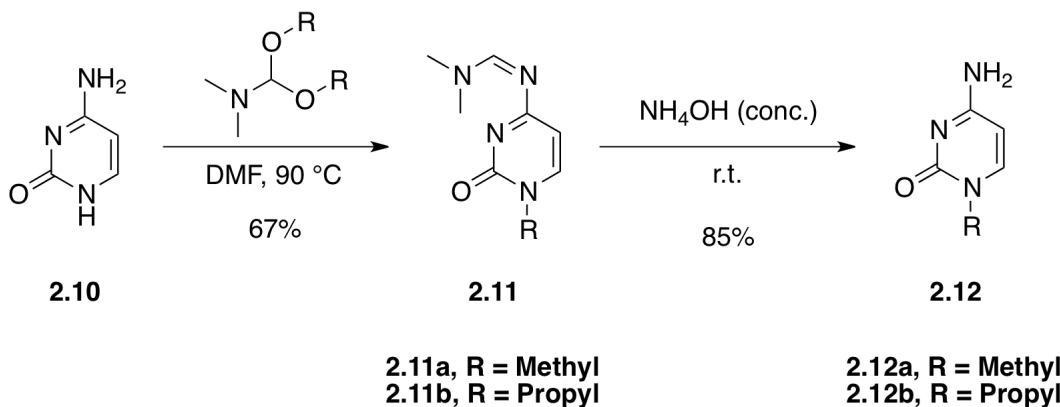
¹Decomposition checked by HPLC. ²Decomposition also analyzed by ¹H NMR.

Less decomposition refers to fewer non-product peaks observed by HPLC.

As it became obvious that the major product of MeQM-dC N3 oxidation was too unstable to be isolated, a new direction was needed to characterize the MeQM alkylation and subsequent oxidative trapping of the cytosine base. A simple approach would be to remove the ribose ring of deoxycytidine and replace it with a methyl group to form 1-methylcytosine (1-MeC, **2.12a**) (**Scheme 2.6**). This substitution would simplify the aliphatic region of the ¹H NMR spectra and should increase the solubility of the subsequent MeQM adduct in organic solvents. The increase in solubility would eliminate the need for aqueous purification of the oxidation reaction,

and possibly make purification and isolation of the MeQM-dC N3 oxidized adduct simpler by avoiding reverse phase HPLC.

Scheme 2.6. Synthesis of 1-methylcytosine (**2.12a**) and 1-propylcytosine (**2.12b**). Adapted from Hosmane et al.⁸² and Helfer et al.⁸³ Yields are for 1-methylcytosine.

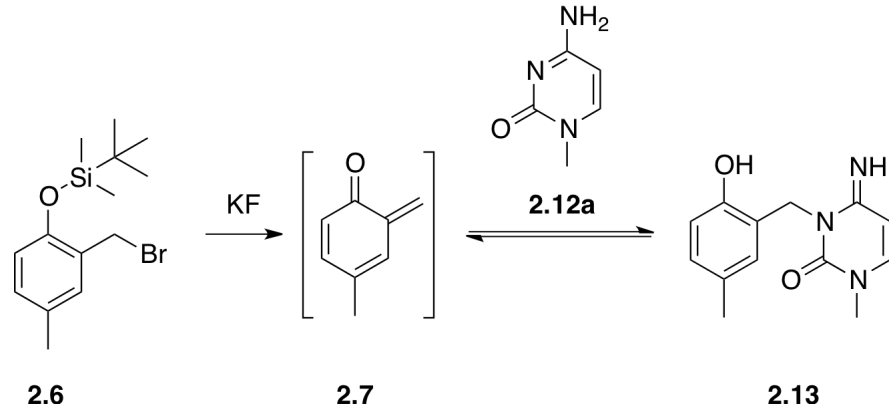


The synthesis of 1-MeC and 1-propylcytosine (1-PrC) were undertaken simultaneously, following literature procedures (**Scheme 2.6**).^{82,83} The synthesis of 1-PrC was attempted to further increase the solubility of the MeQM adduct in organic solvents. As the synthesis of 1-MeC was completed first, it became the focus of the dC substitution studies.

Once the synthesis of 1-MeC was completed, alkylation with MeQM was confirmed (**Scheme 2.7**). Phosphate buffer (pH 7), 4-MeBrQMP, 1-MeC, and KF were combined, at the same ratios as for the formation of MeQM-dC N3, and held at 37 °C for 30 minutes. The reaction mixture was filtered (0.2 µm) and fractionated using reverse phase HPLC with a semi-prep column (5 mL/min). The major product (*t*_r = 35 min) exhibited a λ_{\max} at 223 nm and 279 nm, equivalent to the MeQM-dC N3 adduct. This is consistent with formation of the MeQM-MeC N3 adduct as the chromophore is the same in both adducts. The formation of MeQM-MeC N3 was

further confirmed by ESI⁺-MS (observed m/z 246.10 ($M + H$)⁺ vs. calculated m/z 246.12 ($M + H$)⁺). The only other significant product formed was identified (by t_r and UV-Vis) as the MeQM-H₂O adduct.

Scheme 2.7. Formation of MeQM (**2.7**) and subsequent alkylation of 1-MeC (**2.12a**) resulting in MeQM-MeC N3 (**2.13**).

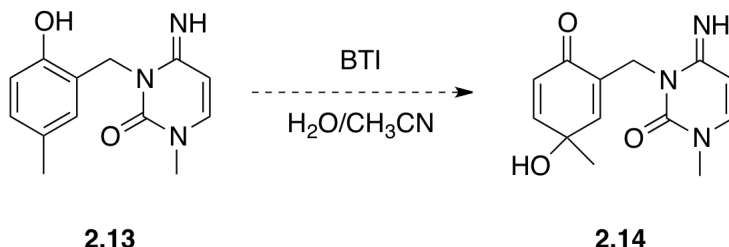


Prior to attempting the oxidative trapping, the ability to extract MeQM-MeC N3 from the eluting solvent (85% 10 mM TEAA pH 4, 15% CH₃CN) into an organic solvent was studied. In small-scale (1 mL) experiments monitored with UV-Vis, extraction with Et₂O was completely unsuccessful, while CH₂Cl₂ proved successful. MeQM-MeC N3 was again formed and purified by HPLC. The collected sample was extracted with CH₂Cl₂ (3 × 20 mL), dried over MgSO₄, and the solvent removed under reduced pressure. The resulting material was dissolved in 200 μL CH₃CN: H₂O (1:1) prior to analysis by HPLC. MeQM-MeC N3 was observed as the major peak (by t_r and UV-Vis) and proved to be stable enough to undergo the extraction procedure, adding to the confidence that the oxidized adduct will also survive the extraction procedure.

After the successful alkylation of 1-MeC by MeQM, the next step was to trap the MeQM-MeC N3 adduct by oxidation with BTI (**Scheme 2.8**). Preliminary

experiments used the same procedure as that used for MeQM-dC N3 oxidized adduct. The starting adduct (MeQM-MeC N3) was fully consumed, but no major product was observed by HPLC, or any product matching the UV-Vis absorbance signature as the previously discussed unstable oxidation product of MeQM-dC N3.

Scheme 2.8. Oxidation of MeQM-MeC N3 (**2.13**) with BTI and the expected product **2.14**.



To test if the oxidized adduct was formed, but not observed due to inherent stability issues or compatibility issues with the HPLC eluting buffer or the silica itself, the above oxidation was repeated and analyzed by ESI⁺-MS prior to the work-up. The mass corresponding to the proposed MeQM-MeC N3 oxidized adduct (**2.14**) was detected (m/z 262.09 ($M + H^+$)) in the crude reaction along with 1-MeC (m/z 126.04 ($M + H^+$)). The remainder of the crude reaction was analyzed by HPLC, but no major product was observed with a UV-Vis absorbance at 348 nm corresponding to both the MeQM-MeC N3 oxidized adduct and the previously discussed MeQM-dC N3 oxidized adduct.

The MeQM-MeC N3 adduct was purified by HPLC and extracted with CH₂Cl₂ in an effort to separate the alkylation and oxidation reactions. This successfully removed the excess 1-MeC and KF, along with the by-products TBDMS-F and Br⁻, and eliminated these species as potential reactants within the oxidation reaction. The MeQM-H₂O was still detected based on its t_r and UV-Vis

absorbance. The presence of MeQM-H₂O was due to the release of MeQM from the MeQM-MeC N3 adduct and not from the initial formation of MeQM-H₂O. Once the CH₂Cl₂ was removed, MeQM-MeC N3 was redissolved with a mixture of solvents ideal for BTI oxidation (300 µL CH₃CN, 100 µL H₂O). An equal volume of BTI (200 mM in CH₃CN) was added to the solution and kept at room temperature for 1 hour. The solution was filtered (0.2 µm) prior to HPLC analysis. Once again, the starting material was completely consumed, but there was no compound matching the UV-Vis absorbance signature ($\lambda_{\text{max}} = 238 \text{ nm}, 289 \text{ nm}, 348 \text{ nm}$) of the previously discussed MeQM-dC N3 oxidized adduct. Substituting phosphate buffer (pH 7) for the water in the oxidation did not change the HPLC profile of the reaction.

While these results were discouraging, the procedures still relied on HPLC as the final purification step of the oxidized adduct. If the MeQM-MeC N3 oxidized adduct did decompose on reverse phase silica, HPLC would need to be avoided as any purification after the introduction of BTI to the reaction. Extraction of the MeQM-MeC N3 oxidized adduct with CH₂Cl₂ would leverage the increased solubility of the 1-MeC in organic solvents. The MeQM-MeC N3 oxidized adduct was formed as described above, but after a 1 hr oxidation using the same conditions the reaction was washed with saturated diethyl ether. This wash should remove oxidation by-products such as iodobenzene while hopefully leaving the MeQM-MeC N3 oxidized adduct in the aqueous phase, as MeQM-MeC N3 was previously shown to prefer aqueous conditions to diethyl ether. The aqueous layer was extracted with CH₂Cl₂ (3 × 1 mL), dried over MgSO₄, and the solvent removed under reduced pressure. The expected mass (*m/z* 262.09 (M + H⁺)) was detected by ESI⁺-MS but ¹H

NMR revealed a complex spectra that was either the result of a mixture of compounds or product decomposition. Incidentally, a new mass (m/z 244.15 ($M + H^+$)) was observed here, but not in the crude reaction. At the time it was not identified, but later was proposed to be a spiro product analogous to the eventual MeQM-dC N3 oxidized adduct (2.15). While the MeQM-MeC N3 oxidized adduct seemed unstable to the HPLC conditions, it would not be pure enough to be characterized by NMR without a final purification procedure. Additionally, the lengthy oxidation (1 hr) may also have aided in driving the reaction from a stable MeQM adduct towards an unstable oxidized MeQM adduct.

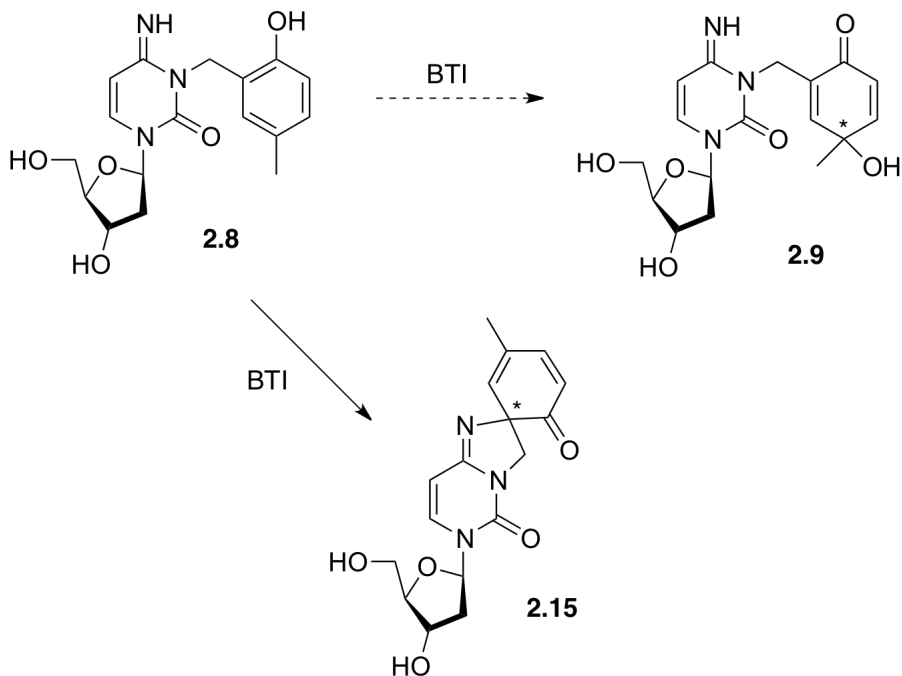
2.2.5. Oxidation of MeQM-dC N3.

With the 1-MeC studies at an apparent standstill, focus shifted back to the dC studies. As described above, purification conditions of the MeQM-dC N3 oxidation were thought to be possibly to blame for the failure to isolate the major product. Therefore, with the focus shifted back to oxidation of MeQM-dC N3, the HPLC elution buffer was changed to find a new buffer that the MeQM-dC N3 oxidized adduct was stable in. Triethylamine based buffers were avoided due to their persistence during lyophilization and the possibility that triethylamine acetate may be involved in the decomposition of the MeQM-dC N3 oxidized adduct. Ammonium formate, at pH 6.9, is a common volatile buffer for fractionating nucleoside adducts and is less nucleophilic than triethylamine acetate. It was chosen as the first elution buffer to be tested, at 10 mM to match the previous concentration of TEAA. Concurrently, the oxidation reaction time was optimized in a model oxidation of

phenol in the presence of dC. The model oxidation consisted of dC (25 mM), phenol (25 mM), and lastly BTI (100 mM) combined in a solution of 5:3 CH₃CN:H₂O. Upon addition of BTI, the clear solution instantly turned purple-brown and gradually changed to yellow-brown over 5 minutes. After a 30 minute incubation at room temperature, the reaction was analyzed, without work-up, by HPLC using CH₃CN as the organic phase and 10 mM ammonium formate pH 6.9 as the aqueous phase with a semi-prep column (5 mL/min). The dC was unaffected by the oxidation while the phenol was completely consumed and the BTI oxidation by-product iodobenzene was present. The oxidation of phenol in the presence of dC was repeated with the reaction time decreased from 30 minutes to 1 minute. Even with an oxidation of 1 minute, the phenol was completely consumed.

The new reaction and purification conditions, consisting of ammonium formate (10 mM, pH 6.9) as the eluting buffer and a reduced BTI oxidation time of 20 minutes from 1 hour, were successfully applied to the isolation of the MeQM-dC N3 oxidized adduct. Fractionation by reverse phase HPLC revealed the previously observed unstable compound at $t_r = 38$ minutes ($\lambda_{max} = 239, 284, 348$ nm) along with an increased yield for the compound (**2.15**) at $t_r = 27$ minutes ($\lambda_{max} = 235, 283, 340$ nm). Preliminary analysis with ¹H NMR revealed that the compound eluting at 27 minutes is stable upon isolation and is likely the elusive oxidized MeQM-dC N3 adduct (**Scheme 2.9**). Furthermore, the isolated compound is stable (>85%, 24 hrs) in an aqueous solution (9 mM ammonium formate pH 6.8, 12% CH₃CN) at physiological pH as detected by HPLC.

Scheme 2.9. Oxidative trapping of MeQM-dC N3 (**2.8**) with BTI. Oxidation product **2.15** was isolated and characterized while **2.9** was not observed.



Preliminary characterization by ^1H NMR confirmed that over-oxidation, as seen in **2.2**, was effectively blocked by the *para* methyl group. Initial evidence consisted of coupling between adjacent vinyl protons of **2.15** and no observable ^1H signals downfield of 8 ppm (Figure 2.2). ESI $^+$ -MS further confirmed that oxidation of MeQM-dC N3 did not result in the loss of two carbon atoms or the incorporation of a bromine atom. ESI $^+$ -MS also gave the first indication, from a $(\text{M} + \text{H})^+$ of m/z 346.18, that the oxidized product **2.15** (calculated m/z 346.14 $(\text{M} + \text{H})^+$) had formed instead of the anticipated product **2.9** (calculated m/z 364.15 $(\text{M} + \text{H})^+$) (Scheme 2.9).

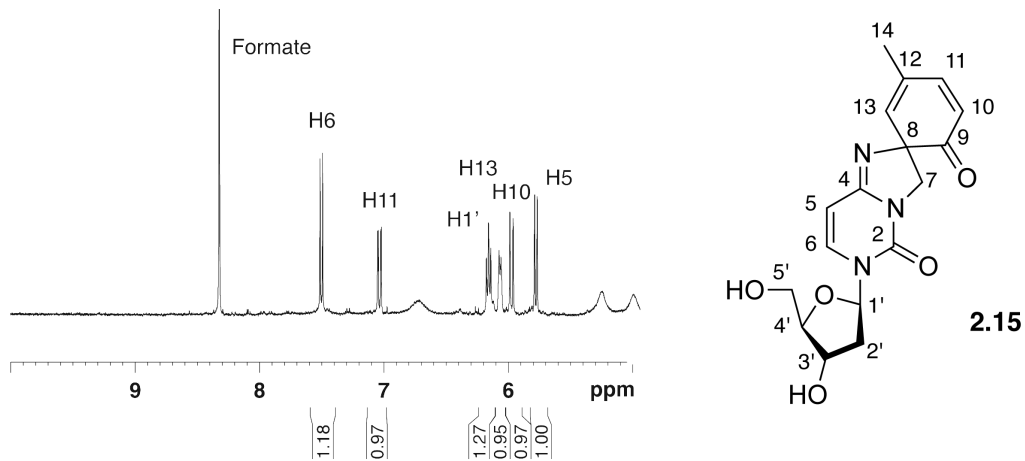
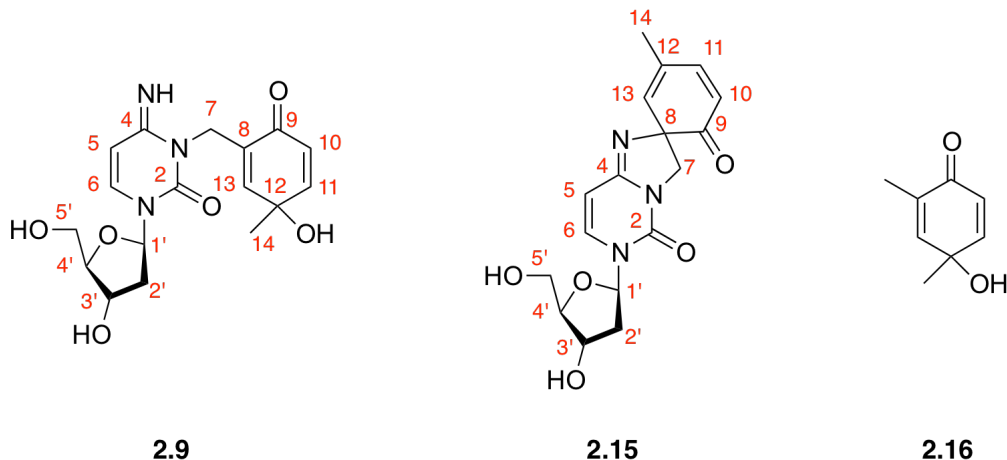


Figure 2.2. ^1H NMR of **2.15** in $\text{DMSO}-d_6$ at 400 MHz. All signals observed downfield of 5 ppm are shown.

Signals (^1H and ^{13}C) for both the pyrimidine and ribose groups were once again observed based on literature values,⁷⁷ and their assignments were confirmed by ^1H - ^{13}C HSQC and ^1H - ^{13}C HMBC analysis (**Appendix A.18 and A.19**). Data from these 2D spectra were also used to establish the connectivities of the oxidized MeQM-dC N3 adduct (**2.15**). A key atom in the structure elucidation of the oxidized MeQM-dC N3 adduct is carbon 8 (C8). C8 was identified by its correlations to the protons attached to C7. The ^{13}C chemical shift of C8 (73.1 ppm) was most consistent with the sp^3 hybridization of the proposed spiro carbon of compound **2.15** (**Scheme 2.9**). The observed chemical shift is quite different from that predicted for the corresponding sp^2 carbon (C8) in **2.9** (ca. 133 ppm).⁶⁸ The comparison was with the compound 4-hydroxy-2,4-dimethyl-2,5-cyclohexadien-1-one (**2.16**). This compound was chosen as a *para*-quinol model compound, as this was the expected transformation upon oxidation by BTI (**Scheme 2.10**).⁶⁸

Scheme 2.10. Two possible products from the BTI oxidation of MeQM-dC N3 (**2.9** and **2.15**). A model compound used for comparison with the *para*-quinol moiety is also shown (**2.16**).⁶⁸



Another key correlation was observed between the *para*-methyl protons (H14) and the adjacent vinyl proton (H13) by ^1H - ^1H COSY NMR (Appendix A.17), as expected for **2.15** due to the conjugation between these protons. This correlation would not be present for **2.9** or observed in **2.16** due to the lack of this conjugation.⁶⁸ The final key correlations center on C7 and the two attached protons (H7A and H7B). Restricted rotation of C7 is apparent from the diastereotopic relationship of the attached protons and their proximity to the carbonyl oxygen of C9 that alternatively extends in front or behind C8 (Figure 2.3). A pair of doublets in the ^1H NMR is created from this configuration. The spectrum is further complicated by the diastereomeric mixture of **2.15** (**2.15a** and **2.15b**) formed by the oxidation of MeQM-dC N3 by BTI (Figure 2.3).

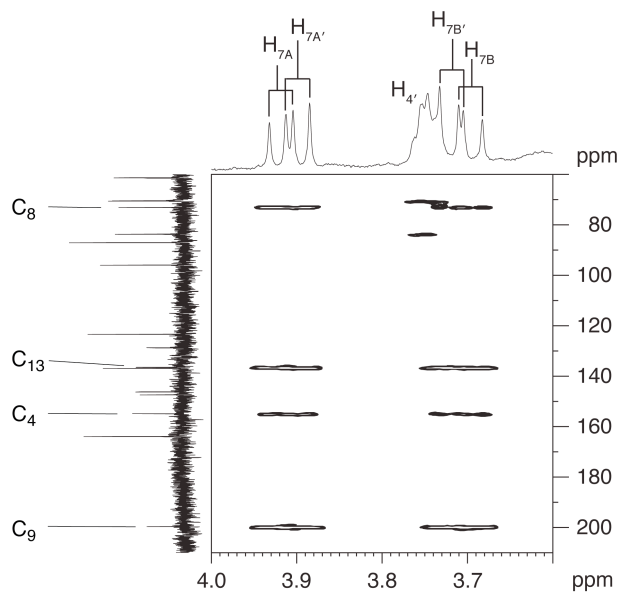
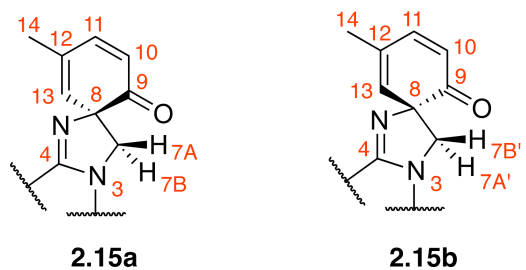


Figure 2.3. ^1H - ^{13}C HMBC of **2.15** in $\text{DMSO}-d_6$ at 400 MHz.

The oxidized MeQM-dC N3 adduct **2.15** is proposed to be formed through an intramolecular attack of the *exo*-imine to a position *ortho* to the phenolic oxygen in competition with an intermolecular attack of water to a position *para* to the phenolic oxygen. While many literature examples show only intermolecular attack of water,⁷²⁻^{74,84} examples show when a nitrogen or oxygen nucleophile is present at an ideal position which would form a 5 or 6 member ring it will outcompete water due, in part, to the proximity effect.^{71,85-87}

2.3. Summary.

Oxidative de-aromatization by BTI of the labile adduct formed between MeQM and dC results in the formation of a stable and identifiable compound. The oxidative trapping by BTI meets the criteria outlined for application to MeQM-DNA adducts. Specifically, BTI reacts quickly, quantitatively, and selectively with the QM phenol under physiological conditions. The oxidative trap based on BTI will, for the first time, allow for the determination of the intrinsic selectivity and efficiency of *o*-QM alkylation of DNA.

Initial studies with QM-dC N3 highlight the necessity of an alkyl substituent *para* to the phenolic oxygen to block over-oxidation and subsequent rearrangement and reincorporation of bromine to the final product. The novel precursor 4-MeBrQMP (**2.6**) will therefore be applied to oxidative trapping studies with dG and dA. The oxidized products of MeQM-dG and MeQM-dA will be characterized in a similar manner as the MeQM-dC N3 oxidized adduct. This will allow for their use as analytical standards in the HPLC analysis of MeQM alkylation of DNA.

2.4. Materials and Methods.

Starting materials, reagents, and solvents were obtained commercially and used without further purification. [Bis(trifluoroacetoxy)iodo]benzene (BTI) was purchased from Acros and CH₃CN (HPLC grade) was purchased from Fisher Scientific. Water was purified to a resistivity of 18.2 MΩ-cm. The silyl-protected quinone methide precursor **1.40** was prepared as described previously.^{55,58} NMR

experiments were performed on Bruker 400, 500, and 600 MHz spectrometers using deuterated solvents. The residual non-deuterated solvent peaks were used as internal standards. Chemical shifts (δ) and coupling constants (J) are reported in parts per million (ppm) and Hertz (Hz), respectively. HPLC analysis employed a reverse-phase, Alltech C18 Econosphere semi-preparative column (10 mm \times 250 mm) for isolation of the nucleoside products and Varian C18 Microsorb column (4.6 mm \times 250 mm) for analytical studies. Mass spectrometry analysis was performed at UMD on a JEOL AccuToF-CS ESI-MS in ESI $^+$ ionization mode. Mass spectrometry analysis was also performed at FDA on a Waters Corporation Q-TOF Premier (Quadrupole-TOF-MS) in ESI $^+$ ionization mode and a Thermo-Electron Corporation “Exactive” FT-ICR-MS in ESI $^+$ ionization mode.

Formation and oxidation of the dC N3 adduct (1.42) generated by the *ortho* quinone methide (1.28). Alkylation was initiated by addition of aqueous KF (32 μ L, 3.13 M) to a mixture of dC in DMF (70 μ L, 143 mM), the QM precursor **1.40** in DMF (70 μ L, 143 mM), and potassium phosphate (28 μ L, 50 mM, pH 7). The reaction was stirred at 37 °C for 20 minutes to form the dC N3 adduct (**1.42**) *in situ* before subsequent oxidation by addition of an equal volume of BTI in CH₃CN (0.10 M, 4 equivalents compared to **1.40**). The resulting mixture was stirred at room temperature for 20 min and then raised from pH 5 to pH 7 by addition of saturated NaHCO₃ and washed with diethyl ether to remove iodobenzene. The aqueous phase was filtered through a 0.2 μ m syringe filter and fractionated by preparative reverse-phase C18 chromatography (3%-10% aqueous CH₃CN over 10 min and 10%-25%

aqueous CH₃CN over a subsequent 30 minutes, 5 mL/min). The oxidized dC adduct **2.2** was collected ($t_r = 30$ minutes) and lyophilized to yield a brown solid. A reliable yield could not be measured due to the small amounts of product isolated from each HPLC separation. ¹H NMR (600 MHz, DMSO-*d*₆): δ 2.23 (m, 2H), 3.62 (m, 2H), 3.87 (m, 1H), 4.30 (m, 1H), 5.15 (br, 1H), 5.34 (br, 1H), 6.39 (t, *J*=6.6 Hz, 1H), 6.78 (d, *J*=8.0 Hz, 1H), 7.85 (d, *J*=8.0 Hz, 1H), 8.39 (s, 1H), 8.63 (s, 1H), 9.44 (s, 1H). ¹³C NMR (600 MHz, DMSO-*d*₆): δ 40.2, 61.1, 70.2, 85.6, 87.9, 98.1, 116.6, 124.4, 129.9, 138.7, 143.2, 145.4, 145.2, 187.6. ¹⁵N NMR (600 MHz, DMSO-*d*₆): δ 149.1, 193.9, 253.9. ESI⁺-MS: *m/z* 384.0141 (M + H⁺). Calcd for C₁₄H₁₅BrN₃O₅ (M + H⁺): 384.0195. $\lambda_{\text{max}} = 219, 271, 335$ nm (diode array detector, 20% aq. CH₃CN).

2-(*tert*-Butyldimethylsilyl)oxy-5-methylbenzaldehyde (2.4). 5-

Methylsalicylaldehyde (1.93 g, 14.2 mmol) was dissolved in 50 mL anhydrous DMF. *tert*-Butyldimethylsilyl chloride (TBDMS-Cl, 6.63 g, 44.0 mmol) and imidazole (6.63 g, 97.4 mmol) were added sequentially to the reaction solution while stirring under N₂ at room temperature. Stirring was continued at room temperature for 26 hours and then the reaction was quenched by addition of water (150 mL). The mixture was extracted with CH₂Cl₂ (4 × 150 mL). The organic fractions were combined, washed with brine (6 × 100 mL), dried over MgSO₄ and evaporated under reduced pressure to a yellow oil. Purification of the desired material by silica gel column chromatography (hexanes/diethyl ether, 80:20) yielded a very pale yellow oil (2.88 g, 81 % yield). ¹H NMR (500 MHz, *d*₄-methanol) δ 10.36 (s, 1H), 7.53 (d, *J*=2.0 Hz, 1H), 7.34 (dd, *J*=8.3, 2.0 Hz, 1H), 6.87 (d, *J*=8.3 Hz, 1H), 2.28 (s, 3H), 1.02 (s, 9H),

0.26 (s, 6H). ^{13}C NMR (500 MHz, d_4 -methanol) δ 191.3, 158.3, 138.1, 132.5, 129.2, 128.2, 121.7, 26.4, 20.6, 19.4, -4.1. ESI $^+$ -MS: m/z 251.19 ($\text{M} + \text{H}$) $^+$. Calcd for $\text{C}_{14}\text{H}_{23}\text{O}_2\text{Si}$ ($\text{M} + \text{H}$) $^+$: 251.15.

2-Hydroxymethyl-4-methyl-*O*-(*tert*-butyldimethylsilyl)phenol (2.5). Borane/THF (1 M, 15 mmol) was slowly added over 5 min to a solution of 2-(*tert*-butyldimethylsilyl)oxy-5-methylbenzaldehyde (2.47 g, 9.86 mmol) in 50 mL anhydrous THF while stirring under N_2 at 0 °C. The reaction was stirred for an additional 2.5 hr at 0 °C under N_2 and then quenched slowly by addition of 150 mL water. The resulting mixture was extracted with CH_2Cl_2 (4 \times 150 mL). The organic fractions were combined, washed with water (4 \times 100 mL), brine (6 \times 100 mL), dried over MgSO_4 and evaporated under reduced pressure to a very pale yellow oil. The crude product was used directly without purification for the next synthetic procedure.

2-Bromomethyl-4-methyl-*O*-(*tert*-butyldimethylsilyl)phenol (2.6).⁷⁹ A solution of PBr_3 (0.99 mL, 10 mmol) in anhydrous CH_2Cl_2 (20 ml) was added dropwise under N_2 at 0 °C to the crude product generated above (2.50 g, \leq 9.90 mmol) in 10 mL anhydrous CH_2Cl_2 . The reaction was stirred for 1.5 hr at 0 °C under N_2 and then concentrated under reduced pressure to an orange oil. The oil was dissolved with 60 mL ethyl acetate and washed with 50 mL H_2O . The aqueous fraction was extracted with an additional 60 mL ethyl acetate, and all the organic fractions were combined, washed with H_2O (2 \times 50 mL), dried with MgSO_4 and evaporated under reduced pressure to a pale yellow oil. The yellow oil was purified by silica gel radial

chromatography (chromatotron) using hexanes/ethyl acetate (19:1) to yield a clear oil (1.74 g, 56 % yield). ^1H NMR (400 MHz, d_3 -acetonitrile) δ 7.16 (d, $J=2.1$ Hz, 1H), 7.02 (dd, $J=8.2, 2.1$ Hz, 1H), 6.78 (d, $J=8.2$ Hz, 1H), 4.54 (s, 2H), 2.24 (s, 3H), 1.05 (s, 9H), 0.27 (s, 6H). ^{13}C NMR (500 MHz, d_3 -acetonitrile) δ 152.6, 132.6, 131.7, 131.6, 129.2, 119.6, 30.8, 26.3, 20.6, 19.0, -3.9. ESI $^+$ -MS: m/z 235.17 ($\text{M} - \text{Br}$) $^+$. Calcd for $\text{C}_{14}\text{H}_{23}\text{OSi} (\text{M} - \text{Br})^+$: 235.15.

Formation of the dC N3 adduct (2.8) generated by the precursor 2.6 and its MeQM intermediate (2.7). Alkylation was initiated by addition of aqueous KF (20 μL , 2.50 M) to a mixture the MeQM precursor **2.6** in CH_3CN (25 μL , 200 mM), dC in DMF (45 μL , 112 mM), and potassium phosphate (10 μL , 50.0 mM, pH 7). The reaction was stirred at 37 °C for 20 min and then cooled, filtered and fractionated by preparative reverse-phase HPLC using a 3 - 25% gradient of CH_3CN in ammonium formate pH 6.8 over 76 min (5 mL/min). The MeQM-dC N3 adduct **2.8** was collected ($t_r = 60$ minutes) and lyophilized to yield a white solid. A reliable yield could not be measured due to the small amounts of product isolated from each HPLC separation. ^1H NMR (500 MHz, $\text{DMSO}-d_6$): δ 2.07 (m, 2H), 2.16 (s, 3H), 3.53 (m, 2H), 3.76 (m, 1H), 4.22 (m, 1H), 4.89 (d, $J=4.7$ Hz, 2H), 5.90 (d, $J=8.0$ Hz, 1H), 6.21 (t, $J=6.9$ Hz, 1H), 6.62 (d, $J=8.2$ Hz, 1H), 6.93 (dd, $J=8.2, 2.0$ Hz, 1H), 7.22 (d, $J=2.0$ Hz, 1H), 7.45 (d, $J=8.0$ Hz, 1H). ^{13}C NMR (500 MHz, $\text{DMSO}-d_6$): δ 20.2, 39.3, 41.4, 61.3, 70.4, 84.8, 87.3, 100.0, 117.5, 123.1, 127.1, 130.1, 132.2, 133.5, 150.2, 154.6, 158.3. ESI $^+$ -MS: m/z 348.25 ($\text{M} + \text{H}^+$), 232.17 ($\text{M} - \text{drb} + \text{H}^+$). Calcd for $\text{C}_{17}\text{H}_{21}\text{N}_3\text{O}_5 (\text{M} + \text{H}^+)$: 348.16. Calcd for $\text{C}_{12}\text{H}_{13}\text{N}_3\text{O}_2 (\text{M} - \text{drb} + \text{H}^+)$: 232.11. $\lambda_{\text{max}} =$

219, 279 nm (diode array detector, 20% CH₃CN in ammonium formate, 8 mM, pH 6.8).

Oxidation of the dC N3 adduct 2.8 to form 2.15. The dC adduct **2.8** was generated *in situ* as described above at 37 °C for 20 minutes and then treated with an equal volume of BTI in CH₃CN (0.10 M) for 20 min at room temperature. The mixture was then diluted with water (25% v/v) and washed with diethyl ether. The aqueous phase was filtered through a 0.2 µm syringe filter and fractionated by preparative reverse-phase C18 HPLC using a 3 - 25% gradient of CH₃CN in ammonium formate pH 6.8 over 76 min (5 mL/min). The product **2.15** was collected (*t*_r = 26 min) and lyophilized to yield a yellow solid. A reliable yield could not be measured due to the small amounts of product isolated from each HPLC separation. ¹H NMR (400 MHz, DMSO-*d*₆): δ 1.90 (d, *J*=1.2 Hz, 3H), 2.04 (m, 2H), 3.53 (m, 2H), 3.70 (d, *J*=11.2 Hz, 1H), 3.75 (m, 1H), 3.92 (d, *J*=11.2 Hz, 1H), 4.22 (m, 1H), 4.99 (br, 1H), 5.24 (br, 1H), 5.78 (d, *J*=8.2 Hz, 1H), 5.97 (d, *J*=9.9 Hz, 1H), 6.06 (bd, *J*=6.4 Hz, 1H), 6.16 (t, *J*=7.0 Hz, 1H), 7.03 (dd, *J*=9.9, 2.2 Hz, 1H), 7.50 (d, *J*=8.2 Hz, 1H). ¹³C NMR (500 MHz, DMSO-*d*₆): δ 20.3, 39.5, 51.5, 61.4, 70.5, 73.1, 83.8, 87.1, 96.0, 123.5, 128.8, 136.6, 137.0, 146.3, 147.5, 154.9, 199.7. ESI⁺-MS: *m/z* 346.18 (M + H⁺). Calcd for C₁₇H₂₀N₃O₅ (M + H⁺): 346.14. $\lambda_{\text{max}} = 235, 283, 340$ nm (diode array detector, 12% CH₃CN in ammonium formate, 9 mM, pH 6.8).

Chapter 3: Formation and Oxidation of MeQM-dG Adducts

3.1. Introduction.

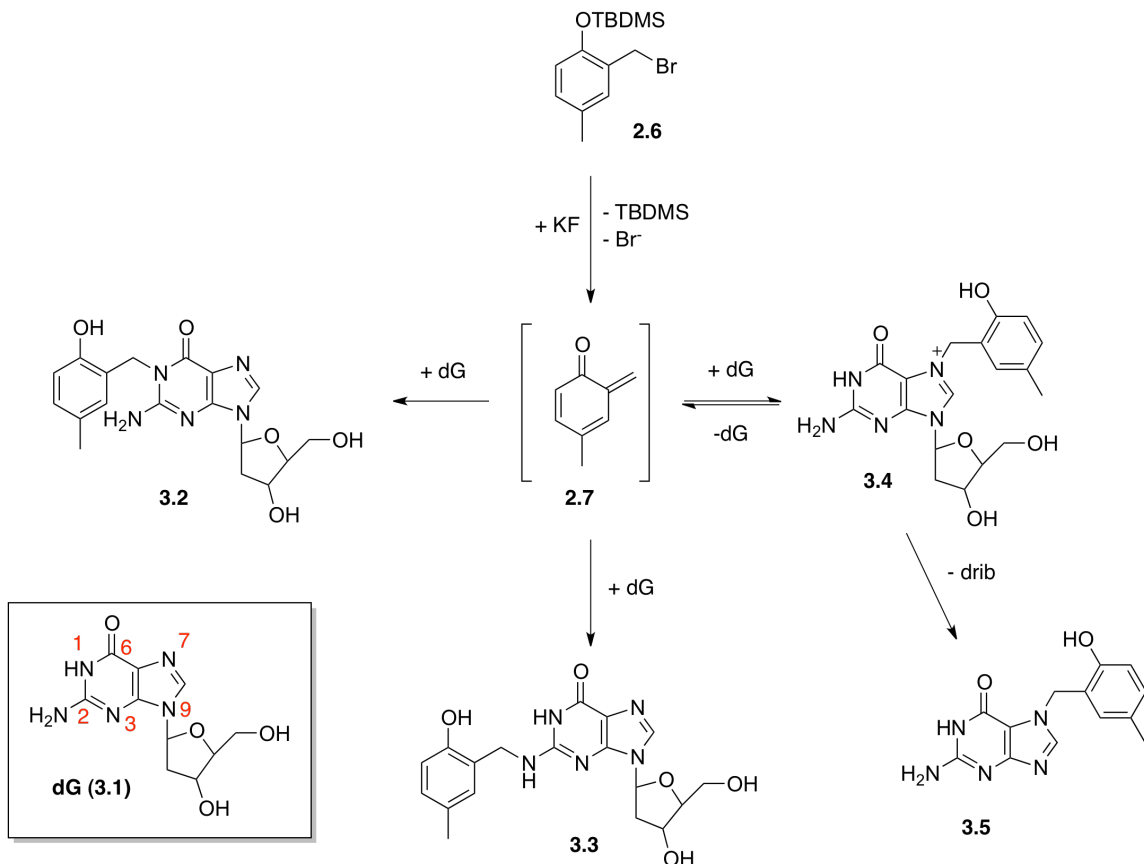
Oxidative de-aromatization of the phenolic product formed between MeQM and dC has been proven to quench the reversible alkylation and allow the MeQM-dC N3 adduct to survive at least 24 hours for enzymatic digestion and HPLC analysis.⁷⁶ The usage of BTI allows the oxidative trapping to occur quickly, quantitatively, and selectively with the QM phenol under physiological conditions. These properties are necessary considering the ultimate goal of analyzing the alkylation profile of MeQM and DNA over short times by quickly trapping the reaction prior to enzymatic digestion.

To properly quantify the HPLC data for the alkylation of DNA by MeQM, each of the potential oxidized MeQM-dN adducts must be synthesized and characterized for use as analytical standards. The aforementioned MeQM-dC N3 oxidation product was synthesized and fully characterized by 1D and 2D NMR, ESI⁺-MS, and UV-vis.⁷⁶ The next nucleoside to be studied was 2'-deoxyguanosine (dG) as it contains the most nucleophilic position (dG N7) and produces the largest number of adducts at three.

MeQM is expected to react with dG at the same positions as previously observed with the simple *o*-QM (**Scheme 3.1**). Of the three initial alkylation products formed between MeQM and dG, the product at dG N7 is the most important as it is proposed to be the most physiologically relevant. The N7 position of dG is the most

nucleophilic site of the DNA bases, and as such, is the most reactive site towards many electrophiles, the strongly electrophilic *o*-QMs included.^{14,58}

Scheme 3.1. Structures of products formed from the alkylation of dG (**3.1**) by MeQM (**2.7**).



Along with being the nucleophilic position in DNA, dG N7 is also the most accessible of the strong nucleophiles in DNA. Unlike dC N3 and dA N1, which participate in hydrogen bonding in dsDNA, dG N7 is available in the major groove. (**Figure 3.1**). This availability allows unobstructed access to dG N7 for electrophiles, while reaction with dC N3 or dA N1 necessitates the breaking of a hydrogen bond.

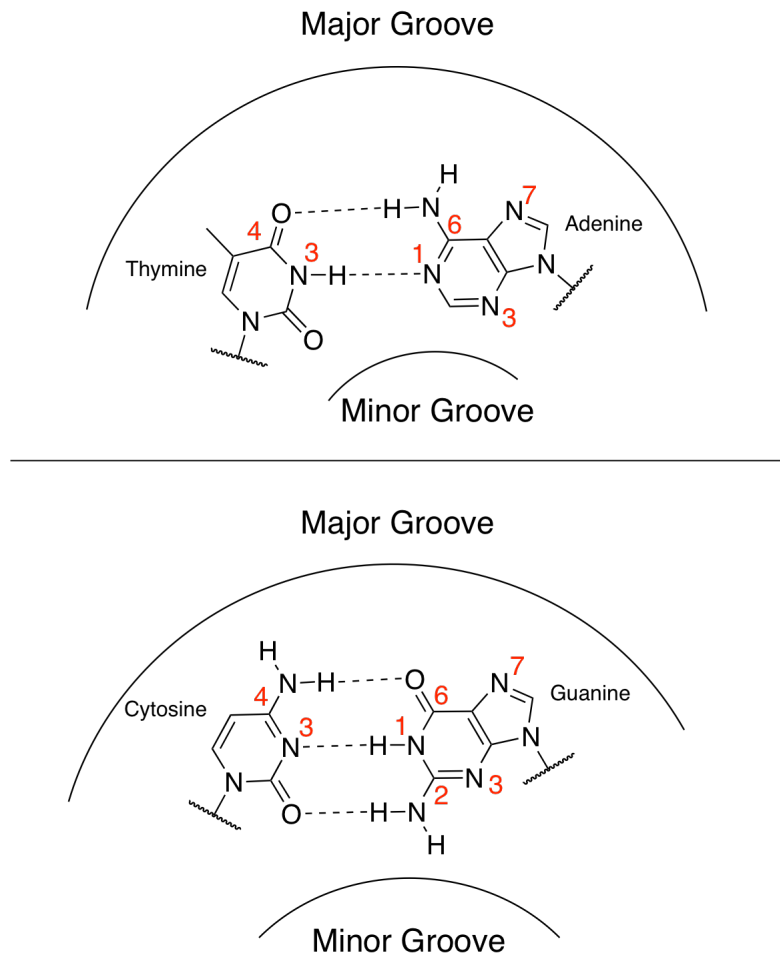


Figure 3.1. Watson-Crick base pairing in DNA with the major and minor grooves labeled. The top pair is T-A and the bottom pair is C-G.

The alkylation of dG by MeQM was expected to be a greater challenge to the oxidative trapping than dC, partly due to the lower solubility of dG in aqueous conditions when compared to dC. Adding to the challenge of dG is that previous work determined that the alkylation of dG by a simple *o*-QM results in the formation of four unique adducts (dG N1, dG N², dG N7, and guanine N7) instead of the single adduct formed by dC (dC N3) (**Scheme 1.12**).⁵⁶ The formation of multiple adducts could complicate the HPLC isolation of individual products due to difficulties in their resolution. Further complicating the reaction of *o*-QM with dG is that there are two

competing processes in the reaction of the dG N7 adduct, reversibility to free *o*-QM and deglycosylation to form the guanine N7 adduct. These processes limit the yield of QM-dG N7 and make it difficult to observe the adduct after DNA alkylation.

Despite these challenges, each of the oxidation products of MeQM-dG must be isolated and fully characterized for use as an analytical standard in the quantification of MeQM alkylation of DNA.

3.2. Results and Discussion.

3.2.1. Alkylation of dG with MeQM.

The oxidized MeQM-dC N3 adduct was formed in a one-pot reaction in which the MeQM-dC N3 adduct was formed *in situ* and subsequently treated with four equivalents of BTI prior to work-up and HPLC purification.⁷⁶ These reaction conditions were applied to the alkylation of dG by MeQM to rapidly isolate the four oxidized MeQM-dG products. 4-MeBrQMP (50.0 mM), dG (22.5 mM), potassium phosphate (5 mM, pH 7), and KF (500 mM) were combined in a solution of CH₃CN (25%), DMF (45%), and H₂O (30%). The reaction was held at 37 °C for 20 minutes prior to addition of a four-fold excess of BTI. This was then removed from heat for another 10 minutes followed by a work-up consisting of a saturated diethyl ether wash and HPLC analysis. Unfortunately, the resulting HPLC chromatogram contained a number of low intensity peaks and there was no major product identified (**Figure 3.2**). The reason for this failure is not known, but it may be due to any number of reactions between any of the chemical species in solution, leading to decomposition. To avoid this, each adduct was isolated prior to their oxidation.

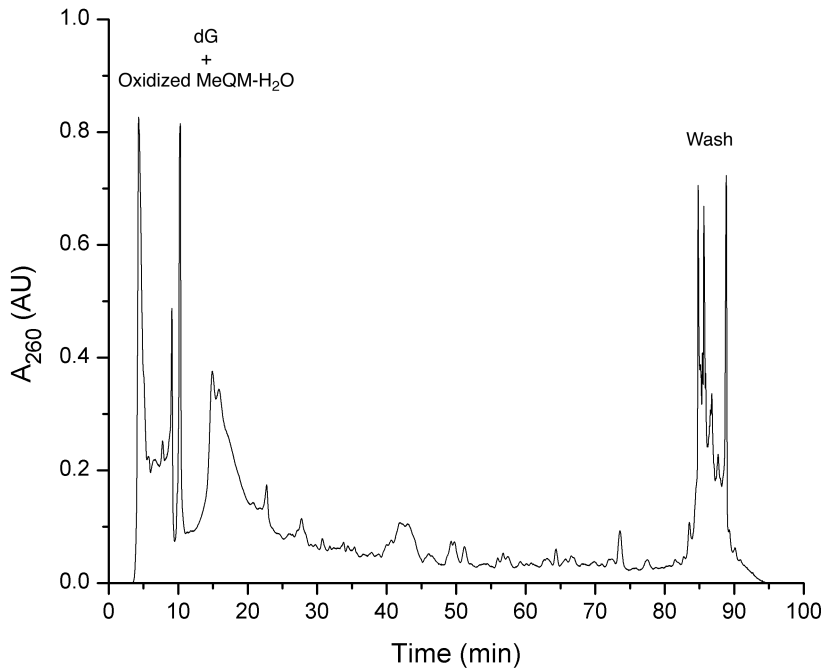


Figure 3.2. HPLC analysis of a “one-pot” MeQM-dG oxidation. The MeQM-dG adducts were generated *in situ* prior to oxidation by BTI. The reaction was analyzed with Gradient 1 using the analytical column (1 mL/min).

The alkylation of dG with MeQM consisted of combining 4-MeBrQMP (**2.6**) (10 mM), dG (10 mM), and KF (500 mM) in 2:1 DMF:H₂O. This mixture was held at 37 °C for 1 hour prior to filtration (0.2 µm) and analysis by HPLC using a semi-prep column (**Figure 3.3**). There were five products observed by HPLC and the product at $t_r = 46$ minutes was the major product. ¹H NMR confirmed that the compound was a MeQM-dG adduct by the presence of protons correlated to dG and MeQM. The compound was later identified as MeQM-dG N1 (**3.2**).

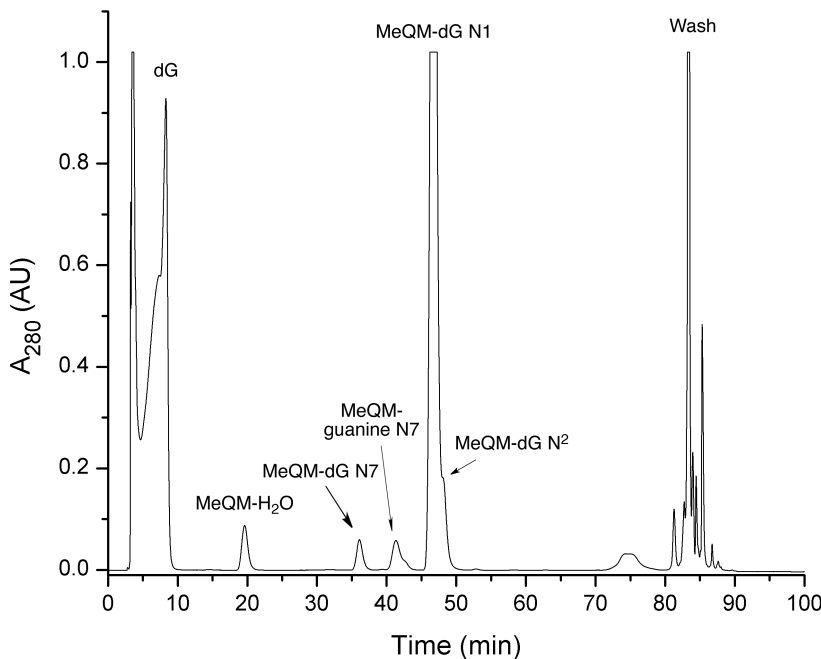


Figure 3.3. HPLC analysis of the alkylation of dG with MeQM. The reaction combined 10 mM each dG and 4-MeBrQMP in a 2:1 solution of DMF:H₂O for 1 hour at 37 °C. HPLC analysis used Gradient 1 with the semi-prep column (5 mL/min). Peak identification was confirmed with additional data from future experiments.

Since the reactivity of MeQM was expected to be similar to the previously studied *o*-QM,⁵⁸ it was expected that the MeQM-dG N7 adduct would form quickest of the adducts. The above experiment demonstrated that after one hour at 37 °C produced primarily the MeQM-dG N1 adduct, which suggested that the MeQM reacted faster than the unsubstituted QM. The MeQM-dG N1 adduct became the major product between QM and dG after approximately 8 hours. A series of reactions were carried out at temperatures varying from 0 °C to 37 °C with a reaction time at one minute from KF activation of MeQM to HPLC analysis. These reactions consisted of a 1:1:2 mixture of DMF:CH₃CN:H₂O containing dG (12.5 mM), 4-MeBrQMP (12.5 mM), potassium phosphate buffer (12.5 mM, pH 7), and KF (625 mM). Unfortunately, these conditions did not result in the primary formation of

MeQM-dG N7. While the lower temperature managed to slow the rate of adduct formation, the rate decreased proportionally for each adduct and did not maximize the amount of MeQM-dG N7 formed. While MeQM reacted at the same positions of dG as QM, it appears that the product profile may have changed.

The reaction conditions were adjusted due to the low overall yield of the previous alkylations. The goal was to increase the yield of each MeQM-dG adduct instead of focusing on any individual adduct. The concentrations of 4-MeBrQMP and dG were increased to 50 mM and 22.5 mM, respectively, in a 1.8:1:1.2 mixture of DMF:CH₃CN:H₂O. The dG concentration was limited by its low solubility in the reaction solvents. The HPLC analysis used an analytical column to obtain better resolution than the previously used semi-prep column (**Figure 3.4**). There were four products isolated by HPLC, but only MeQM-dG N1 had sufficient yield for ¹H NMR analysis. The reaction was scaled up 2-fold and the subsequent HPLC purification used a semi-prep column to accommodate the larger reaction size. Unfortunately, the resolution of adducts decreased and at least two of these co-eluted (**Figure 3.5**).

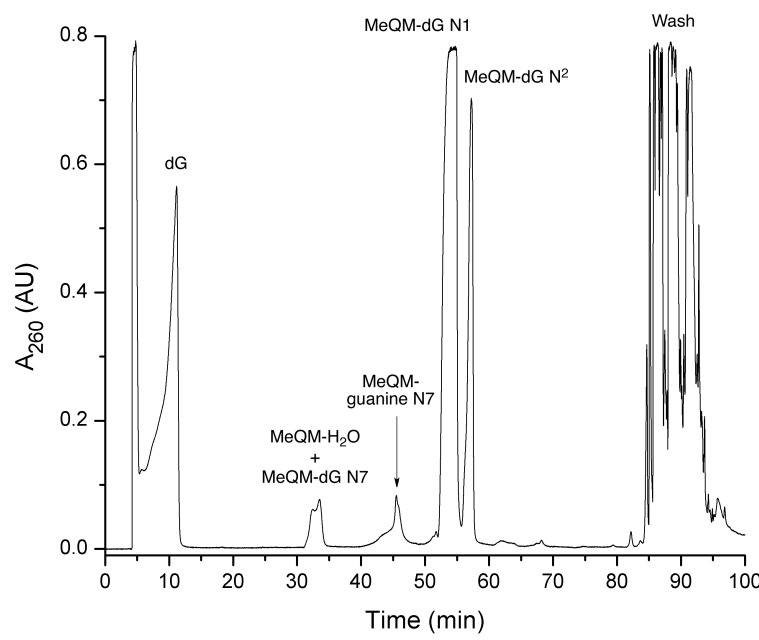


Figure 3.4. HPLC analysis of MeQM-dG alkylation with 50 mM 4-MeBrQMP and 22.5 mM dG in a 1.8:1:1.2 mixture of DMF:CH₃CN:H₂O. The reaction was held at 37 °C for 20 minutes and fractionated using Gradient 1 with an analytical column (1 mL/min). Injection volume was 180 µL.

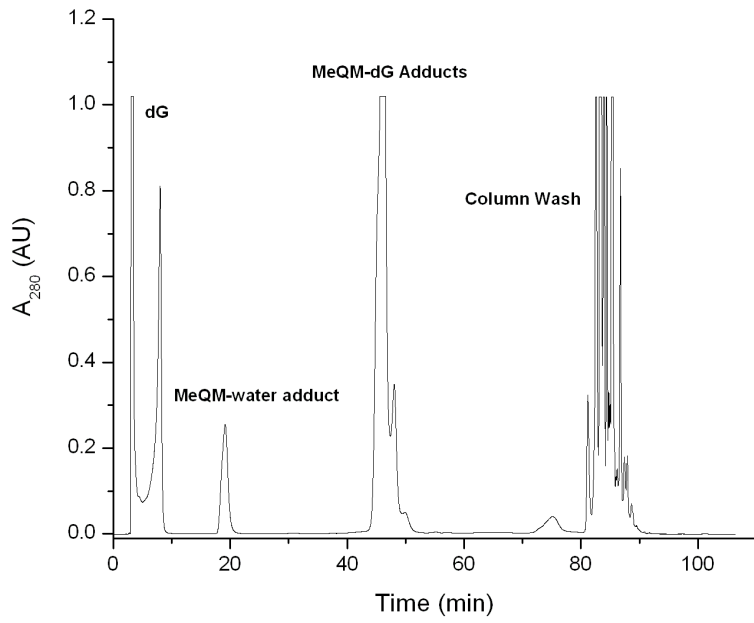


Figure 3.5. HPLC analysis of a 2x scale MeQM-dG alkylation of **Figure 3.4**. The analysis used Gradient 1 with a semi-prep column (5 mL/min). Injection volume was 370 µL. The scale-up resulted in the co-elution of at least two of the MeQM-dG adducts between $t_r = 40 - 50$ minutes.

The reaction conditions were again varied in an attempt to form more of the other MeQM-dG adducts (dG N² and dG N7). New conditions were inspired by previously optimized conditions to form QM-dG N² consisting of a 1:1 mixture of DMF:H₂O with 4-MeBrQMP (25.0 mM), dG (12.5 mM), and KF (250 mM).⁵⁶ This mixture was held at 37 °C for between 30 minutes and 23 hours before HPLC analysis. The HPLC analysis utilized an analytical column for the improved resolution. The different reaction times were used to find an ideal reaction length for the formation of the various adducts (**Figure 3.6**). As expected, the yield of MeQM-dG N7 decreases for reaction times over 30 minutes. MeQM-guanine N7, however, increases in yield for reaction times over 30 minutes. This relationship is expected as MeQM-guanine N7 forms from the deglycosylation of MeQM-dG N7. MeQM-dG N1 and N² appear to have a constant yield over the range of 30 minutes to 23 hours. These amounts were determined by comparing the peak area at A₂₆₀ for each compound.

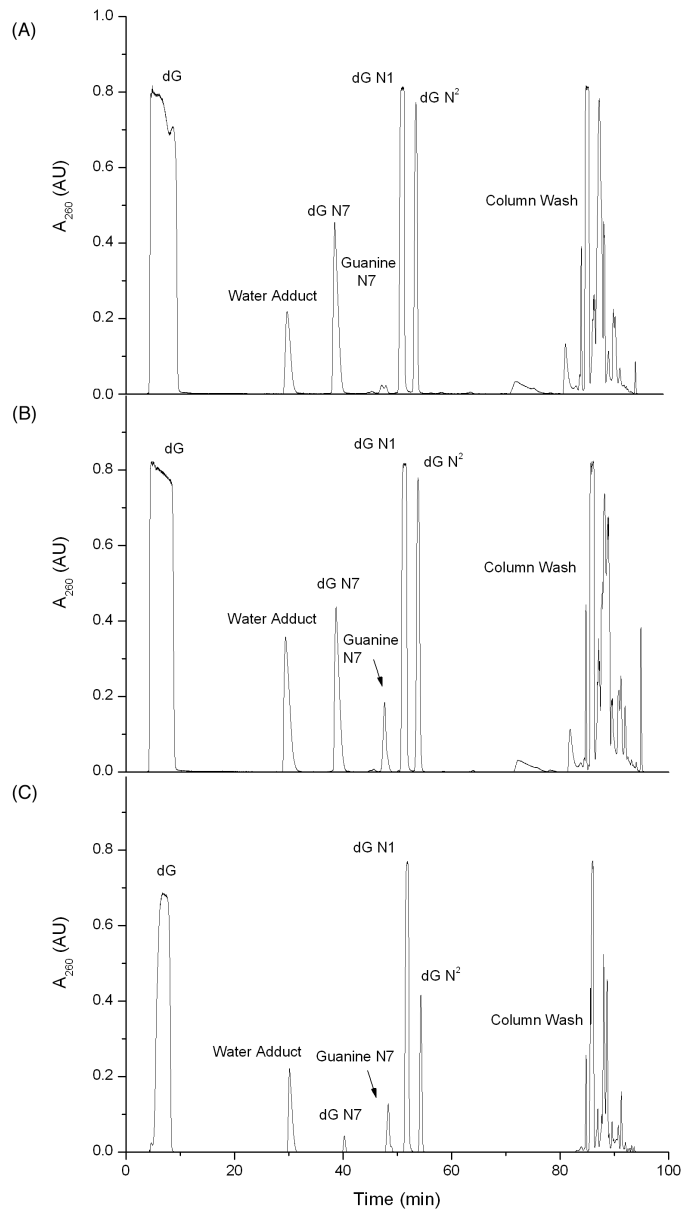


Figure 3.6. HPLC analysis of the MeQM-dG alkylation that consisted of a 1:1 mixture of DMF:H₂O with 4-MeBrQMP (25.0 mM), dG (12.5 mM), and KF (250 mM). The reaction was monitored by analyzing 100 μ L aliquots by HPLC at 30 minutes (A) and 3 hours (B). The reaction was also monitored by analyzing a 50 μ L aliquot at 23 hours (C). Gradient 1 was used with an analytical column (1 mL/min).

Each of the five MeQM adducts observed by HPLC (including MeQM-H₂O) were collected over the course of four runs and lyophilized overnight. Initially,

identification of the adducts was done by comparing t_r and UV-Vis data with the unsubstituted QM data (**Table 3.1**).⁵⁶

Table 3.1. Comparison of UV-Vis and t_r data between MeQM-dG and QM-dG.⁵⁶

Adduct	Experimental λ_{max} for MeQM-dG (nm)	Literature λ_{max} for QM-dG (nm)	Order of Elution for MeQM-dG	Order of Elution for QM-dG
dG N7	259, 279	260	1	1
guanine N7	283	280	2	2
dG N1	255, 271	257, 275	3	3
dG N ²	247, 275	256, 280	4	4

Each of the lyophilized MeQM-dG products were then individually combined with 100 μ L H₂O and 100 μ L CH₃CN and analyzed by HPLC immediately to assess their stability. There was no observed decomposition of MeQM-dG N1, MeQM-dG N², or MeQM-guanine N7 after the overnight lyophilization. This is expected as these three adducts were determined to be irreversible with the unsubstituted QM.⁵⁸ MeQM-dG N7, however, does show a small amount (< 2%) of MeQM-guanine N7, but no water adduct. This indicates that, under lyophilizing conditions, the reversibility of MeQM-dG N7 is of small concern while the deglycosylation of MeQM-dG N7 does occur, albeit slowly (**Appendix B.1**).

The reaction was repeated several times to obtain enough material for ¹H NMR analysis of each product (**Appendix B.3 – B.6**). The ¹H NMR chemical shifts were compared with the literature values for the QM-dG adducts in order to confirm the MeQM-dG adduct identities (**Table 3.2**).⁵⁶ Specifically, the methylene bridge protons and the lone proton on guanine (H8) were used as points of direct comparison.

Table 3.2. ^1H NMR comparison between MeQM-dG and QM-dG (ppm). All MeQM-dG adducts analyzed in DMSO- d_6 . QM-dG N7 was not analyzed by NMR, QM-guanine N7 was analyzed in NaOD/D₂O, QM-dG N1 and QM-dG N² were analyzed in DMF- d_7 .⁵⁶

Adduct	MeQM-dG Methylene Bridge (ppm)	QM-dG Methylene Bridge (ppm)	MeQM-dG H8 (ppm)	QM-dG H8 (ppm)
dG N7	5.52	n/a	9.18	n/a
guanine N7	5.30	5.39	7.84	7.64
dG N1	5.06	5.28	7.96	8.05
dG N²	4.36	4.58	7.90	7.99

ESI⁺-MS was carried out on each of the NMR samples of the MeQM-dG adducts. To facilitate ionization and flow through the tubing, the DMSO- d_6 samples were diluted to 40% water prior to analysis. Each of the MeQM-dG adducts was observed along with their deglycosylated fragments. The remaining NMR samples were analyzed by HPLC to observe their stability both dry in the freezer and in DMSO- d_6 . The MeQM-dG N7 adduct decomposed such that only approximately 50% of the original adduct remained after one day frozen at 0 °C in DMSO- d_6 (**Figure 3.7**). Surprisingly, the major decomposition product was MeQM-dG N1 (~50% of the dG N7 peak area at A₂₆₀). This result suggests that the rate of reversibility is faster than the rate of deglycosylation, further highlighting the importance of trapping the MeQM-dG N7 adduct. The other decomposition products MeQM-H₂O (<1% of dG N7) and MeQM-guanine N7 adduct (<7% dG N7) formed in very low concentrations. The MeQM-dG N1 and MeQM-guanine N7 adducts did not show any detectable decomposition, confirming that they are irreversible products. The MeQM-dG N² adduct showed a small amount (<10%) of MeQM-dG N1 adduct, which was probably collected during the initial purification of the crude alkylation reaction.

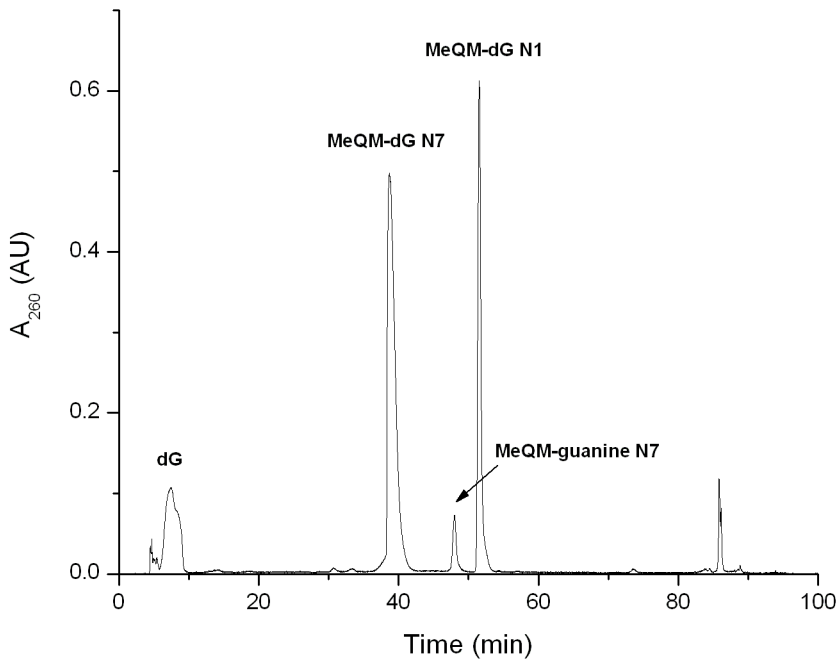


Figure 3.7. HPLC analysis of the MeQM-dG N7 NMR sample that was stored in DMSO- d_6 for 24 hours at -20 °C.

The alkylation described above would yield a maximum of 3.9 mg MeQM-dG adducts (total) per 400 μ L reaction. Due to the high reactivity of MeQM the yield does not approach 100%, although the actual yield is difficult to determine due to the small amounts of product formed. This low yield necessitated a scaled up reaction capable of delivering mgs of each MeQM-dG adduct in a shorter period of time.

The solubility of dG was greatly improved by using a 70:30 mixture of DMF:H₂O to produce a 100 mM stock solution of dG resulting in a final concentration of 25.0 mM dG in a reaction solvent consisting of 57.5% H₂O and 42.5% DMF. This increased the maximum yield of the alkylation reaction 2-fold when considering all adducts. Initial reaction purifications utilized the same HPLC gradient as before, Gradient 1 (**Table 3.3**), and a 200 μ L reaction to confirm that the same products were formed as the less concentrated reaction (**Figure 3.8**). Each of

the previously observed MeQM adducts was observed by HPLC and identified by t_r and UV-Vis absorbance. Once this was accomplished, the same gradient was run on the semi-preparative column in anticipation of larger injection volumes. The same reaction was analyzed using five different HPLC gradients, each one improving on the separation of MeQM adducts of the previous gradient while decreasing the time for each run (**Table 3.3**). The optimal gradient was Gradient 6 due to the separation of the MeQM-dG adducts from the by-products and the shorter method length (**Figure 3.9**).

Table 3.3. HPLC gradient optimization for the fractionation of the MeQM-dG alkylation. The aqueous buffer is 10 mM TEAA pH 5. The flow rate was 5 mL/min with the semi-prep column.

Gradient		Starting CH ₃ CN (%)	Ending CH ₃ CN (%)	Time (min)	Rate (%/min)
1	Step 1	3	25	76	0.289
	Step 1	3	10	14	0.500
2	Step 2	10	18	40	0.200
	Step 3	18	25	14	0.500
3	Step 1	3	11.2	16.4	0.500
	Step 2	11.2	16.2	50	0.100
4	Step 1	3	12	18	0.500
	Step 2	12	14	40	0.050
5	Step 1	3	12	10	0.900
	Step 2	12	12	40	isocratic
	Step 3	12	14	10	0.200
6	Step 1	3	12	10	0.900
	Step 2	12	12	30	isocratic

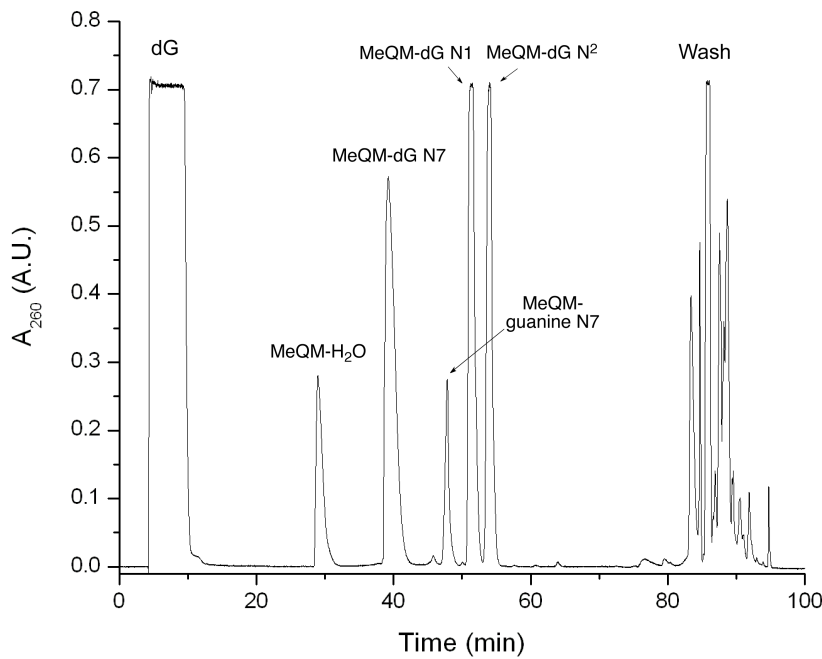


Figure 3.8. HPLC analysis of MeQM-dG alkylation using a 42.5% DMF percentage. The reaction was held at 37 °C for 2 hours and fractionated using Gradient 1 with an analytical column (1 mL/min). Injection volume was 200 μ L.

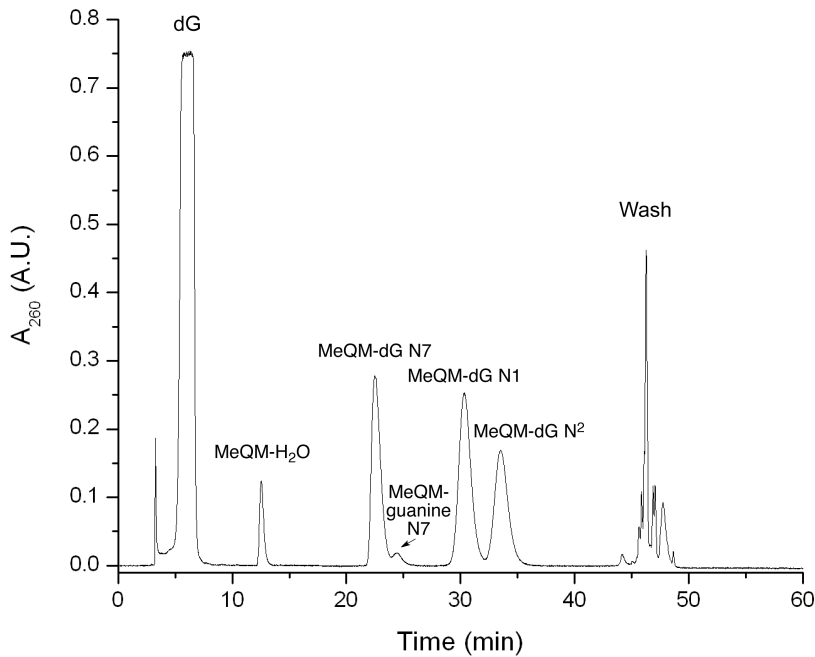


Figure 3.9. HPLC analysis of MeQM-dG alkylation. The reaction was held at 37 °C for 1 hour and fractionated using Gradient 6 with a semi-prep column (5 mL/min). Injection volume was 200 μ L.

With an optimized HPLC gradient, the alkylation reaction was gradually scaled up from 200 μ L to 1 mL. The optimized 1 mL alkylation reaction consisted of 4-MeBrQMP in DMF (250 μ L, 100 mM), dG in 70% aqueous DMF (250 μ L, 100 mM), and aqueous KF (500 μ L, 500 mM) and was stirred at 37 °C for 1- 5 hr (**Figure 3.10**). The new reaction increased the theoretical yield 2.5-fold to 9.7 mg total adducts formed. It was demonstrated that the alkylation products of MeQM-dG could be isolated in mg quantities sufficient for ^1H NMR. The next step was to develop an efficient method for forming and isolating the oxidized products of MeQM-dG.

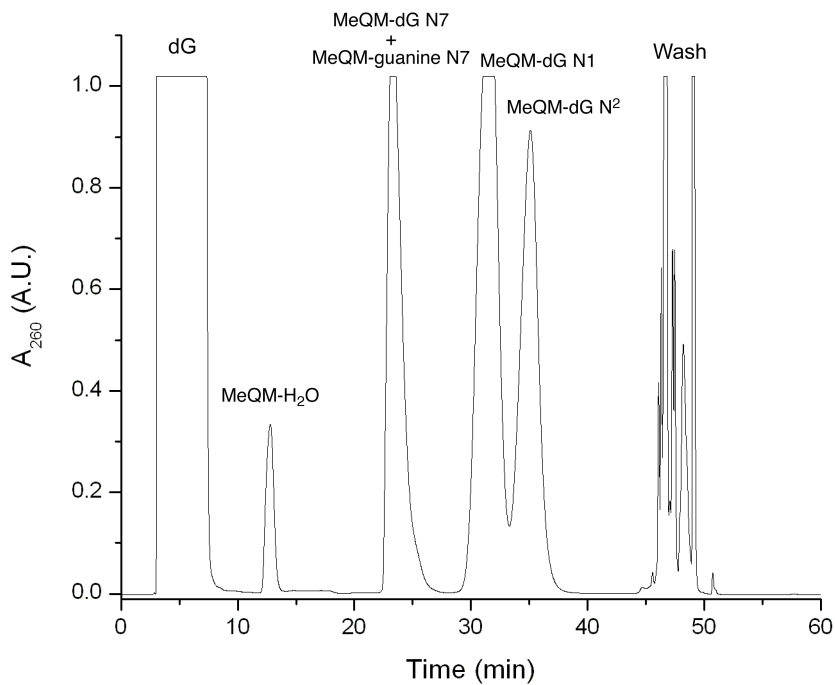


Figure 3.10. HPLC analysis of MeQM-dG alkylation using Gradient 6. The reaction was held at 37 °C for 1 hour and was fractionated using a semi-prep column (5 mL/min). The injection volume was 1 mL.

3.2.2. Oxidation and Isolation of the MeQM-dG adducts.

Since MeQM-dG N1 formed in the highest yield (35 – 55% of the total MeQM adducts measured by peak area at A_{260}) it was the logical choice to start the individual oxidation studies. The lyophilized MeQM-dG N1 adduct was dissolved in 125 μ L water and 125 μ L CH₃CN to prepare it for oxidation. This solution was transferred to an Eppendorf tube and 200 μ L BTI (200 mM in CH₃CN) was added. The reaction was mixed and allowed to stand at room temperature for 20 minutes. Over the course of the reaction, the solution changed from pale yellow to orange in color. Water (100 μ L) was added to the reaction and the mixture was washed with water saturated diethyl ether (3 \times 0.5 mL). The aqueous layer was collected and filtered (0.2 μ m) prior to analysis by HPLC (**Figure 3.11**).

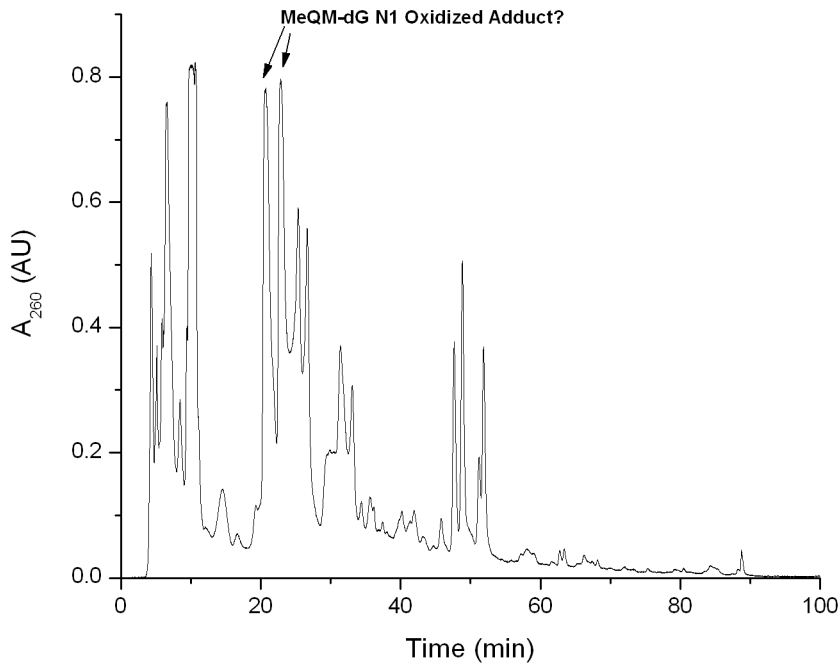


Figure 3.11. Crude oxidation of MeQM-dG N1 with BTI. The reaction was held at room temperature for 20 minutes prior to HPLC analysis. Gradient 1 was used with the analytical column (1 mL/min).

The oxidation of MeQM-dG N1 yielded a very complex mixture. The major products eluting between 20 - 24 minutes, 47 - 50 minutes, and 51 - 53 minutes were collected and lyophilized overnight for ^1H NMR analysis. Of these collected compounds, only the 2 peaks at 20 - 24 minutes yielded enough material for ^1H NMR (**Figure 3.12**).

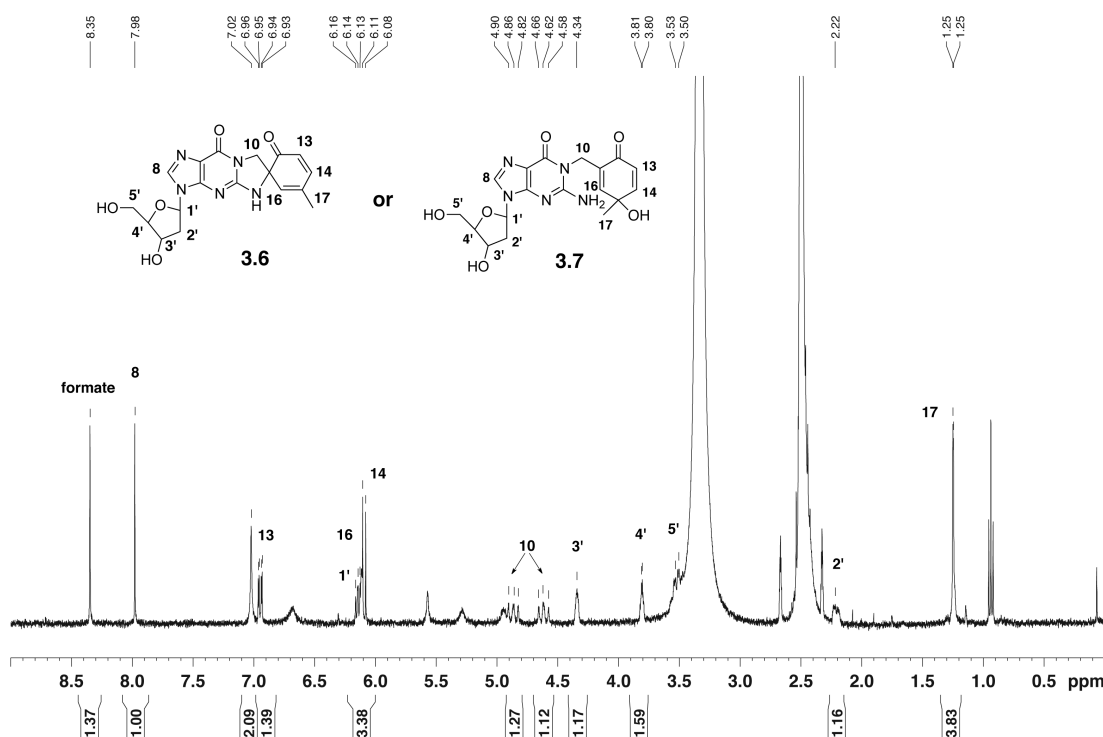


Figure 3.12. ^1H NMR of the product formed by oxidation of MeQM-dG N1 in $\text{DMSO}-d_6$ at 400 MHz. Two possible structures are shown as **3.6** and **3.7**.

The structure for the oxidized product of MeQM-dG N1 was initially proposed to be a spiro-compound (**3.6**) due to the similarities between the ^1H NMR of this compound and the MeQM-dC oxidized adduct which was determined to be a spiro compound. Similarities include a downfield shift and small splitting (<2 Hz) of the 4-Me protons (H17). The complex splitting of the (presumed) methylene bridge protons (H10) also mirrors that of the equivalent protons in the MeQM-dC oxidized

adduct. Additionally, upon HPLC analysis of the NMR sample, two compounds ($t_r = 25.5$ and 26.5 min) with identical UV-Vis absorbances eluted, which also corresponds to the formation of a diastereomeric mixture as seen with the MeQM-dC oxidized adduct (**Appendix B.2**). The synthesis of more MeQM-dG N1 oxidized adduct was necessary to perform additional 1D and 2D NMR to confirm the structure of the isolated compound.

Fortunately, using the optimized alkylation conditions and purification using Gradient 6 (**Table 3.3**) synthesis of MeQM-dG N1 became efficient. Under these conditions MeQM-dG N1 and MeQM-dG N² elute sequentially with t_r 30 and 33 minutes and are not fully resolved (**Figure 3.6**). Instead of attempting to collect the adducts separately, they were collected together for oxidation in the same reaction vessel which should produce two unique, stable compounds. Lyophilized samples of the MeQM-dG N1 and MeQM-dG N² were dissolved in a 1:1 solution of potassium phosphate (50 mM, pH 7) and CH₃CN at an average of 50 μ L solvent per vial of lyophilized adduct and then subjected to 20 mmol BTI for 5 minutes at room temperature. These oxidation conditions were milder than previously used (40 mmol BTI for 20 minutes at room temperature) in an effort to reduce the number of by-products simplify purification and increase yield. The initial HPLC purification using Gradient 1 with the analytical column resulted in a number of compounds of similar UV-Vis spectra ($\lambda_{max} =$ approximately 243 and 271 nm) eluting from 21 - 36 minutes which were collected together for ¹H NMR analysis (**Figure 3.13**).

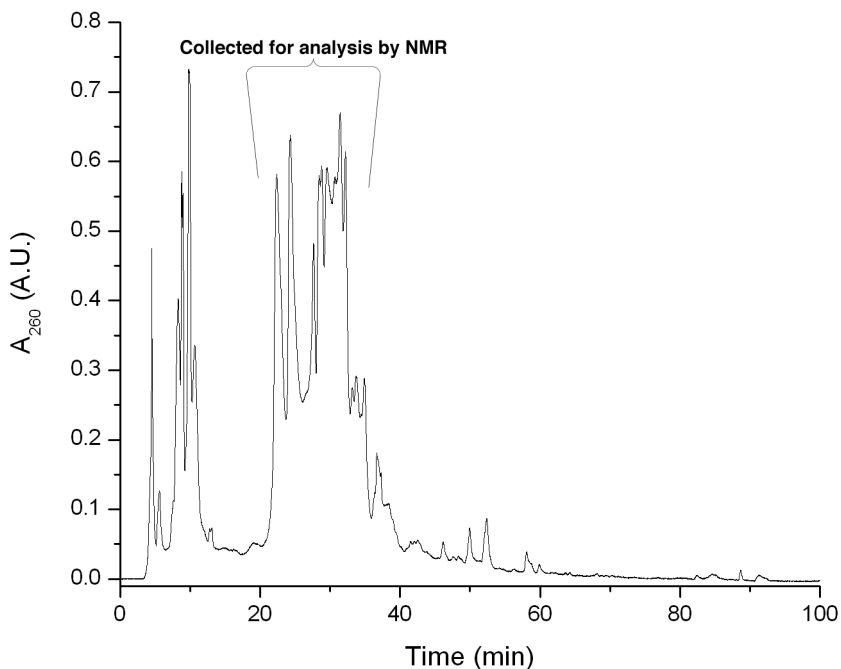


Figure 3.13. HPLC analysis of the crude oxidation of the mixture of MeQM-dG N1 (3.2) and MeQM-dG N² (3.3) with BTI. The reaction was held at room temperature for 5 minutes. Gradient 1 was used with the analytical column (1 mL/min).

¹H NMR of the collected sample suggested a mixture of two unique MeQM-dG adducts from the presence of two proton signals for each H8, H17, and H10 (**Figure 3.14**). The aromatic region also appeared more complex than what would result from a single MeQM-dG adduct. HPLC analysis of the NMR sample, which was first diluted by 50% with H₂O, showed two pairs of peaks with much better resolution with retention times of approximately 24.5, 26.0, 29.0, and 30.0 minutes (**Figure 3.15**). As the same column and gradient was used as the previous purification (**Figure 3.13**) this suggests that the initial purification of the oxidation reaction slightly overloaded the HPLC column, shifting the retention times of the adducts forward. Each of the four peaks has an identical λ_{max} (243 and 271 nm) suggesting a diastereomeric mixture for each product.

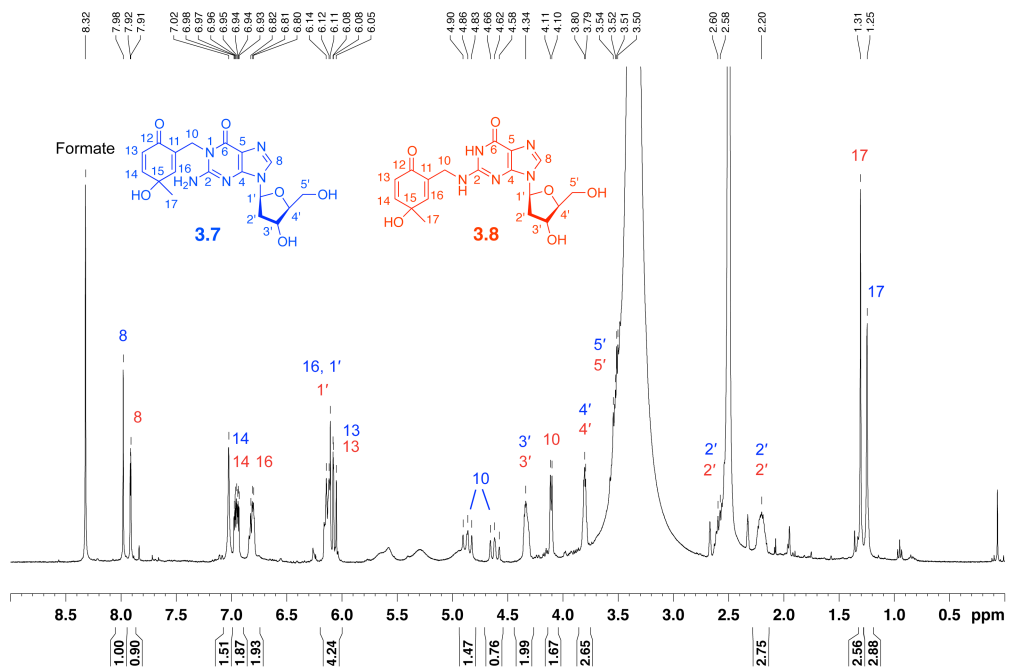


Figure 3.14. ^1H NMR of the material collected between 21 and 36 minutes of HPLC analysis of the crude oxidation of the mixture of MeQM-dG N1 (**3.2**) and MeQM-dG N² (**3.3**) with BTI (**Figure 3.13**).

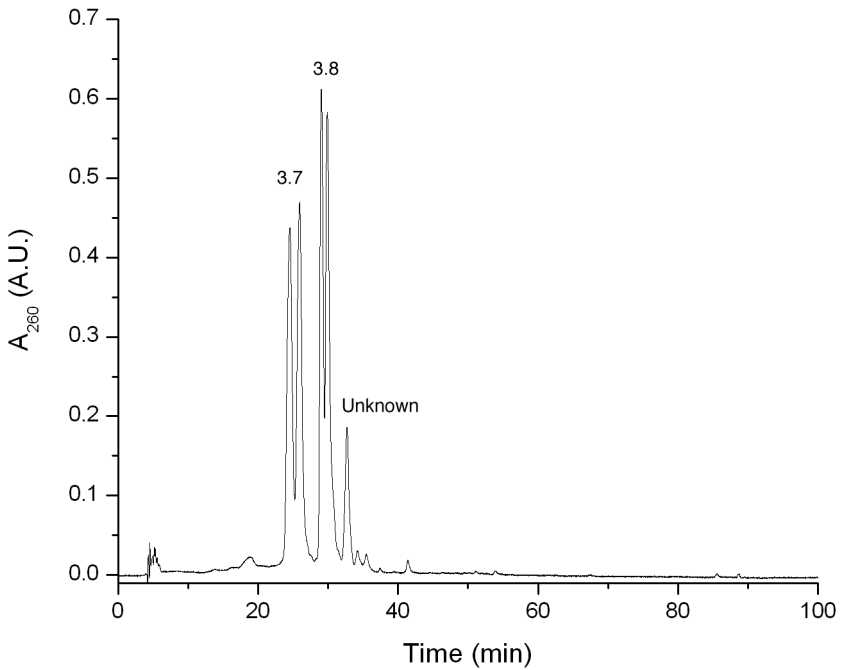
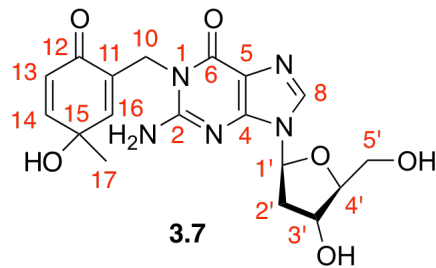


Figure 3.15. HPLC analysis of the ^1H NMR sample from **Figure 3.14**. The NMR sample was diluted with H_2O to 50% aqueous $\text{DMSO}-d_6$ prior to re-injection into the HPLC. Gradient 1 was used with the analytical column (1 mL/min).

The two pairs of compounds were collected separately, lyophilized overnight, and analyzed by ^1H NMR. Preliminary results showed that the first eluting compound was the oxidized product of MeQM-dG N1 (**3.7**) while the second compound was the oxidized product of MeQM-dG N² (**3.8**). These characterizations were based largely on the chemical shifts of H8 and H10 compared to the non-oxidized adducts. The oxidation was repeated until sufficient product was collected for 2D NMR.

Scheme 3.2. Proposed structure of the product (**3.7**) formed by oxidation of MeQM-dG N1 (**3.2**).



The first compound characterized was the oxidized product of MeQM-dG N1 (**3.7**) (**Scheme 3.2**). NMR signals (^1H and ^{13}C) corresponding to the purine and ribose moieties of **3.7** were again assigned from literature values for dG and N1 alkylated dG derivatives^{56,88,89} and confirmed by ^1H - ^{13}C HSQC and ^1H - ^{13}C HMBC spectra (**Appendix B.7 – B.10**). The compound 4-hydroxy-2,4-dimethyl-2,5-cyclohexadien-1-one (**3.9**) was used as a model for the *p*-quinol moiety (**Appendix Table B.4**).⁶⁸ Specifically, the ^{13}C chemical shift of the sp² hybridized C11 (129.5 ppm) and the sp³ hybridized C15 (66.5 ppm) are in agreement with the corresponding carbons in the model compound (133.3 ppm and 67.3 ppm, respectively).

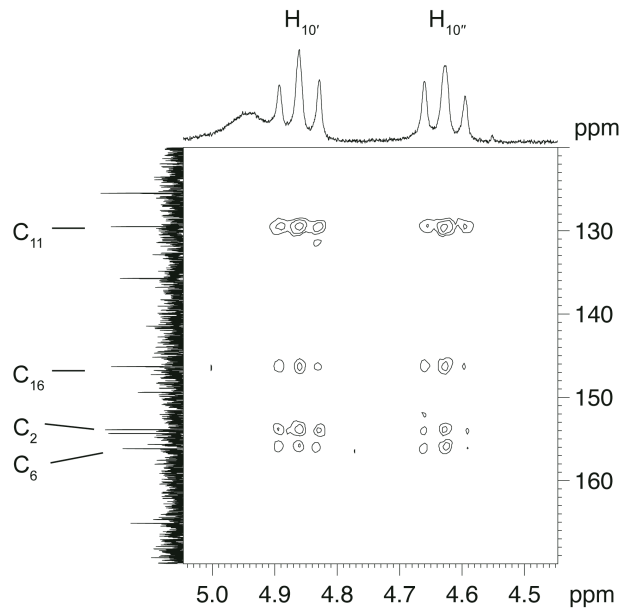
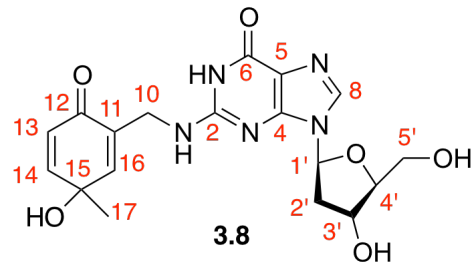


Figure 3.16. $^1\text{H} - ^{13}\text{C}$ HMBC of **3.7** in $\text{DMSO}-d_6$ at 600 MHz.

Alkylation of the N1 position of dG was confirmed by $^1\text{H}-^{13}\text{C}$ HMBC NMR, which detected correlations between the methylene protons (H10) and C2, C6, C11, and C16 (**Figure 3.16**). Only alkylation of N1 would satisfy these data. The presence of diastereomers observed by HPLC was also seen in the splitting pattern of the methylene protons (H10). The coupling constant ($J=15.7$ Hz) between the two protons is characteristic of geminal coupling, the result of restricted rotation around C10. The splitting pattern is similar to the overlapping doublet of doublets observed in the ^1H NMR spectra of MeQM-dC N3 oxidized adduct.⁷⁶ Again, this unique splitting pattern is the result of the diastereomeric mixture of compounds along with the diastereotopic relationship of the protons (H10). ESI $^+$ -MS provided a m/z 404.13 ($\text{M} + \text{H})^+$ that corresponds with the proposed structure of **3.7** (calculated m/z 404.16 ($\text{M} + \text{H})^+$). The above evidence confirms that the *p*-quinol product is formed, not the

initially proposed spiro-cyclized product **3.6** (calculated m/z 386.15 ($M + H$)⁺) observed with the MeQM-dC N3 oxidized adduct.

Scheme 3.3. Proposed structure of the product (**3.8**) formed by oxidation of MeQM-dG N² (**3.3**).



The next compound to be characterized was the oxidized product of MeQM-dG N² (**3.8**) (**Scheme 3.3**). NMR signals (¹H and ¹³C) corresponding to the purine and ribose moieties of **3.8** were again assigned from literature values for dG and N² alkylated dG derivatives^{56,88} and confirmed by ¹H-¹³C HSQC and ¹H-¹³C HMBC spectra (**Appendix B.11 – B.14**). The compound 4-hydroxy-2,4-dimethyl-2,5-cyclohexadien-1-one (**3.9**) was again used as a model for the *p*-quinol moiety.⁶⁸ Specifically, the ¹³C chemical shift of the sp² hybridized C11 (131.7 ppm) and the sp³ hybridized C15 (66.4 ppm) are in agreement with the corresponding carbons in the model compound (133.3 ppm and 67.3 ppm, respectively). The ¹H chemical shifts of H13 (6.06 ppm) and H14 (6.96 ppm), along with their coupling constants (*J* = 10.0 Hz and *J* = 10.0 Hz, 2.9 Hz, respectively), also agree reasonably well with the corresponding values of the model compound (6.01 ppm, *J* = 9.9 Hz and 6.81 ppm, *J* = 9.9, 2.9 Hz).

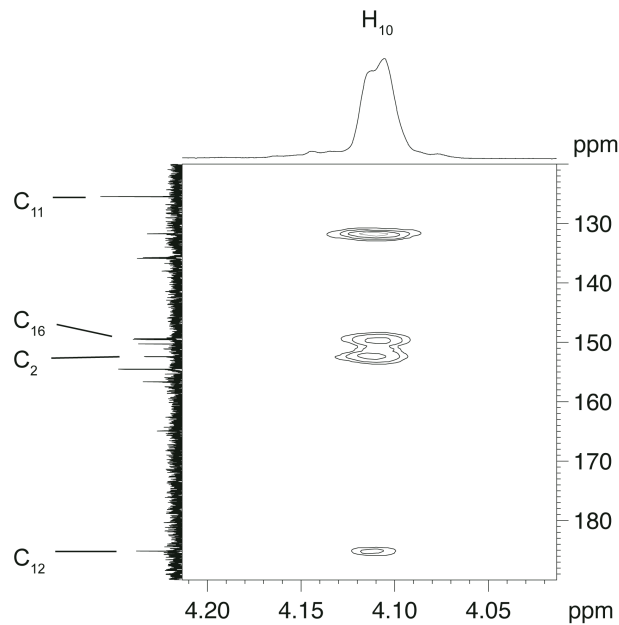
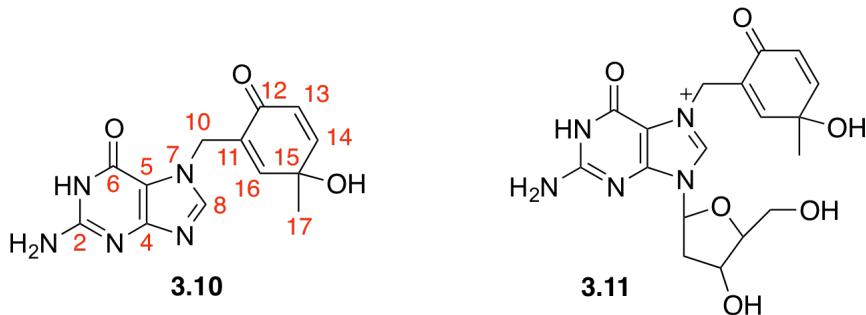


Figure 3.17. $^1\text{H} - ^{13}\text{C}$ HMBC of **3.8** in $\text{DMSO}-d_6$ at 600 MHz.

The connectivity of C10 to the N^2 position of dG was confirmed with $^1\text{H}-^{13}\text{C}$ HMBC NMR (**Figure 3.17**). Protons H10 display correlations to C2, C11, C12, and C16, but not to C6. A correlation to C6 would be indicative of an alkylation of the N1 position of dG. Protons H10 are not observed as diastereomers despite the diastereomeric composition of the NMR sample, as shown by HPLC analysis (**Figure 3.15**). This is perhaps due to less hindered rotation about the C10 - N^2 bond that is not possible in the other adduct, **3.7**. Protons H10 instead display a splitting pattern consistent with one adjacent proton (N-H). ESI⁺-MS showed a m/z 404.18 ($\text{M} + \text{H}$)⁺ that corresponds with the proposed structure of **3.8** (calculated m/z 404.16 ($\text{M} + \text{H}$)⁺).

Scheme 3.4. Proposed structure of the product (**3.11**) formed by oxidation of MeQM-dG N7 (**3.4**) and the subsequent deglycosylated product (**3.10**).



For the remaining two oxidized products of MeQM-dG, dG N7 (**3.11**) and guanine N7 (**3.10**), the two adducts were collected together since MeQM-guanine N7 is the result of deglycosylation of MeQM-dG N7. The co-collection of these two products would facilitate the isolation of the lone stable oxidation product, **3.10** (**Scheme 3.4**). The two adducts were collected together after following the 1 mL alkylation reaction and purification previously used with MeQM-dG N1 and MeQM-dG N² (**Table 3.3**). After overnight lyophilization, the two adducts were dissolved in a 1:1 solution of potassium phosphate (50 mM, pH 7) and CH₃CN at an average of 50 μL solvent per vial of lyophilized adduct and then subjected to the mild oxidation conditions (20 mmol BTI, 5 min, room temperature). Using gradient 1 with an analytical column for increased resolution, a major product was collected with a retention time of 9 - 13 minutes (**Figure 3.18**). Analysis by ¹H NMR suggested the presence of both the oxidized products of MeQM-dG N7 (**3.4**) and MeQM-guanine N7 (**3.5**) due to the observation of two signals for H8, H17, and H10 (**Figure 3.19**). The presence of the deglycosylated adduct (guanine N7) could be inferred by the ribose protons that integrated to only one set of signals for H8 and the QM fragment. ESI⁺-MS analysis showed fragments corresponding to the mass of the two oxidized

adducts (m/z 404.16 and 288.11 respectively). Unfortunately, product **3.10** is also the major fragmentation product of **3.11** under ESI⁺ conditions, so further NMR analysis was necessary to characterize the products.

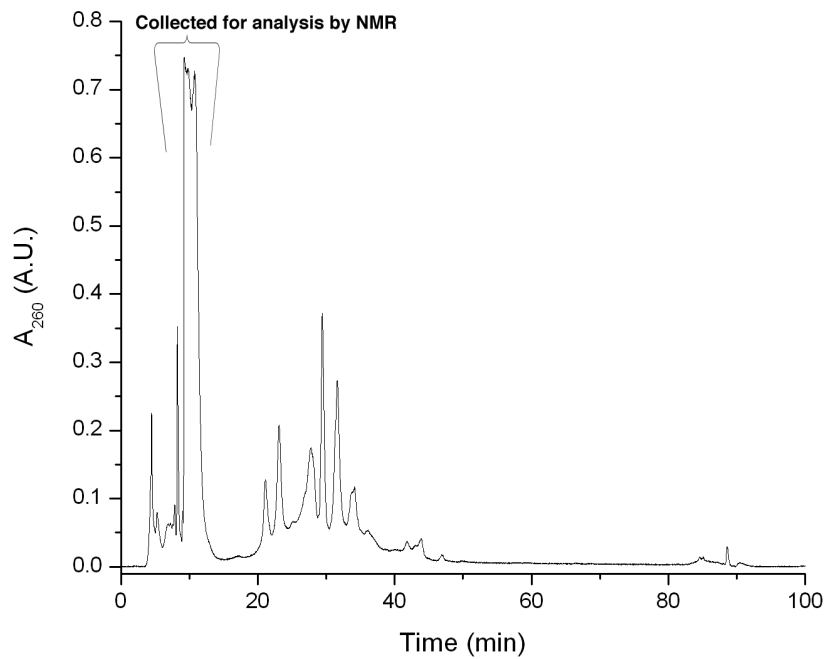


Figure 3.18. HPLC analysis of the crude oxidation of the mixture of MeQM-dG N7 (**3.4**) and MeQM-guanine N7 (**3.5**) with BTI. Reaction with BTI was held at room temperature for 5 minutes then worked-up and analyzed using Gradient 1 with the analytical column (1 mL/min).

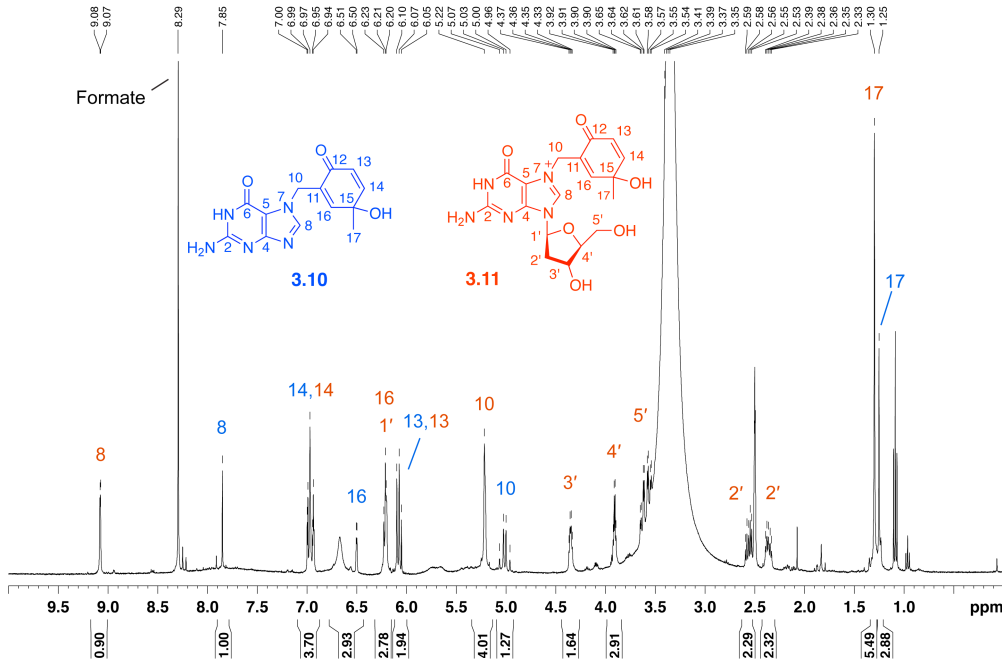


Figure 3.19. ^1H NMR of the material collected between 9 and 13 minutes of HPLC analysis of the crude oxidation of the mixture of MeQM-dG N7 (**3.4**) and MeQM-guanine N7 (**3.5**) with BTI (**Figure 3.18**).

Interestingly, two compounds with different retention times (20 and 21 minutes) and different λ_{max} (239, 280 nm and 235, 277 nm) eluted upon HPLC analysis of the NMR sample shown above (**Figure 3.20**). These two compounds were combined and ^1H NMR analysis again showed a mixture of oxidized adducts **3.10** and **3.11**. This result again suggests that the initial purification of the oxidation reaction slightly overloaded the HPLC column, shifting the retention times of the adducts forward. The initial NMR sample that was analyzed contained less material, and the adducts eluted at what is assumed to be their normal retention times (20 and 21 minutes).

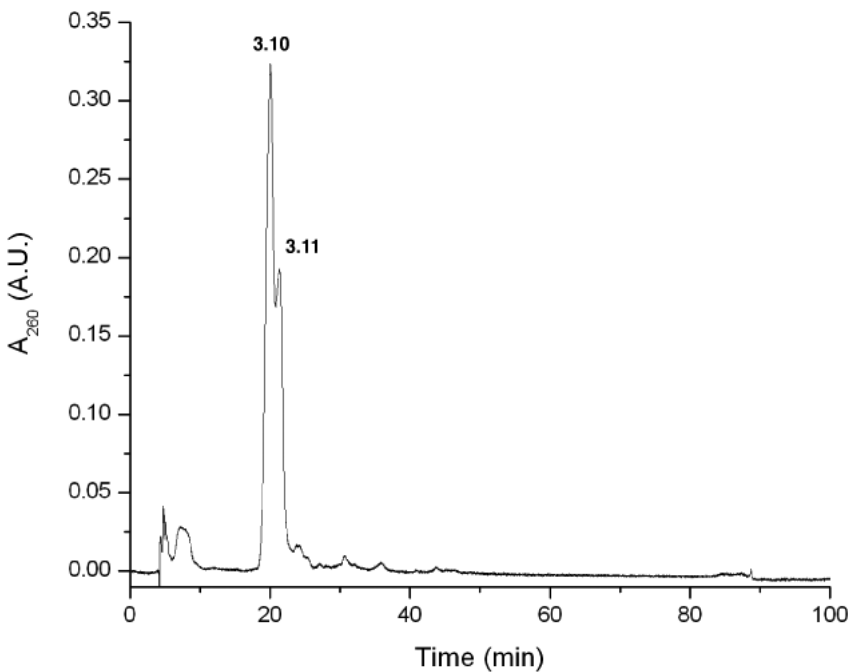


Figure 3.20. HPLC analysis of the ^1H NMR sample from **Figure 3.19**. The NMR sample was diluted with H_2O to 50% aqueous $\text{DMSO}-d_6$ prior to re-injection into the HPLC. Gradient 1 was used with the analytical column (1 mL/min).

The 1 mL scale alkylation reaction previously used with MeQM-dG N1 and MeQM-dG N² was used again to collect **3.4** and **3.5** together after HPLC purification using gradient 6 with a semi-prep column (5 mL/min) (**Table 3.3**). This will allow enough purified **3.10** to be obtained for analysis by 2D NMR. After lyophilization to remove the elution buffer, the adducts were subjected to a 5 minute oxidation discussed above. Purification by HPLC followed, again using gradient 1, and all compounds that eluted between 9 - 13 minutes were collected. After another round of lyophilization, the remaining solid was dissolved with 600 μL of a 1:1 DMSO: H_2O solution and held at 37 °C for 2 - 6 hours to complete the deglycosylation of **3.11** to form **3.10**. The solution was purified by HPLC using 200 μL per injection to avoid overloading the analytical column. A single compound eluted for each run from 19 -

23 minutes, which was collected and lyophilized overnight. This compound was fully characterized using ^1H , ^{13}C , ^1H - ^{13}C HSQC, and ^1H - ^{13}C HMBC NMR (**Appendix B.15 – B.18**).

The structure of **3.10** was proposed to be the *p*-quinol product (**Scheme 3.4**). The lack of 2'-deoxyribose sugar NMR signals indicated that this was not the oxidized product of MeQM-dG N7 (**3.11**). Assignment of the purine ^{13}C NMR signals of C2 (154.4 ppm), C4 (159.7 ppm), C5 (107.9 ppm), and C6 (152.9 ppm) were based on literature precedence of 7-methyl guanine.⁹⁰ The ^1H and ^{13}C NMR signals for C8 (7.84 and 143.4 ppm) were assigned based on ^1H - ^{13}C HSQC. The site of alkylation was confirmed by the observed correlation between the methylene bridge protons (H10) and carbons C5 and C8 associated with guanine and carbons C11, C12, and C16 associated with the former MeQM segment (**Figure 3.21**). The same correlations were previously observed for the QM-guanine N7 adduct.⁵⁶ C11 was identified by its proximity to protons H10, H13, and H16. Carbon C15 was identified by its proximity to protons H13 and H17. The ^{13}C chemical shift of C11 (131.3 ppm) was consistent with sp^2 hybridization, while the ^{13}C chemical shift of C15 (66.3 ppm) was consistent with sp^3 hybridization, which agree with ^{13}C chemical shifts of the corresponding carbons in the model compound 4-hydroxy-2,4-dimethyl-2,5-cyclohexadien-1-one (**3.9**).⁶⁸ The protons at C10 show splitting consistent with a diastereomeric relationship due to the introduction of a chiral center at C15 and restricted rotation of the methylene bridge. The two protons appear as doublets with a coupling constant of $J=15.7$ Hz, consistent with their geminal relationship. ESI⁺-MS resulted in a $(\text{M} + \text{H})^+$ of m/z 288.11 and corresponds with the structure of **3.10**.

(calculated m/z 288.11 ($M + H^+$)). Due to the location of nearby nitrogens it is mechanistically impractical for MeQM-guanine N7 or MeQM-dG N7 to form the spiro-cyclized product upon oxidation by BTI. The above evidence confirms that the *p*-quinol product is formed and not the spiro-cyclized product observed with the oxidized product of MeQM-dC N3.⁷⁶

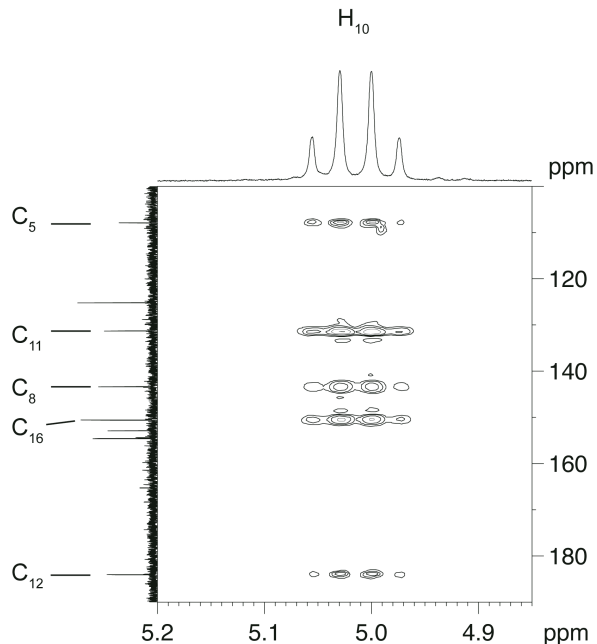


Figure 3.21. $^1\text{H} - ^{13}\text{C}$ HMBC of **3.10** in $\text{DMSO}-d_6$ at 600 MHz.

Each of the MeQM-dG adducts was confirmed to form the *p*-quinol product upon oxidation with BTI. This result serves to highlight the unique environment necessary for the spiro-cyclization to occur, especially since MeQM-dG N1 **3.2** and MeQM-dG N² **3.3** contain primary and secondary amines in the equivalent position as a primary imine in the MeQM-dC N3 adduct (**2.8**) (Figure 3.22). The position of each nitrogen does not, however, take into account the nucleophilicity of the nitrogen. The primary imine in MeQM-dC N3 (**2.8**) would be expected to be the most

nucleophilic of the three compounds and therefore would be the most likely to form the spiro-cyclized product.

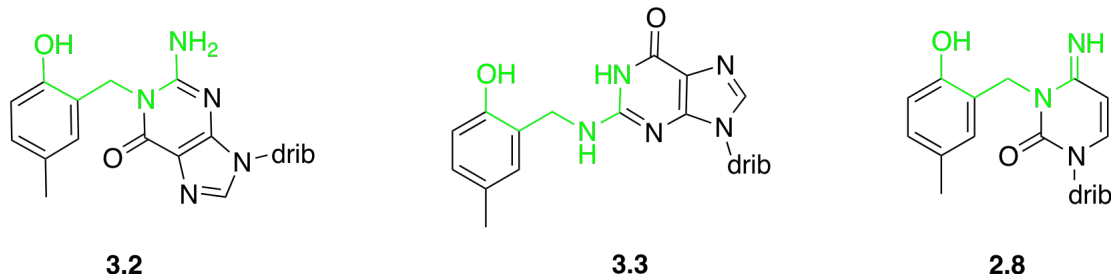


Figure 3.22. Structural similarities, labeled in green, between MeQM-dG N1 (**3.2**), MeQM-dG N² (**3.3**), and MeQM-dC N3 (**2.8**).

3.3. Summary.

The goal of oxidative de-aromatization by BTI of the adducts formed between MeQM and dG has been accomplished. Oxidation of the four MeQM-dG adducts (dG N7, dG N1, dG N², and guanine N7) yields four unique products. Due to the deglycosylation of MeQM-dG N7 to MeQM-guanine N7, only three of the oxidation products were fully characterized by 1D NMR, 2D NMR, and ESI⁺-MS as these are the only oxidized products expected to survive the enzymatic digestion of DNA. The transformation of the QM phenol to a *p*-quinol was further confirmed by comparison to a model compound, 4-hydroxy-2,4-dimethyl-2,5-cyclohexadien-1-one (**3.9**).⁶⁸ The *p*-quinol forms through an intermolecular addition of H₂O, as opposed to the intramolecular addition of the dC *exo*-imine leading to the spiro-cyclized MeQM-dC N3 product.⁷⁶ These results demonstrate the influence of the reaction environment on the oxidative de-aromatization of phenol analogues by BTI, specifically the

nucleophilicity of atoms capable of adding to the QM phenol upon its activation by BTI.

In addition to the synthesis and characterization of the oxidized MeQM-dC N3 adduct,⁷⁶ the synthesis and characterization of the oxidized MeQM-dG adducts yielded four of the six analytical standards necessary for the eventual study of MeQM alkylation with DNA. The remaining two analytical standards are the oxidized MeQM-dA adducts (dA N1 and dA N⁶), which will be characterized in a similar manner as the oxidized MeQM-dG adducts by my undergraduate mentee Omer Ad.

3.4. Materials and Methods.

Formation of the dG N1, dG N², dG N7, and guanine N7 adducts (3.2, 3.3, 3.4, 3.5) generated by the precursor 2.6 and its MeQM intermediate 2.7. Alkylation was initiated by addition of aqueous KF (500 µL, 500 mM) to a mixture of the MeQM precursor **2.6** in DMF (250 µL, 100 mM) and dG in 70% aqueous DMF (250 µL, 100 mM). The reaction was mixed and held at either room temperature (20-25 °C) or 37 °C for 1 - 5 hr. The reaction was then cooled and fractionated by semi-preparative reverse-phase C-18 HPLC using a gradient of 3 - 12% over 10 min followed by 12% isocratic over 30 min of CH₃CN in triethylammonium acetate (10 mM, pH 5) at 5 mL/min.

MeQM-dG N1 (3.2): ¹H NMR (400 MHz, DMSO-d₆): δ 2.10 (s, 3H), 2.19 (m, 1H), 2.45 (m, 1H), 3.52 (m, 2H), 3.80 (m, 1H), 4.34 (m, 1H), 5.06 (s, 2H), 6.13 (q, *J*=6.9 Hz, 1H), 6.76 (s, 1H), 6.78 (d, *J*=8.2 Hz, 1H), 6.90 (d, *J*=8.2 Hz, 1H), 7.96 (s, 1H). ESI⁺-MS: *m/z* 388.26 (M + H)⁺. Calcd for C₁₈H₂₂N₅O₅⁺ (M + H)⁺: 388.16. $\lambda_{\text{max}} =$

255, 271 nm (diode array detector, 18% CH₃CN in triethylammonium acetate, 8 mM, pH 5).

MeQM-dG N² (3.3): ¹H NMR (400 MHz, DMSO-d₆): δ 2.17 (s, 3H), 2.22 (m, 1H), 2.61 (m, 1H), 3.53 (m, 2H), 3.82 (m, 1H), 4.35 (m, 1H), 4.36 (s, 2H), 6.18 (t, *J*=6.9 Hz, 1H), 6.72 (d, *J*=8.3 Hz, 1H), 6.89 (dd, *J*=8.3, 1.6 Hz, 1H), 7.03 (d, *J*=1.6 Hz, 1H), 7.90 (s, 1H). ESI⁺-MS: *m/z* 388.27 (M + H)⁺. Calcd for C₁₈H₂₂N₅O₅⁺ (M + H)⁺: 388.16. λ_{max} = 247, 275 nm (diode array detector, 19% CH₃CN in triethylammonium acetate, 8 mM, pH 5).

MeQM-dG N7 (3.4): ¹H NMR (600 MHz, DMSO-d₆): δ 2.17 (s, 3H), 2.33 (m, 1H), 2.56 (m, 1H), 3.60 (m, 2H), 3.89 (m, 1H), 4.36 (m, 1H), 5.52 (d, *J*=5.8 Hz, 2H), 5.86 (s, 2H), 6.21 (t, *J*=6.2 Hz, 1H), 6.74 (d, *J*=8.3 Hz, 1H), 6.98 (dd, *J*=8.3, 1.8 Hz, 1H), 7.22 (d, *J*=1.8 Hz, 1H), 9.18 (s, 1H). λ_{max} = 259, 279 nm (diode array detector, 15% CH₃CN in triethylammonium acetate, 9 mM, pH 5).

MeQM-guanine N7 (3.5): ¹H NMR (400 MHz, DMSO-d₆): δ 2.11 (s, 3H), 5.30 (s, 2H), 6.72 (d, 1H), 6.80 (d, 1H), 6.90 (dd, 1H), 7.84 (s, 1H). ESI⁺-MS: *m/z* 272.18 (M + H)⁺. Calcd for C₁₃H₁₄N₅O₂⁺ (M + H)⁺: 272.11. λ_{max} = 283 nm (diode array detector, 17% CH₃CN in triethylammonium acetate, 8 mM, pH 5).

Oxidation of the dG N7 and guanine N7 adducts 3.4 and 3.5 to form 3.10. The adducts **3.4** and **3.5** were combined with 100 μL CH₃CN and 100 μL potassium phosphate (50 mM, pH 7). The starting amount of **3.4** and **3.5** were unknown due to the small amounts isolated from each HPLC separation. Instead, an average of 50 μL solvent per vial was used as a guideline to dissolve **3.4** and **3.5**. The mixture was

treated with 100 μ L BTI (200 mM in CH₃CN) for 5 minutes at room temperature. The reaction was then diluted with water (100 μ L) and washed with diethyl ether (3 \times 500 μ L). The aqueous phase was filtered through a 0.2 μ m syringe filter and fractionated by analytical reverse-phase C-18 HPLC using a linear gradient of 3 - 25% CH₃CN in ammonium formate (10 mM, pH 6.9) over 76 min (1 mL/min). The product **3.10** was collected (t_r = 20 min) and lyophilized to yield a white solid. A reliable yield could not be measured due to the small amounts of product isolated from each HPLC separation. ¹H NMR (600 MHz, DMSO-d₆): δ 1.25 (s, 3H), 4.99 (d, J =15.7 Hz, 1H), 5.04 (d, J =15.7 Hz, 1H), 6.06 (d, J =10.1 Hz, 1H), 6.51 (s, 1H), 6.95 (dd, J =2.8, 10.1 Hz, 1H), 7.84 (s, 1H). ¹³C NMR (600 MHz, DMSO-d₆): δ 27.1, 43.8, 66.3, 107.9, 125.2, 131.3, 143.4, 150.6, 154.6, 184.1. ESI⁺-MS: *m/z* 288.11 (M + H)⁺. Calcd for C₁₃H₁₄N₅O₃⁺ (M + H)⁺: 288.11. $\lambda_{\text{max}} = 239, 283$ nm (diode array detector, 9% CH₃CN in ammonium formate, 9 mM, pH 6.9).

Oxidation of the dG N1 and dG N² adducts **3.2 and **3.3** to form **3.7** and **3.8**.**

The oxidation of **3.2** and **3.3** was identical to the above procedure for **3.4** and **3.5**. The two products **3.7** and **3.8** were collected separately (t_r = 25 min and 30 min) and lyophilized to yield a yellow solid (**3.7**) and a white solid (**3.8**). A reliable yield could not be measured due to the small amounts of product isolated from each HPLC separation.

MeQM-dG N1 Oxidized adduct (3.7**):** ¹H NMR (600 MHz, DMSO-d₆): δ 1.25 (s, 3H), 2.22 (m, 1H), 2.54 (m, 1H), 3.53 (m, 2H), 3.81 (m, 1H), 4.34 (m, 1H), 4.62 (d, J =15.7 Hz, 1H), 4.88 (d, J =15.7 Hz, 1H), 6.09 (d, J =10.0 Hz, 1H), 6.13 (m, 1H), 6.15

(t, $J=6.9$ Hz, 1H), 6.95 (dd, $J=2.9, 10.0$ Hz, 1H), 7.97 (s, 1H). ^{13}C NMR (600 MHz, DMSO-d₆): δ 27.4, 39.4, 39.5, 61.7, 66.5, 70.8, 82.2, 87.6, 115.6, 125.5, 129.5, 135.7, 146.3, 149.4, 153.9, 154.3, 156.2, 184.8. ESI⁺-MS: m/z 404.13 (M + H)⁺. Calcd for C₁₈H₂₂N₅O₆⁺ (M + H)⁺: 404.16. m/z 442.06 (M + K)⁺. Calcd for C₁₈H₂₁KN₅O₆⁺ (M + K)⁺: 442.11. $\lambda_{\max} = 243, 271$ nm (diode array detector, 10% CH₃CN in ammonium formate, 9 mM, pH 6.9).

MeQM-dG N² Oxidized adduct (3.8): ^1H NMR (600 MHz, DMSO-d₆): δ 1.31 (s, 3H), 2.19 (m, 1H), 2.58 (m, 1H), 3.50 (m, 2H), 3.80 (m, 1H), 4.11 (d, $J=5.3$ Hz), 4.32 (m, 1H), 6.06 (d, $J=10.0$ Hz, 1H), 6.14 (t, $J=6.9$ Hz, 1H), 6.80 (m, 1H), 6.96 (dd, $J=2.9, 10.0$ Hz, 1H), 7.91 (d, $J=2.5$ Hz, 1H). ^{13}C NMR (600 MHz, DMSO-d₆): δ 27.3, 38.9, 39.3, 61.8, 66.4, 70.8, 82.8, 87.6, 117.0, 125.5, 131.7, 135.7, 149.4, 150.3, 152.4, 154.5, 156.6, 185.1. ESI⁺-MS: m/z 404.18 (M + H)⁺. Calcd for C₁₈H₂₂N₅O₆⁺ (M + H)⁺: 404.16. $\lambda_{\max} = 243, 271$ nm (diode array detector, 12% CH₃CN in ammonium formate, 9 mM, pH 6.9).

HPLC gradients used in this chapter can found in **Table 3.3**.

Chapter 4: Alkylation of DNA by MeQM and Subsequent Enzymatic Digestion

4.1. Introduction.

Identification of the complete profile of adducts formed between MeQM and DNA is necessary for understanding the selectivity of MeQM towards DNA. While standard analysis of DNA alkylating agents would consist of a lengthy (24 hr) enzymatic digestion of alkylated DNA followed by LC/MS, this method fails for MeQM for two reasons. The first reason is that multiple MeQM adducts at a particular nucleoside would have the same mass. Therefore MS would be unable to provide important information about the position of the covalent linkage between MeQM and DNA. The second reason is that the alkylation profile of DNA by MeQM would change drastically over the course of enzymatic digestion because some of the MeQM-DNA adducts are labile.

Oxidative de-aromatization of the QM phenol with BTI followed by HPLC analysis would solve both of the issues stated above. The oxidative trapping of MeQM-DNA adducts would transform the labile adducts to stable adducts, allowing them to survive the enzymatic digestion. Also, to eliminate the need to isolate and characterize the oxidized MeQM-DNA adducts (by LC/MS or NMR), analytical standards for each oxidized adduct were synthesized and fully characterized (**Figure 4.1**). The synthesis and characterization of oxidized MeQM-dC N3 (**2.15**) was

discussed in Chapter 2.⁷⁶ The synthesis and characterization of oxidized MeQM-dG N1 (**3.7**), MeQM-dG N² (**3.8**), and MeQM-guanine N7 (**3.10**) were discussed in Chapter 3. Synthetic studies and structure elucidation of oxidized MeQM-dA N1 (**4.4**) and oxidized MeQM-dA N⁶ (**4.3**) were carried out simultaneously by my undergraduate mentee Omer Ad.

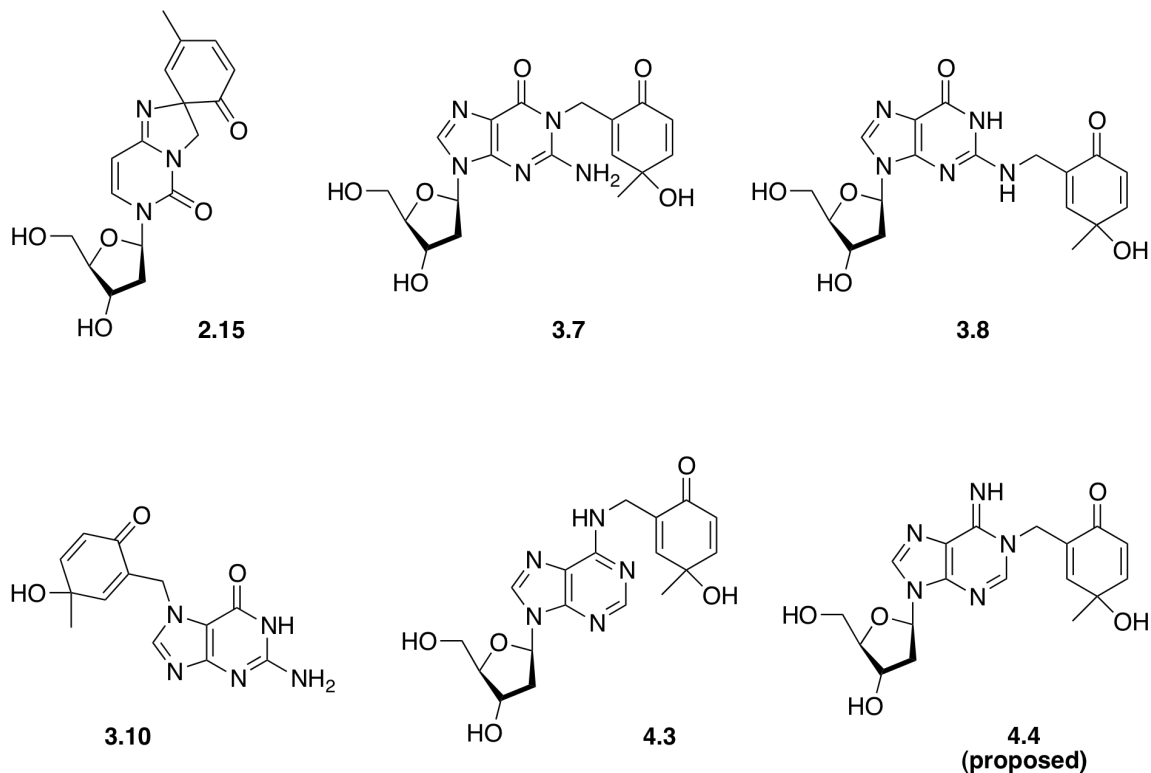


Figure 4.1. Fully characterized products of the BTI oxidation of MeQM-dC N3 (**2.15**), MeQM-dG N1 (**3.7**), MeQM-dG N² (**3.8**), MeQM-guanine N7 (**3.10**), and MeQM-dA N⁶ (**4.3**). The oxidation product of MeQM-dA N1 (**4.4**) has not been confirmed.

The MeQM-dA N1 (**4.1**) and MeQM-dA N⁶ (**4.2**) adducts were successfully synthesized using procedures optimized for the formation of each adduct.⁹¹ As the dA N1 position is more reactive than the dA N⁶ position, the formation of MeQM-dA N1 was favored at short reaction times (20 minutes) while the formation of MeQM-dA N⁶ was favored at longer reaction times (72 hours). The formation of both adducts

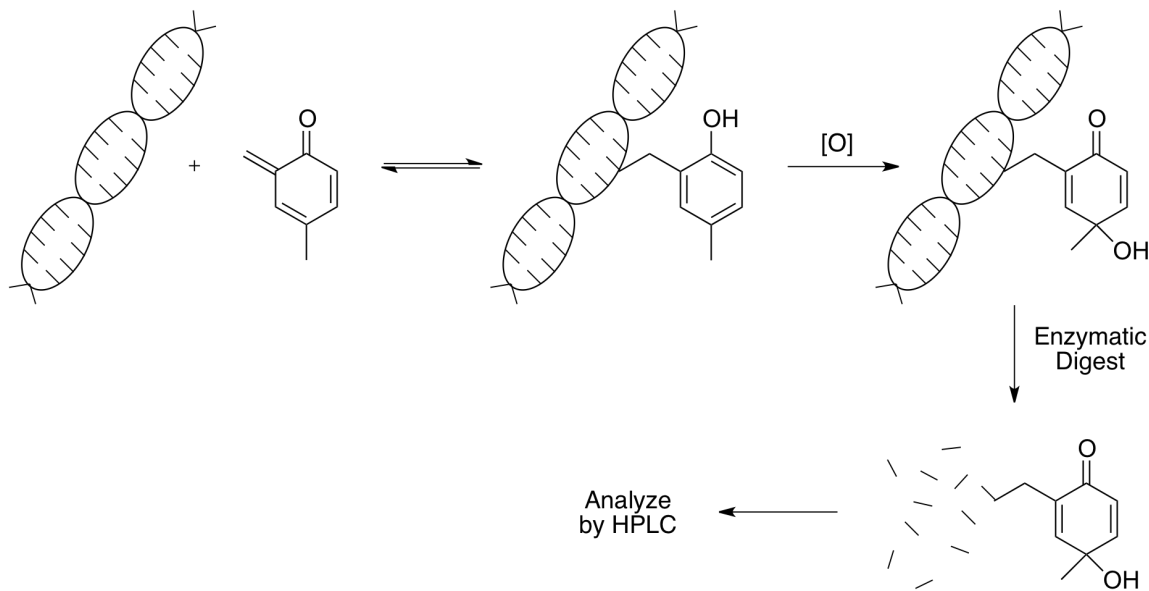
was initiated by the addition of KF to a solution of 4-MeBrQMP, dA, and potassium phosphate in a 1:1.8:1.2 mixture of CH₃CN:DMF:H₂O. The structure of both MeQM-dA N1 and MeQM-dA N⁶ was elucidated with ¹H NMR, ¹³C NMR, and ESI⁺-MS.⁹¹

MeQM-dA N1 and MeQM-dA N⁶ were oxidized separately, after HPLC purification, using the same procedure that was used to form the oxidized MeQM-dG adducts. The structure of oxidized MeQM-dA N⁶ (**4.3**) was elucidated with 1D and 2D NMR along with ESI⁺-MS and comparison to model compounds N⁶-Me-dA,⁹² N1-Me-dA,⁹³ and 4-hydroxy-2,4-dimethyl-2,5-cyclohexadien-1-one (**3.9**).⁶⁸ Unfortunately, oxidized MeQM-dA N1 (**4.4**) was not characterized due to instability of the product. This remains the only uncharacterized oxidation product of MeQM alkylation of dN and studies are ongoing to remedy this issue. Until that time, oxidation studies with MeQM-DNA that yield a single unknown product can only assume and not confirm that the product is the result of oxidation of MeQM-dA N1.

The alkylation of dsDNA by a simple *o*-QM has been previously studied by the Rokita laboratory.⁶² These studies observed predominant formation of QM-dG N². At the time, this preference was explained solely by the ability of the *exo*-amino group of dG to maintain its reactivity from nucleosides to dsDNA.⁶² It was later discovered that the alkylation profile of nucleosides varies greatly over the time needed for enzymatic digestion of DNA (24 hours).⁵⁸ Specifically, the initial alkylations occur with the stronger nucleophilic positions (dG N7, dA N1, and dC N3), but these adducts are reversible. Alkylation with the weaker nucleophilic positions (dG N1, dG N², and dA N⁶) occurs slower, but since the adducts are

irreversible they will accumulate over time. The result of these processes is a significantly different alkylation profile at the beginning of DNA digestion than at the end of DNA digestion, when the mixture is analyzed by HPLC. The oxidative de-aromatization of QM phenols by BTI discussed earlier has the potential to trap the labile MeQM-DNA adducts prior to enzymatic digestion (**Scheme 4.1**). This will allow, for the first time, quantification of MeQM alkylation of DNA at short, but biologically relevant, time points.

Scheme 4.1. Oxidative de-aromatization can trap labile MeQM-DNA adducts. The trapped MeQM-DNA adducts are stable enough to persist through enzymatic digestion of the DNA and the subsequent analysis by HPLC.



4.2. Results and Discussion.

4.2.1. Optimization of the Enzymatic Digestion of DNA.

The early studies of QM alkylation of DNA were based on the following experiments involving the formation and subsequent oxidation of MeQM-DNA adducts.⁶² One aspect of the MeQM-DNA experiments to be optimized is the enzymatic digestion of DNA. The complete enzymatic digestion of DNA to the nucleoside level is necessary for the subsequent HPLC analysis. The individual nucleosides and nucleoside adducts are well resolved using a gradient of 3 – 11% CH₃CN in 50 mM TEAA, pH 4 over 24 minutes (1 mL/min) followed by 11 – 25% CH₃CN in 50 mM TEAA pH 4 over the next 85 minutes (1 mL/min).⁶² The different compounds are well resolved due to the large change in structure of each nucleoside adduct by the addition of MeQM. Undigested DNA containing MeQM adducts, however, would elute as an unresolved peak. This is because even several MeQM additions have little influence on a molecule the size of polymeric DNA and differing amounts of alkylation would not be distinguished by HPLC.

The two enzymes involved in the digestion are phosphodiesterase I (from *Crotalus adamanteus* venom) and alkaline phosphatase (from *Escherichia coli*). Phosphodiesterase I is an exonuclease responsible for breaking the 3' phosphorus-oxygen bond in DNA stepwise from the 3' terminus^{94,95} while alkaline phosphatase dephosphorylates the resulting mononucleotides at their 5' position. When used together, the two enzymes digest DNA to monomeric nucleosides free of phosphate. Alkaline phosphatase was stored at a concentration of 0.1 unit/μL in a solution of 50 mM Tris-HCL pH 8, 50 μM ZnSO₄, 10 mM MgCl₂, and 50% glycerol.

Phosphodiesterase I was initially stored at a concentration of 0.001 unit/ μ L in 100 mM TEAA pH 10. For later studies, phosphodiesterase I was stored at a concentration of 0.005 unit/ μ L in a solution of 50 mM Tris-HCL pH 8, 50 μ M ZnSO₄, 10 mM MgCl₂, and 50% glycerol. These storage conditions protect against degradation from repeated freezing and thawing while providing Mg²⁺ and Zn²⁺ needed for the catalytic activity of the enzymes.^{96,97}

The work-up and digestion conditions after alkylation of DNA were based on previous work by Gao et al.,⁹⁸ Lewis et al.,⁴³ and Pande et al.⁶² Initially for a 200 μ L scale alkylation, once the alkylation and oxidation reactions are complete, the CH₃CN was removed under a stream of N₂ (15 minutes). The DNA was precipitated by adding EtOH (55 μ L, 100 %) and cooling to -20 °C for 30 minutes. The EtOH was evaporated under reduced pressure and the remaining DNA was washed with additional EtOH (140 μ L, 80 %), frozen with liquid N₂, and centrifuged (15 minutes, 14,800 rpm). The supernatant was decanted from the Eppendorf tube and the remaining solid was dissolved in 100 mM TEAA (100 μ L, pH 10) and hydrolyzed by alkaline phosphatase (0.2 units per 1 mM nts DNA) and phosphodiesterase I (0.006 units per 1 mM nts DNA). The digestion mixture was held at 37 °C for 24 hours, followed by neutralization to pH 7 with 1% aqueous acetic acid (5 μ L). The mixture was filtered through a 0.2 μ m syringe filter (with an addition of 50 μ L H₂O when necessary) and fractionated by analytical reverse-phase C18 chromatography (3% CH₃CN in 9.7 mM ammonium formate, pH 6.9, to 11% CH₃CN in 8.9 mM ammonium formate, pH 6.9, over 24 minutes (1 mL/min), followed by 11% CH₃CN in 8.9 mM ammonium formate, pH 6.9, to 25% CH₃CN in 7.5 mM ammonium

formate, pH 6.9, over the next 85 minutes). This is the only HPLC gradient used in this chapter. This procedure for enzymatic digestion of DNA is known as **Method 1**.

Prior to alkylation and oxidation studies, a number of control experiments were necessary to optimize conditions that resulted in the complete enzymatic digestion of the target DNA, along with confirming that the alkylation and oxidation conditions were compatible with enzymatic digestion. The initial target DNA was calf thymus DNA (ctDNA), a large molecular weight DNA historically used to represent a large duplex DNA of random sequence.^{43,56,62} The findings are summarized in **Table 4.1**. Experiments 1-4 did not contain 4-MeBrQMP or BTI and served as blank controls, containing only ctDNA and potassium phosphate pH 7 in a 70:30 solution of H₂O:CH₃CN. Experiment 1 revealed that 2 mM nucleotides (nts) of ctDNA was insufficient to determine digestion by HPLC. Experiments 2-4 confirmed that 10 mM nts ctDNA was sufficient to observe digestion by HPLC. An effective ratio of enzymes to ctDNA was also determined. In experiment 5, ctDNA was alkylated by a ten-fold excess of 4-MeBrQMP activated with KF (525 mM) in 30% aqueous CH₃CN for 30 minutes prior to enzymatic digestion, to simulate the alkylation conditions. The complete enzymatic digestion of ctDNA was observed by HPLC. In experiment 6, 4-MeBrQMP was omitted, but an excess of BTI (167 mM) was added to the ctDNA solution and the mixture was kept at room temperature for 5 minutes followed by enzymatic digestion, to simulate the oxidation conditions. Again, complete enzymatic digestion of ctDNA was observed by HPLC.

Table 4.1. Enzymatic digestion conditions for the initial ctDNA experiments, compared to the literature precedent.⁶²

Exp	[Nucleotides] (mM)	Alkaline Phosphatase	Phosphodiesterase I	Complete Digestion?
Literature ⁶²	20	10 units	0.27 units	yes
1	2	1 unit (10 µL)	0.03 units (30 µL)	Insufficient DNA
2 - 6	10	2 units (20 µL)	0.06 units (60 µL)	yes

While the ctDNA was completely digested in each experiment, including experiment 6 containing BTI, one issue needed to be addressed. This issue was that in experiment 6, precipitation occurred upon addition of the BTI. If the precipitate was ctDNA, then it may prove to be difficult to oxidize the MeQM-DNA adducts. A series of trials involving the alkylation conditions and the addition of BTI addressed the precipitation issue. For these trials, three different duplex DNAs were used to observe any influence by the oligo length or sequence. The three duplex DNAs were ctDNA, salmon sperm DNA (salDNA) which is another large molecular weight DNA historically^{99,100} used as a large duplex DNA of random sequence, and **OD1/OD3** which was conveniently available as excess material from Dr. Jen Buss from an unrelated project (**Figure 4.2**). In each case that duplex DNA (ctDNA, salDNA, or **OD1/OD3**) was included in the mixture, a precipitate was formed upon addition of BTI. A large concentration (>31 mM) of K⁺ also seemed to result in precipitate formation upon addition of BTI. A large concentration (225 mM) of Na⁺ did not result in a precipitate upon addition of BTI. Fluoride was also added at a concentration of 200 mM without precipitate formation upon addition of BTI. Washing the reaction with saturated diethyl ether (3 × 200 µL) 5 minutes after BTI addition appeared to decrease the amount of precipitate, suggesting that not all of the

precipitate was DNA. These trials lead to general conditions for the alkylation and subsequent oxidation of duplex DNA. These conditions for enzymatic digestion of DNA, further known as **Method 2**, effectively solved the precipitation issue and included the use of Na^+ counter ions where possible and a saturated diethyl ether wash ($3 \times 200 \mu\text{L}$) prior to EtOH precipitation of the DNA.

OD1 = 5'-d(TGATAGCGGCCGCTAATGGTGATGGTGATGGTGTACTGT)
OD3 = 3'-d(ACTATGCCGGCGATTACCACTACCACATGACA)

Figure 4.2. Synthesized complimentary oligonucleotide sequences used as target duplex DNA.

A series of experiments used the improved reaction conditions (**Method 2**) to confirm that the alkylation and oxidation conditions were compatible with enzymatic digestion. For these experiments, ctDNA was replaced by salDNA as the random sequence duplex DNA because the remainder of ctDNA in the laboratory was dissolved in potassium phosphate buffer and a large quantity of lyophilized salDNA was available. The first experiment was to dissolve the salDNA (8 mM nts) under alkylation and oxidation conditions without the presence of 4-MeBrQMP or BTI. The reaction was then worked-up and digested according to **Method 2** using 2 units of alkaline phosphatase ($20 \mu\text{L}$) and 0.06 units of phosphodiesterase I ($60 \mu\text{L}$). This resulted in fully digested salDNA with no background compounds eluting after the nucleosides ($t_r > 20$ minutes) providing a clean baseline for the detection of nucleoside adducts (**Figure 4.3**). The nucleosides are identified by comparison of t_r to the literature.⁶²

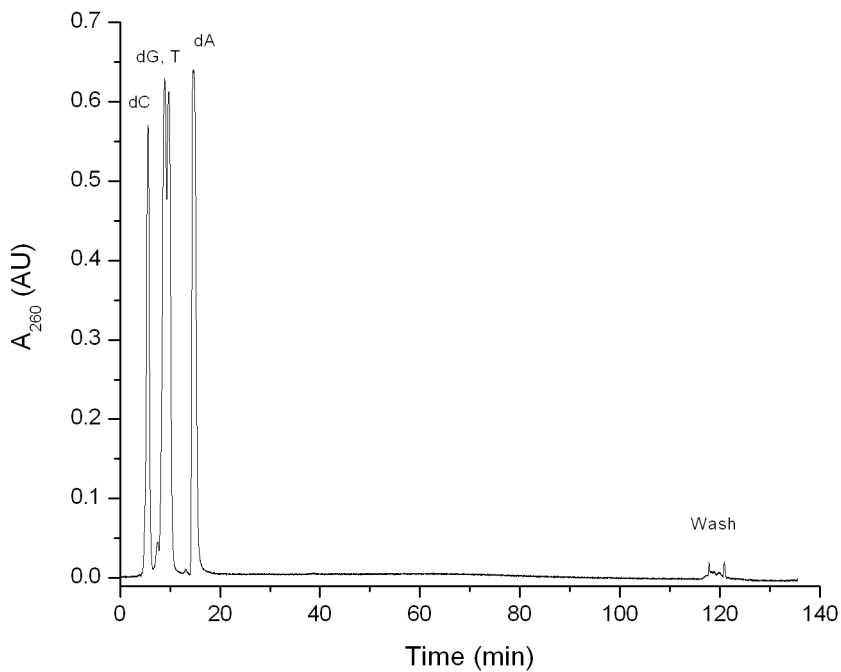


Figure 4.3. HPLC analysis of the enzymatic digestion of a reaction consisting of salDNA (8 mM nts), sodium phosphate (25 mM, pH 7), and NaF (200 mM) in an 80:20 solution of H₂O:CH₃CN. The reaction was worked-up and digested according to **Method 2** using alkaline phosphatase (2 units, 20 μ L) and phosphodiesterase I (0.06 units, 60 μ L).

The next experiment aimed to determine if BTI would inhibit the enzymatic digestion of salDNA. Again, salDNA (8 mM nts) was combined with sodium phosphate (25 mM, pH 7), and NaF (200 mM) in an 80:20 mixture of H₂O:CH₃CN (200 μ L). BTI (20 μ L, 91 mM) was added to the reaction and held for 5 minutes at room temperature prior to work-up following **Method 2**, using 2 units of alkaline phosphatase (20 μ L) and 0.06 units of phosphodiesterase I (60 μ L). The salDNA was completely digested, with no observable background noise or oxidation by-products eluting after the nucleosides ($t_r > 20$ minutes) (**Figure 4.4**).

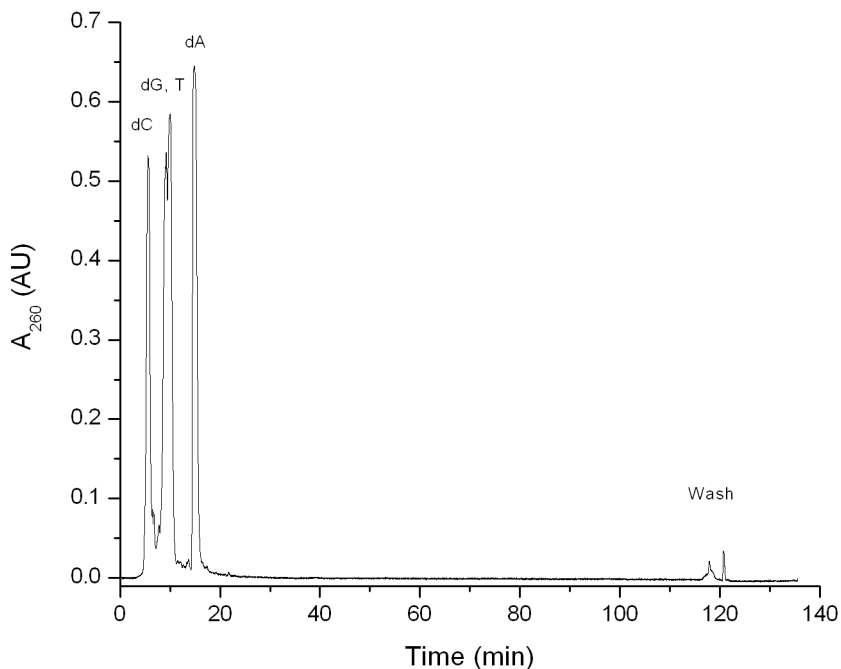


Figure 4.4. HPLC analysis of the enzymatic digestion of a reaction consisting of salDNA (8 mM nts), sodium phosphate (25 mM, pH 7), and NaF (200 mM) in an 80:20 solution of H₂O:CH₃CN. BTI (91 mM) was added to the reaction and held for 5 minutes prior to work-up and digestion according to **Method 2** using alkaline phosphatase (2 units, 20 µL) and phosphodiesterase I (0.06 units, 60 µL).

Through the course of these experiments, the phosphodiesterase I purchased from Sigma-Aldrich was exhausted and a new supplier (Worthington Biochemical) was found to offer significantly more enzyme activity (100 units vs. 0.6 units) for approximately the same price, which would be advantageous due to the large amount of enzyme needed for future experiments. Unfortunately, the new phosphodiesterase I failed to fully digest salDNA in a series of experiments using previously successful reaction conditions.

To improve the solubility of the duplex DNAs (ctDNA and salDNA), a new duplex DNA was chosen to test the less active phosphodiesterase I. The new DNA, **OD1/OD3**, was 40 base pairs long and was easily dissolved in the digestion buffer

after work-up, unlike ctDNA and salDNA which required more time to completely dissolve (**Figure 4.2**). **OD1/OD3** was also unsuccessfully digested by the phosphodiesterase I from Worthington Biochemical in a series of experiments, which included increasing the amount of enzyme from 0.06 units to 0.75 units while keeping the concentration of DNA at 8 mM nts.

At this point there appeared to be enough evidence that the phosphodiesterase I from Worthington Biochemical was inferior to that from Sigma-Aldrich. Due to the inability of the phosphodiesterase I from Worthington Biochemical to completely digest the target DNA, further experiments utilized the more expensive, but effective phosphodiesterase I from Sigma-Aldrich. The large difference in activity of phosphodiesterase I from two different suppliers highlights the need to test chemicals and enzymes from previously unused suppliers to confirm their effectiveness.

The activity of phosphodiesterase I from Sigma-Aldrich was tested by digesting a reaction that consisted of **OD1/OD3** (20 mM nts), sodium phosphate (25 mM, pH 7), and KF (500 mM) in a 70:30 solution of H₂O:CH₃CN. The reaction was subjected to work-up and digestion conditions from **Method 2** using alkaline phosphatase (10 units, 100 µL) and phosphodiesterase I (0.28 units, 56 µL). This resulted in complete digestion of the target DNA (**Figure 4.5**).

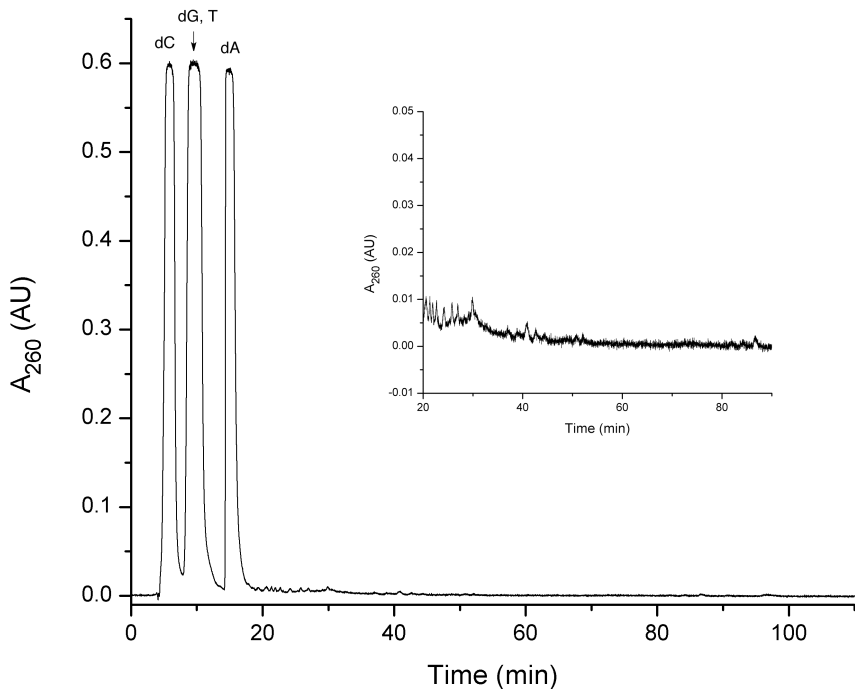


Figure 4.5. HPLC analysis of the enzymatic digestion of a reaction consisting of **OD1/OD3** (20 mM nts), sodium phosphate (25 mM, pH 7), and KF (500 mM) in an 70:30 solution of $\text{H}_2\text{O}:\text{CH}_3\text{CN}$. The reaction was subjected to work-up and digestion according to **Method 2** using alkaline phosphatase (10 units, 100 μL) and phosphodiesterase I (0.28 units, 56 μL).

Now that the enzymatic digestion of target DNA has been optimized, the alkylation of the target DNA by MeQM could be investigated.

4.2.2. Alkylation of DNA by MeQM.

Early experiments using ctDNA as the target DNA observed no alkylation when the reactions were analyzed by HPLC (**Table 4.1**). This would make it impossible to observe the subsequently formed oxidized MeQM-DNA adducts. A series of experiments replaced DNA in the alkylation reaction with an equimolar solution of nucleosides (dC, dG, dA, and dT) to determine the amount of dN and 4-MeBrQMP needed to observe alkylation by HPLC. The first reaction combined 8

mM dN, 25 mM sodium phosphate pH 7, 200 mM NaF, and 67 mM 4-MeBrQMP in a 80:20 aqueous: CH₃CN solution. The reaction was incubated in a 1.5 mL plastic Eppendorf tube for 30 minutes at 37 °C, filtered (0.2 µm), and analyzed by HPLC (**Figure 4.6**). There was almost no detectable alkylation.

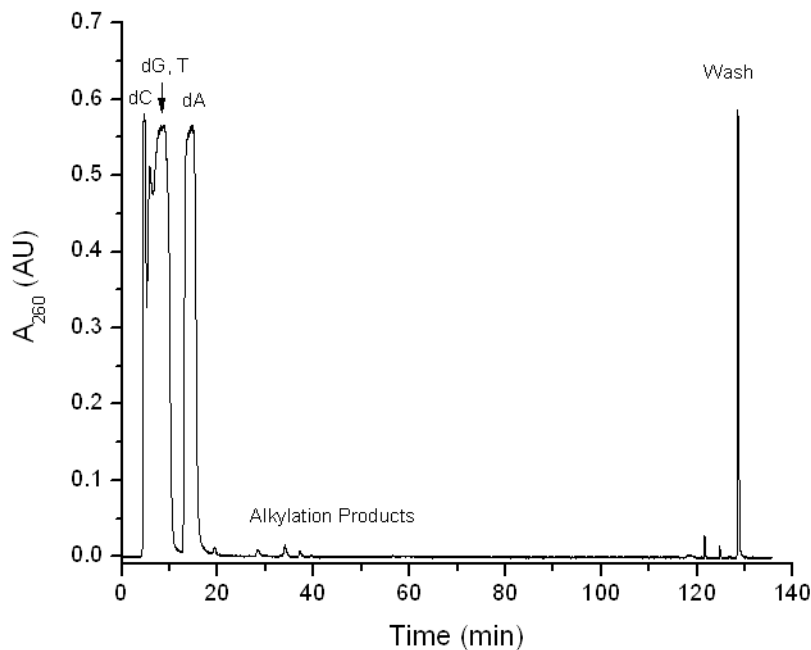


Figure 4.6. HPLC analysis of an alkylation reaction consisting of 2 mM each dN, 25 mM sodium phosphate (pH 7), 200 mM NaF, and 67 mM 4-MeBrQMP in an 80:20 solution of H₂O:CH₃CN. The reaction was carried out in a 1.5 mL plastic Eppendorf tube for 30 minutes at 37 °C.

The next reaction increased the concentration of 4-MeBrQMP to 160 mM, but these conditions still failed to produce a significant amount of alkylation (measured by integration of the peak area at A₂₆₀, **Figure C.1**) compared to the baseline (**Figure 4.5**). Further increasing 4-MeBrQMP concentration to 240 mM, substituting KF (500 mM) for NaF (200 mM) due to the higher solubility of KF in H₂O, and increasing the CH₃CN percentage from 20% to 30% slightly increased the alkylation yield (**Figure C.2**). Lengthening the reaction time from 30 minutes to one hour further increased

the alkylation yield (**Figure C.3**), while a larger increase came with switching from plastic Eppendorf tubes to 0.3 mL glass Reacti-vials equipped with Teflon stirbars (**Figure C.4**). This effect is most likely the result of stirring the reaction as opposed to allowing the reagents to react through diffusion. The most promising results came when the concentration of nucleosides was increased to 20 mM total dN while 4-MeBrQMP was kept at 240 mM (**Figure 4.7**).

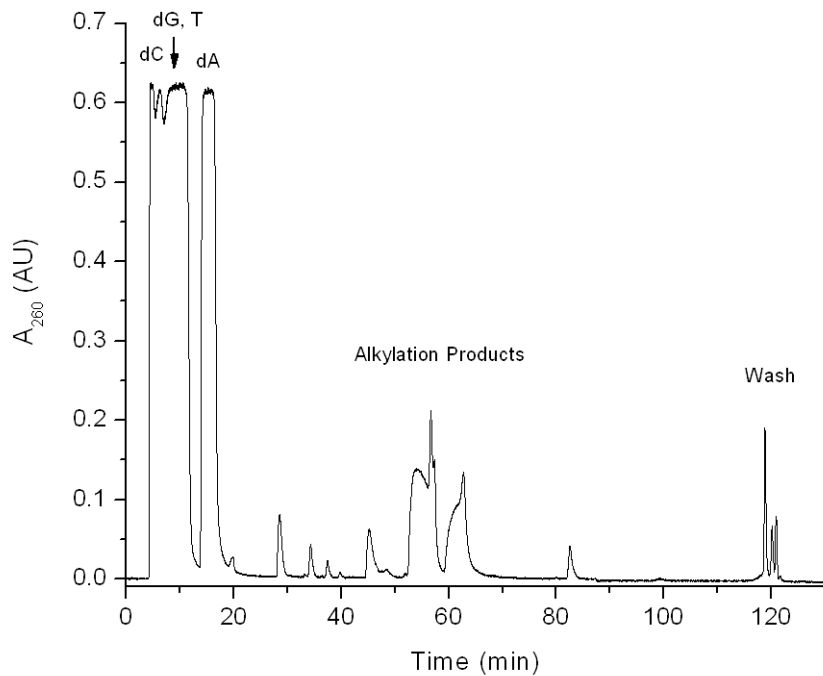


Figure 4.7. HPLC analysis of an alkylation reaction consisting of 5 mM each dN, 25 mM sodium phosphate (pH 7), 500 mM KF, and 240 mM 4-MeBrQMP in a 70:30 solution of H₂O:CH₃CN. The reaction was stirred in a 0.3 mL glass Reacti-vial for 1 hour at 37 °C.

The next experiment used the optimum alkylation conditions of dN and applied them to the alkylation of salDNA. Guided by the earlier nucleoside results, a 200 µL reaction mixture consisting of 20 mM nts salDNA, 25 mM sodium phosphate pH 7, 500 mM KF, and 240 mM 4-MeBrQMP in a 70:30 aqueous: CH₃CN solution was stirred in a 0.3 mL glass Reacti-vial for 1 hour at 37 °C. To simulate the BTI

addition, an additional 40 μ L CH₃CN was added after the 1 hour. The reaction was worked-up and digested according to **Method 2** using 6 units of alkaline phosphatase (60 μ L) and 0.18 units of phosphodiesterase I (90 μ L). Despite compensating for the 2.5 fold increase in salDNA by increasing the amount of enzymes (units) by 3 fold, undigested salDNA was present in the analysis (**Figure 4.8**). Another problem was that little to no alkylation was observed, which may have been due to the high concentration of 4-MeBrQMP that did not appear to be fully miscible in the reaction mixture.

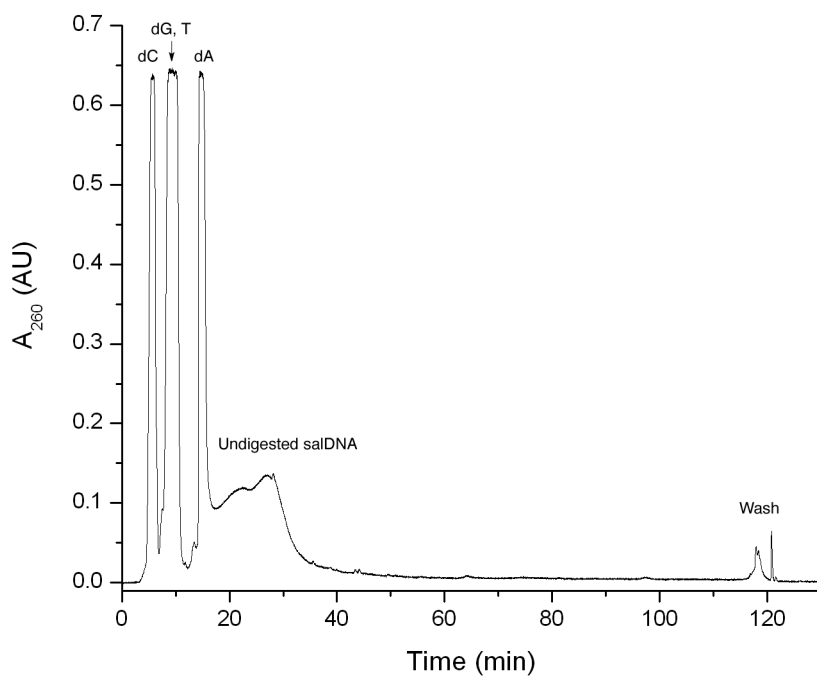


Figure 4.8. HPLC analysis of an alkylation reaction consisting of 20 mM salDNA, 25 mM sodium phosphate (pH 7), 500 mM KF, and 240 mM 4-MeBrQMP in a 70:30 solution of H₂O:CH₃CN. The reaction was stirred in a 0.3 mL glass Reacti-vial for 1 hour at 37 °C prior to an addition of 40 μ L CH₃CN to simulate the addition of BTI. The reaction was worked-up and digested according to **Method 2** using alkaline phosphatase (6 units, 60 μ L) and phosphodiesterase I (0.18 units, 90 μ L).

To adjust for these two problems, the next experiment increased the amount of enzymes 4-fold to 8 units (80 μ L) alkaline phosphatase and 0.24 units (120 μ L) phosphodiesterase I while the concentration of 4-MeBrQMP was decreased from 240 mM to 100 mM. The ensuing reaction mixture was fully miscible and resulted in a complete digestion of the salDNA, but only trace amounts of alkylation were observed (**Figure 4.9**) when compared to the optimized dN alkylation (**Figure 4.7**).

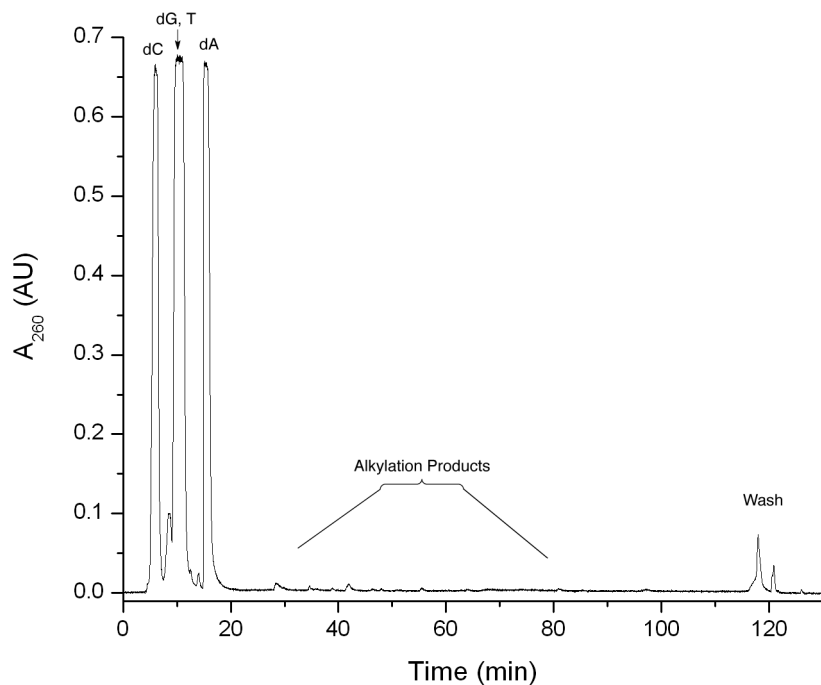


Figure 4.9. HPLC analysis of an alkylation reaction consisting of 20 mM salDNA, 25 mM sodium phosphate (pH 7), 500 mM KF, and 100 mM 4-MeBrQMP in a 70:30 solution of $H_2O:CH_3CN$. The reaction was stirred in a 0.3 mL glass Reacti-vial for 1 hour at 37 °C prior to an addition of 40 μ L CH_3CN to simulate the addition of BTI. The reaction was worked-up and digested according to **Method 2** using alkaline phosphatase (8 units, 80 μ L) and phosphodiesterase I (0.24 units, 120 μ L).

A possible complication with a large target DNA, such as ctDNA or salDNA, is the potential for it to form complex secondary structures that may suppress alkylation by MeQM. The large target DNA was also difficult to dissolve following the work-up prior to enzymatic digestion. The shorter duplex DNA **OD1/OD3** was

easily dissolved at the same concentration and was used as the target in future experiments of MeQM alkylation. The exact sequence had no significance, merely that there was not an excess of any one base-pair (52.5% G:C) and the melting temperature was above 37 °C (calculated at 69 °C by the supplier Integrated DNA Technologies) to limit the presence of single stranded DNA. **OD1/OD3** met these criteria as the target duplex DNA. The reaction conditions were the same as used above with salDNA. Specifically, **OD1/OD3** (20 mM nts), sodium phosphate (25 mM, pH 7), KF (500 mM), and 4-MeBrQMP (100 mM) were combined in a solution of 70:30 H₂O:CH₃CN. The reaction was stirred in a 0.3 mL Reacti-vial for 1 hour prior to work-up and digestion using alkaline phosphatase (10 units, 100 µL) and phosphodiesterase I (0.28 units, 56 µL) (**Method 2**). After enzymatic digestion for 24 hours, the mixture was analyzed by HPLC (**Figure 4.10**). The identification of the alkylated products was made with UV-Vis and t_r comparisons to the individual nucleoside reactions (**Figure 4.11, Appendix C.5**).

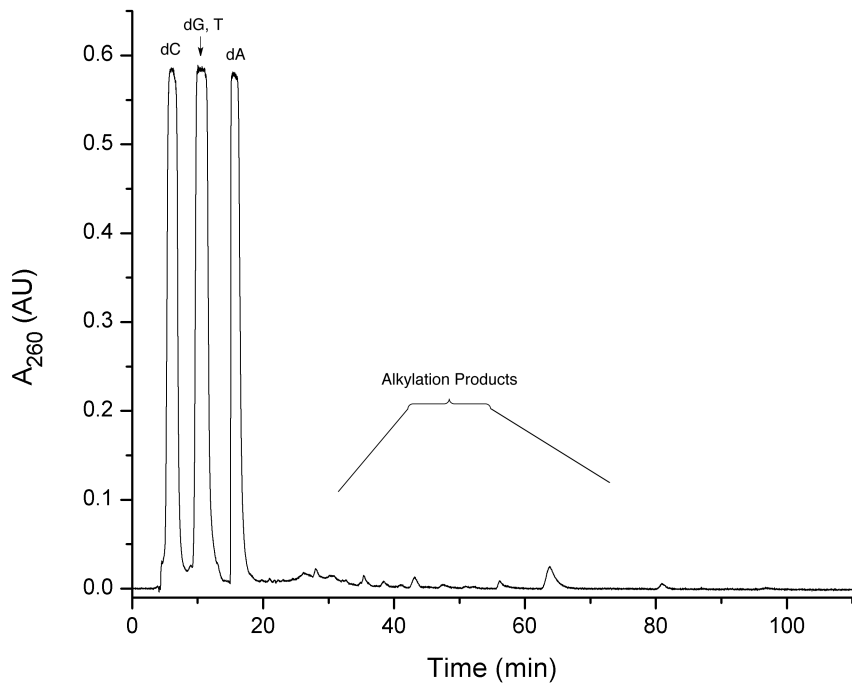


Figure 4.10. HPLC analysis of an alkylation reaction consisting of 20 mM **OD1/OD3**, 25 mM sodium phosphate (pH 7), 500 mM KF, and 100 mM 4-MeBrQMP in a 70:30 solution of $\text{H}_2\text{O}:\text{CH}_3\text{CN}$. The reaction was stirred in a 0.3 mL glass Reacti-vial for 1 hour at 37 °C prior to an addition of 40 μL CH_3CN to simulate the addition of BTI. The reaction was worked-up and digested according to **Method 2** using alkaline phosphatase (10 units, 100 μL) and phosphodiesterase I (0.28 units, 56 μL).

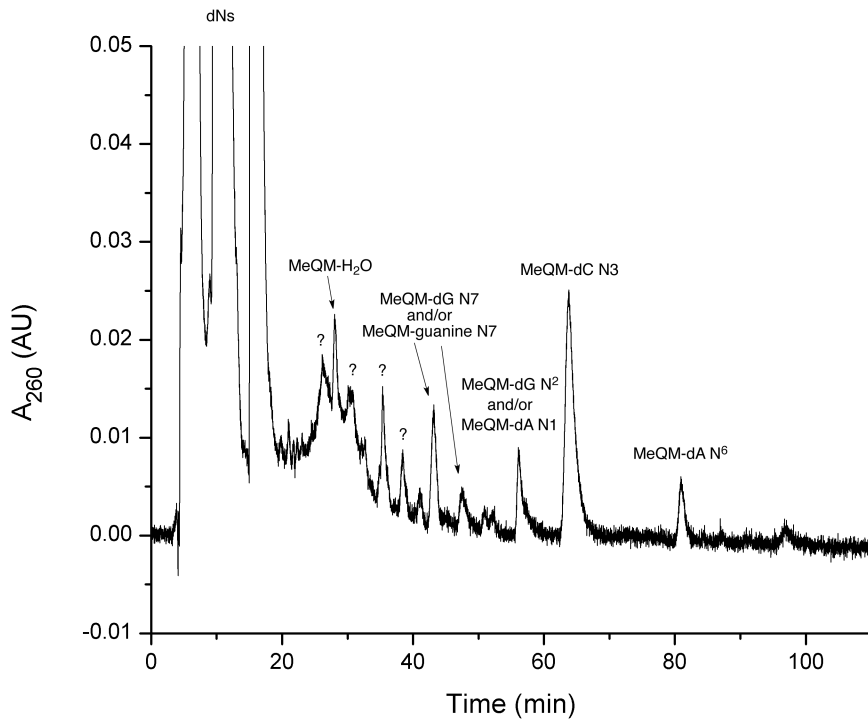


Figure 4.11. Expansion of **Figure 4.10** to better show the products of MeQM alkylation of **OD1/OD3**. The same reaction without 4-MeBrQMP is shown in **Figure 4.5**.

HPLC analysis of the MeQM alkylation of **OD1/OD3** confirmed that there was a higher yield of alkylation products formed when compared to salDNA (**Figure 4.9**). Unfortunately, there was still not a significant amount of MeQM alkylation products formed. A low yield of alkylation products would be problematic for the planned oxidation and HPLC analysis due to the sensitivity of the HPLC and diode array detector. The MeQM alkylation reaction shown in **Figures 4.10** and **4.11** revealed that the alkylation products are very close to the limit of detection.

To confirm that the alkylation yield is insufficient for further oxidation studies, the reaction above (**Figure 4.10**) was repeated with an addition of BTI (40 μ L, 167 mM final concentration) after the 1 hour alkylation. The work-up and digestion was identical to the previous alkylation reaction, using **Method 2**.

Unfortunately, HPLC analysis confirmed that the amount of oxidized MeQM-DNA adducts produced was insufficient for quantification (**Figure 4.12**). At this point, a new method of analysis, such as Ultra High Performance Liquid Chromatography (UHPLC) or tandem Liquid Chromatography – Mass Spectrometry (LC/MS) may be necessary to continue the study of MeQM alkylation of DNA and the subsequent oxidative trapping of reversible adducts.

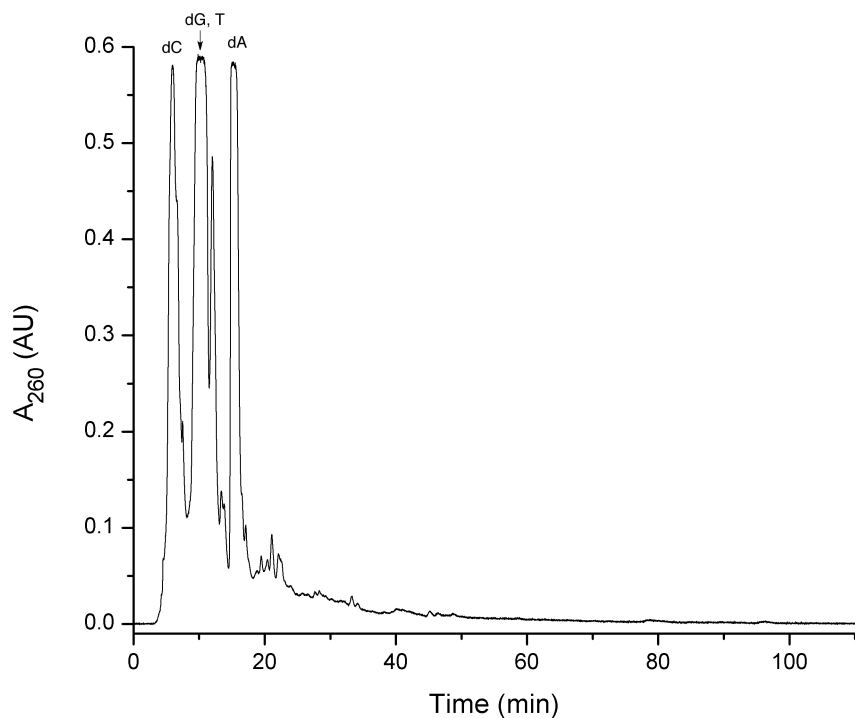


Figure 4.12. HPLC analysis of an alkylation reaction consisting of 20 mM **OD1/OD3**, 25 mM sodium phosphate (pH 7), 500 mM KF, and 100 mM 4-MeBrQMP in a 70:30 solution of $\text{H}_2\text{O}:\text{CH}_3\text{CN}$. The reaction was stirred in a 0.3 mL glass Reacti-vial for 1 hour at 37 °C prior to an addition of 40 μL BTI in CH_3CN (167 mM final concentration). The reaction was stirred for 5 minutes at room temperature prior to work-up and digestion according to **Method 2** using alkaline phosphatase (10 units, 100 μL) and phosphodiesterase I (0.28 units, 56 μL).

4.3. Summary.

The enzymatic digestion of DNA has proven to be effective after both alkylation and oxidation conditions are applied to a target DNA. The efficiency of alkylation by MeQM of target DNA decreases as the target is changed from monomeric nucleosides to a short duplex DNA (**OD1/OD3**) and decreases further as the target DNA is changed to a long duplex DNA (salDNA). Unfortunately, it has become apparent that the sensitivity of UV analysis of HPLC chromatograms is not high enough to quantify the formation of product from the MeQM alkylation of duplex DNA (salDNA or **OD1/OD3**). This leads to an inability to quantify the products of oxidation of MeQM alkylated DNA. Either a new method of detection is needed to increase sensitivity or new alkylation conditions are needed to increase the amount of MeQM-DNA adducts formed.

4.4. Materials and Methods.

Calf thymus DNA (ctDNA) was purchased from Sigma-Aldrich and salmon sperm DNA (salDNA, Na⁺salt, highly polymerized) was purchased from NBCo Biochemicals (now MP Bio), both as lyophilized solids. **OD1** and **OD3** were purchased from Integrated DNA Technologies with “standard desalting” and were not further purified prior to use. To form duplex DNA, **OD1** and **OD3** were dissolved in either potassium or sodium phosphate buffer, mixed, heated to 90 °C for 5 minutes and slowly cooled to room temperature over several hours. Alkaline phosphatase from *Escherichia coli* (P5931) and phosphodiesterase I from *Crotalus adamanteus*

venom (P3243) were purchased from Sigma-Aldrich as lyophilized solids and each was stored at a concentration of 0.1 unit/ μ L and 0.005 unit/ μ L, respectively, in a solution of 50 mM Tris-HCl pH 8, 50 μ M ZnSO₄, 10 mM MgCl₂, and 50% glycerol.

DNA work-up and digestion – Method 1. For a 200 μ L scale alkylation, once the alkylation and oxidation reactions were complete, the CH₃CN was removed under a stream of N₂ (15 minutes). The DNA was precipitated by adding EtOH (55 μ L, 100 %) and cooling to -20 °C for 30 minutes. The EtOH was evaporated under reduced pressure and the remaining DNA was washed with additional EtOH (140 μ L, 80 %), frozen with liquid N₂, and centrifuged (15 minutes, 14,800 rpm). The supernatant was decanted from the Eppendorf tube and the remaining solid was dissolved in 100 μ L TEAA (100 mM, pH 10) and hydrolyzed by alkaline phosphatase (0.2 units per 1 mM nts DNA) and phosphodiesterase I (0.006 units per 1 mM nts DNA). The digestion mixture was held at 37 °C for 24 hours, followed by neutralization by 1% aqueous acetic acid (5 μ L). The mixture was filtered through a 0.2 μ m syringe filter (with an addition of 50 μ L H₂O when necessary) and fractionated by analytical reverse-phase C18 chromatography (3% CH₃CN in 9.7 mM ammonium formate, pH 6.9, to 11% CH₃CN in 8.9 mM ammonium formate, pH 6.9, over 24 minutes (1 mL/min), followed by 11% CH₃CN in 8.9 mM ammonium formate, pH 6.9, to 25% CH₃CN in 7.5 mM ammonium formate, pH 6.9, over the next 85 minutes).

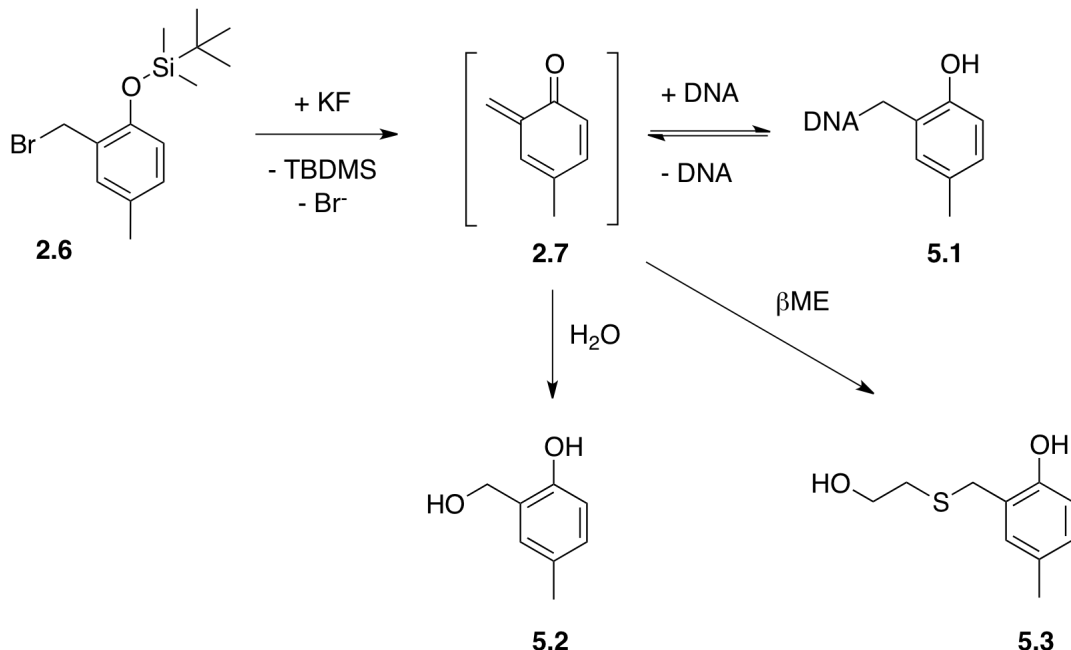
DNA work-up and digestion – Method 2. For a 200 µL scale alkylation, once the alkylation and oxidation reactions were complete, the reaction mixture was washed with saturated diethyl ether ($3 \times 300 \mu\text{L}$). Ethanol (400 µL, 100%, 0 °C) was added to the aqueous phase and the solution was kept at -20 °C for 30 minutes to facilitate precipitation of the DNA. The solution was centrifuged (5 minutes, 14,800 rpm) and the supernatant removed by pipette. The remaining DNA was washed with 80% aqueous ethanol (140 µL) and centrifuged (5 minutes, 14,800 rpm). The supernatant was removed by pipette and the remaining solid was dissolved in 100 µL TEAA (100 mM, pH 10) and 44 µL MgCl₂ (66.7 mM, 15 mM final concentration of Mg²⁺). The DNA was hydrolyzed by 100 µL alkaline phosphatase (10 units for 20 mM nts DNA) and 56 µL phosphodiesterase I (0.28 units for 20 mM nts DNA). The digestion mixture was held at 37 °C for 24 hours, followed by neutralization by 1% aqueous acetic acid (5 µL). The mixture was filtered through a 0.2 µm syringe filter and fractionated by analytical reverse-phase C18 chromatography (3% CH₃CN in 9.7 mM ammonium formate, pH 6.9, to 11% CH₃CN in 8.9 mM ammonium formate, pH 6.9, over 24 minutes (1 mL/min), followed by 11% CH₃CN in 8.9 mM ammonium formate, pH 6.9, to 25% CH₃CN in 7.5 mM ammonium formate, pH 6.9, over the next 85 minutes).

Chapter 5: Quantifying Quinone Methide Release from DNA with β -Mercaptoethanol

5.1. Introduction.

Oxidative trapping of *o*-QM-DNA adducts can provide data on the intrinsic selectivity of a model *o*-QM (MeQM, **2.7**) towards the nucleophilic positions on nucleosides. Nucleophilic trapping of the *o*-QM released from DNA can provide complimentary data that allows for the quantification of how much of the *o*-QM-DNA alkylation products are reversible. Specifically, released QM from its adducts can be trapped by a nucleophile (such as β -mercaptoproethanol, β ME) and quantified. The kinetics of release can be observed by measuring QM release at various times between fluoride initiation of a precursor (to form *o*-QM) and nucleophile addition (to form *o*-QM- β ME product) (**Scheme 5.1**). For this project β ME was chosen as a nucleophile for the trapping of MeQM as it reacts quickly with previous *o*-QMs and has been proven to be an effective trap of *o*-QM.^{61,101} Phenylhydrazine is another nucleophile previously used to trap the release of QM from QM-dG N7 adducts.⁵⁸ Subsequent studies completed prior to my arrival in the Rokita group replaced phenylhydrazine as a trapping nucleophile because decomposition of phenylhydrazine resulted in a more complicated HPLC chromatogram than equivalent trapping with β ME.

Scheme 5.1. Reaction scheme for nucleophilic trapping of MeQM (**2.7**) with β ME to form MeQM- β ME (**5.3**).



As mentioned above, β ME is an effective nucleophilic trap of active *o*-QM.^{61,101} In these previous studies, β ME suppressed cross-linking of a bisQM precursor with DNA by successfully competing with other nucleophiles such as water and dA to react irreversibly with an active bisQM present in solution to form QM- β ME. This method provided the starting point for an alternative method for quantifying the reversibility of QMs. Previously, transfer of a bisQM between complementary oligonucleotides has been used to observe the reversibility of the bisQM.^{61,102} Trapping of the released QM with a low molecular weight nucleophile would allow the reaction to be followed by HPLC. The trapped products can also be unambiguously identified with analytical standards by comparing UV-Vis absorbencies and retention times. Furthermore, the trapped products can be quantified with the help of molar extinction coefficients and an internal standard.

The goal for the following studies is to, for the first time, quantify the reversible alkylation of DNA by using a model QM (MeQM, **2.7**). The release of QM from nucleosides, single stranded DNA (ssDNA), and double stranded DNA (dsDNA) was measured through the use of β ME as a nucleophilic trap followed by HPLC analysis and quantification of the β ME and water adducts of MeQM. The expectation is that the β ME product will form in high yield initially and gradually decrease as the QM is allowed more time to form irreversible adducts with H_2O and the weaker nucleophiles of DNA (**Scheme 5.1**).

5.2. Results and Discussion.

5.2.1. Synthesis of the Water and β -Mercaptoethanol Adducts of MeQM.

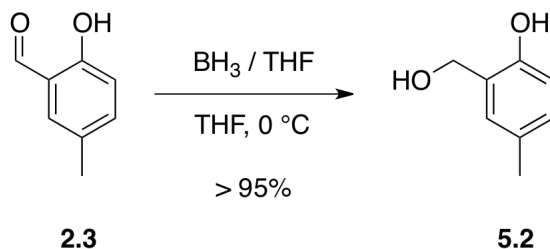
The first step in this project was to synthesize the MeQM- H_2O adduct (2-(hydroxymethyl)-4-methylphenol, **5.2**) and the MeQM- β ME adduct (4-methyl-2-[(2-hydroxyethylthio)methyl]phenol, **5.3**) as standards to measure their molar extinction coefficients (ϵ) and obtain their HPLC retention times (t_r).

Synthesis of the MeQM- H_2O adduct (**5.2**) was first attempted by combining 4-MeBrQMP (**2.6**) and KF in a 3:2 solution of $CH_3CN:H_2O$. The reaction was allowed to stir at room temperature for 26 hours to allow for the full reaction between MeQM and H_2O . The compound appeared to be MeQM- H_2O from comparison of the HPLC t_r to previous reactions with 4-MeBrQMP, which always contain a small amount of MeQM- H_2O as a side product. Additionally, 1H NMR confirmed the loss of the silyl protecting group and the presence of a significant amount of triethylammonium

acetate (TEAA) leftover from the HPLC buffer after lyophilization. ESI⁺-MS was unable identify a parent ion or fragment that corresponded to MeQM-H₂O, possibly due to TEAA repressing the signal. Contamination with TEAA would also change the measured mass of MeQM-H₂O and would introduce error into the molar extinction coefficient determination. To minimize impurities, such as TEAA, a new method was needed to obtain pure MeQM-H₂O.

MeQM-H₂O was synthesized by reduction of 5-methylsalicylaldehyde (**2.3**) with a 1 M borane/THF solution in high yield (> 95%) (**Scheme 5.2**). The new synthesis had a shorter reaction time (< 2 hr), was much easier to scale up to gram quantities if needed and avoided the use of HPLC purification and 4-MeBrQMP (that required 3 steps to synthesize) as a starting material. Most importantly, the product was observed to be pure based on ¹H NMR and was characterized by ¹H NMR, ¹³C NMR, and ESI⁺-MS (**Appendix D1 – D3**).

Scheme 5.2. Synthesis of MeQM-H₂O (**5.2**) in one step by reduction of 5-methylsalicylaldehyde (**2.3**).

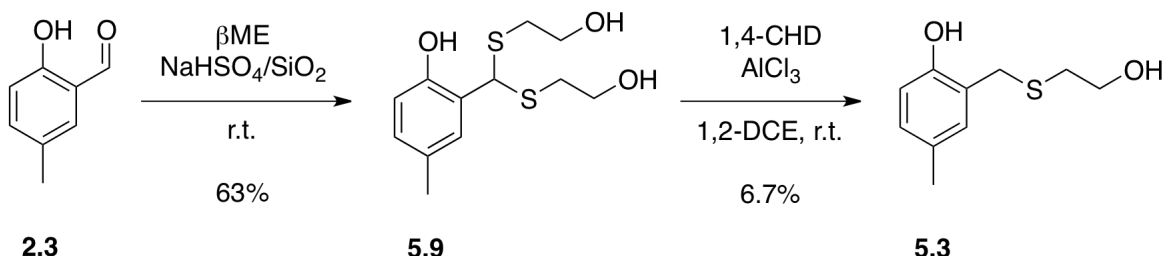


The second standard to be synthesized was the MeQM-βME adduct (**5.3**). The first attempt at this synthesis was based on literature precedent.¹⁰³ In the reaction vessel, βME was combined with KF prior to slow addition of 4-MeBrQMP for a 1:1 reaction solution of DMF:H₂O. After 10 minutes the reaction was worked-up and purified by silica column chromatography to yield unreacted **2.6**. The reaction time

was then increased from 10 minutes to 26 hours and the amount of β ME was increased 1.5-fold. The starting material was completely consumed under these later conditions and a total of five compounds were isolated by HPLC. Unfortunately, ESI⁺-MS was unable to identify the expected product, possibly due to TEAA that was still present from the final HPLC purification after multiple rounds of lyophilization that suppressed the MS signals. The TEAA would also interfere with the determination of the molar extinction coefficient. Another drawback of this synthetic method was again the need to use 4-MeBrQMP. An alternative synthesis was developed to address the drawbacks of the earlier synthetic scheme by starting with a simpler, commercially available reagent and avoiding the use of buffered HPLC solvents.

The new synthesis started from 5-methylsalicylaldehyde (**2.3**) and formed the product MeQM- β ME (**5.3**) in two steps (**Scheme 5.3**). The silica supported sodium hydrogen sulfate catalyst (NaHSO₄/SiO₂) was prepared from the literature procedure.¹⁰⁴ The first attempt at dithiolation followed the literature procedure except for substituting 5-methylsalicylaldehyde (**2.3**) for the reported salicylaldehyde. 5-Methylsalicylaldehyde (**2.3**) was combined with β ME and stirred slowly at room temperature while NaHSO₄/SiO₂ was slowly added. Immediately, the mixture formed a yellow paste that stopped stirring. Petroleum ether was added to the paste, but did not dissolve the mixture. TLC (3:1, hexanes: ethyl acetate) of the petroleum ether phase suggested the presence of only the starting material, **2.3**. The unsuccessful attempt was confirmed upon further work-up and ¹H NMR (CDCl₃).

Scheme 5.3. Synthesis of MeQM- β ME (**5.3**) from 5-methylsalicylaldehyde (**2.3**) through a dithioacetal intermediate (**5.9**). 1,4-CHD: 1,4-cyclohexadiene. 1,2-DCE: 1,2-dichloroethane.



The second attempt at dithiolation of **2.3** was successful. The amount of β ME used was increased by more than 3-fold to alleviate the stirring difficulties involved with the paste formation. 5-Methylsalicylaldehyde (**2.3**) was again combined with β ME and stirred slowly at room temperature while $\text{NaHSO}_4/\text{SiO}_2$ was slowly added to the mixture, stopping to add additional β ME when a paste began to form. Immediately after the catalyst was completely added petroleum ether was added to the reaction, causing a solid to precipitate. No compounds were observed by TLC (3:1, hexanes: ethyl acetate) in the liquid phase. The petroleum ether was pipetted off of the solid and saved. CHCl_3 was added to dissolve the solid and produced a cloudy opaque solution. TLC (3:1, hexanes: ethyl acetate) showed the presence of at least one compound at the baseline with no starting material (**2.3**) present. The CHCl_3 solution was washed with petroleum ether (including the saved portion) and both layers were saved. Additional CHCl_3 was added to the CHCl_3 layer and washed with H_2O , dried with NaSO_4 , and removed under reduced pressure to yield a clear oil (1.73 g, 63% crude yield). The clear oil mostly crystallized upon standing and the remaining solvent was removed under vacuum overnight. The clear solid was

confirmed to be the expected dithioacetal product **5.9** by ^1H NMR (**Figure 5.1**) and ESI $^+$ -MS (**Appendix D4**).

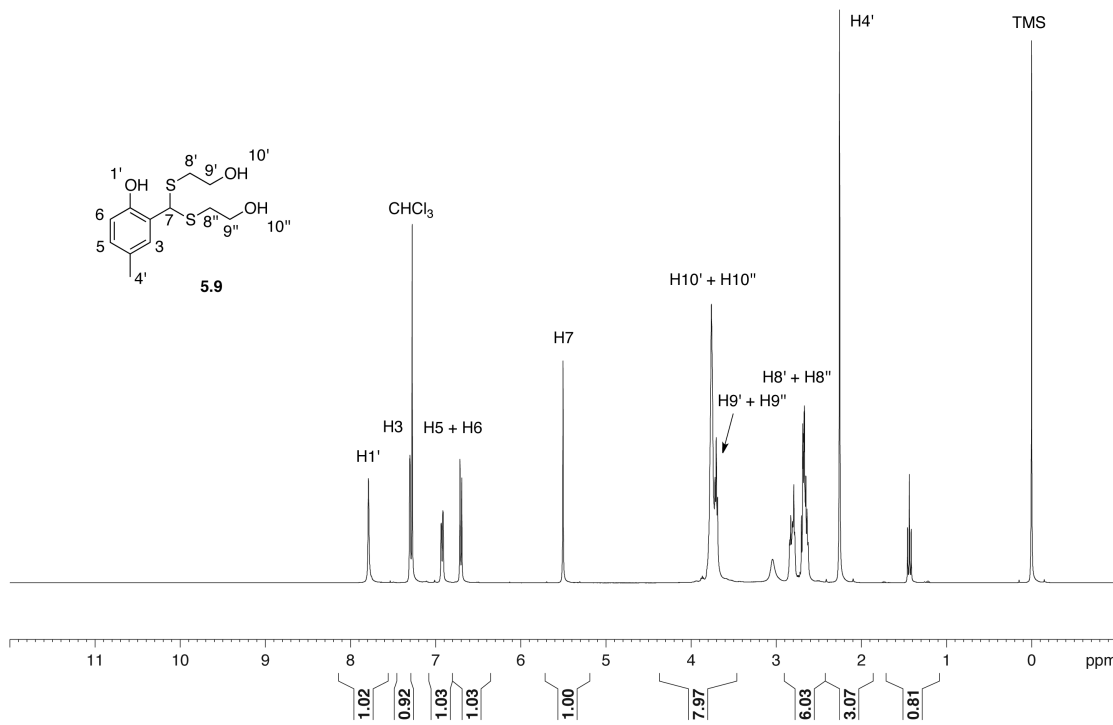
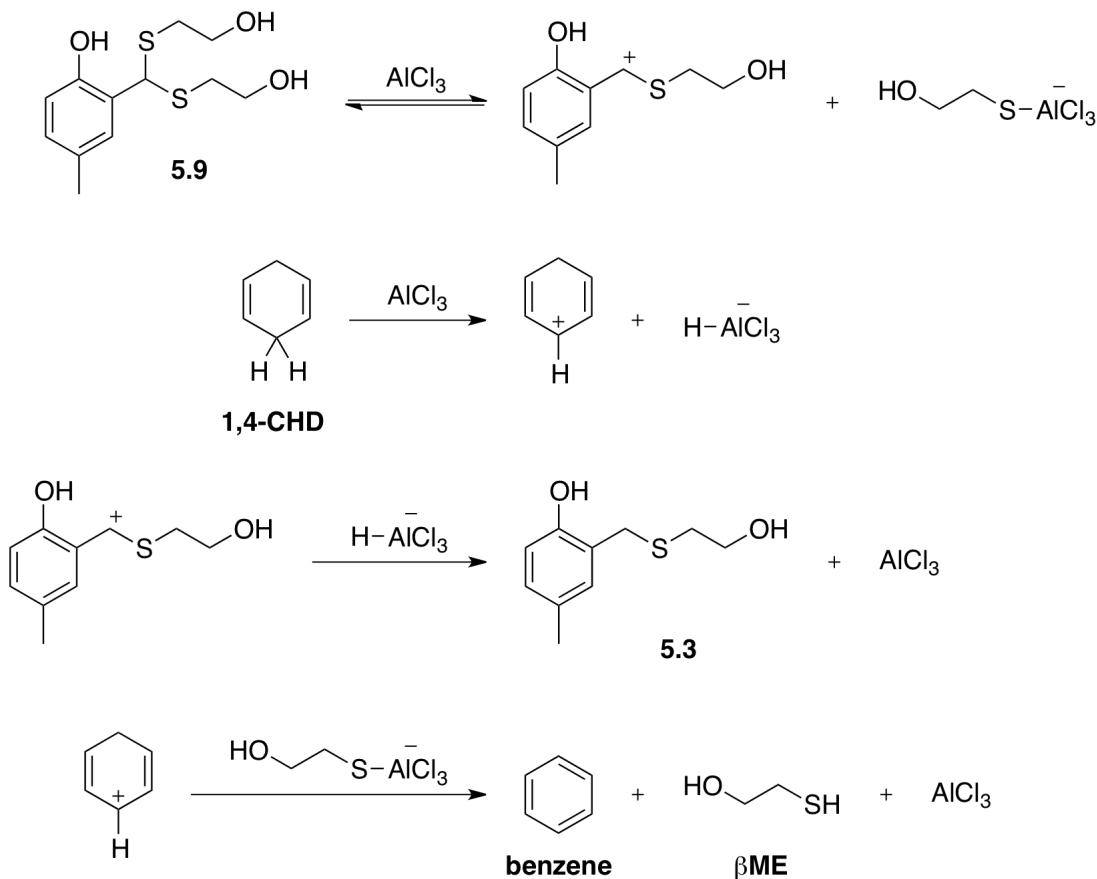


Figure 5.1. ^1H NMR of **5.9** in CDCl_3 at 400 MHz.

In the second step of the synthesis the dithioacetal was reduced to a single thioether.¹⁰⁵ The proposed mechanism by Ikeshita et al.¹⁰⁵ of this transformation is shown in **Scheme 5.4**. The Lewis acid, AlCl_3 , activates dithioacetal **5.9** and also abstracts a hydride from 1,4-cyclohexadiene (1,4-CHD). The AlCl_3 transfers the abstracted hydride to the activated dithioacetal, forming product **5.3** and reforming the catalyst AlCl_3 . The cyclohexadienyl cation reacts with the previously formed AlCl_3 - thioether to regenerate the catalyst AlCl_3 along with benzene and βME , which should be easily separated from the desired product, **5.3**.

Scheme 5.4. Proposed mechanism for the reduction of dithioacetal **5.9** by 1,4-CHD. Adapted from Ikeshita et al.¹⁰⁵



Dithioacetal (**5.9**) and 1,4-CHD were combined with 1,2-dichloroethane (1,2-DCE, 7 mL) under N_2 at room temperature. While stirring, a suspension of AlCl_3 in hexanes was slowly added. Upon addition of AlCl_3 , the solution changed from colorless to a red/orange color. Within 5 minutes, a precipitate formed and the reaction gradually changed to yellow over an hour. The reaction was followed by TLC (2:1, hexanes; ethyl acetate) by removing a 100 μL aliquot and slowly quenching it with 200 μL H_2O in a 1.5 mL Eppendorf tube. CHCl_3 (100 μL) was added to the aliquot containing 1.5 mL Eppendorf, shaken, and the organic layer was sampled for TLC. The first TLC (2 hr 40 min) showed 4 spots, one at the baseline and three mobile spots. The second TLC (4 hr 40 min) showed no change from the

first, but when compared to the starting material, **5.9**, it was determined that the baseline spot was starting material. Further analyzing the aliquot removed at 4 hours 40 minutes by ^1H NMR (CD_3CN) showed some starting material present, but also at least one other compound present, creating a complicated spectra.

After seven hours, 9-fold more of the AlCl_3 suspension was added and the reaction solution became a cloudy red. The reaction was stirred overnight under N_2 at room temperature. After 22 hours, the solution was cloudy yellow with yellow solid on the sides of the round bottom flask. TLC (2:1, hexanes: ethyl acetate) of the liquid phase revealed the same four spots, with the three mobile spots appearing darker. Analysis by $\text{ESI}^+ \text{-MS}$ of the TLC aliquot was inconclusive while ^1H NMR (CD_3CN) gave a similar spectra as the earlier aliquot. Analysis of the ^1H NMR sample by HPLC shows the expected product formed as a minor component of the mixture (**Figure 5.2**). MeQM- βME was identified by retention time and UV-Vis absorbance when compared to independently formed MeQM- βME from 4-MeBrQMP and βME .

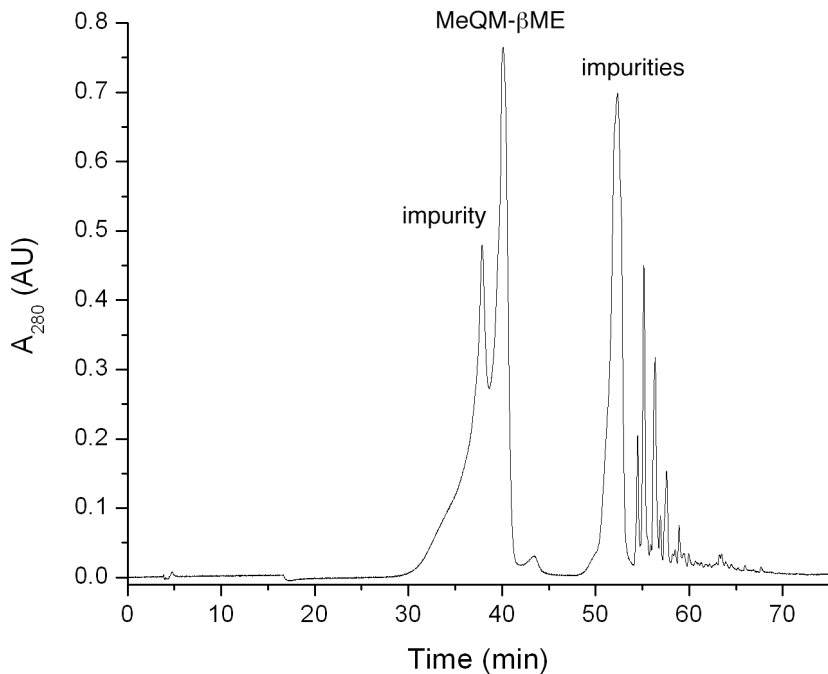


Figure 5.2. HPLC analysis of the ^1H NMR (CD_3CN) sample of the MeQM- β ME reaction at 23 hours. Fractionation by HPLC uses a linear gradient of 5 – 30% CH_3CN in ammonium formate (10 mM, pH 6.9) over 45 minutes (1 mL/min).

An additional 10-fold of the AlCl_3 suspension was added to the reaction after 25.5 hours. The reaction turned a cloudy dark red/brown and became cloudy brown within 45 minutes. TLC (2:1, hexanes: ethyl acetate) at 27.5 hours revealed the same 4 spots as the previous TLCs. At this point, a total of 2 equivalents of AlCl_3 have been added to the reaction. After 28 hours, the reaction was slowly quenched with H_2O and extracted with CHCl_3 . The organic phase was washed with brine, dried over MgSO_4 , and removed under reduced pressure to yield a yellow/brown oil. The oil was stored at 0 °C for 6 days, where a color change occurred leaving a brown/black oil. The oil was dissolved with ethyl acetate and purified by chromatotron. The expected product (**5.3**) was collected with a crude yield of 0.032 g (16 %) and analyzed by ^1H NMR (**Appendix D5**).

Additional purification by HPLC was undertaken due to the high purity necessary for extinction coefficient measurements. To avoid the presence of buffer salts in the lyophilized product, the first HPLC purification used nanopure H₂O as the aqueous phase, with CH₃CN as the organic phase. The desired product was purified using a gradient of 3 - 25% aqueous CH₃CN over 76 minutes (1 mL/min). The 32 mg sample was dissolved into 400 μL CH₃CN and aliquots of 25 - 50 μL were fractionated by HPLC. After the first run using nanopure H₂O as the aqueous phase, the remaining runs used 0.1% trifluoroacetic acid as the aqueous phase to sharpen some of the compounds that were tailing on the column, while avoiding the use of TEAA (**Figure 5.3**).¹⁰⁶

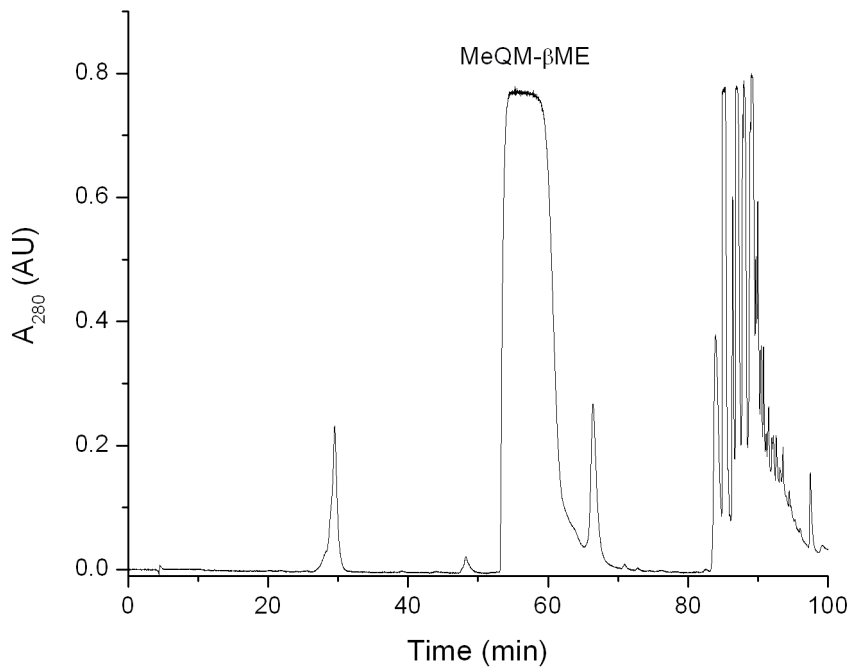


Figure 5.3. HPLC purification of MeQM-βME following a first purification by chromatotron. Crude material (31.6 mg) was dissolved in CH₃CN (400 μL) prior to the injection of a 50 μL aliquot. Fractionation by HPLC used a linear gradient of 3 - 25% CH₃CN in 0.1% aqueous TFA over 76 minutes (1 mL/min).

A total of 8 HPLC runs were needed to purify all of the crude oil. The resulting clear oil was combined and analyzed by ^1H NMR to confirm pure MeQM- β ME for a yield of 0.013 g (6.7 %) (**Appendix D6**). ESI $^+$ -MS and ^{13}C NMR were also used to fully characterize the product (**Appendix D7 – D8**). While the final yield of MeQM- β ME was low (13 mg), there was enough pure compound to obtain a molar extinction coefficient (greater than 10 mg).

Although the necessary amount of MeQM- β ME was obtained from the above procedure, some improvements could be made if more MeQM- β ME is needed in the future. The slow introduction of 3 equivalents (instead of 2) of AlCl₃ to the reaction as a solid should improve the yield. The original use of a suspension of AlCl₃ in hexanes proved difficult to regulate the amount of AlCl₃ added to the reaction. The increase in AlCl₃ will also compensate for the possible interaction between AlCl₃ and the three hydroxy groups present in the starting material **5.9**. The amount of 1,4-CHD should also be increased from 1 equivalent to 2 equivalents if the new AlCl₃ procedure is ineffective, to increase the amount of hydride source in solution.

5.2.2. Determination of Extinction Coefficients for MeQM-H₂O, MeQM- β ME, and Internal Standards.

The molar extinction coefficients of MeQM-H₂O, MeQM- β ME, and the internal standards were determined in the eluting buffer used in the HPLC analysis of the alkylation reaction to compensate for any pH or solvent effect on their absorbance. Quantification of the amounts of MeQM- β ME and MeQM-H₂O observed by HPLC require accurate molar extinction coefficients. Molar extinction

coefficients for the two different internal standards used for HPLC analysis, phenol and *meta*-cresol, were also determined.

For the β ME trapping, three different elution buffers were used in the HPLC analysis. Earlier work used 10 mM TEAA pH 5 as the aqueous phase and later work used either 0.1% aqueous TFA or 10 mM ammonium formate pH 6.9 as aqueous phase. The reasons for these adjustments will be discussed in the following section.

The extinction coefficients at $\lambda = 280$ nm (ϵ_{280}) of phenol and MeQM-H₂O were determined in TEAA and TFA and ϵ_{280} values for *m*-cresol, MeQM-H₂O, and MeQM- β ME were determined in ammonium formate. The wavelength at 280 nm was chosen for detection and ϵ determination because it is between the λ_{max} of MeQM-H₂O (279 nm) and MeQM- β ME (283 nm). This allows for maximum sensitivity to the detection of these compounds in the HPLC assay. The molar extinction coefficient was calculated using the Beer-Lambert law (A = ϵcl) (**Table 5.1**). Stock solutions of each compound at 10 mM in H₂O were prepared in triplicate. Aliquots were then diluted to a final concentration of 0.33 mM with the appropriate aqueous buffer. With accurate ϵ_{280} values for each compound, MeQM-H₂O and MeQM- β ME can be directly compared to a known concentration of internal standard (phenol or *m*-cresol) and the HPLC peak area can be integrated and converted to the moles of compound in the reaction.

Table 5.1. Calculated molar extinction coefficients (ϵ) at $\lambda_{280\text{ nm}}$ of the compounds of interest in the β ME trapping of MeQM.

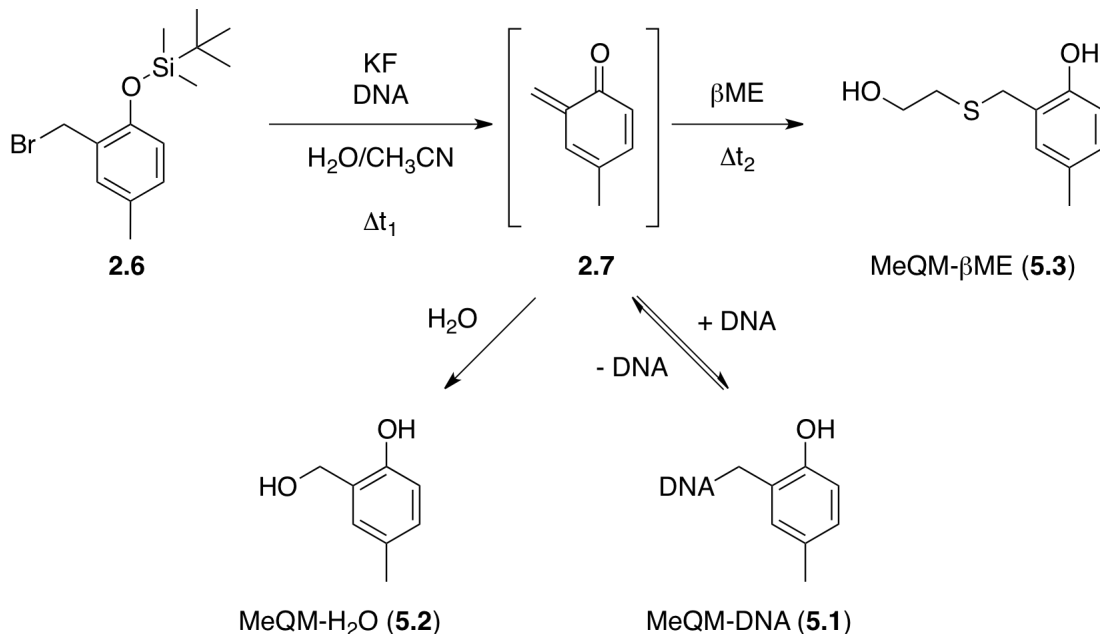
Compound (0.33 mM)	$\epsilon_{280} (\text{M}^{-1}\text{cm}^{-1})$ in 9.7 mM TEAA pH 5	$\epsilon_{280} (\text{M}^{-1}\text{cm}^{-1})$ in 0.097% aqueous TFA	$\epsilon_{280} (\text{M}^{-1}\text{cm}^{-1})$ in 9.7 mM ammonium formate pH 6.9
Phenol	560 ± 8	539 ± 30	572 ± 20
<i>m</i> -Cresol	n/a	n/a	920 ± 30
MeQM-H ₂ O	2170 ± 40	1970 ± 30	1920 ± 60
MeQM- β ME	1420 ± 90	1460 ± 110	2170 ± 220

5.2.3. Quantifying MeQM Released from Nucleoside Adducts by Trapping with β -Mercaptoethanol.

Prior to conducting the β ME trapping studies with both MeQM and a target nucleophile (dN or DNA), a series of control experiments confirmed the HPLC assay accurately measured the amount of MeQM-H₂O, MeQM- β ME, and the internal standard in the reaction mixture. The goals of the control experiments were to confirm that MeQM-H₂O and MeQM- β ME are stable and to measure the persistence of MeQM and 4-MeBrQMP in solution in the absence of nucleophiles capable of forming labile adducts. The rate of MeQM and 4-MeBrQMP persistence with and without the presence of DNA was measured by varying the aging time (Δt_1) followed by addition of β ME and a sufficient trapping time (Δt_2) to allow for complete trapping of released MeQM by β ME. The aging time (Δt_1) is necessary to allow MeQM to partition over time between irreversible reaction with water and reversible reaction with DNA prior to the addition of the β ME trap. The time needed for full transfer of reversible MeQM from DNA to β ME was measured by holding the aging time (Δt_1)

constant and varying the trapping time (Δt_2). MeQM-H₂O (**5.2**) and MeQM- β ME (**5.3**) were quantified by HPLC analysis of each reaction (**Scheme 5.5**).

Scheme 5.5. Scheme for the trapping of MeQM with β ME. Varying the aging time (Δt_1) revealed the persistence of MeQM and 4-MeBrQMP while varying the trapping time (Δt_2) allowed the release of MeQM from DNA to be measured.



The first control reaction did not contain any nucleophiles that could potentially form reversible MeQM adducts (nucleosides or DNA) to measure the persistence of MeQM or 4-MeBrQMP in solution. The initial reaction conditions consisted of 5% aqueous CH₃CN with 50 mM 3-(N-morpholino)propanesulfonic acid (MOPS) pH 7 (buffer), 5 mM phenol (internal standard), 2 mM 4-MeBrQMP (MeQM source), and 500 mM KF (MeQM initiator) (**Table 5.2**). This reaction was combined for a total of 100 μ L in a 1.5 mL plastic Eppendorf vial and held at 37 °C for 1 hour (Δt_1), after the addition of KF to allow MeQM to react with water. After 1 hour, 20 μ L βME (600 mM in 50 mM MOPS pH 7) was added for a 60-fold excess compared to 4-MeBrQMP. The reaction mixture was then held at 37 °C for 24 hours (Δt_2) prior

to HPLC analysis to allow for complete trapping of any reversible MeQM. The HPLC analysis utilized a gradient of 5 – 30% CH₃CN in TEAA (10 mM, pH 5) over 45 minutes with an analytical column (1 mL/min). The one hour reaction time (Δt_1) was expected to result in the maximum amount of MeQM-H₂O and a lack of observable formation of MeQM- β ME due to previous studies determining that the unsubstituted BrQMP (**1.40**) is fully converted to the QM intermediate within 30 minutes under aqueous conditions.⁵⁸ The inclusion of the electron-donating methyl group *para* to the phenolic oxygen in 4-MeBrQMP (**2.6**) stabilized the electron deficient MeQM intermediate (**2.7**).⁸⁰ This was observed to lead to faster generation of MeQM from 4-MeBrQMP than QM from BrQMP allowing for more time for irreversible MeQM-H₂O formation prior to the addition of β ME in the absence of other nucleophiles.⁸⁰ In the presence of DNA, this would also lead to faster formation of MeQM-DNA adducts. Surprisingly, MeQM- β ME was observed in higher yield than MeQM-H₂O (46 nmol vs. 15 nmol), suggesting that MeQM or 4-MeBrQMP persisted for more than 1 hour under aqueous conditions, without a known nucleophile capable of forming a labile MeQM adduct and extending the lifetime of MeQM (**Figure 5.4**).

Table 5.2. Reaction conditions without a DNA nucleophile expected to produce a maximum amount of MeQM-H₂O and a minimum amount of MeQM-βME.

Stock Solution	Volume to Add (μL)	Final Concentration (mM)	Final Volume (μL)
100 mM MOPS pH 7	25	50	
H ₂ O	15		
50 mM Phenol in H ₂ O	10	5	
100 mM MOPS pH 7	25		
40 mM 4-MeBrQMP in CH ₃ CN	5	2	
2.5 M KF in H ₂ O	20	500	100
Trapping:			
600 mM βME in 50 mM MOPS pH 7	20	100	120

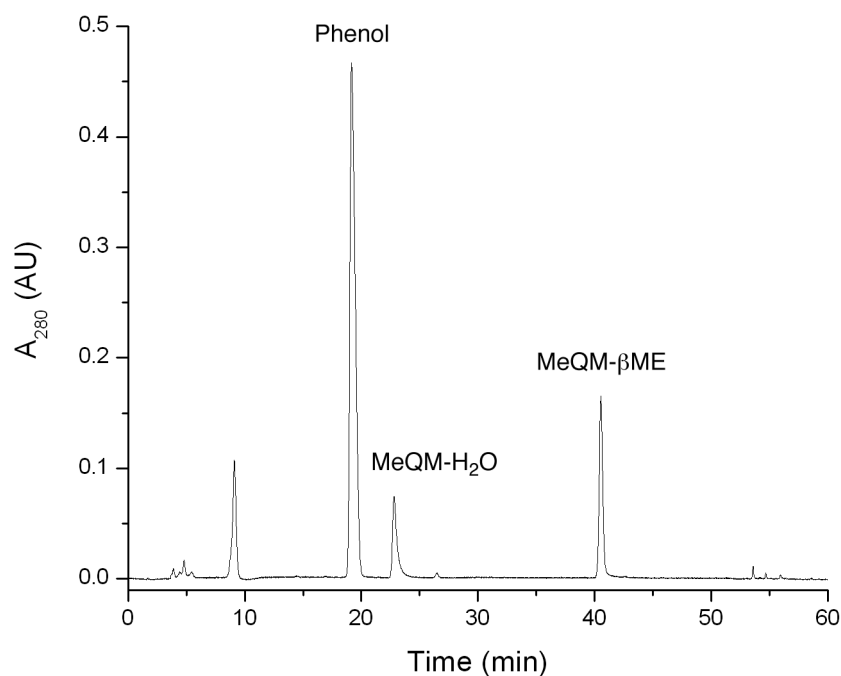


Figure 5.4. HPLC chromatogram from the reaction detailed in **Table 5.2**. The reaction was held for 1 hour at 37 °C after KF initiation of MeQM and for another 24 hours at 37 °C after addition of βME. HPLC analysis used a linear gradient of 5 – 30% CH₃CN in TEAA (10 mM, pH 5).

A series of control (lacking DNA related nucleophiles) experiments were then carried out with the goal of determining the amount of time necessary for MeQM to form from 4-MeBrQMP (Δt_1) and for β ME to react with and trap any free MeQM (Δt_2). The amount of time between KF initiation of MeQM and β ME addition was varied between 0 minutes and 2 hours. MeQM- β ME formation was detected for each time point, suggesting that MeQM or 4-MeBrQMP persists for at least 2 hours in solution. Furthermore, these experiments revealed that only a fraction of the expected 200 nmol of MeQM-H₂O and MeQM- β ME was being detected. The experiments averaged 63 nmol MeQM-H₂O and MeQM- β ME, combined, which is only a 31% yield based on 4-MeBrQMP. Varying a number of reaction variables, including KF concentration, β ME concentration, CH₃CN concentration, and the presence of phenol, failed to affect the yield of the two MeQM adducts or the persistence of MeQM.

One possible explanation for the apparent persistence of MeQM was that one, or both, of MeQM-H₂O and MeQM- β ME formed reversibly. Three experiments were conducted that demonstrated that both adducts were irreversible and stable under the β ME trapping conditions. The first experiment tested the stability of MeQM-H₂O in the β ME trapping conditions by including it at 2 mM as a replacement for an equal amount of 4-MeBrQMP. The mixture was held at 37 °C for 66.5 hours prior to HPLC analysis (**Figure 5.5**). There was no detected formation of MeQM- β ME, which would have formed had MeQM-H₂O regenerated the active MeQM.

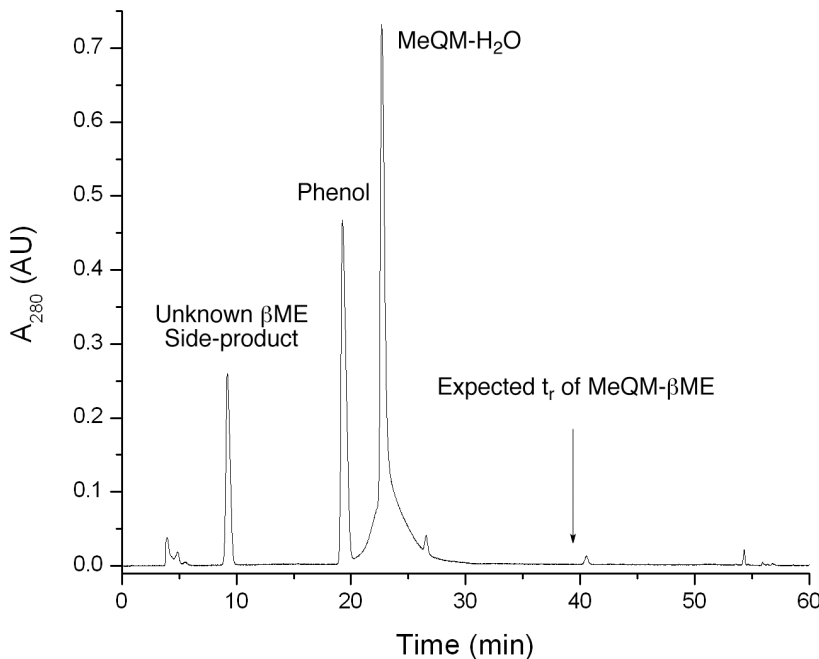


Figure 5.5. HPLC chromatogram of the MeQM-H₂O stability test. MeQM-H₂O was added at 2 mM (100% theoretical yield) to 4.2% aqueous CH₃CN containing 50 mM MOPS pH 7, 5 mM phenol, 4 mM in nucleotides (nts) calf thymus DNA (ctDNA), 500 mM KF, and 100 mM βME. The reaction was held for 66.5 hours at 37 °C prior to HPLC analysis using a linear gradient of 5 – 30% CH₃CN in TEAA (10 mM, pH 5). MeQM-H₂O co-elutes with ctDNA, leading to the broad base of the peak at t_r = 23 minutes.

The second experiment tested the stability of MeQM-βME in the βME trapping conditions by including it at 2 mM as a replacement for an equal amount of 4-MeBrQMP. The mixture was held at 37 °C for 68.5 hours prior to HPLC analysis (**Figure 5.6**). Although a small amount of ctDNA did elute at the expected t_r of MeQM-H₂O, there was no significant formation of MeQM-H₂O which would have been accompanied by a corresponding decrease in the amount of MeQM-βME from its regeneration of the active MeQM. These two experiments also show that there is no interconversion between MeQM-H₂O and MeQM-βME due to nucleophilic attack of βME or H₂O, respectively.

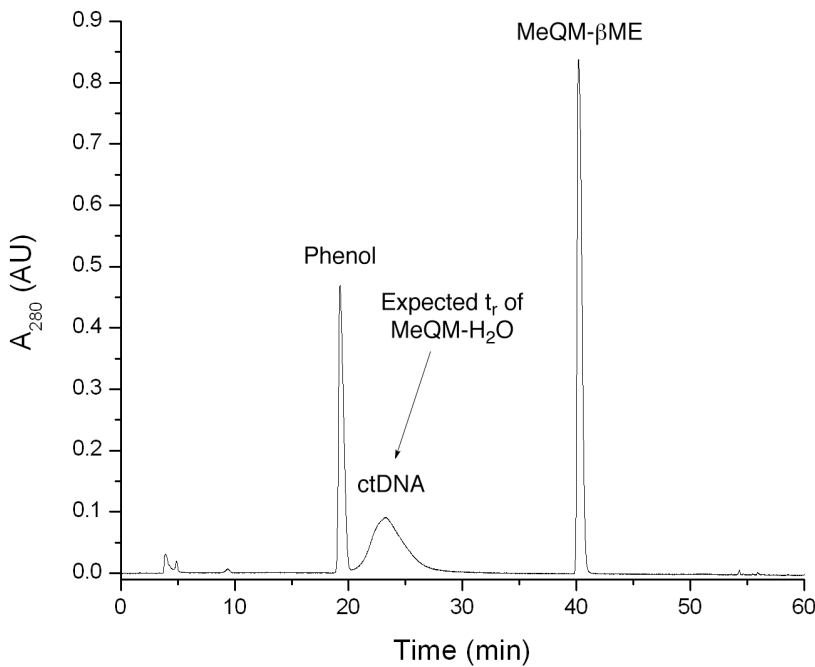


Figure 5.6. HPLC chromatogram of the MeQM- β ME stability test. MeQM- β ME was added at 2 mM (100% theoretical yield) to 4.2% aqueous CH₃CN containing 50 mM MOPS pH 7, 5 mM phenol, 4 mM in nucleotides (nts) calf thymus DNA (ctDNA), and 500 mM KF. The reaction was held for 68.5 hours at 37 °C prior to HPLC analysis using a linear gradient of 5 – 30% CH₃CN in TEAA (10 mM, pH 5).

The third experiment removed any potential MeQM source (4-MeBrQMP, MeQM-H₂O, or MeQM- β ME) from the above stability tests. This experiment tested if ctDNA impurities or β ME side-products (such as thiol dimers) would obscure any of the compounds of interest (MeQM- β ME, MeQM-H₂O, or phenol). After the mixture was incubated at 37 °C for 70 hours, there were no compounds detected by HPLC at the t_r of MeQM- β ME (40 min) or phenol (labeled). Calf thymus DNA, however, eluted at the t_r of MeQM-H₂O (23 min), but this would increase the observed yield of MeQM-H₂O and would not explain the low yields. This result provides evidence that the HPLC signals are not false positives from an impurity in

the reaction mixture or any side-reactions occurring with β ME, as observed at $t_r = 10$ minutes (**Figure 5.7**).

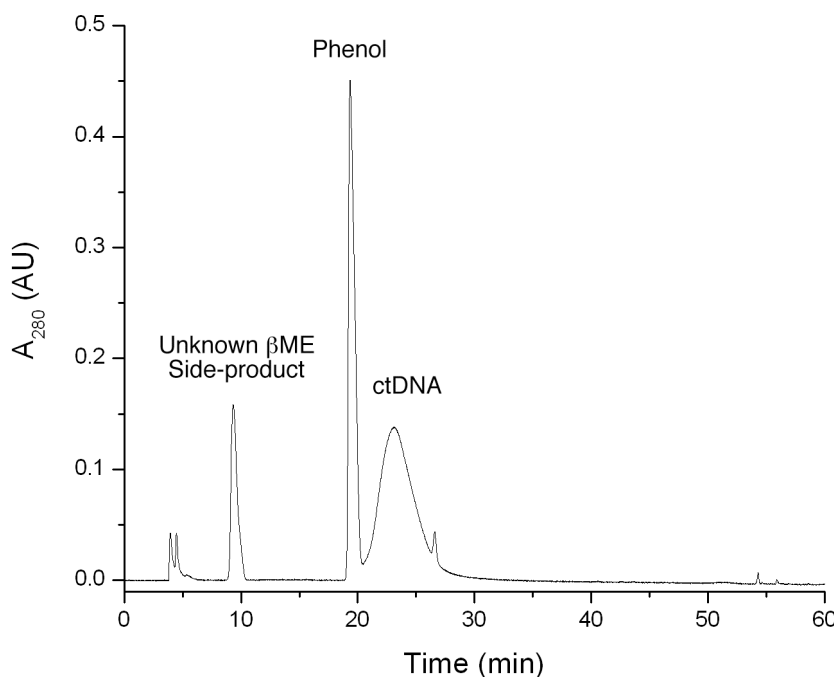


Figure 5.7. HPLC chromatogram of the stability test without a potential MeQM source. A 4.2% aqueous CH_3CN solution containing 50 mM MOPS pH 7, 5 mM phenol, 4 mM in nucleotides (nts) calf thymus DNA (ctDNA), 500 mM KF, and 100 mM β ME was held for 70 hours at 37 °C prior to HPLC analysis using a linear gradient of 5 – 30% CH_3CN in TEAA (10 mM, pH 5).

Next, the reaction vessel was varied to determine if this affected the persistence of MeQM or the yield of MeQM- H_2O and MeQM- β ME. The previous experiments were carried out in polypropylene vials (1.5 mL). The precursor 4-MeBrQMP may interact more strongly with this plastic reaction vessel than a glass reaction vessel, sequestering it from reacting with the available H_2O and β ME. To test glass reaction vessels, a 600 μL auto-sampler brown glass vial was fitted with a rubber septa. Two identical reactions in which KF was added after β ME to yield a maximum amount of MeQM adducts were used to compare the yield of MeQM

adducts between the plastic and glass reaction vessels (**Table 5.3**). The reaction in the glass vessel resulted in 51% increase in the amount of MeQM-H₂O and MeQM-βME formed (175 nmol vs. 74 nmol) and 87.5% of the maximum yield (200 nmol) based on 4-MeBrQMP. It was also discovered that shaking the reaction, as opposed to floating in a water bath, had a more dramatic effect on the yield of both adducts when reaction conditions consisted of 4 hours in between KF initiation of MeQM and addition of βME (Δt_1) (**Table 5.4**). The combined total of MeQM-H₂O and MeQM-βME increased 20% from 79 nmol to 120 nmol. Furthermore, shaking with the glass vessel increased the combined yield of MeQM-H₂O and MeQM-βME by 12% over shaking the plastic reaction vessel (144 nmol vs. 120 nmol). These results suggest that better mixing of the reaction solution is key to obtaining the maximum recovery of MeQM adducts. A change of reaction temperature from 37 °C to room temperature (20 – 25 °C) was also needed because the shaking device was on the benchtop.

Table 5.3. Reaction conditions used to compare the effect of reaction vessel on the persistence of MeQM and subsequent formation of MeQM- β ME. The reactions were carried out in a polypropylene vial (1.5 mL) and a glass auto-sampler vial (600 μ L) at 37 °C for 24 hours with no agitation after the initial mixing.

Stock Solution	Volume to Add (μ L)	Final Concentration (mM)	Final Volume (μ L)
100 mM MOPS pH 7	10	8.3	
H ₂ O	40		
CH ₃ CN	15		
50 mM Phenol in H ₂ O	10	4.2	
40 mM 4-MeBrQMP in CH ₃ CN	5	1.7	
600 mM β ME in 50 mM MOPS pH 7	20	100	
2.5 M KF in H ₂ O	20	416.7	120

Table 5.4. Reaction conditions used to compare the effect of shaking the reaction vessel on the persistence of MeQM and subsequent formation of MeQM- β ME. The reactions were carried out in a polypropylene vial (1.5 mL) and a glass auto-sampler vial (600 μ L) at room temperature for 4 hours after KF initiation (Δt_1) followed by addition of β ME and no agitation at 37 °C for 24 hours (Δt_2).

Stock Solution	Volume to Add (μ L)	Final Concentration (mM)	Final Volume (μ L)
100 mM MOPS pH 7	10	10	
H ₂ O	40		
CH ₃ CN	15		
50 mM Phenol in H ₂ O	10	5	
40 mM 4-MeBrQMP in CH ₃ CN	5	2	
2.5 M KF in H ₂ O	20	500	100
Trapping:			
600 mM β ME in 50 mM MOPS pH 7	20	100	120

Since the reaction conditions were changed significantly from the earlier studies (**Table 5.2**), a new control experiment was needed to measure the persistence of MeQM without the presence of DNA (**Table 5.5**). Again, the aging time between KF initiation (Δt_1) of MeQM and addition of the β ME trap was varied between 0 – 24 hours. The subsequent formation of MeQM- β ME was measured to quantify the persistence of MeQM or 4-MeBrQMP. During this time, the reaction was shaken in the glass vessel at room temperature. After β ME addition, the reaction was kept in a water bath at 37 °C for 24 hours (Δt_2) and subsequently analyzed by HPLC. MeQM- β ME was observed to form after all reaction times (Δt_1) of up to 2 hours, suggesting that MeQM or 4-MeBrQMP still persisted in solution as MeQM- β ME has been shown to only form with MeQM.

Table 5.5. Reaction conditions for the control experiment which measures the persistence of MeQM or 4-MeBrQMP in solution in the absence of DNA. Reaction was shaken at room temperature after KF initiation of MeQM for 0 - 24 hours (Δt_1) and was held at 37 °C for 24 hours after addition of β ME (Δt_2).

Stock Solution	Volume to Add (μ L)	Final Concentration (mM)	Final Volume (μ L)
100 mM MOPS pH 7	10	10	
H ₂ O	30		
CH ₃ CN	25		
50 mM Phenol in H ₂ O	10	5	
40 mM 4-MeBrQMP in CH ₃ CN	5	2	
2.5 M KF in H ₂ O	20	500	100
Trapping:			
pure β ME	10	1290	110

Once it was determined that glass reaction vessels resulted in a higher yield of MeQM adducts, a more permanent solution than the septa capped auto-sampler vial was needed. Glass Reacti-vials were the practical choice as they can use stir bars, can be stirred in the warm room at 37 °C, and they can accommodate a number of reaction volumes (0.3 mL and 5 mL vials). All of the following reactions use Reacti-vials as the reaction vessel.

When ctDNA was introduced into the above reactions, HPLC analysis revealed that it co-elutes with MeQM-H₂O, obscuring the actual amount of MeQM-H₂O in solution (**Figure 5.8**). The broad peak at $t_r = 21$ minutes was confirmed to be ctDNA by its λ_{max} (259 nm) and it matches the t_r of a prepared standard of only ctDNA and the reaction solvents.

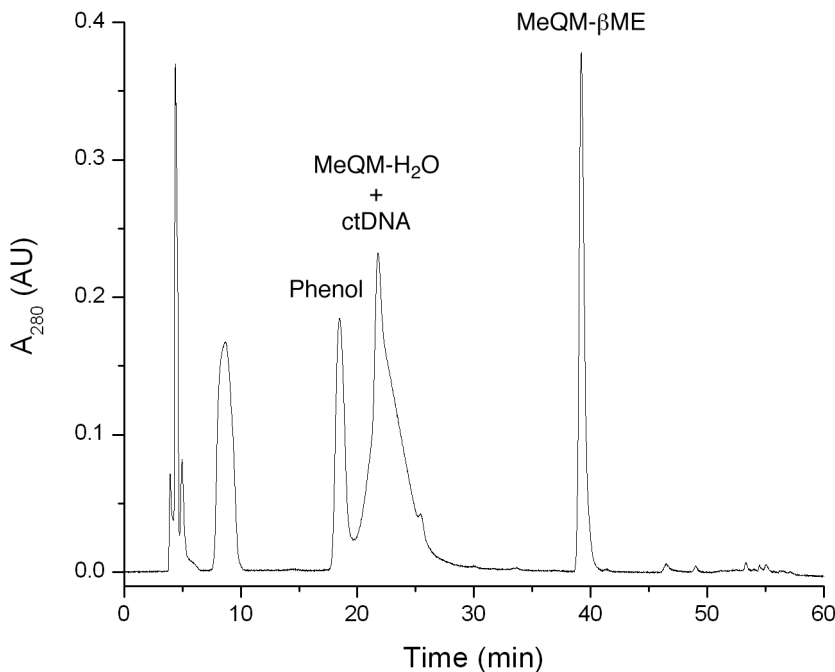


Figure 5.8. Example HPLC chromatogram of the β ME trapping reaction detailed in **Table 5.4**, including ctDNA at 4 mM nts. The reaction was stirred for 14 hours at r.t. after KF initiation of MeQM (Δt_1) followed by stirring for 4 hours at 37 °C after β ME addition (Δt_2). HPLC analysis used a linear gradient of 5 – 30% CH₃CN in TEAA (10 mM, pH 5).

As a simple solution to ctDNA co-eluting with MeQM-H₂O, different aqueous phases were tested to observe any effect of the t_r of ctDNA so that it would not overlap with any of the compounds of interest (phenol, MeQM-H₂O, and MeQM- β ME). The original aqueous phase was 10 mM TEAA pH 5 and the first new aqueous phase tested was 10 mM TEAA pH 4 since the elution of DNA is pH dependant. This resulted in an increased t_r (23 minutes) for ctDNA that still overlapped with MeQM-H₂O. The next aqueous phase tested was 10 mM ammonium formate pH 6.9. The ctDNA now eluted earlier (17 minutes) and did not overlap with MeQM-H₂O. Unfortunately, the ctDNA now co-eluted with phenol. The next aqueous phase tested was 0.1% aqueous trifluoroacetic acid (TFA), with the

expectation that the lower pH (~2) would increase the t_r beyond MeQM-H₂O, but not to MeQM-βME. Using this aqueous phase, the ctDNA did not elute during the course of the gradient as it precipitated out of solution on the column prior to the UV-Vis detector. One last aqueous phase tested was 10 mM ammonium formate pH 3 to avoid precipitation of ctDNA, but the ctDNA once again co-eluted with MeQM-H₂O. The only aqueous phase (in the pH range tolerated by the C18 silica) to clearly resolve the three compounds of interest was 0.1% TFA. To avoid precipitating DNA on the HPLC column, a work-up of the reaction consisting of an addition of 100 μL 0.1% TFA followed by filtration (syringe filter, 0.2 μm) and an addition of another aliquot of 0.1% TFA (50 μL) to push the remainder of the reaction through the filter was utilized when 0.1% TFA was the aqueous phase. The drop in pH upon addition of 0.1% TFA caused the ctDNA to precipitate out of solution. After filtration, the ctDNA was removed from the subsequent HPLC analysis allowing for a cleaner HPLC chromatogram.

An attempt to determine the mechanism behind the surprising persistence of MeQM in aqueous conditions analyzed the reaction prior to the addition of βME. The hypothesis was that an intermediate was formed with the active MeQM that could then reverse to form MeQM or be substituted directly by βME to form MeQM-βME. Either option would give the impression of MeQM persisting for hours in solution. The reaction from **Table 5.5** was analyzed by HPLC after 1 – 2.5 hours after KF activation of MeQM (Δt_1), prior to βME addition. A new compound was observed ($t_r = 15$ min) that does not co-elute with any previous compound and has a unique UV-Vis absorbance ($\lambda_{max} = 287$ nm) which suggested that it was a previously

unobserved MeQM adduct. Multiple reactions without ctDNA and β ME were carried out to allow for the collection of this new compound. The compound proved stable enough in CD_3CN for ^1H NMR (**Figure 5.9**) and ESI $^+$ -MS (**Figure 5.10**).

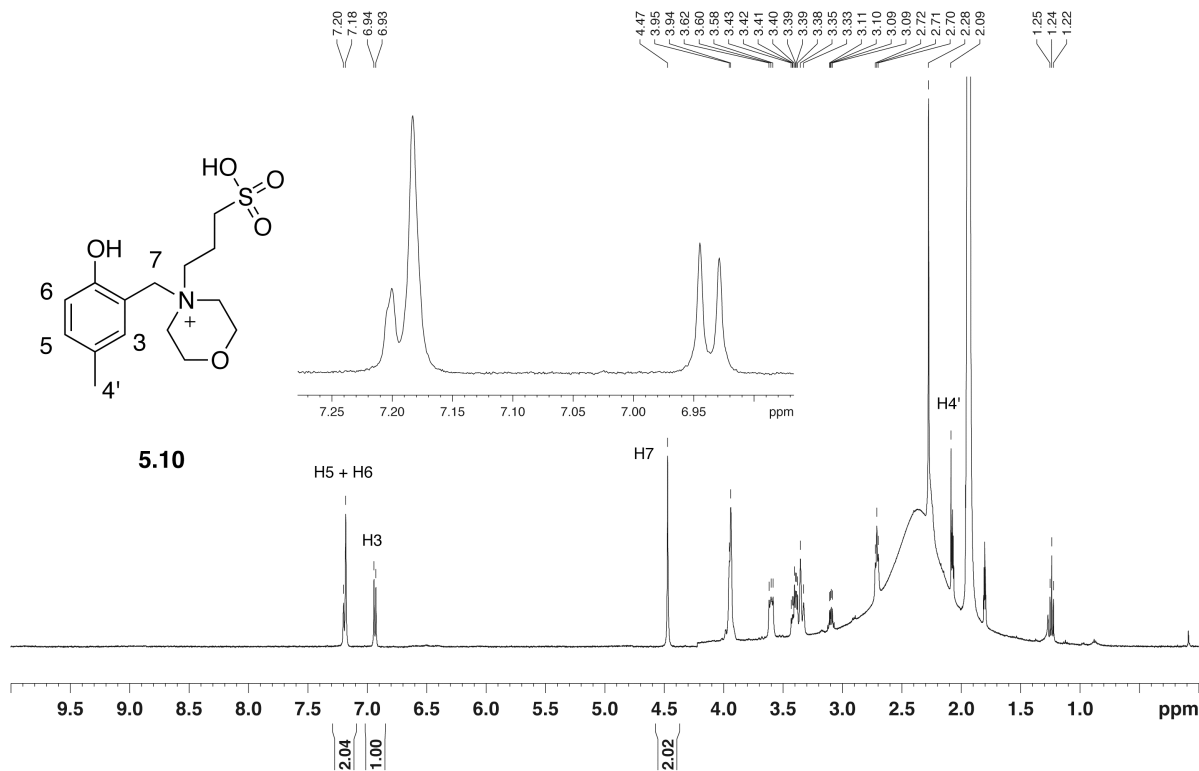


Figure 5.9. ^1H NMR of the proposed MeQM-MOPS adduct (**5.10**) in CD_3CN at 500 MHz. The methylene protons from the MOPS fragment were observed between 2.5 – 4 ppm, but the specific identification was ambiguous.

^1H NMR supports the claim that this is a MeQM adduct due to the characteristic three aromatic protons (H3, H5, H6 - 6.93 - 7.20 ppm), methylene bridge (H7 - 4.47 ppm), and a peak possibly corresponding to the 4-Me group (H4' - 2.28 ppm). Due to H_2O in the NMR sample, integration of the numerous aliphatic protons was not possible. The chemical shifts of the aromatic protons and the methylene bridge do not match any of the previously mentioned MeQM adducts, such as MeQM- H_2O (H7 = 4.61 ppm) or MeQM- β ME (H7 = 3.70 ppm). The possibility

existed that the compound was the deprotected, but not debrominated, 4-MeBrQMP. This theory was disproved by ESI⁺-MS as there were no fragments characteristic of a bromine containing compound or of the deprotected and debrominated compound. There was, however, a fragment corresponding to a MeQM-MOPS adduct (*m/z* 330.16 exp. vs. 330.14 calc.) and free MOPS (*m/z* 210.10 exp. vs. 210.08 calc.) (Figure 5.10).

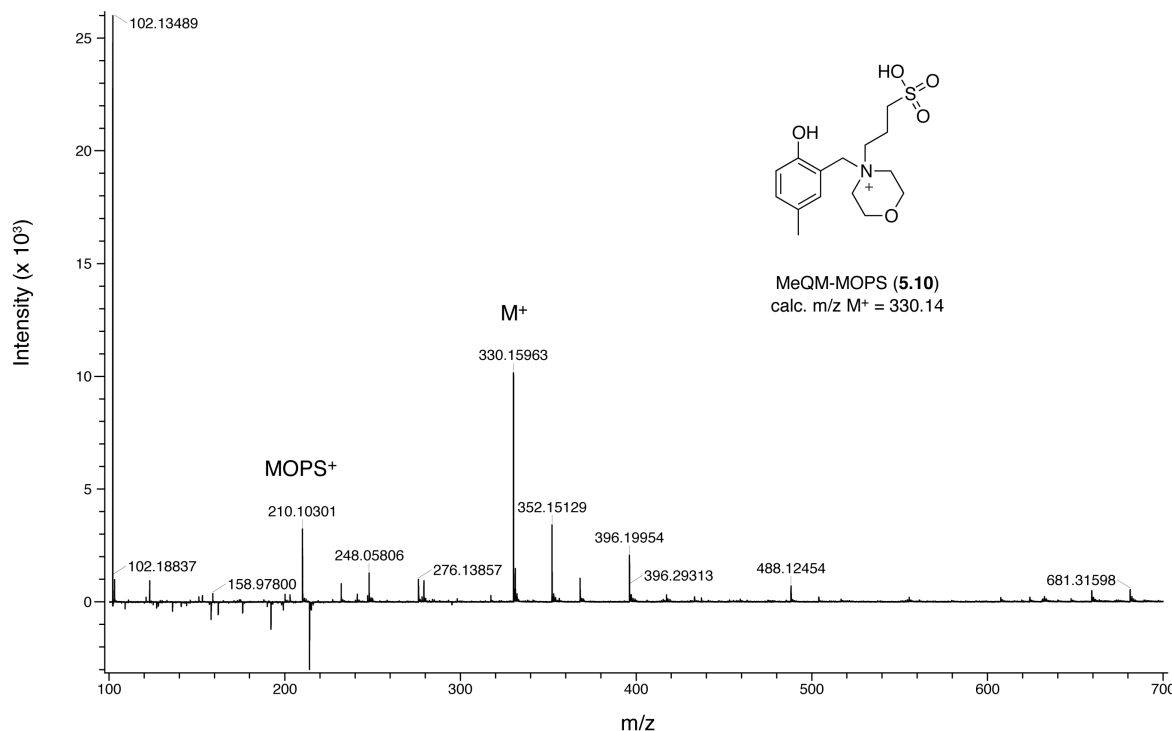


Figure 5.10. ESI⁺-MS of MeQM-MOPS (5.10). The parent compound (5.10, M⁺) and the MOPS fragment are detected.

Additional evidence supporting this structure was the disappearance of the compound at *t*_r = 15 min when only MOPS is removed from the reaction. Unfortunately, attempts to recover the compound from the NMR solvent (CD₃CN) were unsuccessful. A majority of the compound eluted with the injection volume while in 100% CD₃CN and when the sample was diluted to 50% CD₃CN with water.

A portion of the NMR sample (30 μ L in CD₃CN) was subjected to the standard β ME trapping conditions (70 μ L water and 10 μ L β ME stirring for 4 hrs at 37 °C) to test the reversibility of the new MeQM adduct. There was no observed MeQM- β ME adduct, but due to the small amount of starting material in the NMR sample this result may be inconclusive. Further testing of this adduct was not a priority, but provided enough reason to remove the MOPS buffer from the reaction and use a less nucleophilic buffer in its place.

Upon the discovery that MOPS reacts with MeQM discovery, it was thought that this product was contributing to the persistence of MeQM. To investigate this claim, the β ME trapping experiment was repeated by exchanging the MOPS buffer with H₂O or potassium phosphate (50 mM, pH 7 stock solution). Each reaction was incubated at room temperature for 2 hours after KF initiation of MeQM (Δt_1) and another 4 hours at 37 °C after the β ME addition to allow for the complete trapping of any reversible MeQM (Δt_2). These conditions previously resulted in the formation of both MeQM-H₂O and MeQM- β ME to compare the three solvents (MOPS, H₂O, and phosphate). The reaction that included MOPS had the most MeQM- β ME, accounting for 86% of the total adducts formed, while the reaction with H₂O resulted in 17% MeQM- β ME and the potassium phosphate reaction resulted in 10% MeQM- β ME. Potassium phosphate was chosen to replace MOPS as the buffer in the following trapping studies based on this data.

With the replacement of MOPS with potassium phosphate, the ability of ctDNA to extend the effective lifetime of MeQM was again investigated. The reaction conditions followed the previous β ME trapping experiments and consisted of

a 30% aqueous CH₃CN solution with phenol (internal standard), ctDNA (nucleophilic target), 4-MeBrQMP (MeQM source), and KF (MeQM initiator) (**Table 5.6**). This solution was stirred at 37 °C for 30 minutes (Δt_1) to allow for reaction with water or DNA prior to addition of βME (10 μL, 1.29 M final concentration). The solution continued to stir at 37 °C for 4 hours (Δt_2) to allow for full transfer of reversible MeQM from DNA to βME prior to 0.1% TFA work-up and HPLC analysis. These conditions would allow for the capture of the initial MeQM by ctDNA and its subsequent release and trap by βME. A blank reaction, without the ctDNA, was also analyzed by HPLC to quantify the effect of ctDNA on the persistence of MeQM, as measured by MeQM-βME. The reaction containing ctDNA yielded a 2.5-fold increase in MeQM-βME over the blank reaction (35 nmol vs. 14 nmol) (**Figure 5.11**). In order to put this result in context, a number of DNA nucleophiles were also studied. These included nucleosides, shorter dsDNA, and shorter ssDNA.

Table 5.6. Reaction conditions for the comparison between the ability of various nucleoside based nucleophiles to extend the lifetime of MeQM in solution using potassium phosphate as a buffer. ctDNA, **OD1**, **OD2**, **OD1/OD3**, and dNs were investigated at a final concentration of 4 mM in nucleotides.

Stock Solution	Volume to Add (μL)	Final Concentration (mM)	Final Volume (μL)
H ₂ O	15		
CH ₃ CN	25		
50 mM Phenol in H ₂ O	10	5	
16 mM nts DNA in 50 mM potassium phosphate pH 7	25	4 (in nts) 25 (phosphate)	
40 mM 4-MeBrQMP in CH ₃ CN	5	2	
2.5 M KF in H ₂ O	20	500	100
Trapping:			
pure βME	10	1290	110

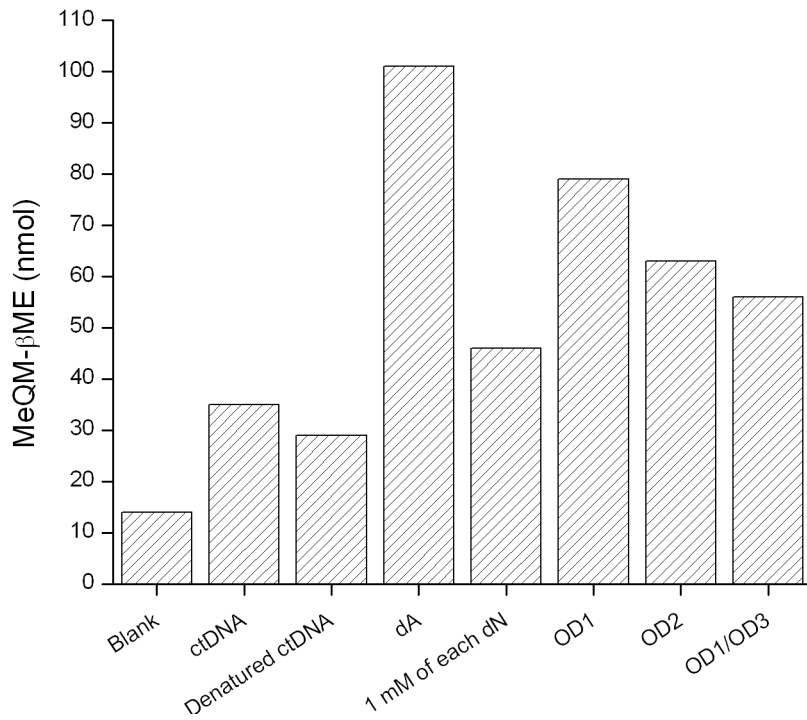


Figure 5.11. Comparing the formation of MeQM- β ME in the presence of various nucleoside based nucleophiles. Each reaction was stirred at 37 °C for 0.5 hr after KF initiation of MeQM (Δt_1) and at 37 °C for 4 hr after β ME addition (Δt_2). **OD1** is an average of two reactions while the other data points are from single reactions. The blank reaction does not contain nucleoside based nucleophiles.

Previous studies have shown that dA will extend the effective lifetime of a bisQM in solution,⁶¹ and has been chosen as a positive control in place of ctDNA in the reaction above (Table 5.6). The effect is observed due to the reversibility of the QM-dA N1 adduct and its ability to efficiently capture and release QM. Formation of a reversible adduct, however, is not the only reason for success in this system as the reversible adducts of dG N7 and dC N3 failed to extend the lifetime of the bisQM under equivalent conditions that were successful with dA N1.¹⁰¹ Although dC N3 forms a reversible adduct with *o*-QM, it is not as good of a nucleophile as dA N1 and cannot efficiently trap and release a bisQM under aqueous conditions.¹⁰¹ While dA

N1 and dC N3 form adducts at high initial yields with *o*-QM, dC N3 reacted slower, reaching a maximum yield after 10 hours versus 30 minutes for dA N1.⁵⁸ The *o*-QM is also released slower by dC N3, when measured by the half-life of QM-dC N3 (approx. 50 hours), than by dA N1 (approx. 4 hours). The adduct formed with dG N7 only forms in low yields and the reverse reaction is in direct competition with deglycosylation leading to the irreversible guanine N7 adduct.⁵⁸ As the other two dG adducts (N1 and N²) are irreversible, dG also does not effectively trap and release an *o*-QM under aqueous conditions.¹⁰¹

Due to its ability to extend the lifetime of *o*-QM, dA was chosen as a positive control with βME trapping (**Table 5.6**). For comparison to ctDNA, dA also utilized a concentration of 4 mM and the same reaction times as the ctDNA study. The reaction with dA resulted in a 7.2-fold increase of MeQM-βME over the blank reaction (101 nmol vs. 14 nmol) and a 2.9-fold increase of MeQM-βME over the ctDNA reaction (101 nmol vs. 35 nmol) (**Figure 5.11**). This result confirmed that dA is a much more effective nucleophile for extending the lifetime of MeQM. An eqimolar mixture of each nucleoside (dA, dG, dC, and dT) was studied also at a total nucleoside concentration of 4 mM. This reaction was to test if dA was the major contributing nucleoside to the increase in effective lifetime of MeQM. The equimolar mixture of dNs resulted in a 3.3-fold increase of MeQM-βME over the blank reaction (46 nmol vs. 14 nmol) and a 1.3-fold increase of MeQM-βME over the ctDNA reaction (46 nmol vs. 35 nmol) (**Figure 5.11**). The equimolar mixture of dNs was 46% as effective as just dA suggesting that dG and dC also increase the lifetime of MeQM in solution, but not as effectively as dA. If dA were the only contributing nucleoside,

the equimolar mixture would be 25% effective as just dA. For each of these reactions, most of the unaccounted MeQM was trapped as MeQM-H₂O (**Appendix D.9**). The remaining MeQM was most likely trapped by the irreversible dN nucleophiles (dA N⁶, dG N1, and dG N²) or polymerized into dimers or trimers.

Denatured ctDNA was used as the source of ssDNA to directly compare the contribution of ssDNA versus dsDNA to extend the effective lifetime of MeQM. The ctDNA was denatured by heating the ctDNA stock solution to 90 °C for 5 minutes followed by quick cooling in an ice bath. The ssDNA is expected to more effectively increase the lifetime of MeQM by providing access to the dA N1 position unencumbered by hydrogen bonding found in dsDNA. The denatured ctDNA, however, resulted in a 0.8-fold decrease in the formation of MeQM-βME when compared to the non-denatured (annealed) ctDNA (29 nmol vs. 35 nmol) (**Figure 5.11, Appendix D.9** for MeQM-H₂O). The most likely reason for similar results with annealed and denatured ctDNA is that the denaturing procedure was not effective, due to the length of ctDNA. To test this hypothesis, a shorter (40 base pairs) oligonucleotide was studied in its ssDNA form and annealed with its complementary strand for its dsDNA form (**Figure 5.12**). The new oligonucleotide, **OD1**, consisted of 40 nucleotides (17.5% A, 30.0% T, 37.5% G, 15.0% C). The exact sequence had no significance, merely that there was not a lack of any one base, it did not form any stable secondary structures (hairpin) at 37 °C, and the melting temperature of its duplex DNA was above 37 °C (calculated at 69 °C as **OD1/OD3**) to limit the presence of ssDNA in future dsDNA studies. **OD1** met these criteria as the ssDNA and was conveniently available as excess material from Dr. Jen Buss from an

unrelated project (as JA2-62 REV). The reaction above (**Table 5.6**) used 4 mM nts **OD1** and yielded a 5.6-fold increase in MeQM- β ME compared to the reaction without nucleosides (79 nmol, vs. 14 nmol) and an increase of 2.7-fold compared to the denatured ctDNA (79 nmol vs. 29 nmol) (**Figure 5.11, Appendix D.9** for MeQM- H_2O). To test if the nucleotide composition of **OD1** contributed to the increase in effective lifetime of MeQM, a second oligonucleotide (**OD2**) was purchased (**Figure 5.12**). **OD2** also consisted of 40 nucleotides (5.0% A, 37.5% T, 40% G, 17.5% C) and featured 12.5% less dA than **OD1**, previously determined to be the major contributing nucleoside to extending the lifetime of MeQM (dA vs. dN). Use of **OD2** did yield a 4.5-fold increase in MeQM- β ME when compared to the reaction without nucleosides (63 nmol vs. 14 nmol), but a 0.8-fold decrease when compared to **OD1** (63 nmol vs. 79 nmol), suggesting that the composition of ssDNA does correlate to its ability to extend the lifetime of MeQM in solution (**Figure 5.11**). **OD2** was still 2.2-fold more effective in extending the lifetime of MeQM than denatured ctDNA (63 nmol vs. 29 nmol), despite the higher dA content of ctDNA (55% A:T).¹⁰⁷ This further shows that denatured ctDNA is not an effective model of ssDNA.



Figure 5.12. Synthesized oligonucleotide sequences used as model of dsDNA and ssDNA. **OD1** and **OD3** are complementary.

OD1 was annealed with its complementary strand **OD3** to form **OD1/OD3** for direct comparison to ctDNA. The comparison will again be based on measuring the

formation of MeQM- β ME as a way to quantify the release of MeQM from DNA. The shorter **OD1/OD3** is expected to have a greater effect on the lifetime of MeQM than ctDNA, based on the results of the ssDNA studies above. The oligonucleotides **OD1** and **OD3** were annealed (**OD1/OD3**) in 50 mM potassium phosphate, pH 7 at 90 °C for 5 minutes followed by slow cooling (overnight) to room temperature. **OD1/OD3** was used in the reaction detailed in **Table 5.9** at 4 mM nts and resulted in a 4.0-fold increase in the formation MeQM- β ME compared to the reaction without nucleosides (56 nmol vs. 14 nmol) (**Figure 5.11, Appendix D.9** for MeQM-H₂O). **OD1/OD3** was 0.7-fold less effective at extending the lifetime of MeQM than just **OD1**, which was expected as two of the positions capable of forming labile adducts with MeQM (dA N1 and dC N3) are occupied in **OD1/OD3** due to hydrogen bond formation. Most importantly, **OD1/OD3** was 1.6-fold more effective at extending the lifetime of MeQM than ctDNA (56 nmol vs. 35 nmol of MeQM- β ME). Based on this result **OD1/OD3** was used the standard dsDNA for the future experiments of MeQM trapping with β ME, while **OD3** will be the standard ssDNA for future experiments due to the increased percentage of dA compared to **OD1** (30% vs. 17.5%).

With a new standard dsDNA (**OD1/OD3**) and new reaction conditions (potassium phosphate in place of MOPS), the release of MeQM from dsDNA needed to be reexamined. Previous studies determined that a trapping time of 4 hours after β ME addition (Δt_2) was sufficient to allow for the full transfer of reversible MeQM from ctDNA to β ME. The subsequent formation of MeQM- β ME was measured while varying the time after β ME addition (Δt_2) from 0 – 24 hours. Unfortunately, these experiments included MOPS buffer, which contributed to the enhanced

persistence of MeQM in solution. The new experiment used the conditions detailed in **Table 5.6** to quantify the release of MeQM from **OD1/OD3** as measured by formation of MeQM- β ME. This information was necessary to determine the time needed after the addition of β ME (Δt_2) for the complete release of MeQM from dsDNA for use in future experiments that vary the aging time (Δt_1). Each reaction was stirred at 37 °C for 30 minutes after KF initiation of MeQM (Δt_1) followed by β ME addition. The reaction was then stirred at 37 °C for 0 – 48 hours (Δt_2) prior to work-up and HPLC analysis. The maximum amount of MeQM- β ME was observed at 24 hours after β ME addition, although the yield may have reached maximum as early as 1 hour, but it is difficult to tell because of the error in the measurements (**Figure 5.13**). Future experiments consistently used 24 hours between β ME addition and work-up to ensure that all of the MeQM was released from the target DNA and for convenience of the analysis.

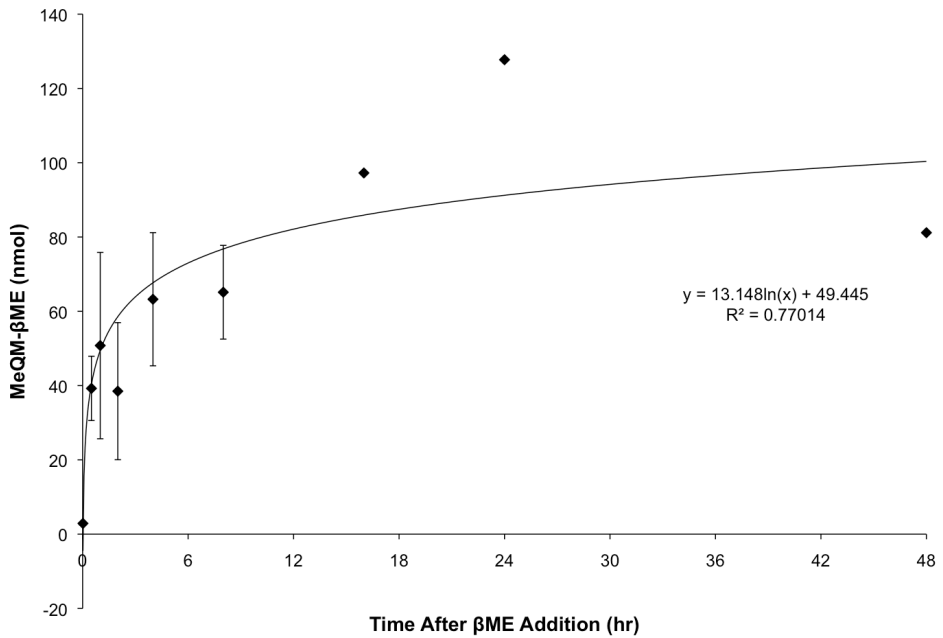


Figure 5.13. Measuring the release of MeQM from **OD1/OD3** by quantifying the amount of MeQM- β ME formed. The data is best fit to a logarithmic trendline only to indicate product trends. Data points prior to 16 hours are an average of three reactions. Data points for 16, 24, and 48 hours are single reactions. The error bars are based on the standard deviation of the data. The amount of MeQM-H₂O formed is shown in **Appendix D.10**.

An issue with the new target dsDNA (**OD1/OD3**) was that, unlike ctDNA, it did not precipitate during the work-up prior to HPLC analysis. While phenol (internal standard) and MeQM- β ME were still well resolved by HPLC, **OD1/OD3** co-eluted with MeQM-H₂O (**Figure 5.14**). Previous attempts to alter the *t_r* of ctDNA determined that higher pH elution buffers decreased the *t_r* of DNA. Specifically, use of ammonium formate (10 mM, pH 6.9) as the elution buffer resulted in both MeQM-H₂O and MeQM- β ME to be well resolved. Unfortunately, phenol was obscured by **OD1/OD3**. The use of a new internal standard that did not co-elute with any other compound in the chromatogram was explored. The compound *m*-cresol differed from phenol only in the addition of a methyl group *meta* to the phenolic oxygen. This difference was enough to alter the *t_r* of *m*-cresol (31 minutes) so that it did not co-

elute with any other compound in the reaction when ammonium formate (10 mM, pH 6.9) was used as the elution buffer. Therefore, *m*-cresol was chosen as the internal standard for the following experiments with the β ME trapping of MeQM (**Figure 5.15**).

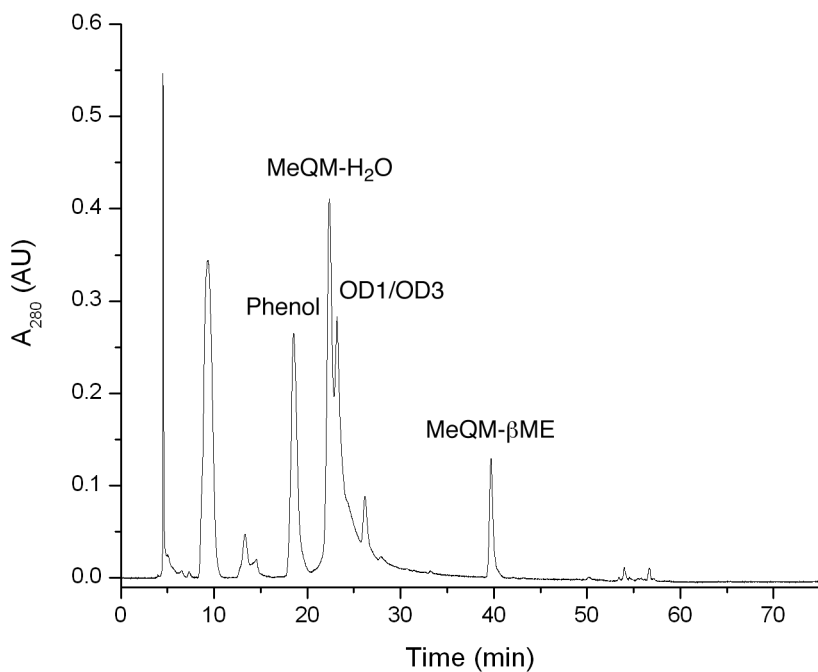


Figure 5.14. HPLC chromatogram of the reaction detailed in **Table 5.6** with **OD1/OD3** as the DNA nucleophile. The reaction was stirred at 37 °C for 30 minutes after KF initiation of MeQM (Δt_1) and 4 hours after β ME addition (Δt_2). HPLC analysis used a linear gradient of 5 – 30% CH₃CN in 0.1% TFA.

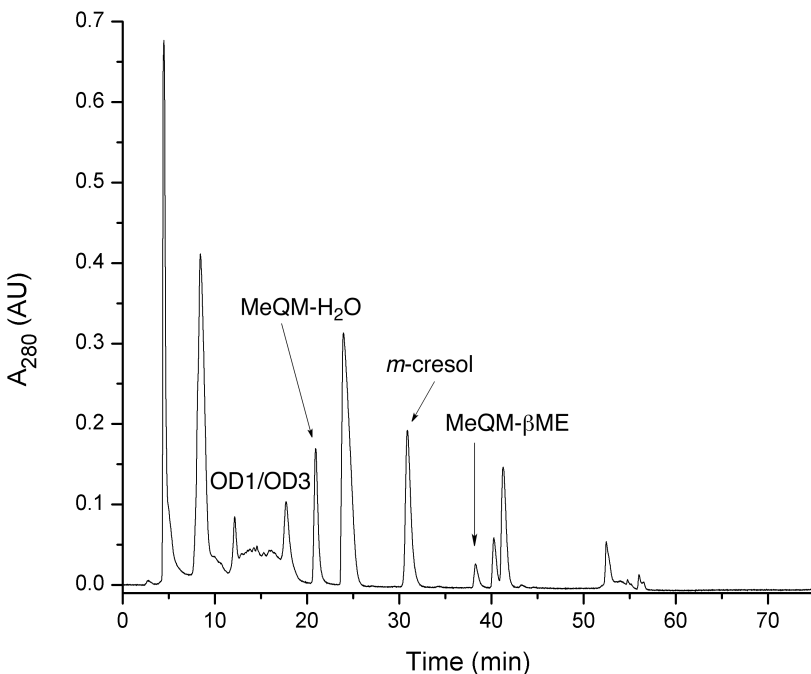


Figure 5.15. HPLC chromatogram of the reaction detailed in **Table 5.7** with **OD1/OD3** as the DNA nucleophile. The reaction was stirred at 37 °C for 30 minutes after KF initiation of MeQM (Δt_1) and 24 hours after β ME addition (Δt_2). Unidentified peaks are mostly β ME by-products. HPLC analysis used a linear gradient of 5 – 30% CH₃CN in ammonium formate (10 mM, pH 6.9).

With a new internal standard, experiments analyzing the release of MeQM from various nucleoside based nucleophiles by measuring MeQM- β ME formation were undertaken. The reaction conditions consisted of a 30% aqueous CH₃CN solution with 5 mM *m*-cresol, 4 mM nts nucleophile (**OD1/OD3** (dsDNA), **OD3** (ssDNA), dA (dN), or no DNA (blank)), 2 mM 4-MeBrQMP, and 500 mM KF (**Table 5.7**). TFA was removed from the work-up as it was no longer needed to precipitate the DNA. In its place 100 μ L of 10 mM ammonium formate pH 6.9 was added to the reaction followed by filtration (0.2 μ m) and HPLC analysis. The new work-up produced a white precipitate which is observed with dsDNA, ssDNA, dA,

and in the blank reaction. It is unknown what the precipitate is, but it does not appear to be any of the compounds of interest (*m*-cresol, MeQM-H₂O, or MeQM-βME).

Table 5.7. Comparison between the ability of various nucleoside based nucleophiles to extend the lifetime of MeQM in solution using *m*-cresol as the internal standard instead of the previously used phenol. **OD1/OD3**, **OD3**, and dA were investigated at a final concentration of 4 mM in nucleotides in 25 mM potassium phosphate.

Stock Solution	Volume to Add (μL)	Final Concentration (mM)	Final Volume (μL)
H ₂ O	15		
CH ₃ CN	25		
50 mM <i>m</i> -Cresol in H ₂ O	10	5	
16 mM nts DNA in 50 mM potassium phosphate pH 7	25	4 (in nts) 25 (phosphate)	
40 mM 4-MeBrQMP in CH ₃ CN	5	2	
2.5 M KF in H ₂ O	20	500	100
Trapping:			
pure βME	10	1290	110

The time points were chosen to give a profile of MeQM release from various nucleoside based nucleophiles by measuring the formation of MeQM-βME. Each time point was an individual 110 μL reaction stirred in a 0.3 mL Reacti-vial at 37 °C. The time points after KF initiation of MeQM (aging, Δt₁) were 0.5, 0.75, 1, 2, and 4 hours, while the time after βME addition (trapping, Δt₂) was a constant 24 hours. The beginning Δt₁ time point (0.5 hr) was chosen based on the length of time necessary for the BrQMP (**1.40**) to fully convert to the active QM intermediate.⁵⁸ As MeQM is more reactive than QM, this should be sufficient time for the initial MeQM to be

captured by DNA and not by β ME. The final Δt_1 time point (4 hr) was chosen because a similar electron-rich QM-dA N1 adduct was observed to have a half-life of less than 4 hours.⁸⁰ As this is the major source of released MeQM in the experiment, it was anticipated that MeQM release after 4 hours would be insignificant. In addition to the reactions without nucleosides, dA, **OD3**, and **OD1/OD3** were present in reactions at a concentration of 4 mM nts (**Figure 5.16**).

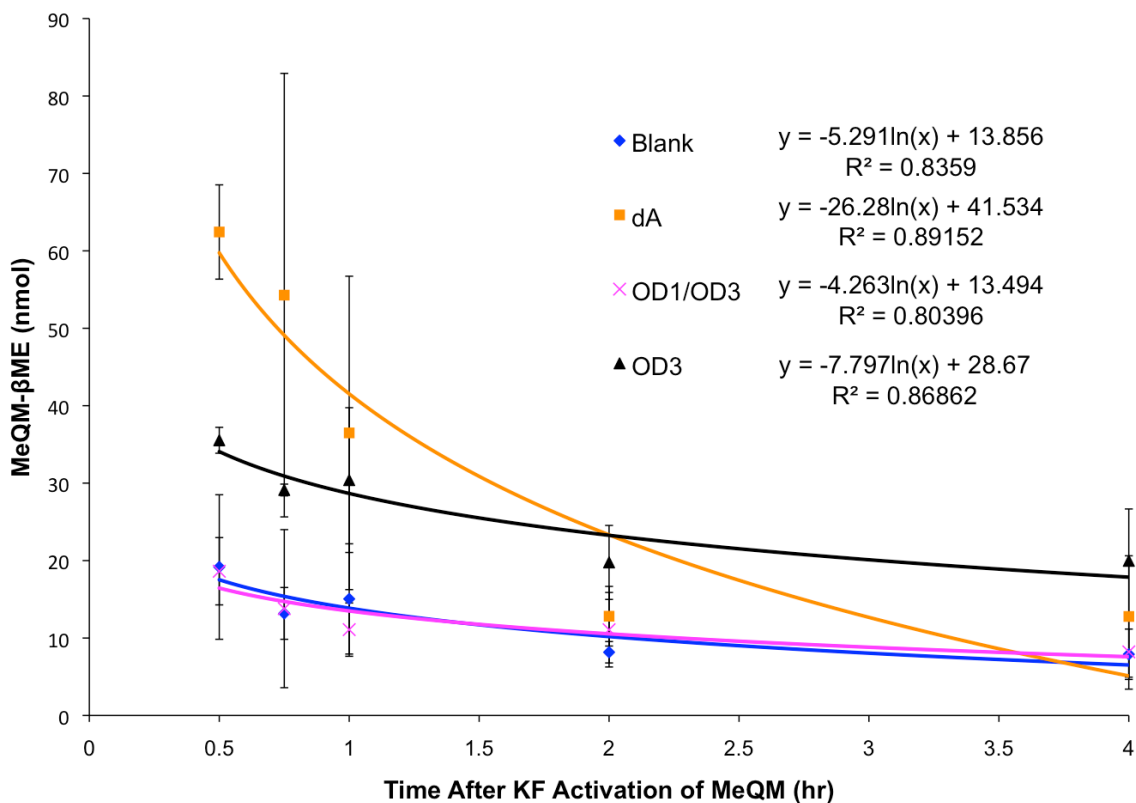


Figure 5.16. Measuring the formation of MeQM- β ME in the presence of various DNA based nucleophiles. Each reaction is stirred at 37 °C for the indicated time after KF initiation (Δt_1) and stirred at 37 °C for 24 hours after addition of β ME (Δt_2). The data is best fit to an exponential trendline only to indicate product trends. Each data point is an average of reactions repeated in triplicate with the error based on the standard deviation.

For this assay, an increase in the formation of MeQM- β ME can be correlated to an increase in the effective lifetime of MeQM in solution. Immediately obvious is the drastic decrease in yield of MeQM- β ME at 30 minutes after KF activation of MeQM (19 nmol) when compared to the previous assay conditions (128 nmol, **Figure 5.13** – 24 hr after β ME addition). The cause of this discrepancy is unknown, but may be due to the new ammonium formate based work-up and eluting buffer (10 mM ammonium formate pH 6.9) in combination with the new internal standard (*m*-cresol) discussed earlier as these were the only conditions altered between the experiments shown in **Figures 5.13** and **5.16**. It is also apparent that over shorter periods of KF initiation of MeQM ($\Delta t_1 < 1$ hr), dA and **OD3** more than double the amount of MeQM that persists in solution. **OD1/OD3**, however, does not effect the lifetime of MeQM in solution when compared to the blank (no nucleoside based nucleophiles) reaction. At 2 hours after KF activation of MeQM (Δt_1), only **OD3** shows increased formation of MeQM- β ME, but not to the extent of the earlier time points.

The ability of dA and **OD3** to apparently extend the lifetime of MeQM can be attributed to their reversible nucleotide adducts dA N1, dC N3, and dG N7. Meanwhile, **OD1/OD3** does not appear to extend the lifetime of MeQM. This can be attributed to the dA N1 and dC N3 positions participating in hydrogen bonding, leaving only dG N7 available in the major groove to form reversible adducts with MeQM. The dG N7 position, as previously discussed, does not efficiently capture and release MeQM due in part to the reverse reaction being in direct competition with deglycosylation leading to the irreversible MeQM-guanine N7. This results in **OD3**

containing 83% of its bases capable of reversible alkylation (based on A, C, and G content), while **OD1/OD3** only contains 26% of its bases capable of reversible alkylation (based on G content), but not the effective dA N1 position. The threefold difference in available reversible alkylation positions should, at least partially, explain why **OD3** is more effective at extending the lifetime of MeQM than **OD1/OD3** (**Figure 5.16**). One problem with this reasoning is that dA should then be consistently better than **OD3** at extending the lifetime of MeQM, but actually is equally effective after one hour. More complex effects such as ssDNA secondary structures that sequester MeQM from the surrounding aqueous environment may provide a mechanism to increase the lifetime of MeQM. The inability of dA to form these secondary structures could contribute to its decreased performance after one hour. Additionally, proximate dA nucleotides in **OD3** may better capture newly released MeQM while the monomeric dA nucleosides won't have the same ability.

5.3. Summary.

The goal of the previous studies was to, for the first time, quantify the release of MeQM from DNA. The release of MeQM from nucleosides, ssDNA, and dsDNA was measured through the use of β ME as a nucleophilic trap followed by HPLC analysis and quantification of the resulting β ME and H_2O adducts of MeQM. The expectation was that the β ME product would form in high yield initially and gradually decrease as MeQM was allowed more time to form irreversible adducts with H_2O and the weaker nucleophiles of DNA.

During the β ME trapping studies a number of variables have been adjusted to allow for the unobstructed reaction of MeQM first with DNA and later with β ME to quantify the release of MeQM from DNA. These adjustments have resulted in the removal of competing compounds (MOPS), changed the reaction vessel (polypropylene to glass), and introduced constant stirring of the reactions. All of these adjustments lead to the near complete consumption of MeQM by both H₂O and β ME. This was necessary to isolate the contribution of various forms of DNA towards extending the effective lifetime of MeQM. Furthermore, HPLC conditions were optimized to ensure that the three compounds of interest (MeQM-H₂O, MeQM- β ME, and *m*-cresol) were eluted fully resolved from each other or any reaction by-products.

The effective lifetime of MeQM under aqueous conditions can be extended by the presence of either dA or a short ssDNA (**OD3**) with dA providing a larger initial effect (< 1 hr). Somewhat surprisingly, a short dsDNA (**OD1/OD3**) appears to have no effect on the effective lifetime of MeQM under aqueous conditions. However, there does seem to be contradicting data on the total yield of MeQM adducts from the experiments shown in **Figures 5.13** and **5.16**. Specifically, the experiments with *m*-cresol as the internal standard and ammonium formate (10 mM, pH 6.9) as the aqueous HPLC phase yield 15% of MeQM adducts as the experiments with phenol as the internal standard and 0.1% TFA as the aqueous HPLC phase. Further analysis of the assay conditions, including possibly selecting a new internal standard and aqueous HPLC phase, may be needed to identify the mechanism behind the apparent differences in these results.

5.4. Materials and Methods.

Organic starting materials, reagents, and solvents were obtained commercially and used without further purification. Silica gel used in the NaHSO₄/SiO₂ catalyst was grade 60 Å, <230 mesh and purchased from Fisher Scientific. All CH₃CN was HPLC grade purchased from Fisher Scientific. UV-Vis spectroscopy was performed on a Hewlett Packard 8453 spectrophotometer. **OD1**, **OD2**, and **OD3** were purchased from Integrated DNA Technologies with “standard desalting” and were not further purified prior to use. To form duplex DNA, **OD1** and **OD3** were dissolved in the indicated buffer, mixed, heated to 90 °C for 5 minutes and slowly cooled to room temperature over several hours.

Synthesis of 2-(hydroxymethyl)-4-methylphenol (MeQM-H₂O, 5.2).

5-Methylsalicylaldehyde (0.809 g, 5.94 mmol) was dissolved in anhydrous THF (40.0 mL), under N₂ at 0 °C. While stirring, a 1 M solution of BH₃/THF (10.0 mL, 10.0 mmol) was slowly added. The reaction was stirred for 1.33 hr under N₂ at 0 °C. The reaction was slowly quenched by addition of 200 mL H₂O and extracted with CH₂Cl₂ (3 × 100 mL). The organic layers were combined, washed with H₂O (2 × 100 mL) and brine (3 × 100 mL), and dried with MgSO₄. The solvent was removed at reduced pressure and the remaining product was purified by chromatotron (1:1, hexanes: ethyl acetate) to yield a white crystalline solid (0.821 g, 100 % yield). ¹H NMR (400 MHz, d₄-methanol) δ 7.06 (d, *J*=2 Hz, 1H), 6.89 (dd, *J*=8, 2 Hz, 1H), 6.65 (d, *J*=8 Hz, 1H), 4.61 (s, 2H), 2.23 (s, 3H). ¹³C NMR (500 MHz, d₄-methanol) δ 154.1, 130.0, 129.8,

129.7, 128.4, 116.0, 61.4, 20.7. ESI⁺-MS: *m/z* 121.0627 ($M + H - H_2O$)⁺. Calcd for $C_8H_9O^+$ ($M + H - H_2O$)⁺: 121.0648. *m/z* 241.1197 ($2M + H - 2H_2O$)⁺. Calcd for $C_{16}H_{17}O_2^+$ ($2M + H - 2H_2O$)⁺: 241.1223. *m/z* 361.1604 ($3M + H - 3H_2O$)⁺. Calcd for $C_{24}H_{25}O_3^+$ ($3M + H - 3H_2O$)⁺: 361.1798. $\lambda_{max} = 223, 279$ nm (diode array detector, 17% CH₃CN in ammonium formate, 8 mM, pH 6.9).

Preparation of NaHSO₄/SiO₂ catalyst.¹⁰⁴ NaHSO₄ (6.9 g, 50 mmol) was dissolved in nanopure water (100 mL) at room temperature. While stirring, <230 mesh silica gel (15 g) was added and the solution stirred at room temperature for 30 minutes. The water was evaporated under reduced pressure to yield a white powder. The white powder was further dried in an oven at 120 °C for 2.5 hr and stored in a sealed 250 mL round bottom flask at room temperature.

Synthesis of 4-methyl-2-[bis[(2-hydroxyethyl)thio]methyl]phenol (5.9).¹⁰⁴ 5-Methylsalicylaldehyde (1.37 g, 10.0 mmol) and β-mercaptopropanol (2.80 mL, 40.0 mmol) were combined in a 50 mL round bottom flask with a magnetic stirrer. NaHSO₄/SiO₂ (2.01g, w/w 23 %) was added slowly over several minutes while stirring at room temperature. As the reaction became more viscous an additional 1.00 mL β-mercaptopropanol was added. Once all of the NaHSO₄/SiO₂ was added, an additional 1.00 mL β-mercaptopropanol was added. The reaction was immediately washed with petroleum ether (20 mL) and the organic layer was checked by TLC (3:1, hexanes:ethyl acetate), but showed no products. The petroleum ether was

removed by pipette once the solid settled to the bottom of the flask and CHCl₃ (10 mL) was added to the reaction producing an opaque solution upon stirring. TLC (3:1, hexanes:ethyl acetate) of the reaction mixture showed complete consumption of the starting material (5-methylsalicylaldehyde). The reaction mixture was extracted by petroleum ether (3 × 20 mL) and the CHCl₃ layer was saved. An additional 20 mL CHCl₃ was added to the CHCl₃ layer and the combined solution was washed with H₂O (2 × 20 mL), dried with Na₂SO₄, and evaporated under reduced pressure to yield a clear oil (1.73 g, 63.0 % crude yield). The clear oil began to crystallize over several hours and the remaining solvent was removed overnight under vacuum. ¹H NMR (400 MHz, CDCl₃) δ 7.79 (s, 1H), 7.30 (d, *J*=1.4 Hz, 1H), 6.92 (dd, *J*= 1.4, 8.2 Hz, 1H), 6.70 (d, *J*= 8.2 Hz, 1H), 5.50 (s, 1H), 3.76 (s, 2H), 3.70 (m, 4H), 2.81 (m, 2H), 2.66 (m, 2H), 2.25 (s, 3H). ESI⁺-MS: *m/z* 197.09 (M + H - βME)⁺. Calcd for C₁₀H₁₃O₂S⁺ (M + H - βME)⁺: 197.06. *m/z* 257.10 (M - OH)⁺. Calcd for C₁₂H₁₇O₂S₂⁺ (M - H₂O)⁺: 257.07. *m/z* 297.09 (M + Na)⁺. Calcd for C₁₂H₁₈NaO₃S₂⁺ (M + Na)⁺: 297.06.

Synthesis of 4-methyl-2-[(2-hydroxyethylthio)methyl]phenol (MeQM-βME, 5.3).¹⁰⁵ The crude product generated above (5.9) (0.27 g, 0.98 mmol) was combined with 1,4-cyclohexadiene (0.09 mL, 0.95 mmol) in 1,2-dichloroethane (7 mL). A suspension of AlCl₃ in hexanes (0.10 mL, 0.96 M, 0.096 mmol) was added dropwise to the reaction solution while stirring under N₂ at room temperature. A color change in the reaction mixture from colorless to red/orange was observed, along with a precipitate formed within five minutes of the addition of AlCl₃. Within one hour, the

reaction solution changed from red/orange to yellow. The reaction was monitored by TLC (2:1, hexanes:ethyl acetate) and ^1H NMR (CD_3CN) after a quick workup in which a 100 μL aliquot of the reaction solution was quenched slowly in a 1.5 mL Eppendorf with 200 μL H_2O . Additional CHCl_3 (100 μL) was added and, after shaking, the organic phase was removed for analysis. A second addition of AlCl_3 in hexanes (0.90 mL, 0.96 M, 0.86 mmol) was added dropwise to the reaction after 5 hours. A color change from yellow to cloudy red was observed and the reaction was stirred under N_2 at room temperature overnight. A third addition of AlCl_3 in hexanes (1.0 mL, 0.96 M, 0.96 mmol) was added dropwise to the reaction after 25.5 hours and a color change from yellow to dark red was observed. The solution became a cloudy, dark brown color within 45 minutes. The reaction was slowly quenched with H_2O (20 mL) after 28 hours. The quenched reaction was extracted with CHCl_3 (3×20 mL), washed with brine (3×20 mL), dried with MgSO_4 , and evaporated under reduced pressure to yield a yellow/brown oil, which changed color to a brown/black oil while stored at 0 °C. The brown/black oil was purified by silica gel radial chromatography (chromatotron) using hexanes, then 2:1 hexanes:ethyl acetate with <1 % methanol, and finally ethyl acetate with <1 % methanol. The second band contained the product, but was not pure by ^1H NMR (CD_3CN) (32 mg, 16 % crude yield). The product was further purified by analytical reverse-phase C18 HPLC using a 3 - 25% gradient of CH_3CN in 0.1% aqueous TFA over 76 minutes (1 mL/min). The product **5.3** was collected ($t_r = 50$ - 60 minutes) and lyophilized to yield a clear oil (13 mg, 6.7 % yield). ^1H NMR (400 MHz, d_3 -acetonitrile) δ 6.99 (s, 1H), 6.92 (d, $J=8.4$ Hz, 1H), 6.71 (d, $J=8.4$ Hz, 1H), 3.71 (s, 2H), 3.64 (t, $J=6.4$ Hz, 2H), 2.57 (t,

J=6.4 Hz, 2H), 2.22 (s, 3H). ^{13}C NMR (500 MHz, d₃-acetonitrile) δ 154.2, 132.3, 130.1, 130.0, 126.1, 116.9, 62.6, 35.2, 31.6, 20.9. ESI⁺-MS: *m/z* 199.0838 (M + H)⁺. Calcd for C₁₀H₁₅O₂S⁺ (M + H)⁺: 199.0787. *m/z* 121.0689 (M - βME)⁺. Calcd for C₈H₉O⁺ (M - βME)⁺: 121.0648. *m/z* 221.0669 (M + Na)⁺. Calcd for C₁₀H₁₄NaO₂S⁺: 221.0607. *m/z* 237.0584 (M + K)⁺. Calcd for C₁₀H₁₄KO₂S⁺: 237.0346. $\lambda_{\text{max}} = 219$, 283 nm (diode array detector, 26% CH₃CN in ammonium formate, 7 mM, pH 6.9).

Chapter 6: Conclusions

A variety of exogenously generated electrophiles have proven to be capable of alkylating DNA. If not repaired, these DNA adducts can lead to mutations and either cancer or cell death. Prediction of the toxicity of any DNA alkylating agent utilizing this mechanism of action would require the determination of its reactivity towards DNA under biologically relevant conditions. An added complication to the determination of the reactivity of an alkylating agent with DNA is that some of these electrophiles can alkylate DNA reversibly, effectively extending their lifetime *in vivo* while making their detection more difficult than that for irreversible alkylating agents. The ability to predict toxicity of a DNA alkylating agent is important because a number of these compounds have found success as chemotherapeutic agents whose mechanism of action is the targeted alkylation of DNA contained in tumor cells. While effective, any non-specific alkylation outside of the tumor can lead to genotoxicity and the devastating side-effects experienced with chemotherapy. The development of a trapping system allowing for the detection and quantification of the reversible DNA adducts would greatly enhance understanding of the reactivity of the reversible DNA alkylating agent and help to guide the synthesis of more selective agents.

Electrophilic *ortho*-quinone methides (*o*-QM) can alkylate DNA and are generated during xenobiotic metabolism of a variety of compounds. From model studies based on nucleosides, *o*-QMs react most readily, but reversibly with strong nucleophiles. Their reaction is less efficient, but irreversible with weak nucleophiles.

The hour time-scale of the reverse reactions complicates analysis of their products in DNA, which requires enzymatic digestion and chromatographic separation. The alkylation profile of DNA can change drastically from the beginning of the digestion to the chromatographic separation. Instead, a chemical trap utilizing bis[(trifluoroacetoxy)iodo]benzene (BTI) has been developed to transform the reversible MeQM-DNA adducts into irreversible derivatives capable of surviving such analysis, allowing the intrinsic selectivity of MeQM alkylation of DNA to be determined for the first time. The goal of this dissertation was to synthesize and characterize the oxidation products of each individual MeQM-dN adduct and then use these products as analytical standards to determine the MeQM alkylation profile of DNA at short time points.

Oxidative trapping studies with the unsubstituted *o*-QM and dC highlight the necessity of an alkyl substituent *para* to the phenolic oxygen to block over-oxidation and the subsequent rearrangement and reincorporation of bromine to the final product. The novel precursor 4-MeBrQMP (**2.6**) included a methyl group *para* to the phenolic oxygen to block the over-oxidation. Initial studies with dC resulted in the formation of MeQM-dC N3 (**2.8**) which was subsequently oxidized to a single stable product (**2.15**). The oxidized MeQM-dC N3 adduct (**2.15**) was fully characterized by 1D NMR, 2D NMR, and ESI⁺-MS.

Oxidation of the four MeQM-dG adducts (dG N7, dG N1, dG N², and guanine N7) yielded four unique products. Due to the deglycosylation of MeQM-dG N7 to MeQM-guanine N7, only three of the oxidation products were fully characterized by 1D NMR, 2D NMR, and ESI⁺-MS as these are the only oxidized products expected to

survive the enzymatic digestion of DNA. Interestingly, BTI oxidation of the MeQM-dG adducts resulted in the transformation of the QM phenol to a *p*-quinol, unlike the oxidation of MeQM-dC N3 that resulted in the transformation of the QM phenol to a spiro-cyclized product. The result of both transformations is the formation of stable products capable of surviving the enzymatic digestion conditions.

Initial studies involving duplex DNA were begun as my undergraduate mentee Omer Ad carried out the synthesis and characterization of the oxidized products of MeQM-dA N1 and MeQM-dA N⁶. The enzymatic digestion of DNA was observed to be sensitive to the quality of enzyme used, specifically phosphodiesterase I. The enzyme supplier has therefore become an important variable to in the digestion of DNA. With suitably high quality enzymes, both from Sigma-Aldrich, enzymatic digestion was determined to be effective after both alkylation and oxidation conditions are applied to a target DNA. It was also observed that the efficiency of alkylation of target DNA by MeQM decreases as the target is changed from monomeric nucleosides to a short duplex DNA (**OD1/OD3**) and decreases further as the target DNA is changed to a long duplex DNA (salDNA). The result is that amount of MeQM-DNA adducts formed is near the level of detection of the HPLC analysis. This leads to conditions that are not sufficient to quantify the products of oxidation of MeQM alkylated DNA. One possible solution is to use a method of analysis that is more sensitive than HPLC/UV-Vis, such as LC/MS or ultra high performance liquid chromatography (UHPLC). The increased sensitivity of either method would lower the limit of detection for the products of oxidation of MeQM-DNA. Another possible solution would be to increase the concentrations of starting

materials in the MeQM alkylation of DNA, either 4-MeBrQMP or target DNA, to increase the amount of MeQM-DNA adducts formed. The subsequent oxidation would lead to a larger amount of oxidized MeQM-DNA adducts formed for analysis. Similar to this solution, increasing the maximum injection volume on the HPLC would allow the alkylation and oxidation reactions to be scaled-up and increase the amount of product analyzed. Another method to increase the amount of MeQM-DNA adducts that are formed would be the use of a shorter duplex DNA as the target DNA.

Experiments were also performed to study a different aspect, but with the same goal, of reversible MeQM alkylation of DNA by analyzing the release of MeQM from alkylated DNA. Oxidative dearomatization of the QM phenol with BTI can trap the reversible MeQM-DNA adducts by transforming these adducts into irreversible DNA adducts while β -mercaptoethanol (β ME) can irreversibly trap MeQM released from DNA to form MeQM- β ME. HPLC quantification of MeQM- β ME can be used to measure the amount of reversible MeQM-DNA adducts still present in a specific target DNA at a specific time. Alkylations of target DNA (dsDNA, ssDNA, and dN) by MeQM for less than 4 hours were subsequently reacted with β ME. These studies showed that the nucleoside dA and the ssDNA **OD3** successfully extended the lifetime of MeQM in solution. The dsDNA **OD1/OD3**, however, had no effect on the lifetime of MeQM when compared to the reaction without a nucleoside based nucleophile. The ability of single stranded **OD3** to effectively capture and release MeQM while double stranded **OD1/OD3** did not capture and release MeQM suggests that **OD3** may have a greater amount of MeQM-

DNA adducts formed initially and, therefore, may be a better target DNA for the oxidative trapping studies than **OD1/OD3**. The presence of reversible MeQM-DNA adducts should allow for a higher yield of oxidized products at short reaction times, increasing the amount of oxidized MeQM-DNA adducts available for HPLC analysis.

The analytical standards necessary for the quantification of the oxidative trapping of reversible MeQM-DNA adducts have been synthesized and characterized. Unfortunately, the alkylation yield of duplex DNA is insufficient for analysis by HPLC. A number of solutions including increasing the concentration of reagents, substituting ssDNA for dsDNA, and utilizing a more sensitive analytical method for the detection of MeQM-DNA adducts have been proposed and will be pursued in the future. Once the oxidative trapping of MeQM-DNA adducts can be accomplished, the alkylation time can be varied to obtain an alkylation profile of MeQM towards DNA. It can also be determined if MeQM alkylates DNA at the most nucleophilic and accessible position (dG N7) or if there is a sequence specificity that influences the reactivity of MeQM towards DNA. If, as predicted, dG N7 is preferentially alkylated initially, MeQM may be useful also as a molecular probe of duplex DNA structure. For example, if there are portions of duplex DNA that are not base paired, the presence of MeQM-dC N3 and MeQM-dA N1 would be detected.

The goal of the studies presented in this dissertation is to develop a method of trapping the reversible QM-DNA adducts to determine the intrinsic selectivity of *o*-QM towards DNA. With the BTI based oxidative trapping system and the synthesized analytical standards, this intrinsic selectivity can be determined. Knowledge of the type, location, and amount of DNA adducts formed by *o*-QM can

be used to assess the potential toxicity of QM-based DNA alkylating agents.

Furthermore, a targeted QM-based DNA alkylating agent can be developed with the hope of finding use as an anti-cancer chemotherapeutic agent with the information gained from the future MeQM-DNA studies.

Appendices

Appendix A. Supporting Information for Chapter 2

Table A.1. ^{13}C and ^1H NMR data for the product (**2.2**) formed by oxidation of QM-dC adduct **1.42** (DMSO- d_6).

Position	^{13}C shift (ppm)	^1H shift (ppm)	HMBC Connectivity
1'	85.6	6.39 (t, $J=6.6$ Hz)	2', 3', 4', 6
2'	40.2	2.23 (m)	4'
3'	70.2	4.30 (m)	2', 4', 5'
4'	87.9	3.87 (m)	2', 3', 5'
5'	61.1	3.62 (m)	2', 3', 4'
2, 4	145.2, 145.2		1', 5, 6, 7
5	98.1	6.78 (d, $J=8.0$ Hz)	6
6	129.9	7.85 (d, $J=8.0$ Hz)	1', 5
7	116.6	8.63 (s)	10
8	138.7		7, 10
10	143.2	8.39 (s)	
11	124.4		10, 12
12	187.6	9.44 (s)	10

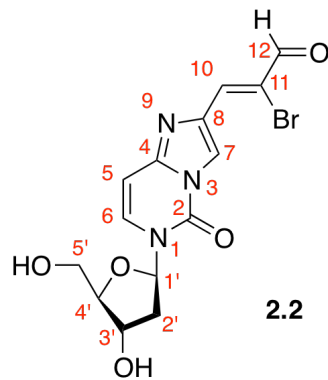
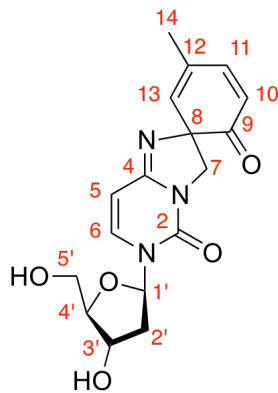


Table A.2. ^{13}C and ^1H NMR data for the product (**2.15**) formed by oxidation of MeQM-dC adduct **2.8** (DMSO- d_6).

Position	^{13}C shift (ppm)	^1H shift (ppm)	HMBC Connectivity
1'	83.8	6.16 (t, $J=7.0$ Hz)	2', 3', 4', 6
2'	39.5	2.04 (m)	
3'	70.5	4.22 (m)	2', 4', 5'
4'	87.1	3.75 (m)	2', 5'
5'	61.4	3.53 (m)	3'
2	147.5		1', 6
4	154.9		5, 6, 7
5	96	5.78 (d, $J=8.2$ Hz)	6
6	137	7.50 (d, 8.2 Hz)	1', 5
7	51.5	3.70 (d, $J=11.2$ Hz), 3.92 (d, $J=11.2$ Hz)	
8	73.1		7, 10
9	199.7		7
10	123.5	5.97 (d, $J=9.9$ Hz)	
11	146.3	7.03 (dd, $J=9.9, 2.2$ Hz)	14
12	128.8		11, 14
13	136.6	6.06 (bd, $J=6.4$ Hz)	7, 10, 11, 14
14	20.3	1.90 (d, $J=1.2$ Hz)	11, 13



2.15

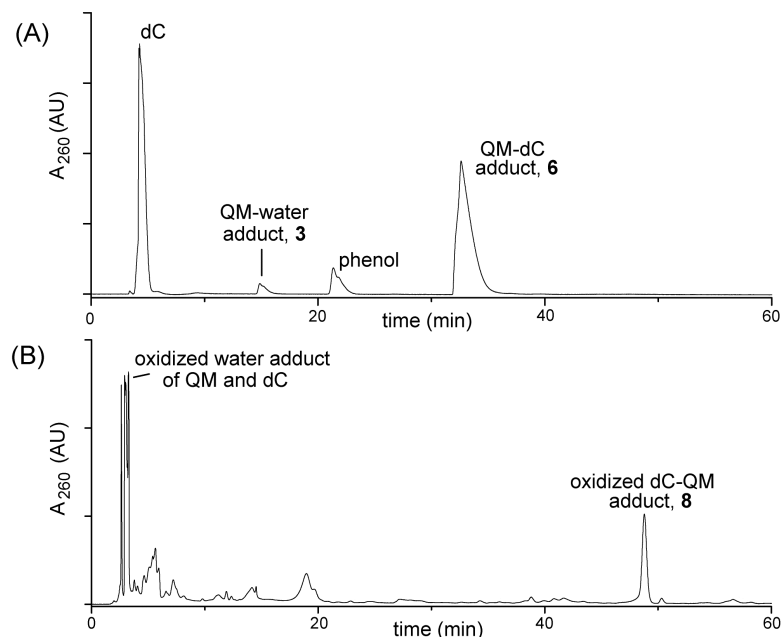


Figure A.1. Reverse-phase C18 chromatography was used to detect and isolate formation and oxidation of the QM-dC N3 adduct (**1.42**). (A) Separation of the QM-dC adduct **1.42** used a gradient of 3 - 25% CH₃CN in triethylammonium acetate pH 5 over 76 min (analytical, 1 mL/min). (B) Separation of the adduct **2.2** after oxidation by BTI used a gradient of 3 - 25% CH₃CN in water over 66 min (preparative, 5 mL/min).

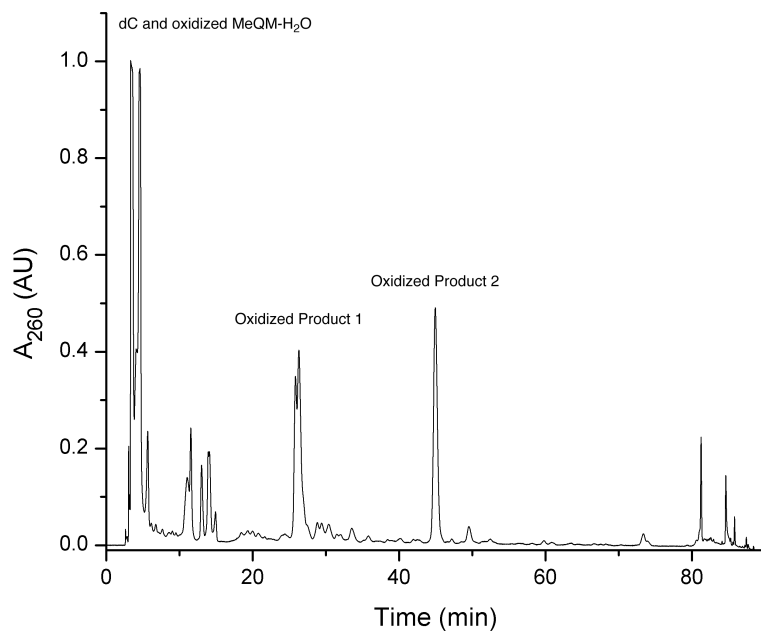


Figure A.2. HPLC analysis of the BTI oxidation of MeQM-dC N3. Oxidized product 2 was the initial focus of the structure elucidation efforts. Unfortunately, oxidized product 1 appears to have been the eventually isolated and characterized MeQM-dC N3 oxidized adduct.

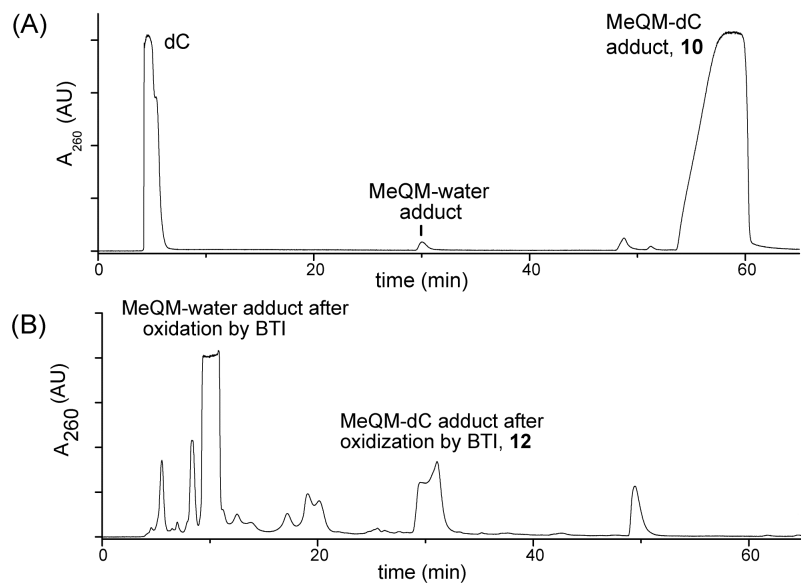


Figure A.3. Reverse-phase C18 chromatography was used to detect and isolate formation and oxidation of the MeQM-dC N3 adduct (**2.8**). (A) Separation of the MeQM-dC adduct **2.8** and (B) its oxidation product **2.15** used a gradient of 3 - 25% CH₃CN in ammonium formate pH 6.8 over 76 min (analytical, 1 mL/min).

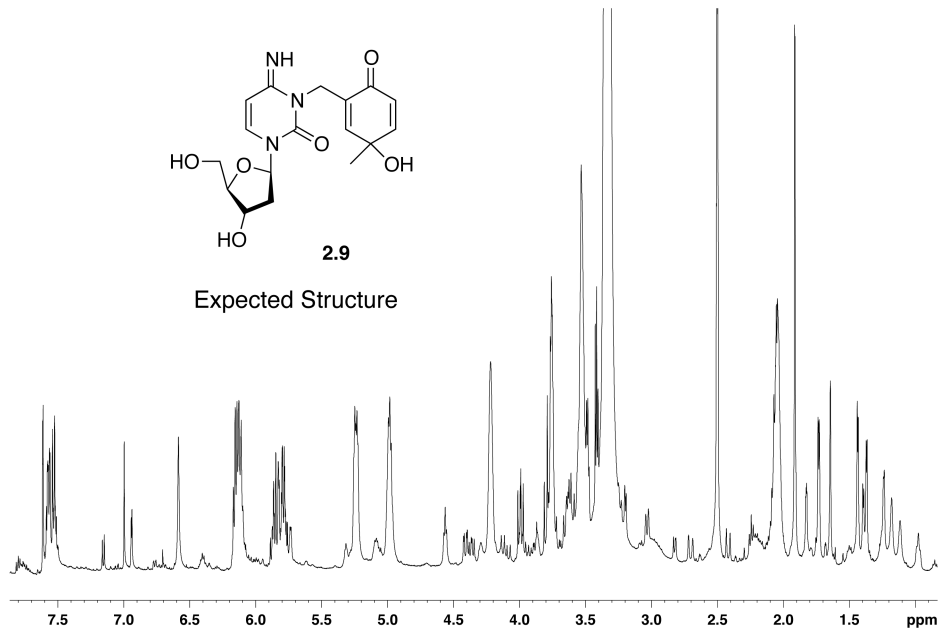


Figure A.4. ¹H NMR of the combined isolated product from the Sep-Pak solvent exchange for 4 oxidations in DMSO-*d*₆ at 500 MHz.

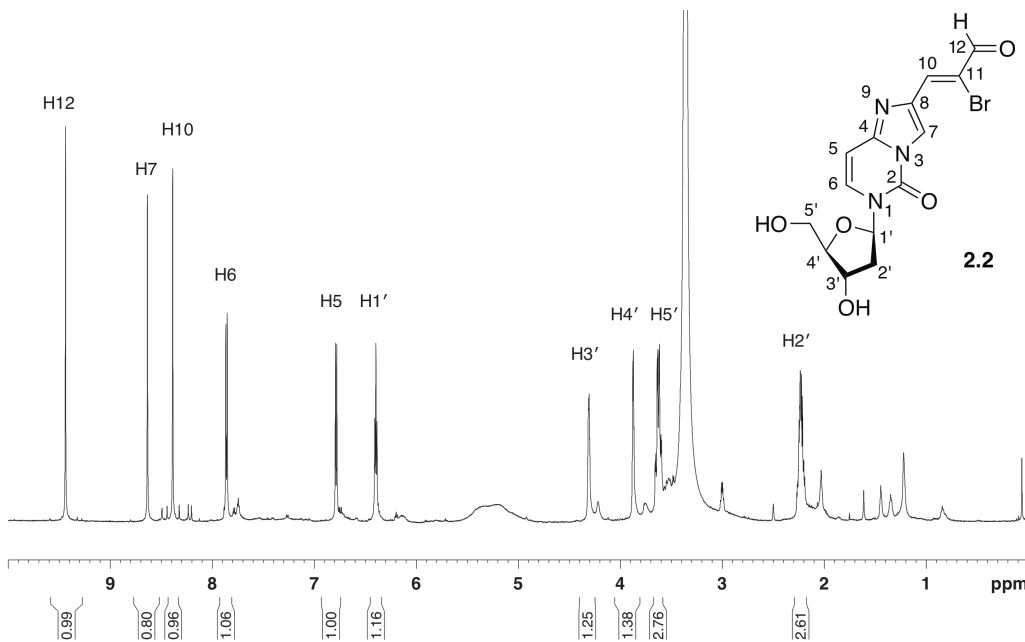


Figure A.5. ^1H NMR of **2.2** in $\text{DMSO}-d_6$ at 600 MHz.

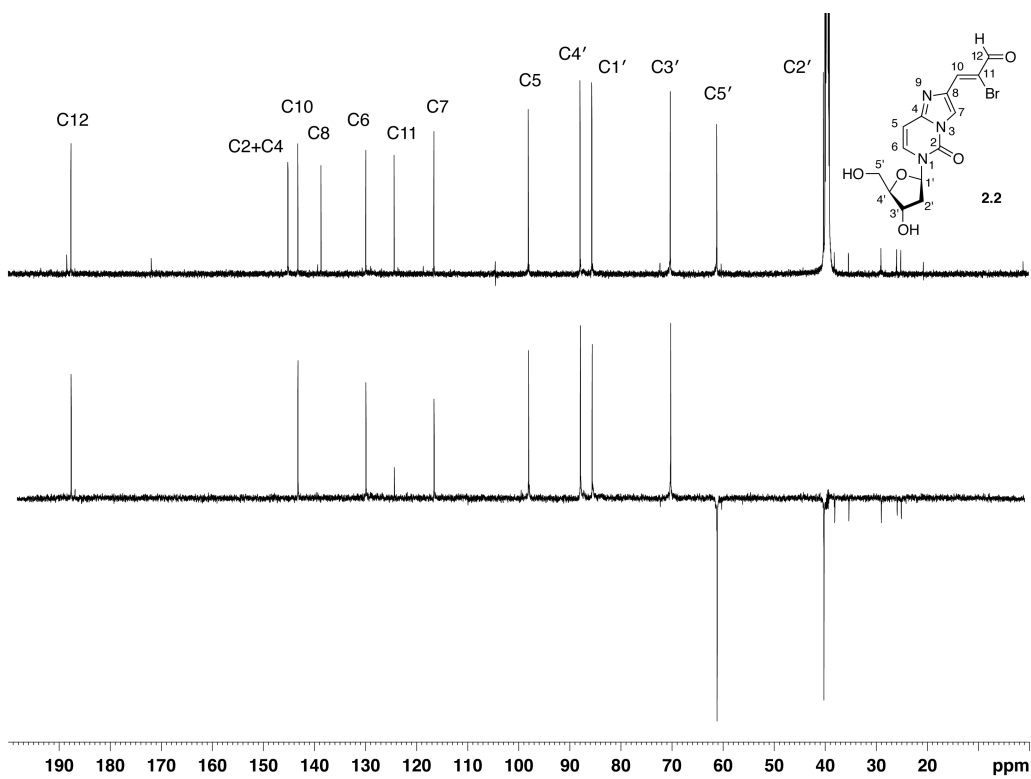


Figure A.6. ^{13}C 1D (top) and DEPT135 (bottom) NMR of **2.2** in $\text{DMSO}-d_6$ at 600 MHz.

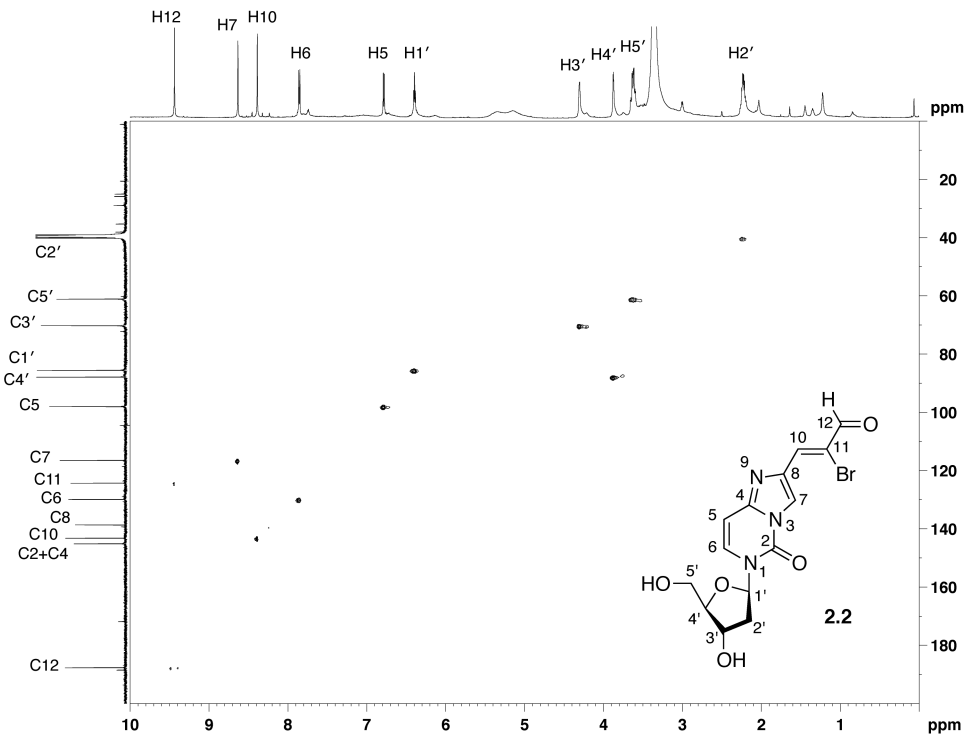


Figure A.7. $^1\text{H} - ^{13}\text{C}$ HSQC of **2.2** in $\text{DMSO}-d_6$ at 600 MHz.

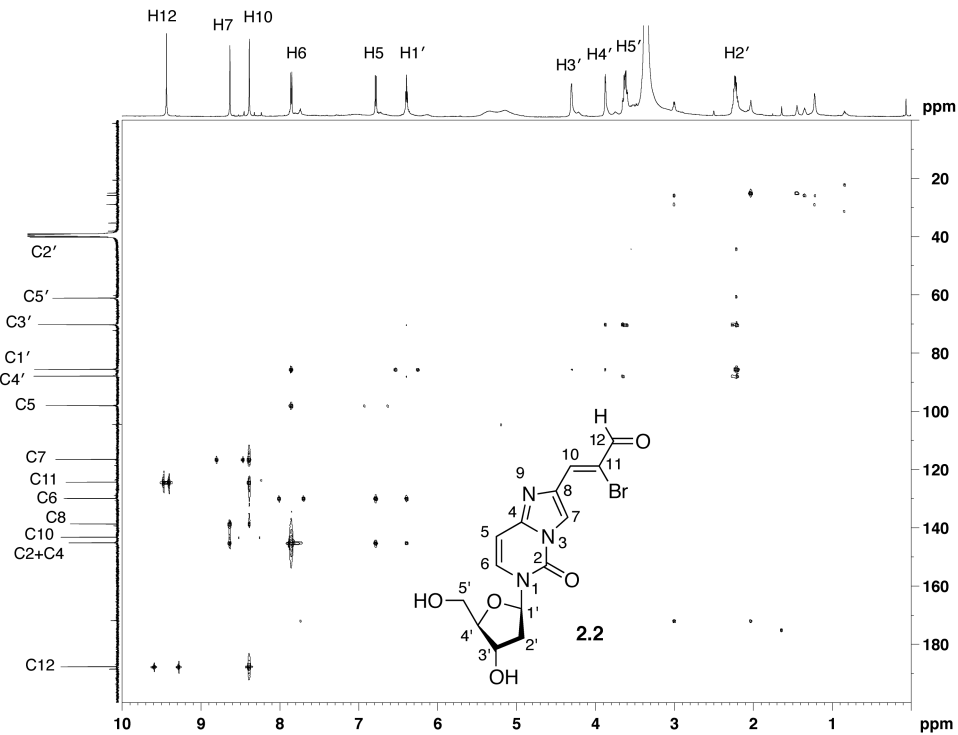


Figure A.8. $^1\text{H} - ^{13}\text{C}$ HMBC of **2.2** in $\text{DMSO}-d_6$ at 600 MHz.

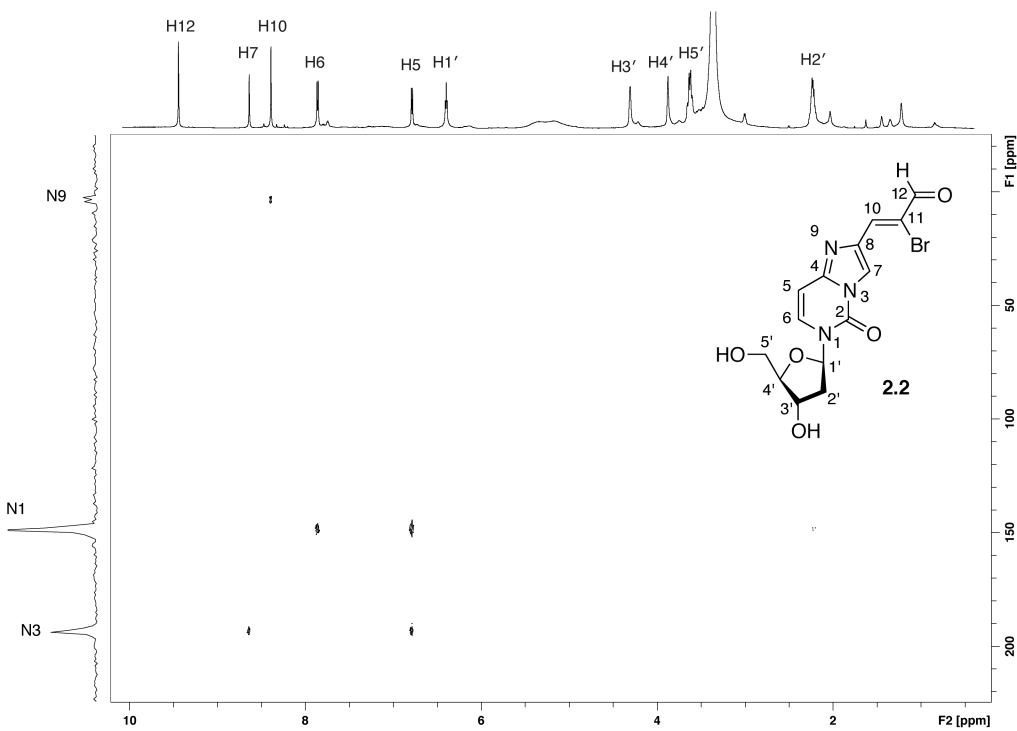


Figure A.9. $^1\text{H} - ^{15}\text{N}$ HMBC of **2.2** in $\text{DMSO}-d_6$ at 600 MHz.

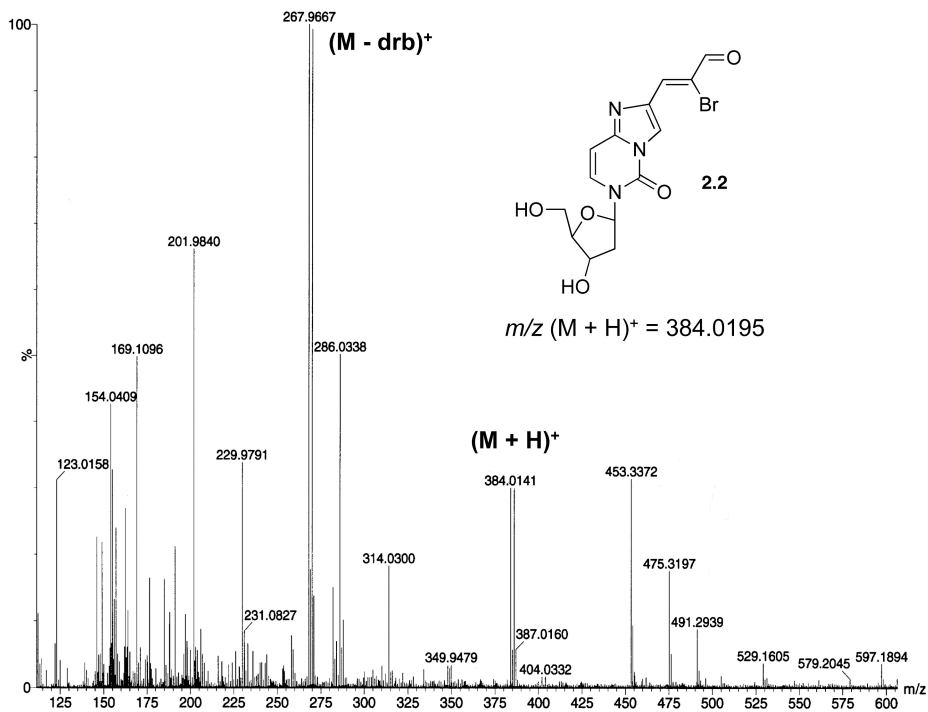


Figure A.10. ESI $^+$ -MS of **2.2**.

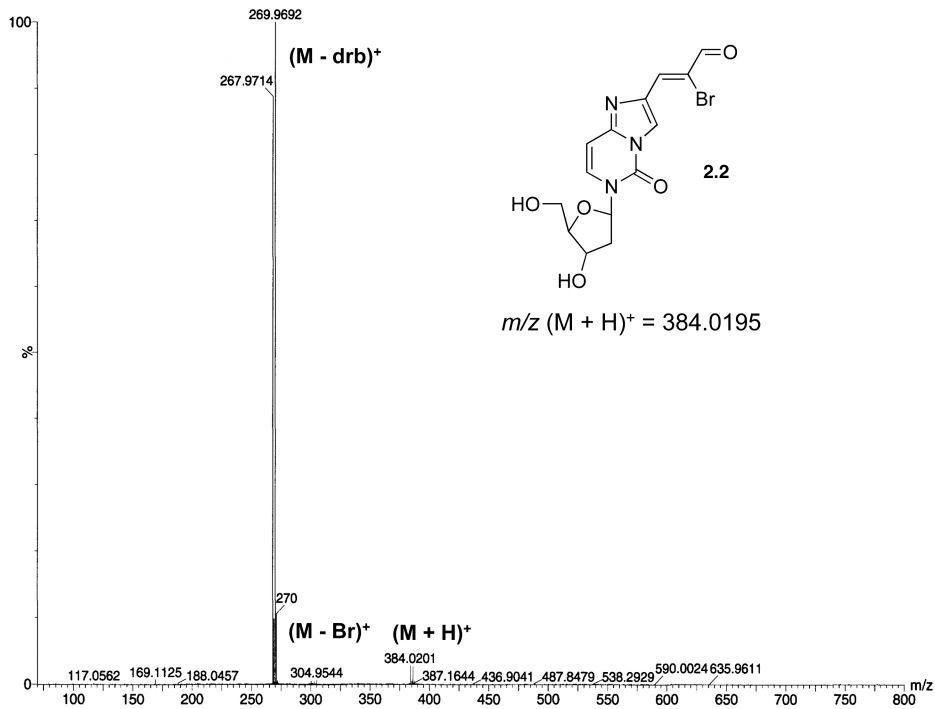


Figure A.11. ESI⁺-MS/MS of **2.2** (m/z 384).

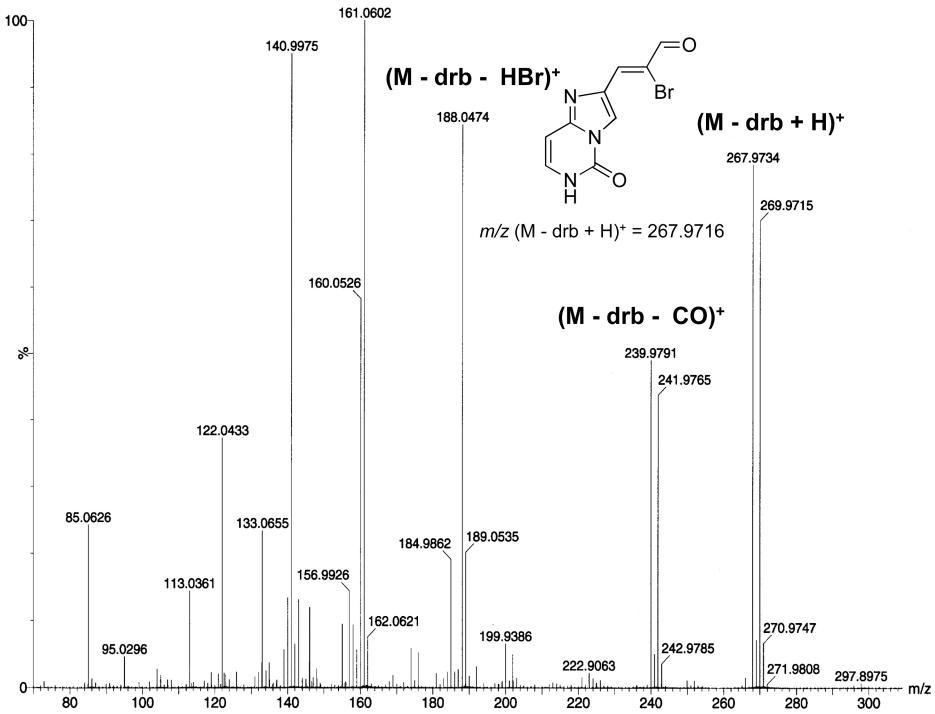


Figure A.12. ESI⁺-MS/MS of deglycosylated **2.2** (m/z 268).

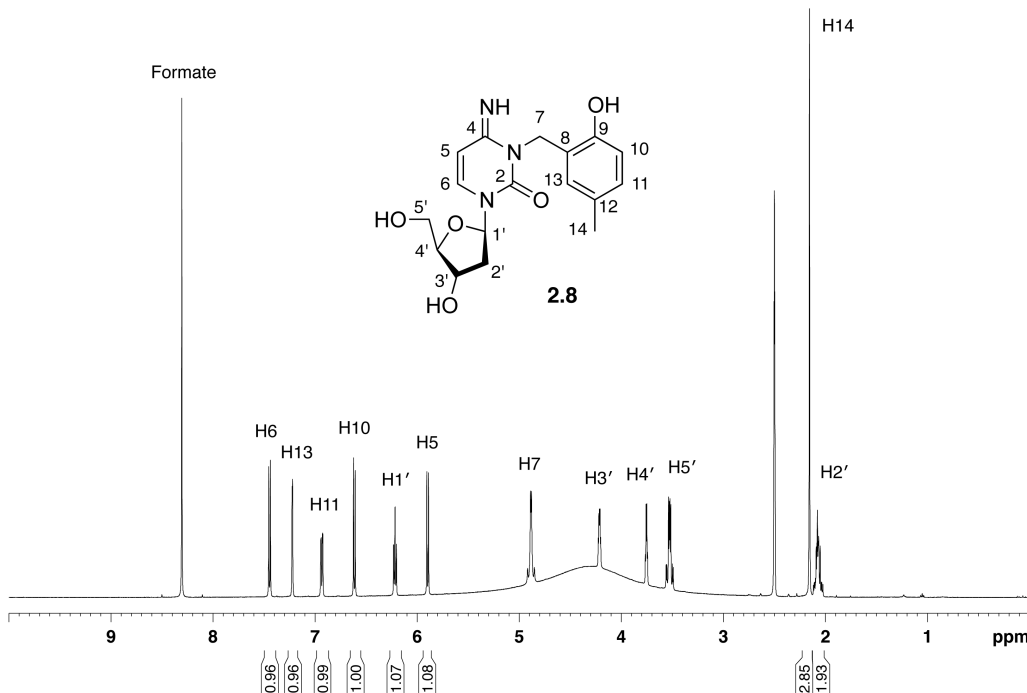


Figure A.13. ^1H NMR of **2.8** in $\text{DMSO}-d_6$ at 500 MHz.

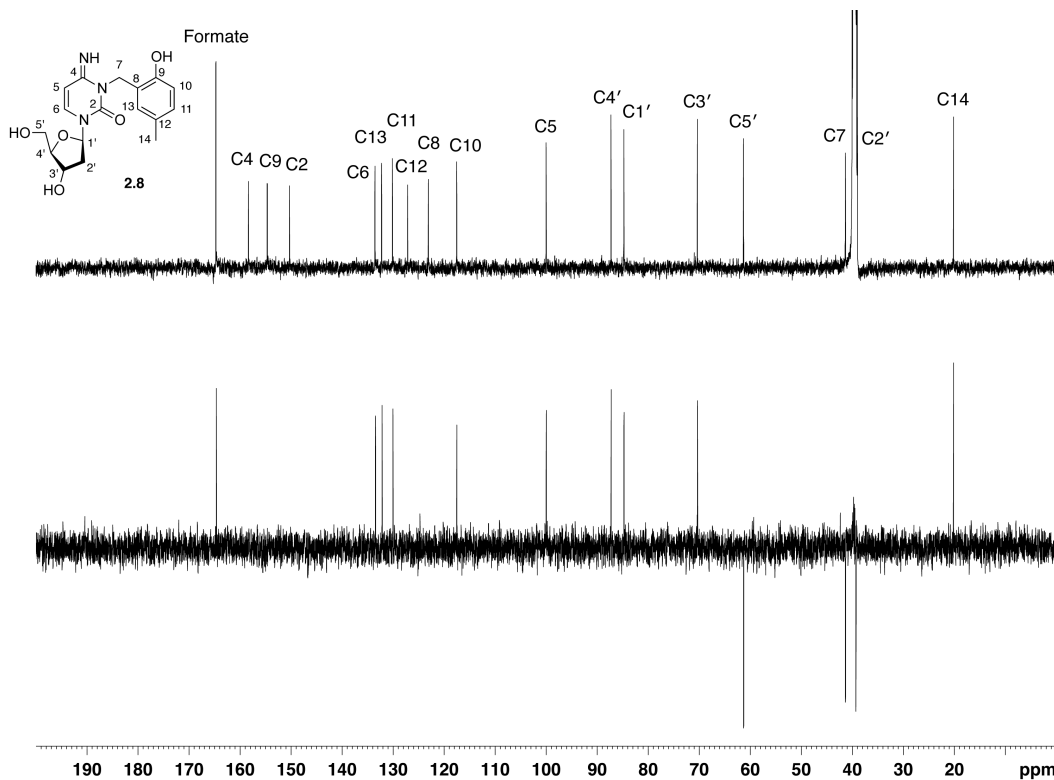


Figure A.14. ^{13}C 1D (top) and DEPT135 (bottom) NMR of **2.8** in $\text{DMSO}-d_6$ at 500 MHz.

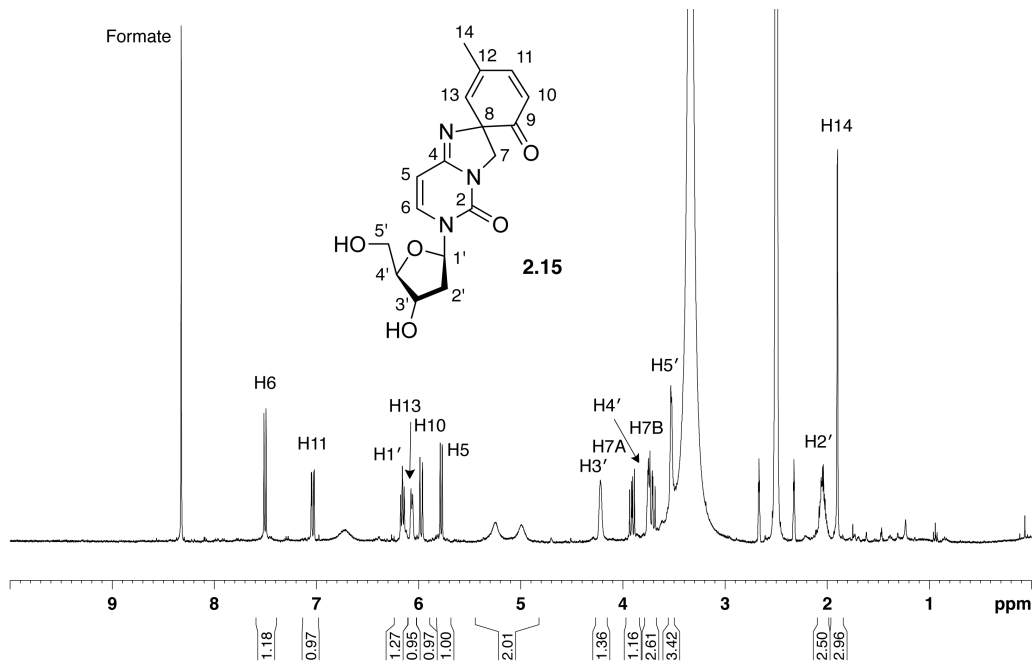


Figure A.15. ^1H NMR of **2.15** in $\text{DMSO}-d_6$ at 400 MHz.

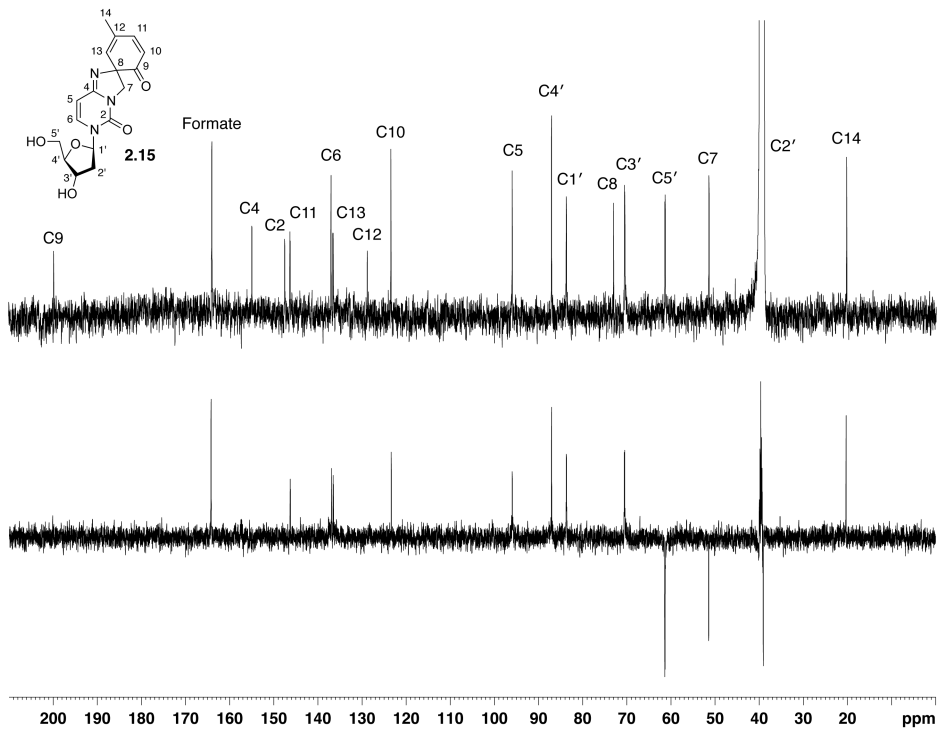


Figure A.16. ^{13}C 1D (top) and DEPT135 (bottom) NMR of **2.15** in $\text{DMSO}-d_6$ at 500 MHz.

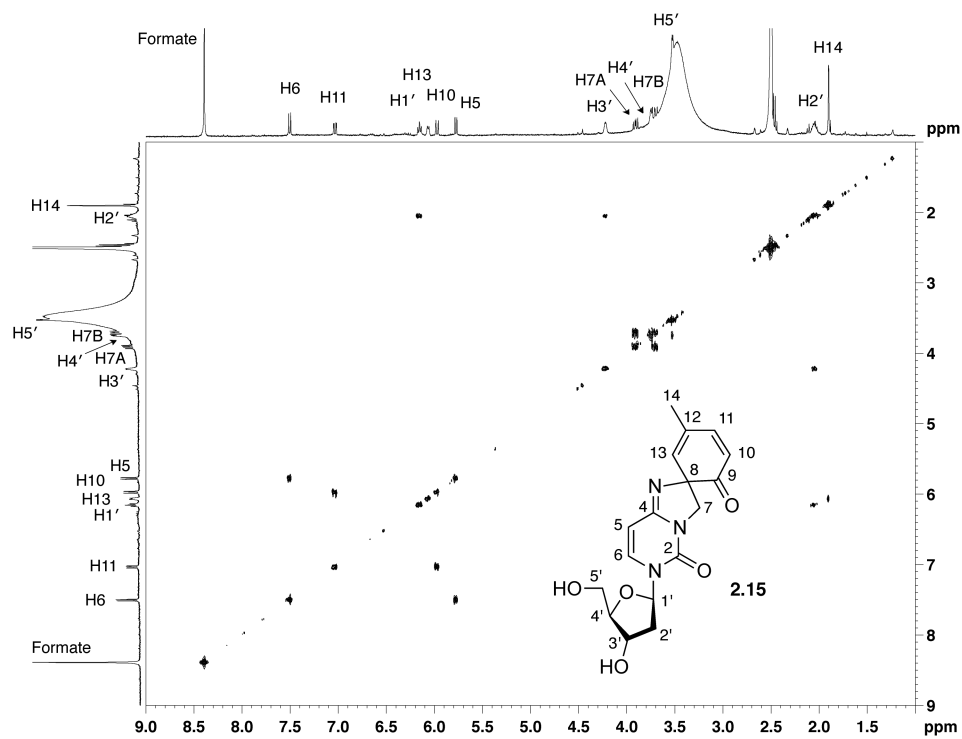


Figure A.17. $^1\text{H} - ^1\text{H}$ COSY of **2.15** in $\text{DMSO}-d_6$ at 400 MHz.

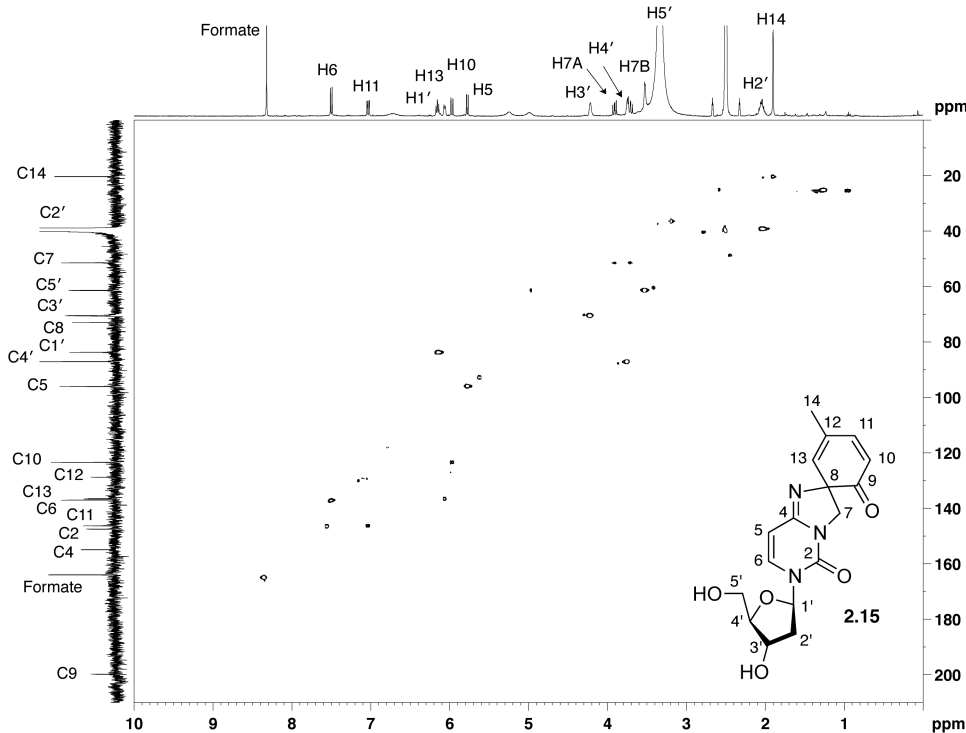


Figure A.18. $^1\text{H} - ^{13}\text{C}$ HSQC of **2.15** in $\text{DMSO}-d_6$ at 400 MHz.

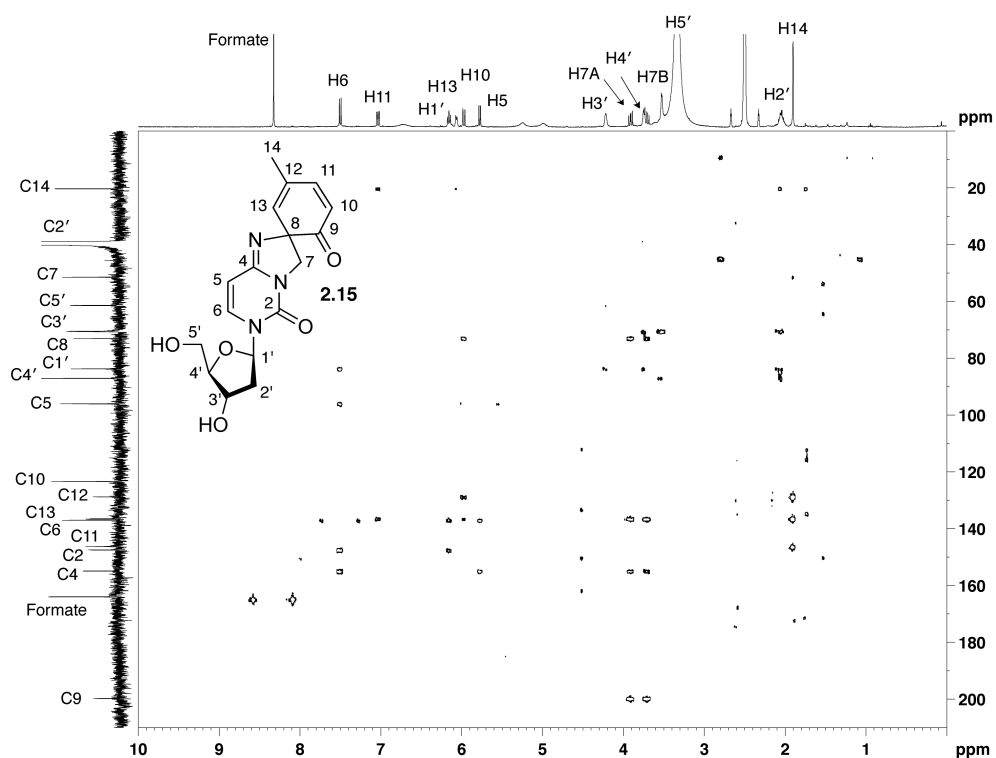


Figure A.19. $^1\text{H} - ^{13}\text{C}$ HMBC of **2.15** in $\text{DMSO}-d_6$ at 400 MHz.

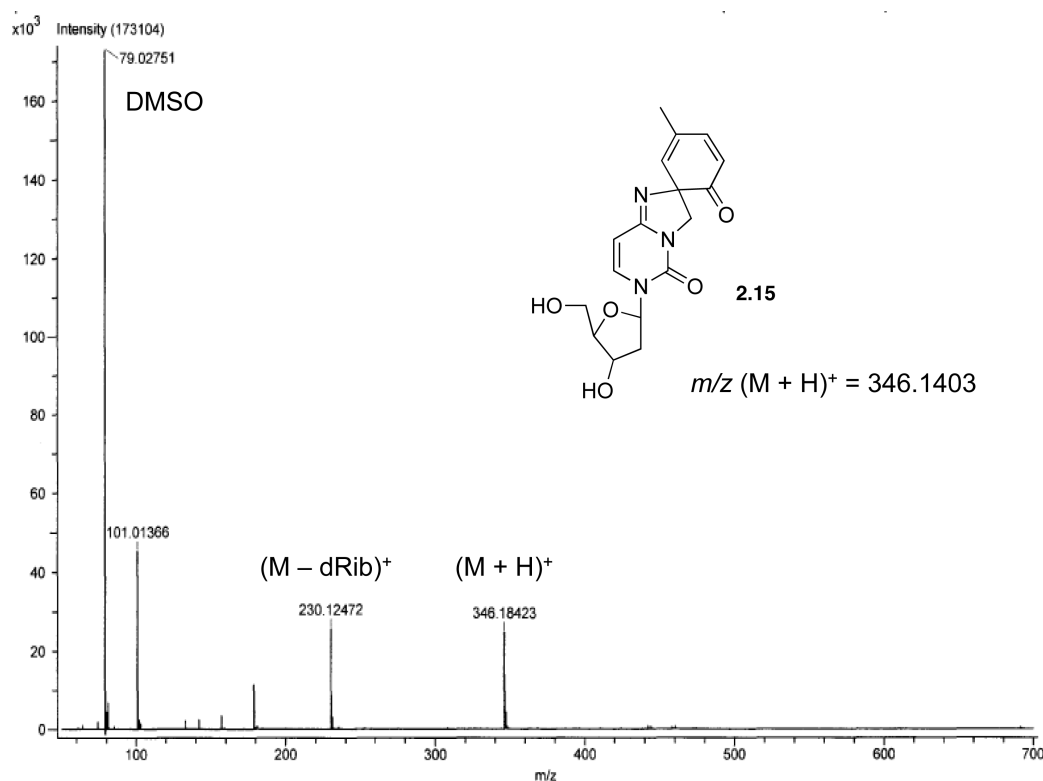


Figure A.20. ESI $^+$ -MS of **2.15**.

Appendix B. Supporting Information for Chapter 3

Table B.1. ^{13}C and ^1H NMR data for the product (**3.7**) formed by oxidation of MeQM-dG N1 (DMSO- d_6).

Position	^{13}C shift (ppm)	^1H shift (ppm)	HMBC Connectivity
1'	82.2	6.15 (t, $J=6.9$ Hz)	2', 3'
2'	39.5	2.54 (m), 2.22 (m)	
3'	70.8	4.34 (m)	2', 4', 5'
4'	87.6	3.81 (m)	2', 5'
5'	61.7	3.53 (m)	
2	153.9		10
4	149.4		1', 8
5	115.6		8
6	156.2		10
8	135.7	7.97 (s)	1'
10	39.4	4.88 (t, $J=15.7$ Hz), 4.62 (t, $J=15.7$ Hz)	16
11	129.5		10, 13
12	184.8		13, 14, 16
13	125.5	6.09 (d, $J=10.0$ Hz)	
14	154.3	6.95 (dd, $J=2.9, 10.0$ Hz)	16, 17
15	66.5		13, 17
16	146.3	6.13 (m)	10, 14, 17
17	27.4	1.25 (d, $J=2.4$ Hz)	

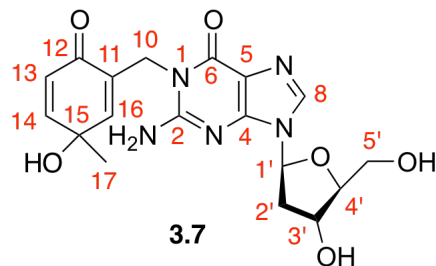


Table B.2. ^{13}C and ^1H NMR data for the product (**3.8**) formed by oxidation of MeQM-dG N² (DMSO- d_6).

Position	^{13}C shift (ppm)	^1H shift (ppm)	HMBC Connectivity
1'	82.8	6.14 (t, $J=6.9$ Hz)	2'
2'	39.3	2.58 (m), 2.19 (m)	
3'	70.8	4.32 (m)	2', 4', 5'
4'	87.6	3.80 (m)	2', 5'
5'	61.8	3.50 (m)	
2	152.4		10
4	150.3		1', 8
5	117.0		8
6	156.6		
8	135.7	7.91 (d, $J=2.5$ Hz)	1'
10	38.9	4.11 (d, $J=5.3$ Hz)	NH
11	131.7		10, 13
12	185.1		10, 14, 16
13	125.5	6.06 (d, $J=10.0$ Hz)	
14	154.5	6.96 (dd, $J=2.9, 10.0$ Hz)	16, 17
15	66.4		13, 17
16	149.4	6.80 (m)	10, 14, 17
17	27.3	1.31 (s)	14

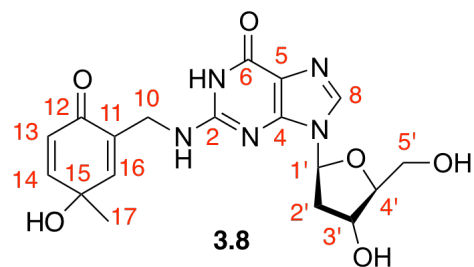


Table B.3. ^{13}C and ^1H NMR data for the product (**3.9**) formed by oxidation of MeQM-guanine N7 (DMSO- d_6).

Position	^{13}C shift (ppm)	^1H shift (ppm)	HMBC Connectivity
2	154.4		
4	159.7		8
5	107.9		8, 10
6	152.9		
8	143.4	7.84 (s)	10
10	43.8	4.99 (d, $J=15.7$ Hz, 1H), 5.04 (d, $J=15.7$ Hz, 1H)	8, 13, 16
11	131.3		10, 13, 16
12	184.1		10, 13, 14, 16
13	125.2	6.06 (d, $J=10.1$ Hz)	
14	154.6	6.95 (dd, $J=2.8, 10.1$ Hz)	16, 17
15	66.3		13, 17
16	150.6	6.51 (s)	10, 14, 17
17	27.1	1.25 (s)	14, 16

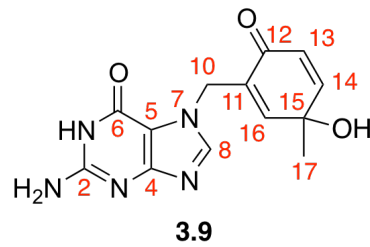
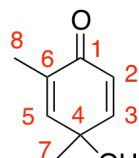


Table B.4. ^{13}C and ^1H NMR data for the *p*-quinol model compound 4-hydroxy-2,4-dimethyl-2,5-cyclohexadien-1-one (**3.9**) (CDCl_3).⁶⁸

Position	^{13}C shift (ppm)	^1H shift (ppm)
1	186.3	
2	126.6	6.01 (d, $J=9.9$ Hz, 1H)
3	152.3	6.81 (d, $J=2.9, 9.9$ Hz, 1H)
4	67.3	
5	148	6.63-6.60 (m, 1H)
6	133.3	
7	26.8	1.40 (s, 3H)
8	15.4	1.79 (d, $J=1.5$ Hz, 3H)



3.9

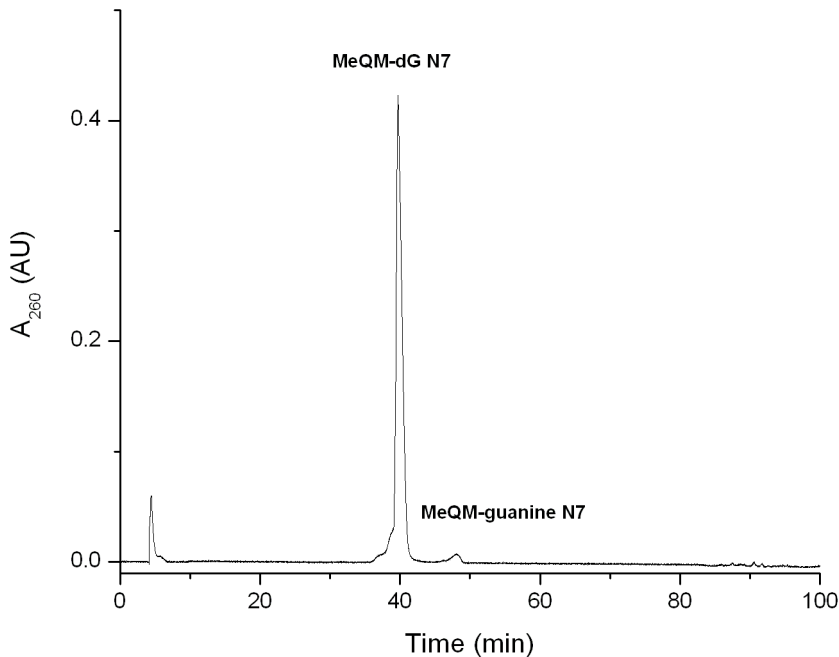


Figure B.1. HPLC analysis of MeQM-dG N7 after overnight lyophilization. The dry product was dissolved in 1:1 H₂O:CH₃CN prior to Gradient 1 using the analytical column (1 mL/min).

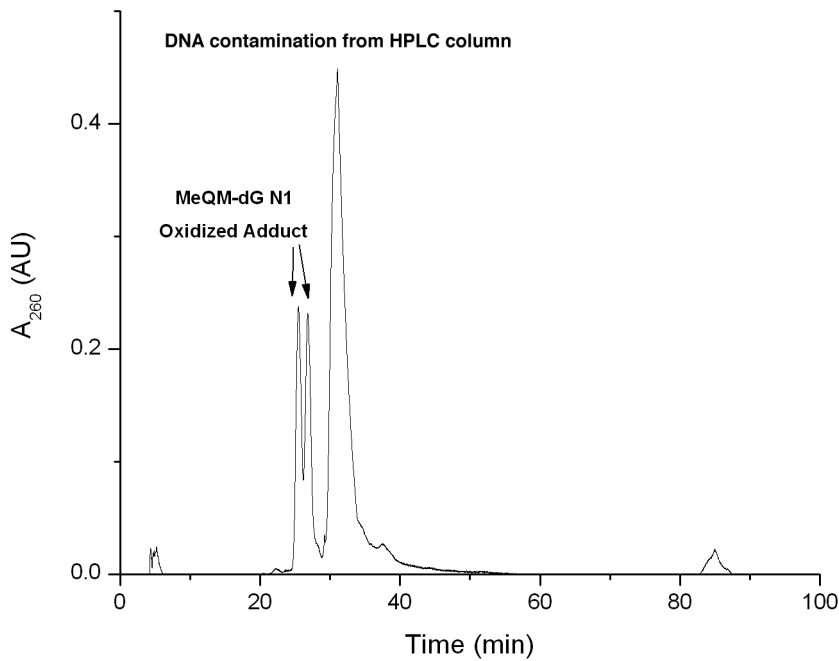


Figure B.2. HPLC analysis of the product formed by oxidation of MeQM-dG N1. The ¹H NMR sample (**Figure 3.12**) was diluted with H₂O to make a 50% aqueous DMSO-*d*₆ solution prior to re-injection into the HPLC. The peak at approximately 30 minutes was DNA contamination from the HPLC column.

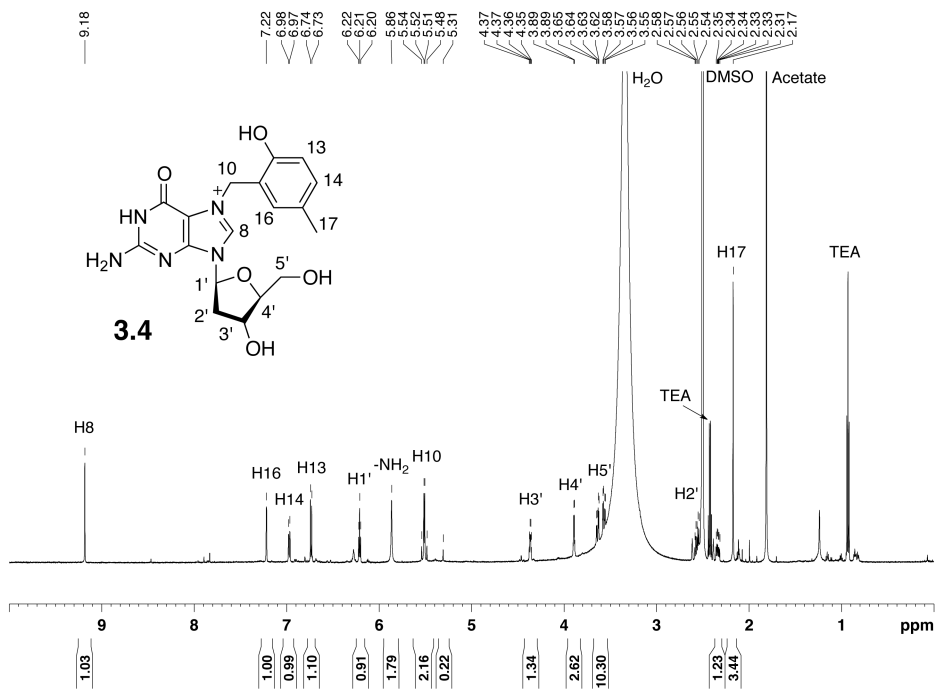


Figure B.3. ^1H NMR of MeQM-dG N7 (**3.4**) in $\text{DMSO}-d_6$ at 600 MHz.

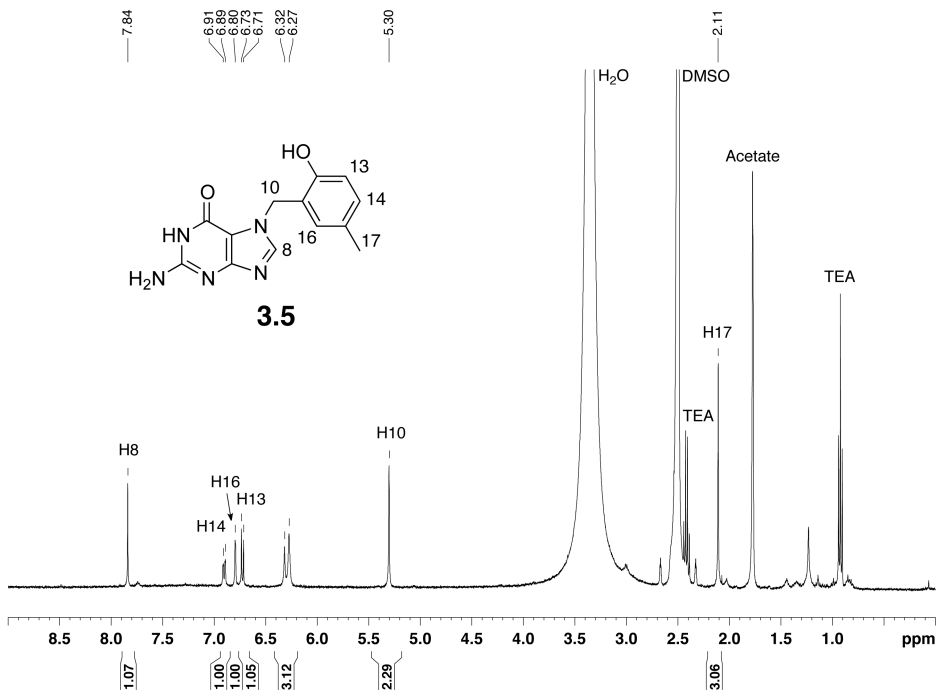


Figure B.4. ^1H NMR of MeQM-guanine N7 (**3.5**) in $\text{DMSO}-d_6$ at 400 MHz.

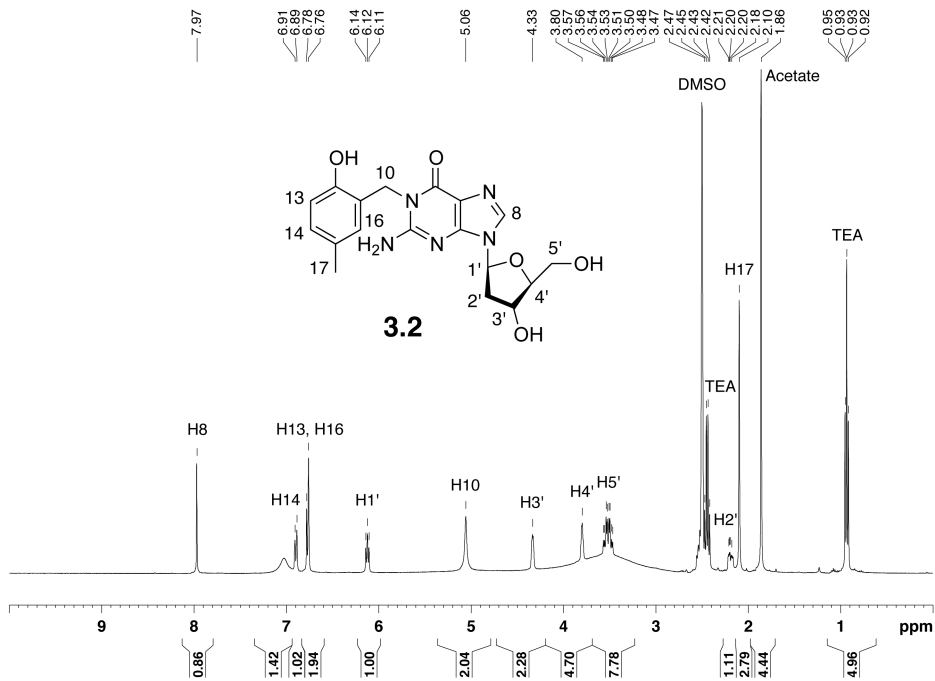


Figure B.5. ^1H NMR of MeQM-dG N1 (**3.2**) in $\text{DMSO}-d_6$ at 400 MHz.

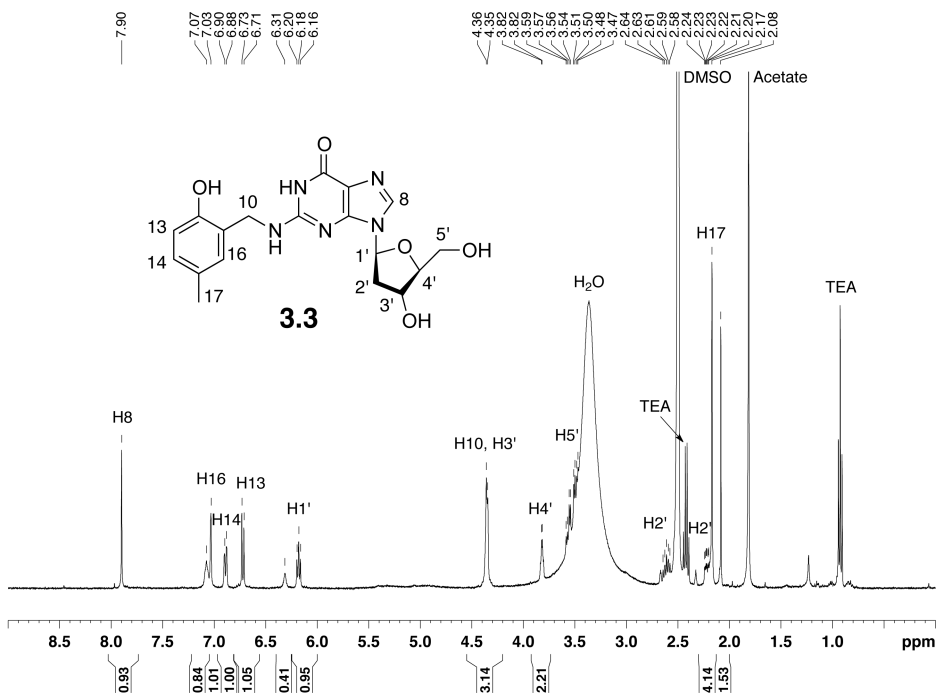


Figure B.6. ^1H NMR of MeQM-dG N² (**3.3**) in $\text{DMSO}-d_6$ at 400 MHz.

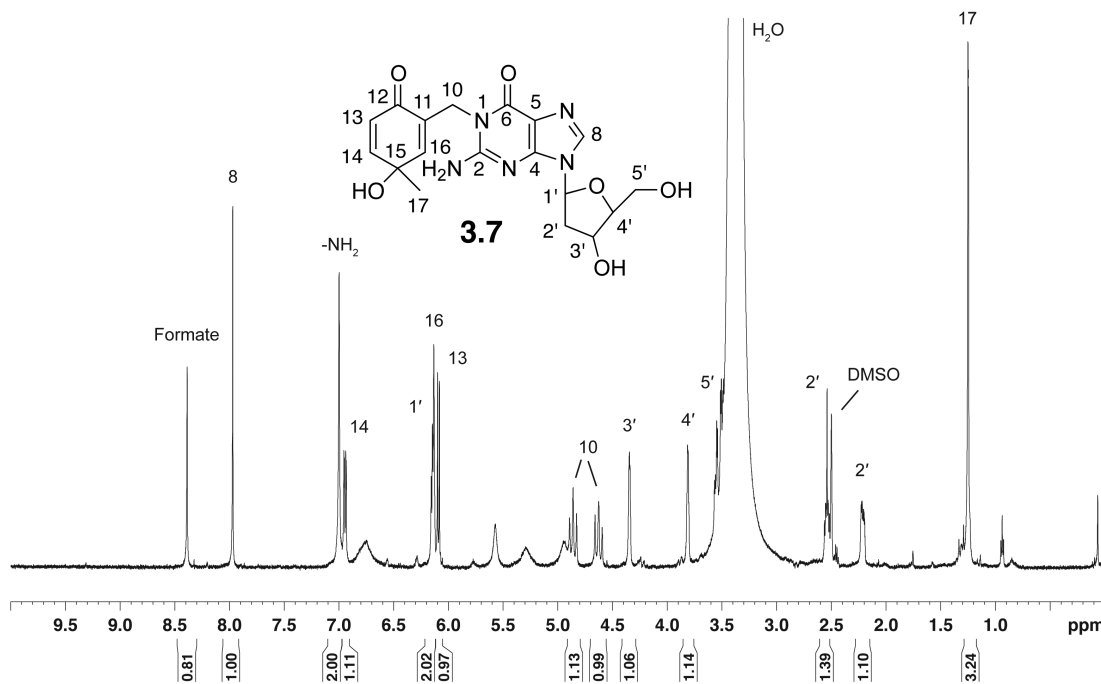


Figure B.7. ^1H NMR of **3.7** in $\text{DMSO}-d_6$ at 600 MHz.

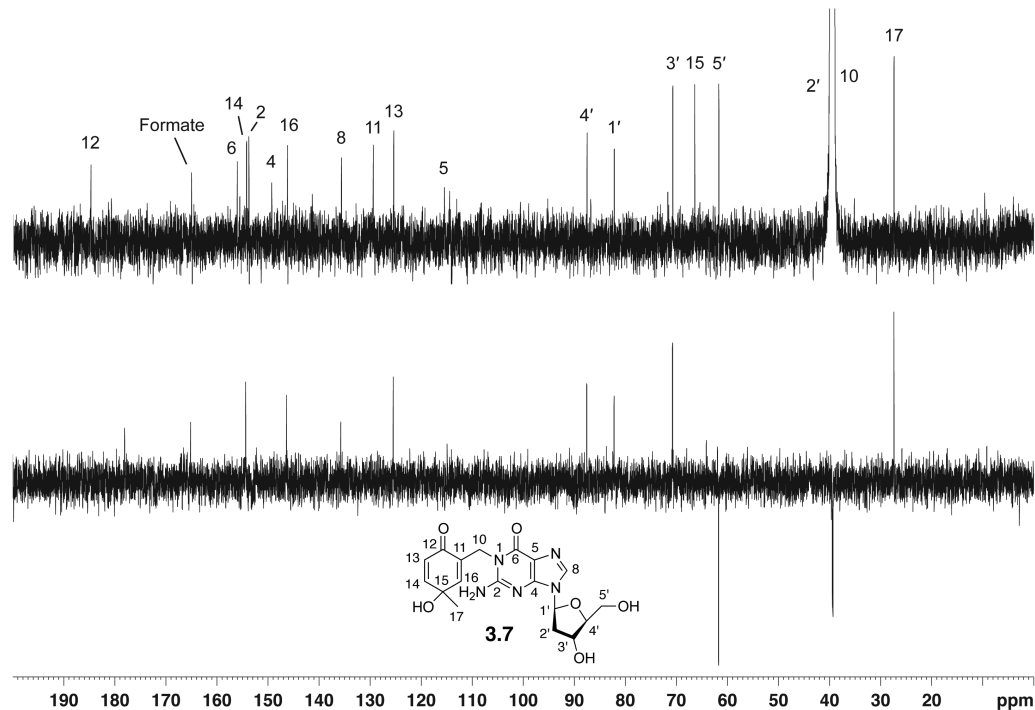


Figure B.8. ^{13}C 1D (top) and DEPT135 (bottom) NMR of **3.7** in $\text{DMSO}-d_6$ at 600 MHz.

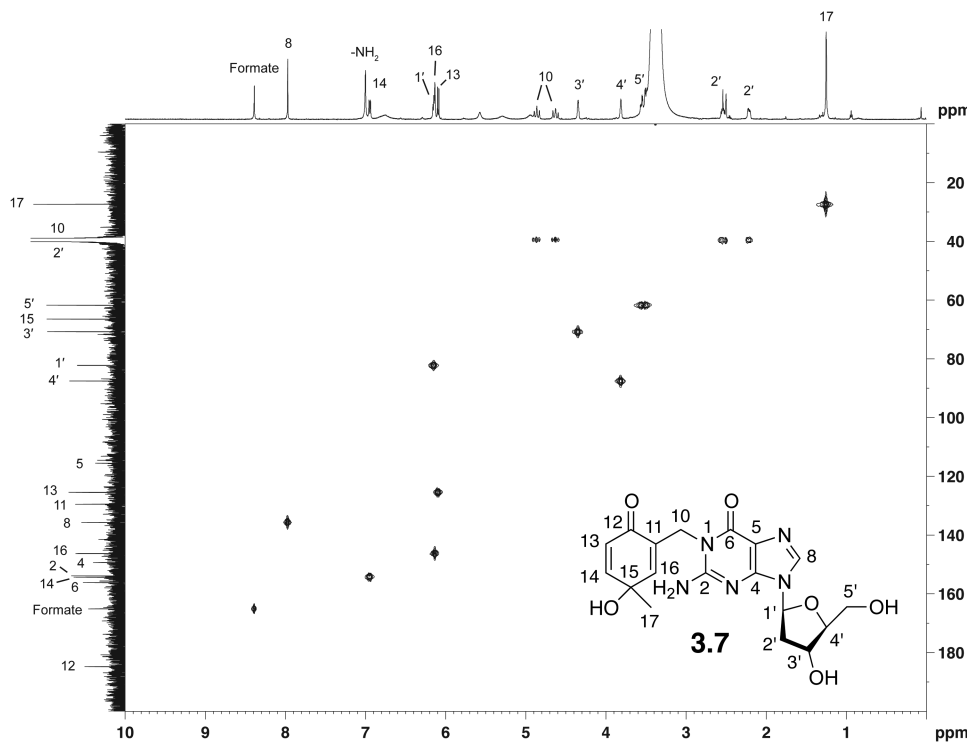


Figure B.9. $^1\text{H} - ^{13}\text{C}$ HSQC of **3.7** in $\text{DMSO}-d_6$ at 600 MHz.

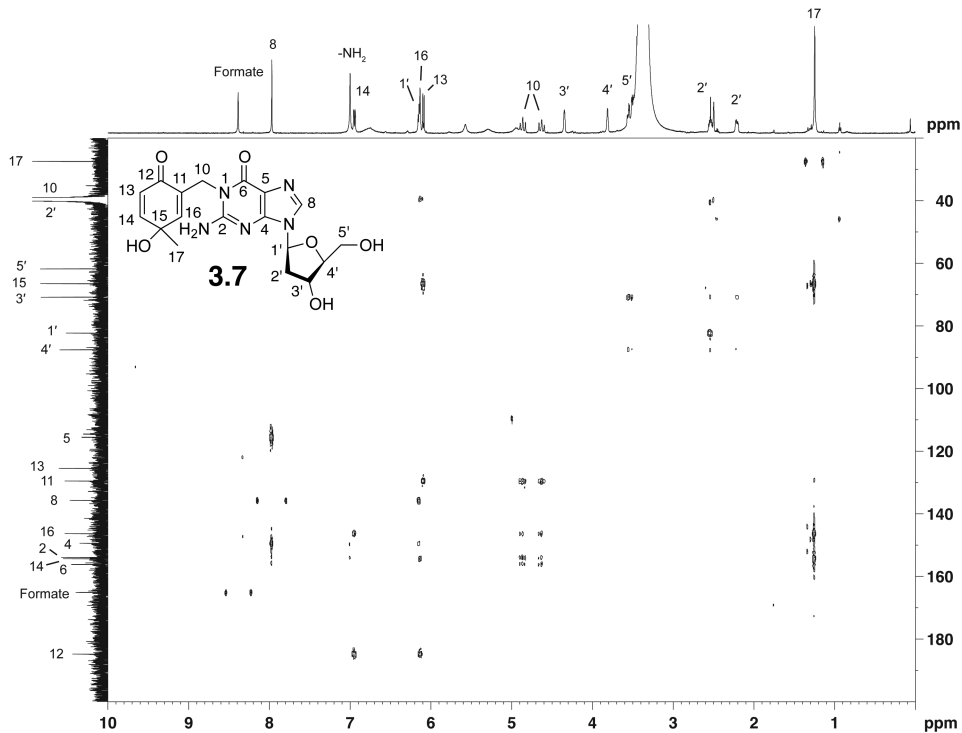


Figure B.10. $^1\text{H} - ^{13}\text{C}$ HMBC of **3.7** in $\text{DMSO}-d_6$ at 600 MHz.

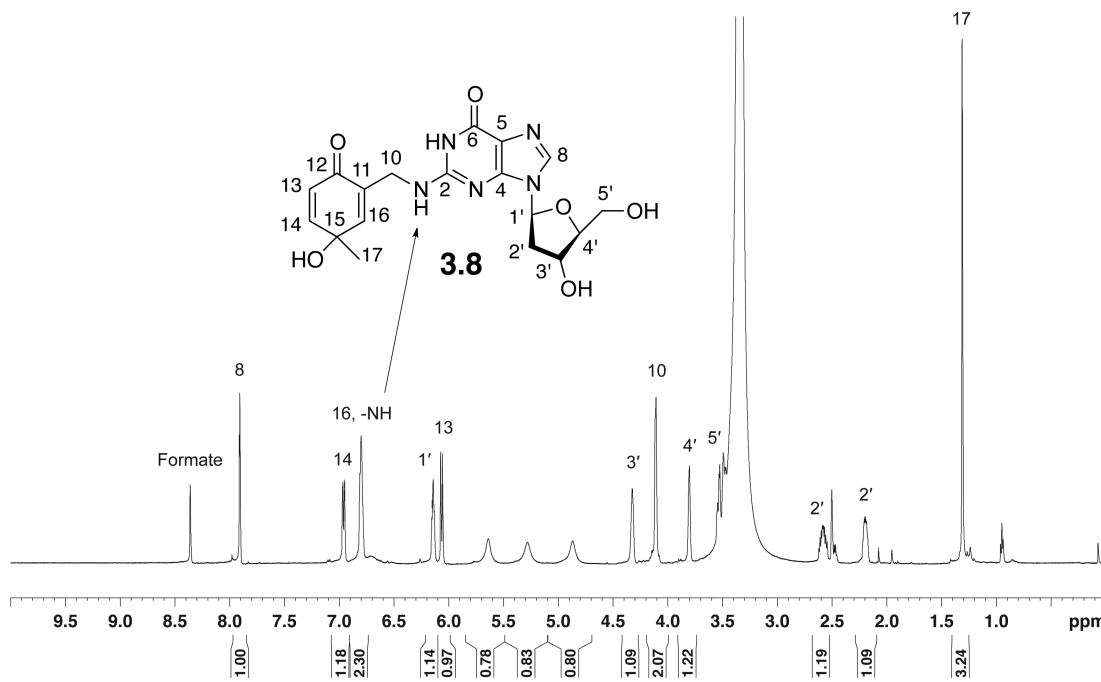


Figure B.11. ^1H NMR of **3.8** in $\text{DMSO}-d_6$ at 600 MHz.

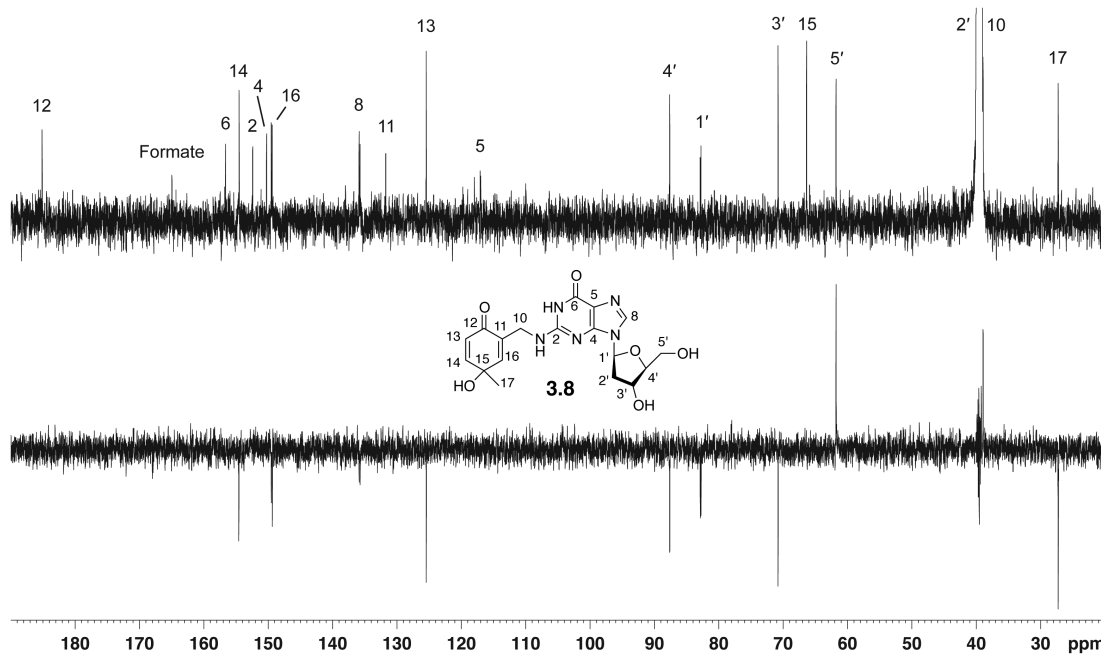


Figure B.12. ^{13}C 1D (top) and DEPT135 (bottom) NMR of **3.8** in $\text{DMSO}-d_6$ at 600 MHz.

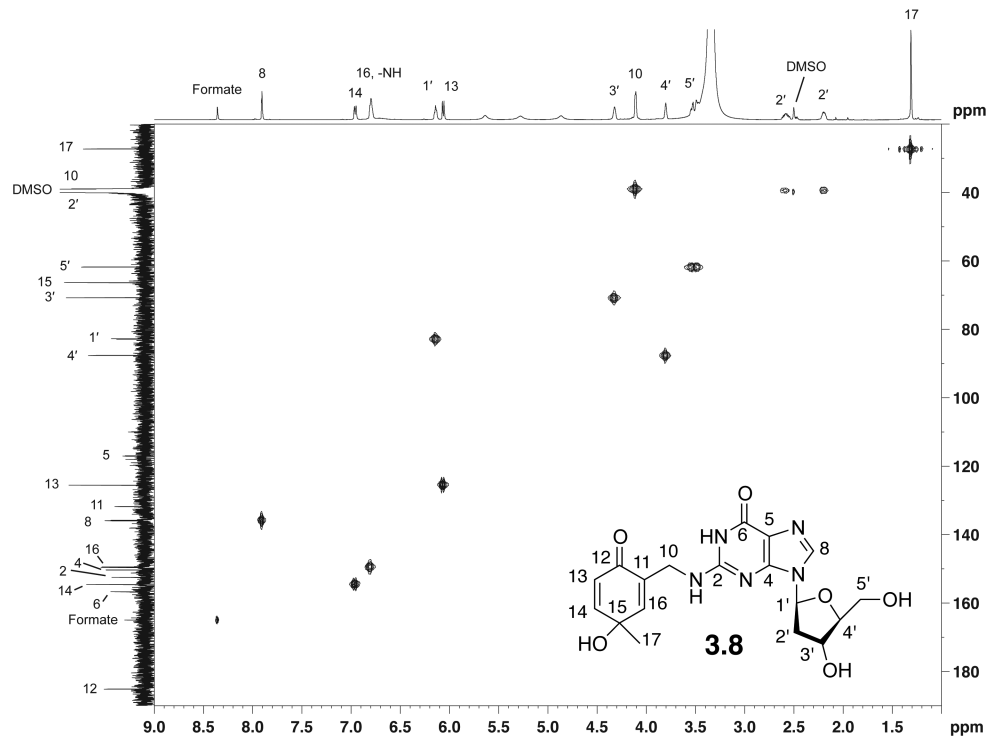


Figure B.13. $^1\text{H} - ^{13}\text{C}$ HSQC of **3.8** in $\text{DMSO}-d_6$ at 600 MHz.

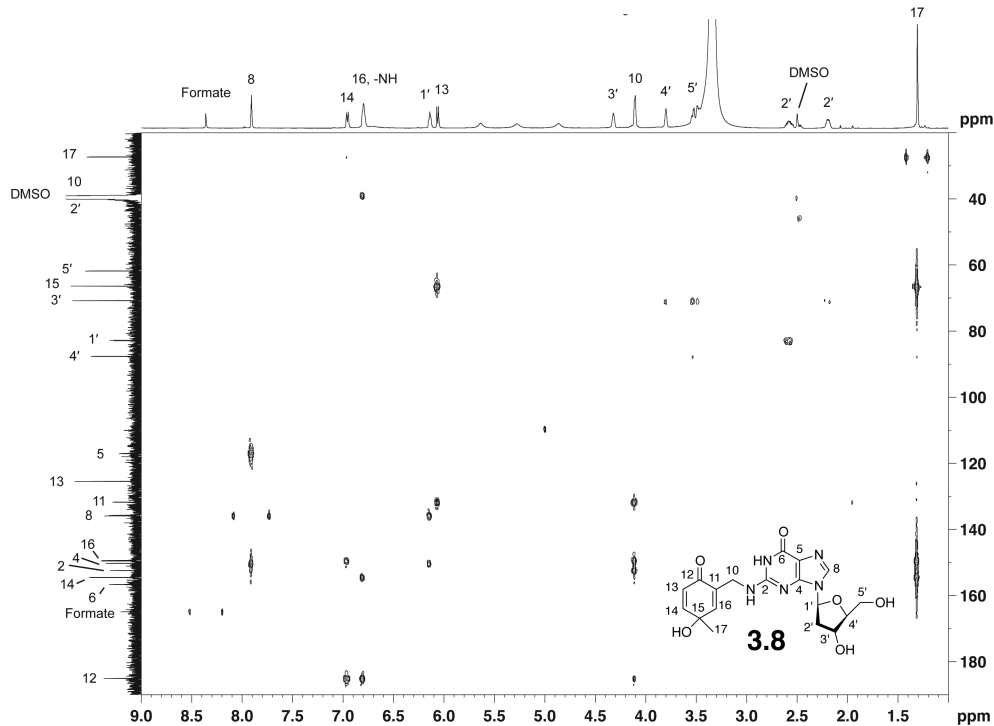


Figure B.14. $^1\text{H} - ^{13}\text{C}$ HMBC of **3.8** in $\text{DMSO}-d_6$ at 600 MHz.

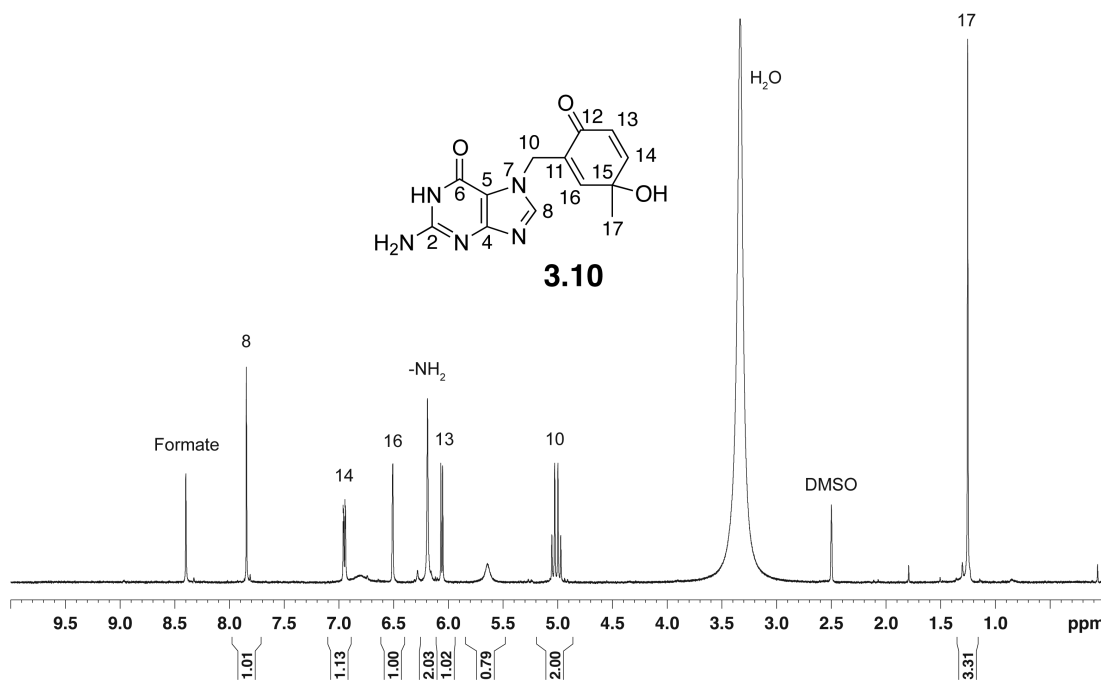


Figure B.15. ^1H NMR of **3.10** in $\text{DMSO}-d_6$ at 600 MHz.

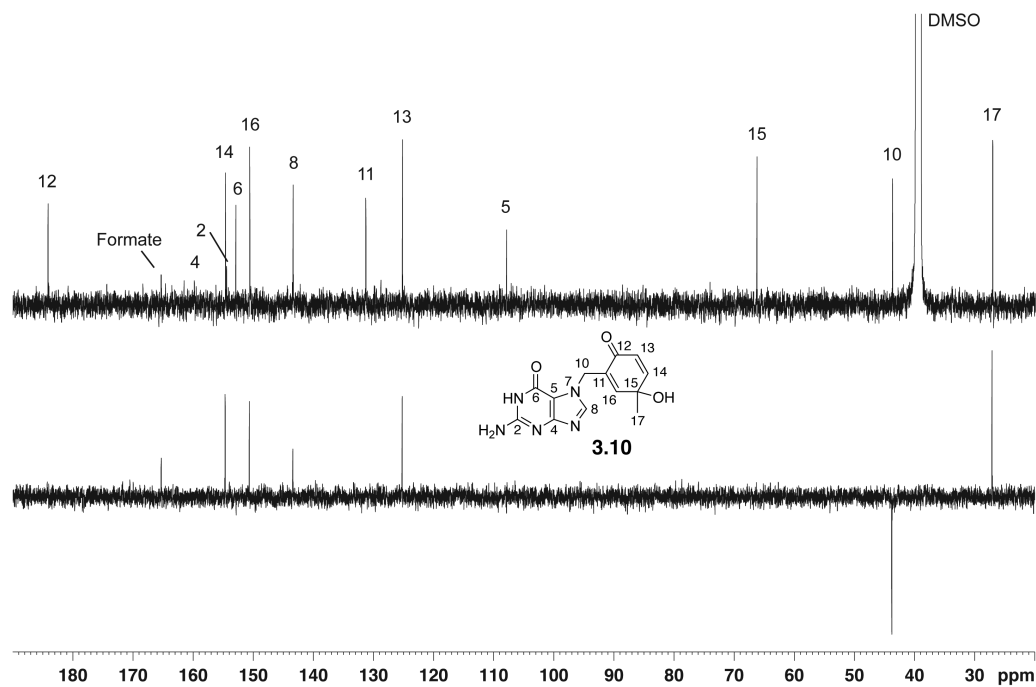


Figure B.16. ^{13}C 1D (top) and DEPT135 (bottom) NMR of **3.10** in $\text{DMSO}-d_6$ at 600 MHz.

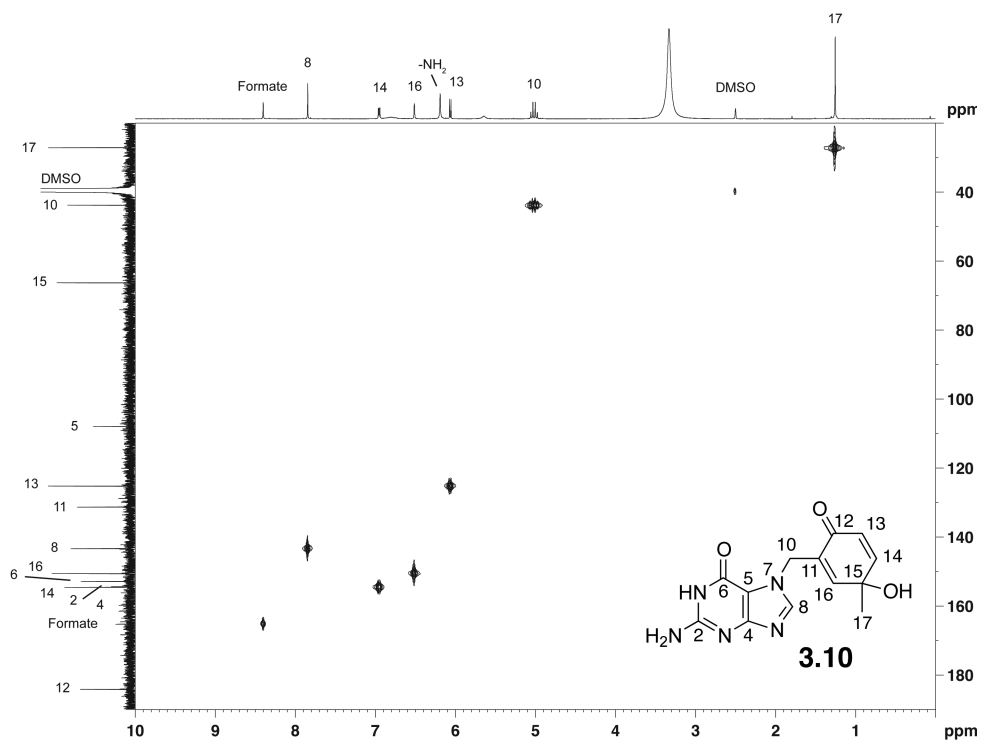


Figure B.17. $^1\text{H} - ^{13}\text{C}$ HSQC of **3.10** in $\text{DMSO}-d_6$ at 600 MHz.

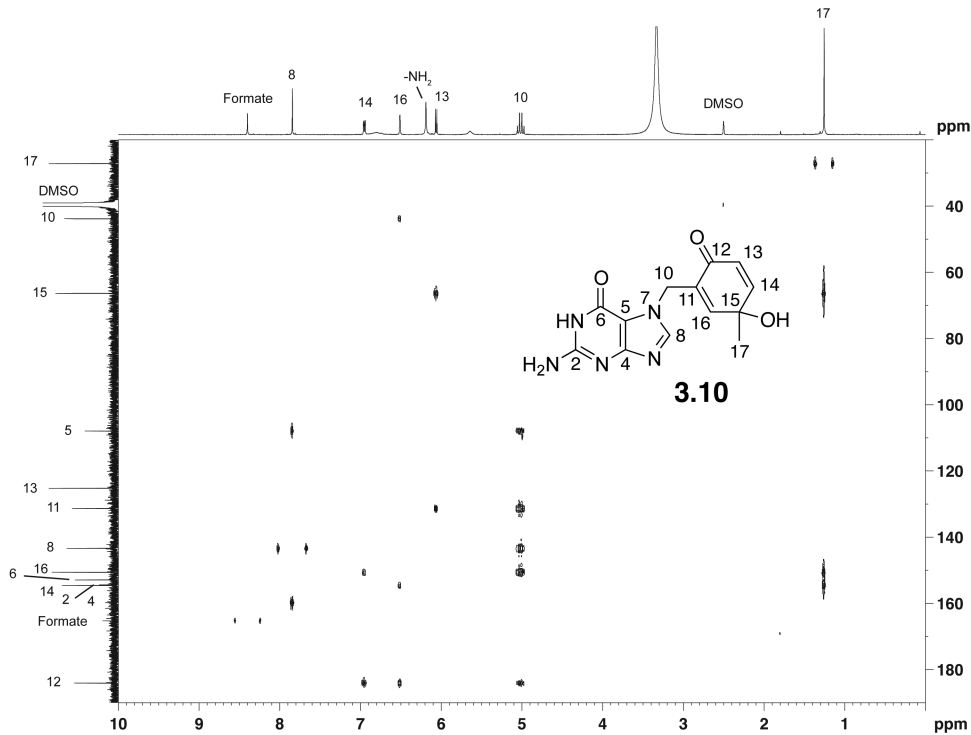


Figure B.18. $^1\text{H} - ^{13}\text{C}$ HMBC of **3.10** in $\text{DMSO}-d_6$ at 600 MHz.

Appendix C. Supporting Information for Chapter 4

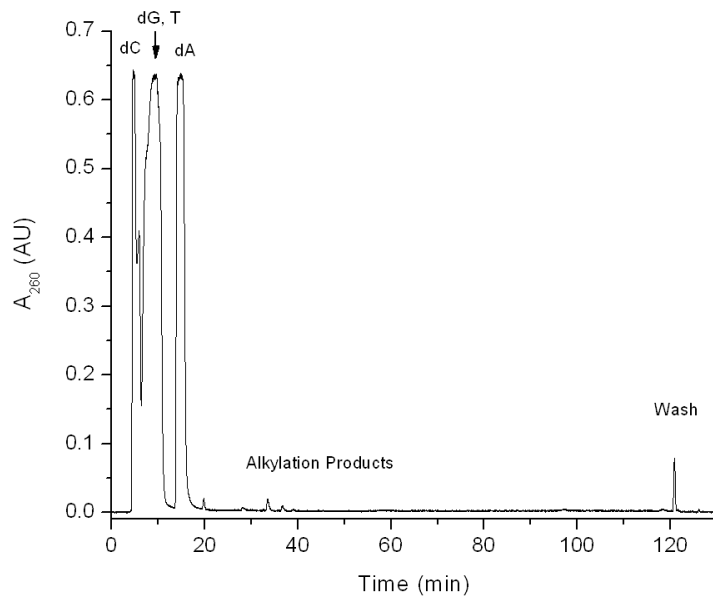


Figure C.1. HPLC analysis of an alkylation reaction consisting of 2 mM each dN, 25 mM sodium phosphate (pH 7), 200 mM NaF, and 160 mM 4-MeBrQMP in an 80:20 solution of H₂O:CH₃CN. The reaction was carried out in a 1.5 mL plastic Eppendorf tube for 30 minutes at 37 °C.

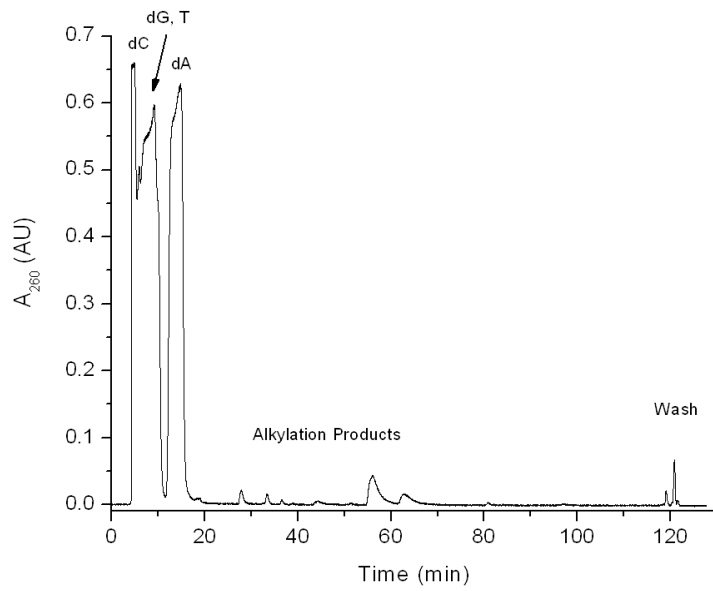


Figure C.2. HPLC analysis of an alkylation reaction consisting of 2 mM each dN, 25 mM sodium phosphate (pH 7), 500 mM KF, and 240 mM 4-MeBrQMP in an 70:30 solution of H₂O:CH₃CN. The reaction was carried out in a 1.5 mL plastic Eppendorf tube for 30 minutes at 37 °C.

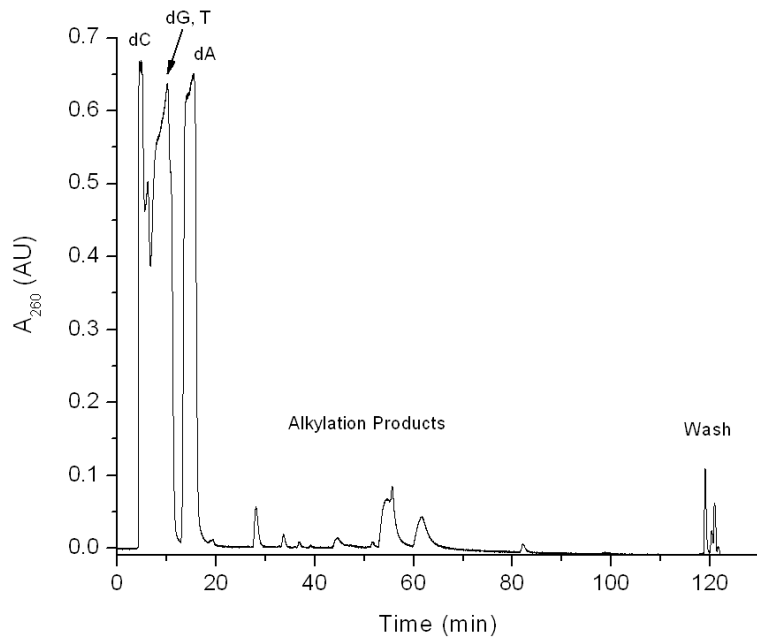


Figure C.3. HPLC analysis of an alkylation reaction consisting of 2 mM each dN, 25 mM sodium phosphate (pH 7), 500 mM KF, and 240 mM 4-MeBrQMP in an 70:30 solution of $\text{H}_2\text{O}:\text{CH}_3\text{CN}$. The reaction was carried out in a 1.5 mL plastic Eppendorf tube for 1 hour at 37 °C.

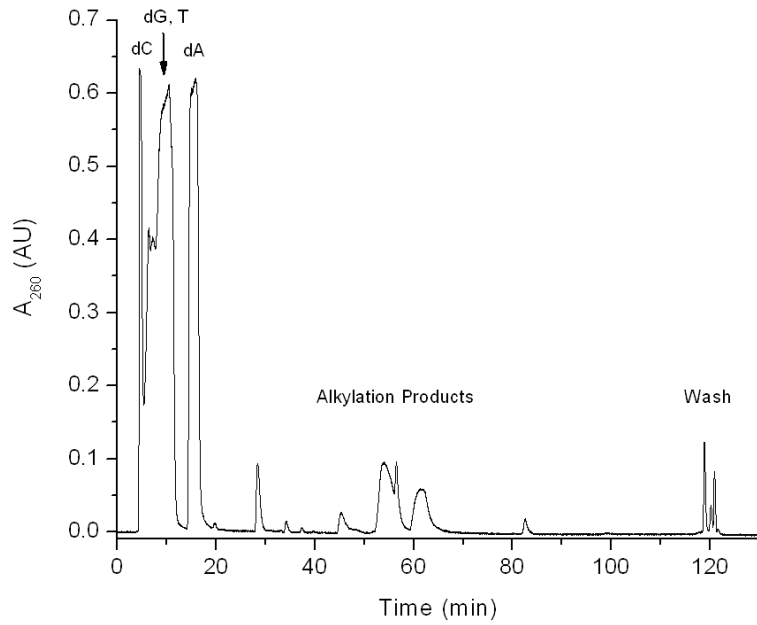


Figure C.4. HPLC analysis of an alkylation reaction consisting of 2 mM each dN, 25 mM sodium phosphate (pH 7), 500 mM KF, and 240 mM 4-MeBrQMP in an 70:30 solution of $\text{H}_2\text{O}:\text{CH}_3\text{CN}$. The reaction was carried out in a 0.3 mL glass Reacti-vial for 1 hour at 37 °C.

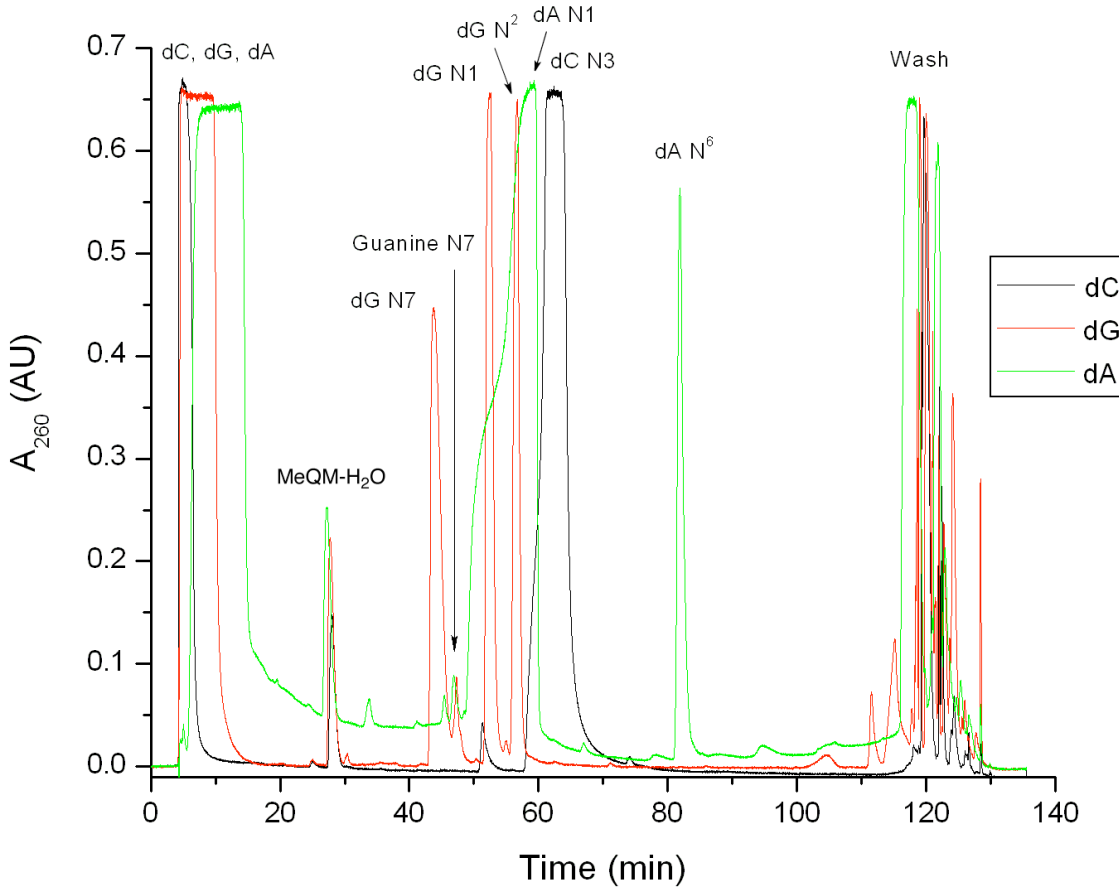


Figure C.5. Overlay of 3 HPLC chromatograms showing the MeQM alkylation of monomeric nucleosides (dC in black, dG in red, and dA in green). Each reaction consisted of 4-MeBrQMP (25 mM), dN (25 mM), and KF (250 mM) in a 1:1 solution of DMF:H₂O. Each reaction was stirred in a 0.3 mL Reacti-vial for 1 hour at 37 °C prior to analysis by HPLC using an analytical column (1 mL/min). The HPLC gradient was identical to the one used for the DNA digestion studies (**Method 2**).

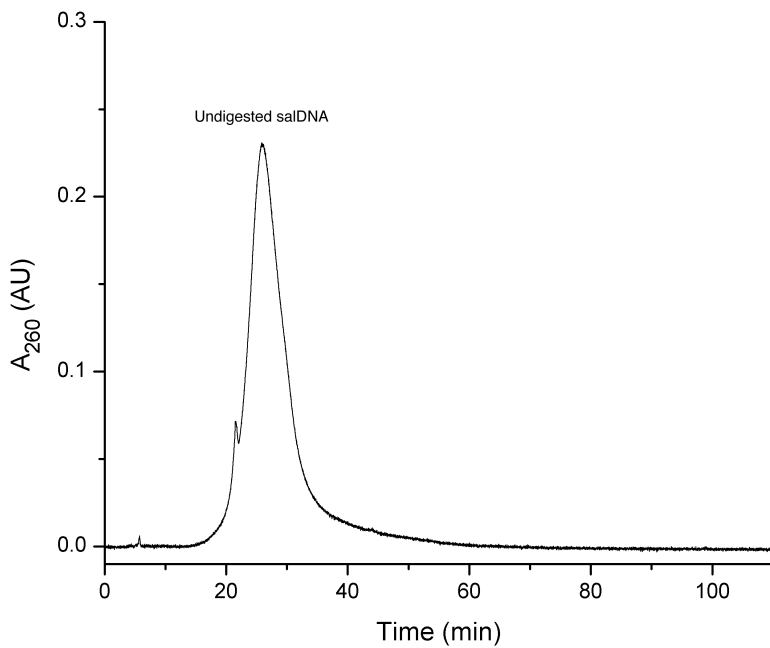


Figure C.6. HPLC analysis of undigested salDNA. A mixture consisting of salDNA (8 mM nts), sodium phosphate (25 mM, pH 7), and NaF (200 mM) in an 80:20 solution of $\text{H}_2\text{O}:\text{CH}_3\text{CN}$ was subjected to work-up and digestion conditions (**Method 2**) without the presence of alkaline phosphatase or phosphodiesterase I.

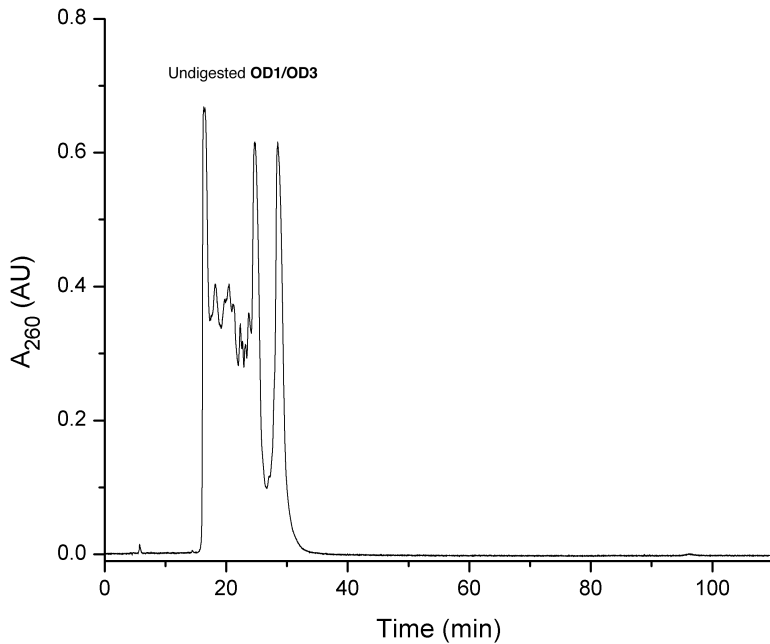


Figure C.7. HPLC analysis of undigested **OD1/OD3**. An aqueous mixture consisting of **OD1/OD3** (16 mM nts) and potassium phosphate (25 mM, pH 7) was subjected to work-up and digestion conditions (**Method 2**) without the presence of alkaline phosphatase or phosphodiesterase I.

Appendix D. Supporting Information for Chapter 5

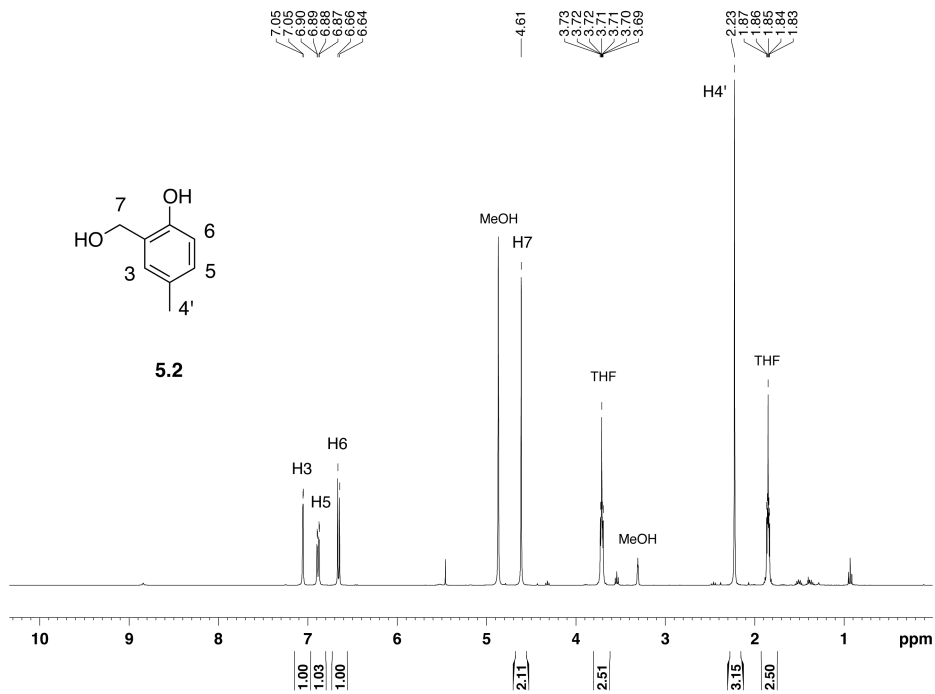


Figure D.1. ^1H NMR of MeQM- H_2O (**5.2**) in d_4 -methanol at 400 MHz.

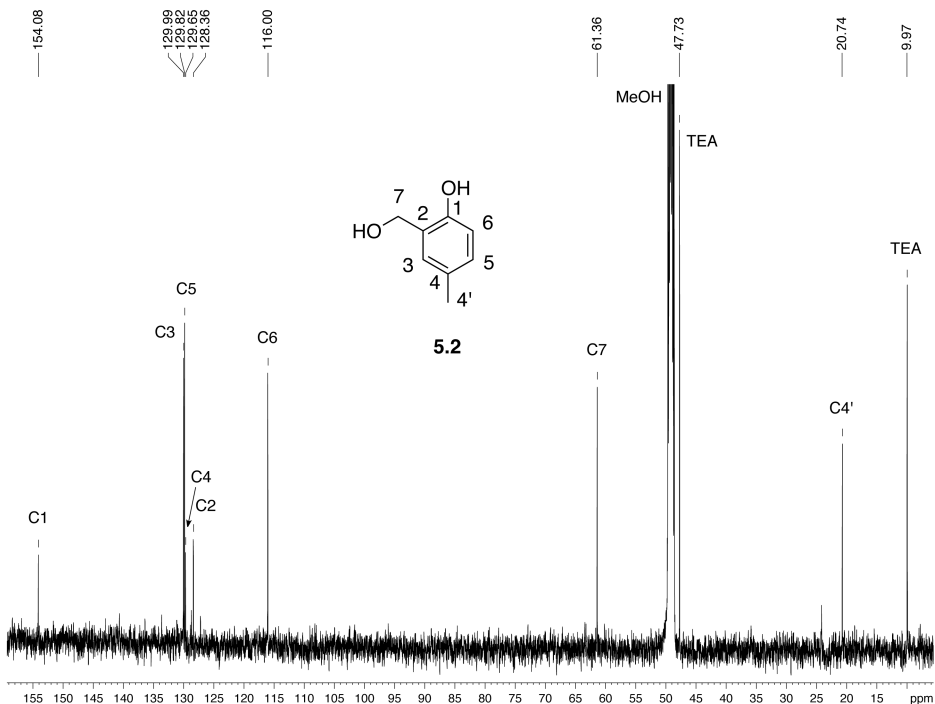


Figure D.2. ^{13}C NMR of MeQM- H_2O (**5.2**) in d_4 -methanol at 500 MHz.

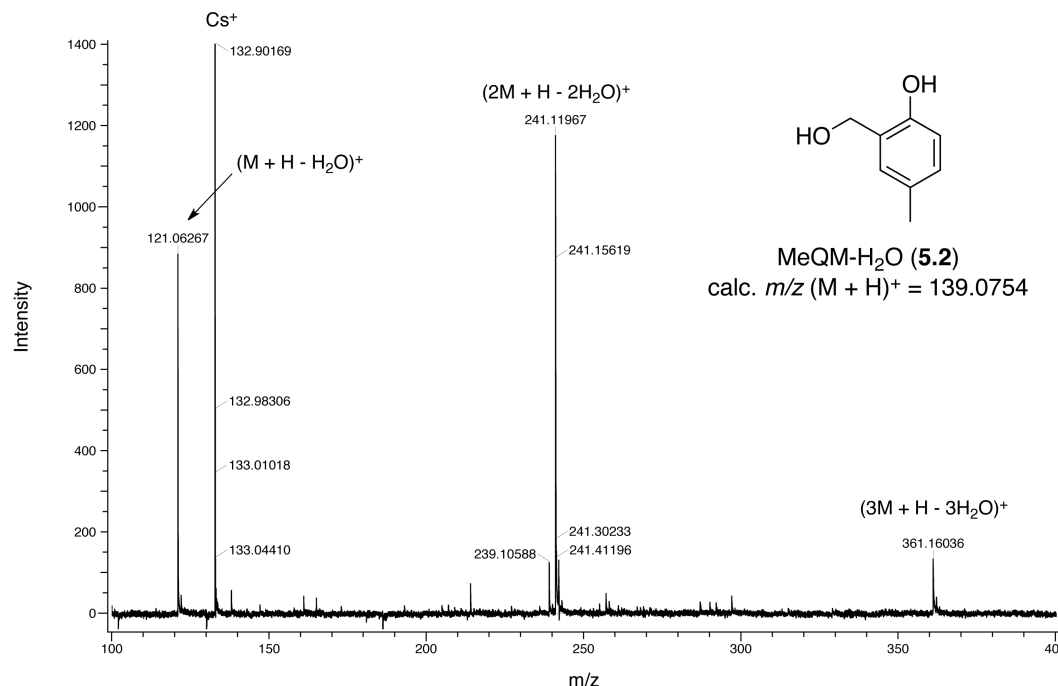


Figure D.3. High resolution ESI⁺-MS of MeQM-H₂O (**5.2**) calibrated with CsI. Mass error is 22.1 ppm (M + H - H₂O)⁺.

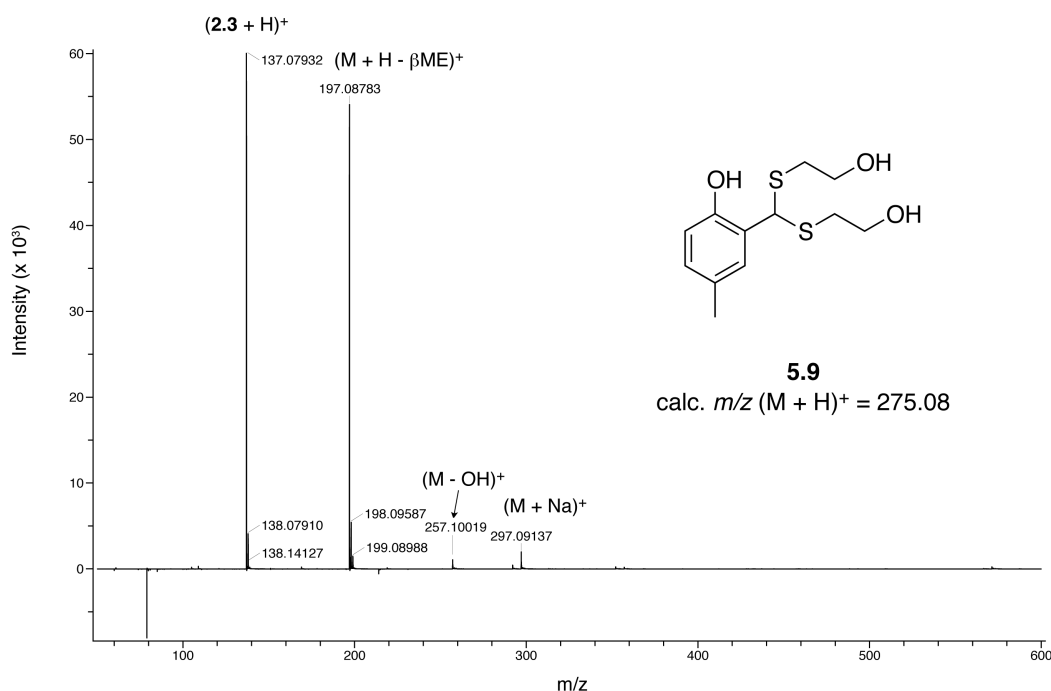


Figure D.4. ESI⁺-MS of the dithioacetal intermediate (**5.9**). Compound **2.3** is residual starting material, 5-methylsalicylaldehyde.

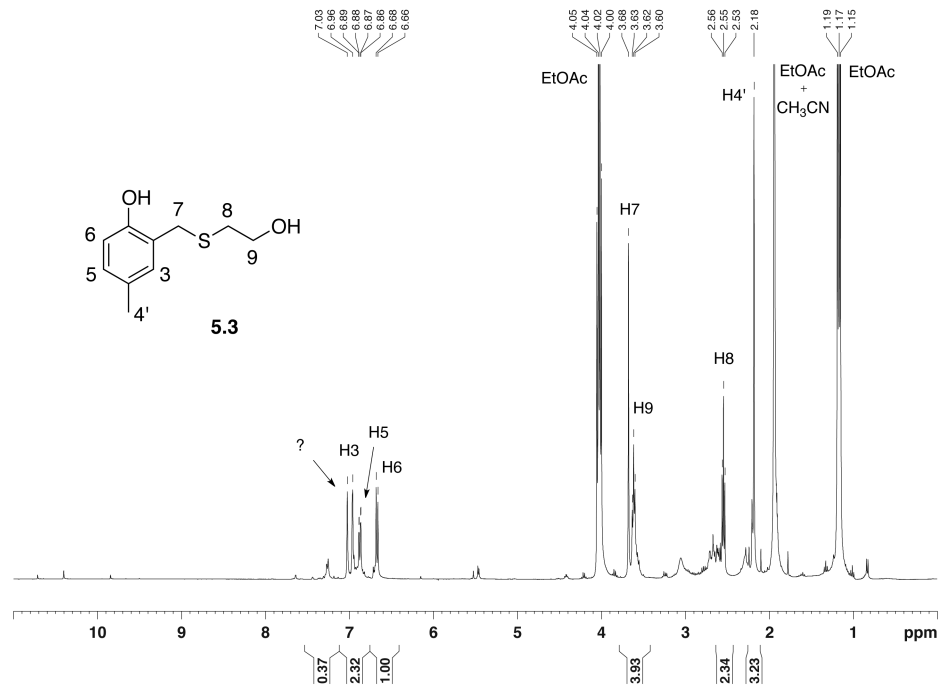


Figure D.5. ^1H NMR of MeQM- β ME (**5.3**) in CD_3CN at 400 MHz after purification by chromatotron.

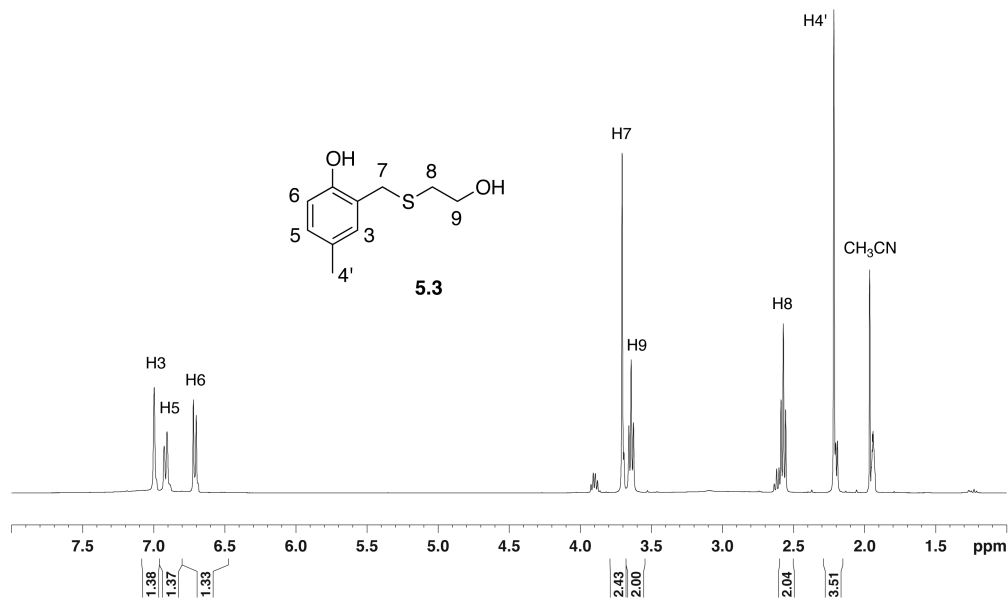


Figure D.6. ^1H NMR of MeQM- β ME (**5.3**) in CD_3CN at 400 MHz after purification by HPLC.

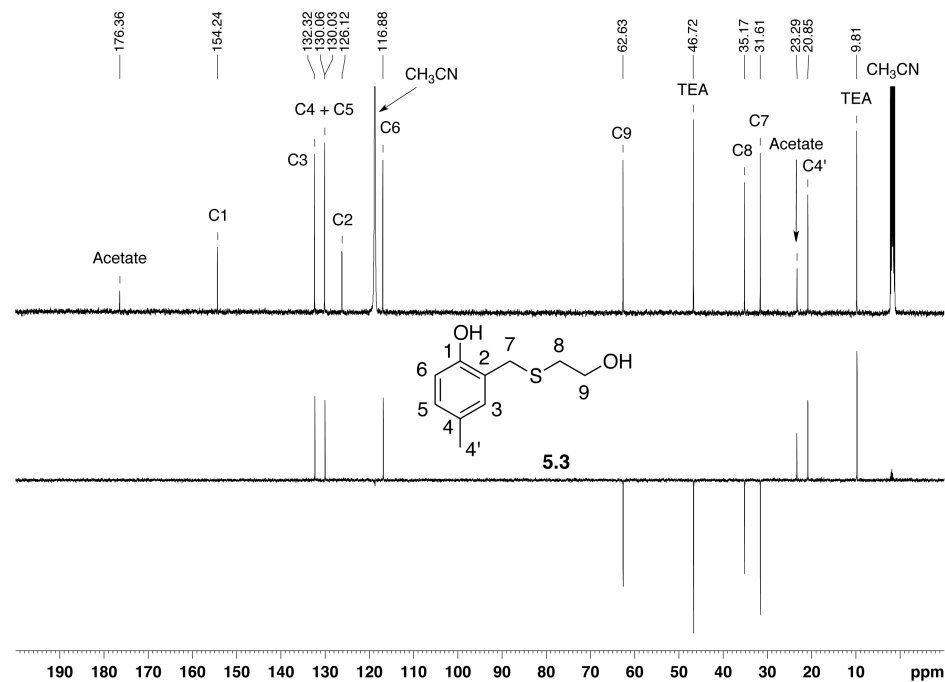


Figure D.7. ^{13}C 1D (top) and DEPT135-SP (bottom) NMR of MeQM- β ME (**5.3**) in CH_3CN at 500 MHz. For DEPT135-SP positive signals are CH and CH_3 carbons, negative signals are CH_2 carbons. Quaternary carbons are not observed.

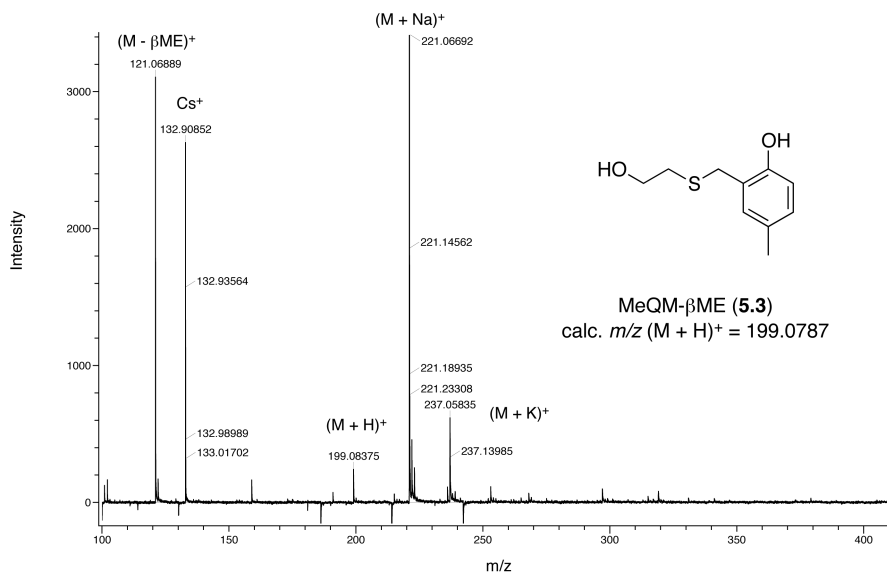


Figure D.8. High resolution ESI $^+$ -MS of MeQM- β ME (**5.3**) calibrated with CsI. Mass error is 22.5 ppm (M + H) $^+$.

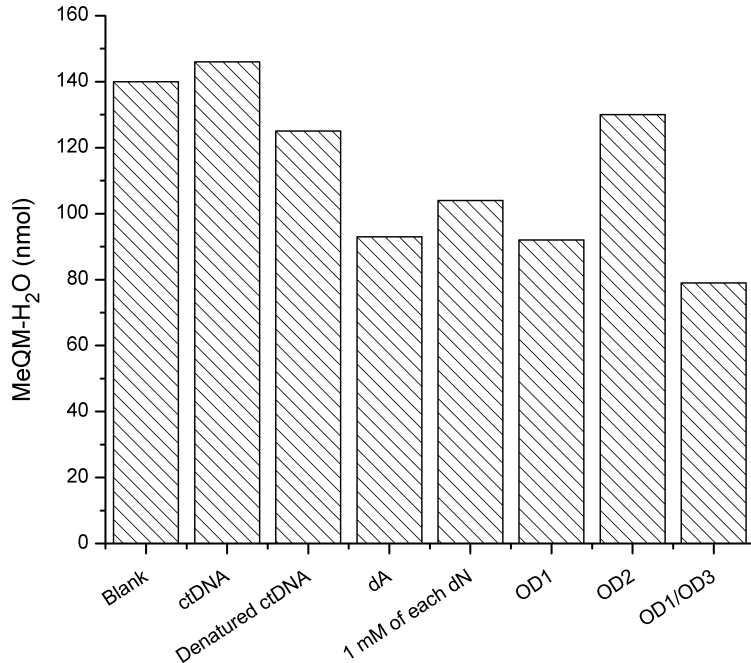


Figure D.9. Comparing the formation of MeQM-H₂O in the presence of various nucleoside based nucleophiles. Each reaction was stirred at 37 °C for 0.5 hr after KF initiation of MeQM (Δt_1) and at 37 °C for 4 hr after β ME addition (Δt_2). **OD1** is an average of two reactions while the other data points are from single reactions. The blank reaction does not contain nucleoside based nucleophiles.

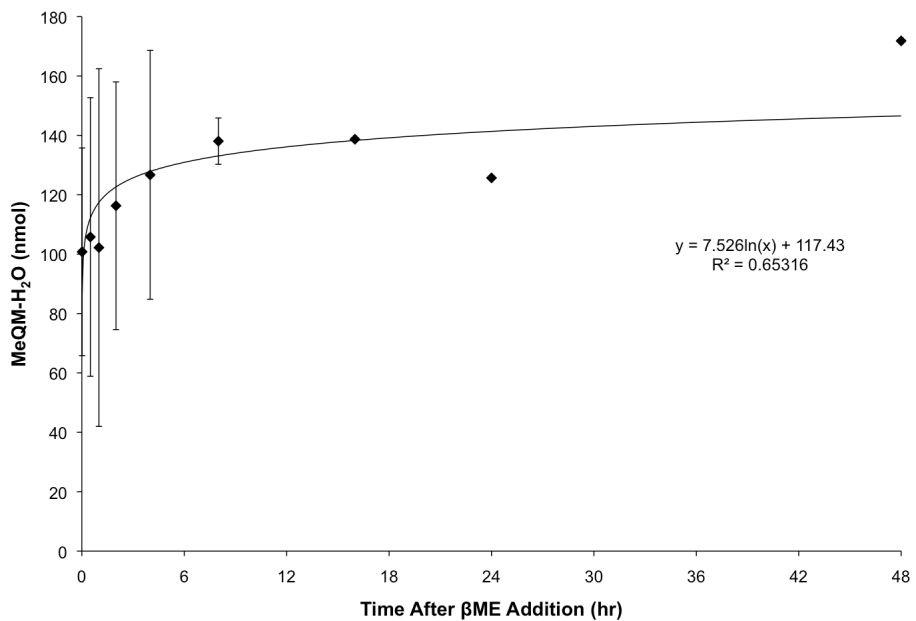


Figure D.10. Measuring the capture of MeQM by H₂O by quantifying the amount of MeQM-H₂O formed. The data is best fit to a logarithmic trendline. Data points prior to 16 hours are an average of three reactions. Data points for 16, 24, and 48 hours are single reactions.

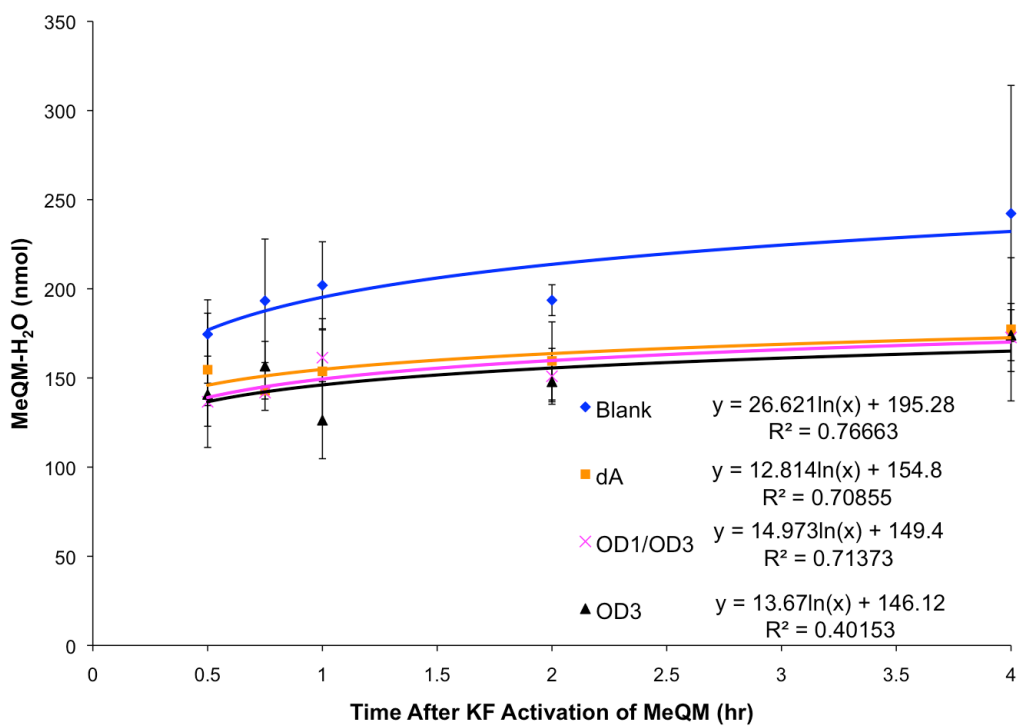


Figure D.11. Measuring the formation of MeQM-H₂O in the presence of various DNA based nucleophiles. Each reaction is stirred at 37 °C for the indicated time and stirred at 37 °C for 24 hours after addition of βME. The data is best fit to an exponential trendline and are an average of reactions repeated in triplicate.

References

- (1) Rydberg, B.; Lindahl, T. Nonenzymatic methylation of DNA by the intracellular methyl group donor S-adenosyl-L-methionine is a potentially mutagenic reaction. *EMBO J.* **1982**, *1*, 211–216.
- (2) Lindahl, T. Instability and decay of the primary structure of DNA. *Nature* **1993**, *362*, 709–715.
- (3) Shrivastav, N.; Li, D.; Essigmann, J. M. Chemical biology of mutagenesis and DNA repair: cellular responses to DNA alkylation. *Carcinogenesis* **2010**, *31*, 59–70.
- (4) Ramsahoye, B.; Davies, C.; Mills, K. DNA methylation: biology and significance. *Blood reviews* **1996**, *10*, 249–261.
- (5) Bird, A. DNA methylation patterns and epigenetic memory. *Genes Dev.* **2002**, *16*, 6–21.
- (6) Robertson, K. D. DNA methylation and human disease. *Nat. Rev. Genet.* **2005**, *6*, 597–610.
- (7) Lawley, P. D.; Phillips, D. H. DNA adducts from chemotherapeutic agents. *Mutat. Res.* **1996**, *355*, 13–40.
- (8) Hurley, L. H. DNA and its associated processes as targets for cancer therapy. *Nat. Rev. Cancer* **2002**, *2*, 188–200.
- (9) Zong, W.-X. W.; Ditsworth, D. D.; Bauer, D. E. D.; Wang, Z.-Q. Z.; Thompson, C. B. C. Alkylating DNA damage stimulates a regulated form of necrotic cell death. *Genes Dev.* **2004**, *18*, 1272–1282.
- (10) Lindahl, T.; Sedgwick, B.; Sekiguchi, M.; Nakabeppu, Y. Regulation and expression of the adaptive response to alkylating agents. *Annu. Rev. Biochem.* **1988**, *57*, 133–157.
- (11) Sedgwick, B. Repairing DNA-methylation damage. *Nat. Rev. Mol. Cell Biol.* **2004**, *5*, 148–157.
- (12) Kleibl, K. Molecular mechanisms of adaptive response to alkylating agents in *Escherichia coli* and some remarks on O(6)-methylguanine DNA-methyltransferase in other organisms. *Mutat. Res.* **2002**, *512*, 67–84.
- (13) Loehler, E. L.; Green, C. L.; Essigmann, J. M. In vivo mutagenesis by O6-methylguanine built into a unique site in a viral genome. *Proc. Natl. Acad. Sci. U. S. A.* **1984**, *81*, 6271–6275.
- (14) Pullman, A.; Pullman, B. Molecular electrostatic potential of the nucleic acids. *Q. Rev. Biophys.* **1981**, *14*, 289–380.
- (15) Beranek, D. T. Distribution of methyl and ethyl adducts following alkylation with monofunctional alkylating agents. *Mutat. Res.* **1990**, *231*, 11–30.
- (16) Gates, K. S.; Nooner, T.; Dutta, S. Biologically relevant chemical reactions of N7-alkylguanine residues in DNA. *Chem. Res. Toxicol.* **2004**, *17*, 839–856.
- (17) Boiteux, S.; Laval, J. Imidazole open ring 7-methylguanine: an inhibitor of DNA synthesis. *Biochem. Biophys. Res. Commun.* **1983**, *110*, 552–558.
- (18) O'Connor, T. R.; Boiteux, S.; Laval, J. Ring-opened 7-methylguanine residues in DNA are a block to in vitro DNA synthesis. *Nuc. Acids Res.* **1988**, *16*, 5879–5894.
- (19) Pawłowicz, A. J.; Munter, T.; Zhao, Y.; Kronberg, L. Formation of Acrolein Adducts with 2'-Deoxyadenosine in Calf Thymus DNA. *Chem. Res. Toxicol.* **2006**, *19*, 571–576.
- (20) Farmer, P. B. DNA and protein adducts as markers of genotoxicity. *Toxicol. Lett.*

- 2004**, *149*, 3-9.
- (21) Liebler, D. C.; Guengerich, F. P. Elucidating mechanisms of drug-induced toxicity. *Nat. Rev. Drug. Discov.* **2005**, *4*, 410–420.
- (22) Basu, A. K.; O'Hara, S. M.; Valladier, P.; Stone, K.; Mols, O.; Marnett, L. J. Identification of adducts formed by reaction of guanine nucleosides with malondialdehyde and structurally related aldehydes. *Chem. Res. Toxicol.* **1988**, *1*, 53–59.
- (23) Dedon, P. C.; Plastaras, J. P.; Rouzer, C. A.; Marnett, L. J. Indirect mutagenesis by oxidative DNA damage: formation of the pyrimidopurinone adduct of deoxyguanosine by base propenal. *Proc. Natl. Acad. Sci. U. S. A.* **1998**, *95*, 11113–11116.
- (24) Plastaras, J. P.; Riggins, J. N.; Otteneder, M.; Marnett, L. J. Reactivity and mutagenicity of endogenous DNA oxopropenylating agents: base propenals, malondialdehyde, and N(epsilon)-oxopropenyllysine. *Chem. Res. Toxicol.* **2000**, *13*, 1235–1242.
- (25) Schnetz-Boutaud, N.; Daniels, J. S.; Hashim, M. F.; Scholl, P.; Burrus, T.; Marnett, L. J. Pyrimido[1,2-alpha]purin-10(3H)-one: a reactive electrophile in the genome. *Chem. Res. Toxicol.* **2000**, *13*, 967–970.
- (26) Riggins, J. N.; Daniels, J. S.; Rouzer, C. A.; Marnett, L. J. Kinetic and thermodynamic analysis of the hydrolytic ring-opening of the malondialdehyde-deoxyguanosine adduct, 3-(2'-deoxy-beta-D-erythro-pentofuranosyl)-pyrimido[1,2-alpha]purin-10(3H)-one. *J. Am. Chem. Soc.* **2004**, *126*, 8237–8243.
- (27) Mao, H.; Schnetz-Boutaud, N. C.; Weisenseel, J. P.; Marnett, L. J.; Stone, M. P. Duplex DNA catalyzes the chemical rearrangement of a malondialdehyde deoxyguanosine adduct. *Proc. Natl. Acad. Sci. U. S. A.* **1999**, *96*, 6615–6620.
- (28) Kozekov, I. D.; Turesky, R. J.; Alas, G. R.; Harris, C. M.; Harris, T. M.; Rizzo, C. J. Formation of Deoxyguanosine Cross-Links from Calf Thymus DNA Treated with Acrolein and 4-Hydroxy-2-nonenal. *Chem. Res. Toxicol.* **2010**, *23*, 1701–1713.
- (29) Pawłowicz, A. J.; Klika, K. D.; Kronberg, L. The structural identification and conformational analysis of the products from the reaction of acrolein with 2'-deoxycytidine, 1-methylcytosine and calf thymus DNA. *Eur. J. Org. Chem.* **2007**, 1429–1437.
- (30) Pawłowicz, A. J.; Kronberg, L. Characterization of adducts formed in reactions of acrolein with thymidine and calf thymus DNA. *Chem. Biodiv.* **2008**, *5*, 177–188.
- (31) Kozekov, I. D.; Nechev, L. V.; Sanchez, A.; Harris, C. M.; Lloyd, R. S.; Harris, T. M. Interchain cross-linking of DNA mediated by the principal adduct of acrolein. *Chem. Res. Toxicol.* **2001**, *14*, 1482–1485.
- (32) Schärer, O. D. DNA interstrand crosslinks: natural and drug-induced DNA adducts that induce unique cellular responses. *ChemBioChem* **2005**, *6*, 27–32.
- (33) Grillari, J.; Katinger, H.; Voglauer, R. Contributions of DNA interstrand cross-links to aging of cells and organisms. *Nuc. Acids Res.* **2007**, *35*, 7566–7576.
- (34) David-Cordonnier, M.-H.; Gajate, C.; Olmea, O.; Laine, W.; la Iglesia-Vicente, de, J.; Perez, C.; Cuevas, C.; Otero, G.; Manzanares, I.; Bailly, C.; Mollinedo, F. DNA and non-DNA targets in the mechanism of action of the antitumor drug trabectedin. *Chem. Biol.* **2005**, *12*, 1201–1210.
- (35) Zewail-Foote, M.; Hurley, L. H. Ecteinascidin 743: a minor groove alkylator that bends DNA toward the major groove. *J. Med. Chem.* **1999**, *42*, 2493–2497.
- (36) Pommier, Y.; Kohlhagen, G.; Bailly, C.; Waring, M.; Mazumder, A.; Kohn, K. W. DNA sequence- and structure-selective alkylation of guanine N2 in the DNA minor groove by ecteinascidin 743, a potent antitumor compound from the

- (37) Caribbean tunicate Ecteinascidia turbinata. *Biochemistry* **1996**, *35*, 13303–13309.
- (38) Zewail-Foote, M.; Hurley, L. H. Differential rates of reversibility of ecteinascidin 743-DNA covalent adducts from different sequences lead to migration to favored bonding sites. *J. Am. Chem. Soc.* **2001**, *123*, 6485–6495.
- (39) Freccero, M.; Di Valentin, C.; Sarzi-Amade, M. Modeling H-bonding and solvent effects in the alkylation of pyrimidine bases by a prototype quinone methide: a DFT study. *J. Am. Chem. Soc.* **2003**, *125*, 3544–3553.
- (40) Richard, J. P.; Toteva, M. M.; Crugeiras, J. Structure–reactivity relationships and intrinsic reaction barriers for nucleophile additions to a quinone methide: a strongly resonance-stabilized carbocation. *J. Am. Chem. Soc.* **2000**, *122*, 1664–1674.
- (41) Noll, D. M.; Mason, T. M.; Miller, P. S. Formation and repair of interstrand cross-links in DNA. *Chem. Rev.* **2006**, *106*, 277–301.
- (42) Tomasz, M. Mitomycin C: small, fast and deadly (but very selective). *Chem. Biol.* **2003**, *2*, 575–579.
- (43) Bolton, J. L.; Sevestre, H.; Ibe, B. O.; Thompson, J. A. Formation and reactivity of alternative quinone methides from butylated hydroxytoluene: possible explanation for species-specific pneumotoxicity. *Chem. Res. Toxicol.* **1990**, *3*, 65–70.
- (44) Lewis, M. A.; Yoerg, D. G.; Bolton, J. L.; Thompson, J. A. Alkylation of 2'-deoxynucleosides and DNA by quinone methides derived from 2, 6-di-tert-butyl-4-methylphenol. *Chem. Res. Toxicol.* **1996**, *9*, 1368–1374.
- (45) Bolton, J. L.; Turnipseed, S. B.; Thompson, J. A. Influence of quinone methide reactivity on the alkylation of thiol and amino groups in proteins: studies utilizing amino acid and peptide models. *Chem.-Biol. Interact.* **1997**, *107*, 185–200.
- (46) Lemercier, J. N.; Meier, B. W.; Gomez, J. D.; Thompson, J. A. Inhibition of glutathione S-transferase P1-1 in mouse lung epithelial cells by the tumor promoter 2,6-di-tert-butyl-4-methylene-2,5-cyclohexadienone (BHT-Quinone methide): Protein adducts investigated by electrospray mass spectrometry. *Chem. Res. Toxicol.* **2004**, *17*, 1675–1683.
- (47) Weng, X.; Ren, L.; Weng, L.; Huang, J.; Zhu, S.; Zhou, X.; Weng, L. Synthesis and biological studies of inducible DNA cross-linking agents. *Angew. Chem., Int. Ed.* **2007**, *46*, 8020–8023.
- (48) Diao, L.; Yang, C.; Wan, P. Quinone methide intermediates from the photolysis of hydroxybenzyl alcohols in aqueous solution. *J. Am. Chem. Soc.* **1995**, *117*, 5369–5370.
- (49) Colloredo-Mels, S.; Doria, F.; Verga, D.; Freccero, M. Photogenerated quinone methides as useful intermediates in the synthesis of chiral BINOL ligands. *J. Org. Chem.* **2006**, *71*, 3889–3895.
- (50) Di Antonio, M.; Doria, F.; Richter, S. N.; Bertipaglia, C.; Mella, M.; Sissi, C.; Palumbo, M.; Freccero, M. Quinone methides tethered to naphthalene diimides as selective G-quadruplex alkylating agents. *J. Am. Chem. Soc.* **2009**, *131*, 13132–13141.
- (51) Sugimoto, H.; Nakamura, S.; Ohwada, T. Generation and application of o-quinone methides bearing various substituents on the benzene ring. *Adv. Synth. Catal.* **2007**, *349*, 669–679.
- (52) Modica, E.; Zanaletti, R.; Freccero, M.; Mella, M. Alkylation of amino acids and glutathione in water by o-quinone methide. Reactivity and selectivity. *J. Org. Chem.* **2001**, *66*, 41–52.

- (53) Marino, J. P.; Dax, S. L. An efficient desilylation method for the generation of o-quinone methides: application to the synthesis of (+)- and (-)-hexahydrocannabinol. *J. Org. Chem.* **1984**, *49*, 3671–3672.
- (54) Li, T. H.; Rokita, S. E. Selective Modification of DNA Controlled by an Ionic Signal. *J. Am. Chem. Soc.* **1991**, *113*, 7771–7773.
- (55) Rokita, S. E.; Yang, J. H.; Pande, P.; Greenberg, W. A. Quinone methide alkylation of deoxycytidine. *J. Org. Chem.* **1997**, *62*, 3010–3012.
- (56) Veldhuyzen, W. F.; Lam, Y. F.; Rokita, S. E. 2'-deoxyguanosine reacts with a model quinone methide at multiple sites. *Chem. Res. Toxicol.* **2001**, *14*, 1345–1351.
- (57) Veldhuyzen, W. F.; Shallop, A. J.; Jones, R. A.; Rokita, S. E. Thermodynamic versus kinetic products of DNA alkylation as modeled by reaction of deoxyadenosine. *J. Am. Chem. Soc.* **2001**, *123*, 11126–11132.
- (58) Weinert, E. E.; Frankenfield, K. N.; Rokita, S. E. Time-dependent evolution of adducts formed between deoxynucleosides and a model quinone methide. *Chem. Res. Toxicol.* **2005**, *18*, 1364–1370.
- (59) Freccero, M.; Gandolfi, R.; Sarzi-Amade, M. Selectivity of purine alkylation by a quinone methide. Kinetic or thermodynamic control? *J. Org. Chem.* **2003**, *68*, 6411–6423.
- (60) Weinert, E. E., Quinone methide alkylation of DNA: Understanding reactivity through reversibility, trapping, and substituent effects. Ph.D. Dissertation, University of Maryland, College Park, MD, 2006.
- (61) Wang, H.; Wahi, M. S.; Rokita, S. E. Immortalizing a transient electrophile for DNA cross-linking. *Angew. Chem., Int. Ed.* **2008**, *47*, 1291–1293.
- (62) Pande, P.; Shearer, J.; Yang, J. H.; Greenberg, W. A.; Rokita, S. E. Alkylation of nucleic acids by a model quinone methide. *J. Am. Chem. Soc.* **1999**, *121*, 6773–6779.
- (63) Weinert, E. E.; Rokita, S. E. Kinetic and trapping studies of 2'-deoxynucleoside alkylation by a quinone methide. *Chem. Res. Toxicol.* **2005**, *18*, 1970–1970.
- (64) Marsch, G. A.; Mundkowski, R. G.; Morris, B. J.; Manier, M. L.; Hartman, M. K.; Guengerich, F. P. Characterization of nucleoside and DNA adducts formed by S-(1-acetoxymethyl)glutathione and implications for dihalomethane-glutathione conjugates. *Chem. Res. Toxicol.* **2001**, *14*, 600–608.
- (65) Wakselman, M. The 1,4 and 1,6 eliminations from hydroxy- and amino-substituted benzyl systems: chemical and biochemical applications. *Nouv. J. Chim.* **1983**, *7*, 439.
- (66) Rodia, J. S.; Freeman, J. H. Methylene bridge formation via carbonium ions in the phenol-formaldehyde reaction. *J. Org. Chem.* **1959**, *24*, 21–26.
- (67) Ishii, Y.; Okamura, T.; Inoue, T.; Fukuhara, K.; Umemura, T.; Nishikawa, A. Chemical structure determination of DNA bases modified by active metabolites of Lucidin-3-O-primeveroside. *Chem. Res. Toxicol.* **2010**, *23*, 134–141.
- (68) Carreno, M. C.; Gonzalez-Lopez, M.; Urbano, A. Oxidative de-aromatization of para-alkyl phenols into para-peroxyquinols and para-quinols mediated by oxone as a source of singlet oxygen. *Angew. Chem., Int. Ed.* **2006**, *45*, 2737–2741.
- (69) Cadet, J.; Ravanat, J.-L.; Martinez, G. R.; Medeiros, M. H. G.; Di Mascio, P. Singlet oxygen oxidation of isolated and cellular DNA: product formation and mechanistic insights. *Photochem. Photobiol.* **2006**, *82*, 1219–1225.
- (70) Deya, P. M.; Dopico, M.; Jeronimo Morey, A. G. R.; Saa, J. M. On the regioselectivity of the fremy's salt oxidation of phenols. *Tetrahedron* **1987**, *43*, 3523–3532.
- (71) Tamura, Y.; Yakura, T.; Haruta, J.; Kita, Y. Hypervalent iodine oxidation of para-

- alkoxyphenols and related-compounds - a general-route to para-benzoquinone monoacetals and spiro lactones. *J. Org. Chem.* **1987**, *52*, 3927–3930.
- (72) Tamura, Y.; Yakura, T.; Tohma, H.; Kikuchi, K.; Kita, Y. Hypervalent iodine oxidation of para-alkoxy-phenol and related phenol - a facile and efficient synthesis of para-quinones. *Synthesis* **1989**, 126–127.
- (73) Barret, R.; Daudon, M. Oxidation of phenols to quinones by bis(trifluoroacetoxy)iodobenzene. *Tetrahedron Lett.* **1990**, *31*, 4871–4872.
- (74) Mckillop, A.; McLaren, L.; Taylor, R. J. K. A simple and efficient procedure for the preparation of p-quinols by hypervalent iodine oxidation of phenols and phenol tripropylsilyl ethers. *J. Chem. Soc., Perkin Trans. 1* **1994**, 2047–2048.
- (75) Moriarty, R. M.; Prakash, O. *Org. React.*; 2001; Vol. 57, p. 327.
- (76) McCrane, M. P.; Weinert, E. E.; Lin, Y.; Mazzola, E. P.; Lam, Y.-F.; Scholl, P. F.; Rokita, S. E. Trapping a labile adduct formed between an ortho-quinone methide and 2'-deoxycytidine. *Org. Lett.* **2011**, *13*, 1186–1189.
- (77) Becker, E. D.; Miles, H. T.; Bradley, R. B. Nuclear magnetic resonance studies of methyl derivatives of cytosine. *J. Am. Chem. Soc.* **1965**, *87*, 5575–5582.
- (78) Pople, J. A.; Bothner-By, A. A. Nuclear spin coupling between geminal hydrogen atoms. *J. Chem. Phys.* **1965**, *42*, 1339–1349.
- (79) Roy, A. K.; B, R.; Batra, S. Insights into the bromination of 3-aryl-5-methyl-isoxazole-4-carboxylate: synthesis of 3-aryl-5-bromomethyl-isoxazole-4-carboxylate as precursor to 3-aryl-5-formyl-isoxazole-4-carboxylate. *Tetrahedron* **2004**, *60*, 2301–2310.
- (80) Weinert, E. E.; Dondi, R.; Colloredo-Melz, S.; Frankenfield, K. N.; Mitchell, C. H.; Freccero, M.; Rokita, S. E. Substituents on quinone methides strongly modulate formation and stability of their nucleophilic adducts. *J. Am. Chem. Soc.* **2006**, *128*, 11940–11947.
- (81) Sun, L.; Singer, B. Reaction of cytidine with ethylating agents. *Biochemistry* **1974**, *13*, 1905–1913.
- (82) Hosmane, R. S.; Leonard, N. J. Simple convenient synthesis of 1-methylcytosine. *Synthesis* **1981**, 118–119.
- (83) Helfer, D. L.; Hosmane, R. S.; Leonard, N. J. Selective alkylation and aralkylation of cytosine at the 1-position. *J. Org. Chem.* **1981**, *46*, 4803–4804.
- (84) Yakura, T.; Omoto, M.; Yamauchi, Y.; Tian, Y.; Ozono, A. Hypervalent iodine oxidation of phenol derivatives using a catalytic amount of 4-iodophenoxyacetic acid and Oxone as a co-oxidant. *Tetrahedron* **2010**, *66*, 5833–5840.
- (85) Wipf, P.; Kim, Y. Studies on the synthesis of Stemona alkaloids; stereoselective preparation of the hydroindole ring system by oxidative cyclization of tyrosine. *Tetrahedron Lett.* **1992**, *33*, 5477–5480.
- (86) Uyanik, M.; Yasui, T.; Ishihara, K. Enantioselective Kita oxidative spirolactonization catalyzed by in situ generated chiral hypervalent iodine(III) species. *Angew. Chem., Int. Ed.* **2010**, *49*, 2175–2177.
- (87) Uyanik, M.; Yasui, T.; Ishihara, K. Chiral hypervalent iodine-catalyzed enantioselective oxidative Kita spirolactonization of 1-naphthol derivatives and one-pot diastereo-selective oxidation to epoxyspirolactones. *Tetrahedron* **2010**, *66*, 5841–5851.
- (88) Pretsch, E.; Bühlmann, P.; Affolter, C. *Structure determination of organic compounds: tables of spectral data*; 3rd ed. Springer: Berlin ; New York, 2000.
- (89) Western, E. C.; Shaughnessy, K. H. Inhibitory effects of the guanine moiety on Suzuki couplings of unprotected halonucleosides in aqueous media. *J. Org. Chem.* **2005**, *70*, 6378–6388.
- (90) Ali, M. S.; Fang, J. J.; Burton, C.; Glenn, B.; Khokhar, A. R. 1-Methyl-4-

- (methylamino)piperidine-platinum(II) adducts with DNA bases. *J. Coord. Chem.* **2007**, *60*, 691–698.
- (91) Ad, O., Trapping quinone methide 2'-deoxyadenosine adducts. Honors Thesis, University of Maryland, College Park, MD 2012.
- (92) El-Kafrawy, S.; Zahran, M.; Pedersen, E. A novel route to N6-alkylated 2'-deoxyadenosine using benzotriazole as a synthetic auxiliary. *Acta Chem. Scand.* **1999**, *53*, 280–283.
- (93) Chang, C. J.; Gomes, J. D. S.; Byrn, S. R. Chemical modification of deoxyribonucleic acids: a direct study by carbon-13 nuclear magnetic resonance spectroscopy. *J. Org. Chem.* **1983**, *48*, 5151–5160.
- (94) Pritchard, A. E.; Kowalski, D.; Laskowski, M. An endonuclease activity of venom phosphodiesterase specific for single-stranded and superhelical DNA. *J. Biol. Chem.* **1977**, *252*, 8652–8659.
- (95) Williams, E. J.; Sung, S. C.; Laskowski, M. Action of venom phosphodiesterase on deoxyribonucleic acid. *J. Biol. Chem.* **1961**, *236*, 1130–1134.
- (96) Pollack, S.; Uchida, T.; Auld, D. Snake-venom phosphodiesterase - a zinc metalloenzyme. *J. Protein. Chem.* **1983**, *2*, 1–12.
- (97) Anderson, R. A.; Bosron, W. F.; Kennedy, F. S.; Vallee, B. L. Role of magnesium in Escherichia coli alkaline phosphatase. *Proc. Natl. Acad. Sci. U. S. A.* **1975**, *72*, 2989.
- (98) Gao, X.; Gaffney, B. L.; Senior, M.; Riddle, R. R.; Jones, R. A. Methylation of thymine residues during oligonucleotide synthesis. *Nuc. Acids Res.* **1985**, *13*, 573–584.
- (99) Wells, R. D.; Larson, J. E. Studies on the binding of actinomycin D to DNA and DNA model polymers. *J. Mol. Biol.* **1970**, *49*, 319–342.
- (100) Ciccarelli, R. B. R.; Solomon, M. J. M.; Varshavsky, A. A.; Lippard, S. J. S. In vivo effects of cis- and trans-diamminedichloroplatinum(II) on SV40 chromosomes: differential repair, DNA-protein cross-linking, and inhibition of replication. *Biochemistry* **1985**, *24*, 7533–7540.
- (101) Wang, H., Reversible quinone methide alkylation of DNA. Ph.D. Dissertation, University of Maryland, College Park, MD 2009.
- (102) Wang, H.; Rokita, S. E. Dynamic cross-linking is retained in duplex DNA after multiple exchange of strands. *Angew. Chem., Int. Ed.* **2010**, *49*, 5957–5960.
- (103) Wahi, M. S., Synthesis of quinone methide precursors as alkylating agents. M.S. Thesis, University of Maryland, College Park, MD 1998.
- (104) Azarifar, D.; Forghaniha, A. A novel chemoselective reaction of aldehydes with 2-mercaptopropanoic acid catalyzed by SiO₂-NaHSO₄ under solvent-free condition. *J Chin. Chem. Soc. - Taip.* **2006**, *53*, 1189–1192.
- (105) Ikeshita, K.-I.; Kihara, N.; Sonoda, M.; Ogawa, A. Lewis acid-catalyzed reduction of dithioacetals by 1,4-cyclohexadiene. *Tetrahedron Lett.* **2007**, *48*, 3025–3028.
- (106) Cai, B.; Li, J. Evaluation of trifluoroacetic acid as an ion-pair reagent in the separation of small ionizable molecules by reversed-phase liquid chromatography. *Anal. Chim. Acta* **1999**, *399*, 249–258.
- (107) Kirk, J. Determination of the base composition of deoxyribonucleic acid by measurement of the adenine/guanine ratio. *Biochem. J.* **1967**, *105*, 673.